

**FOULING AND CLEANING
STUDIES OF PROTEIN
FOULING AT PASTEURISATION
TEMPERATURES**

by

MAJED ALHARTHI

A thesis submitted to

The University of Birmingham

for the degree of

DOCTOR OF PHILOSOPHY

School of Chemical Engineering

The University of Birmingham

2013

UNIVERSITY OF
BIRMINGHAM

University of Birmingham Research Archive

e-theses repository

This unpublished thesis/dissertation is copyright of the author and/or third parties. The intellectual property rights of the author or third parties in respect of this work are as defined by The Copyright Designs and Patents Act 1988 or as modified by any successor legislation.

Any use made of information contained in this thesis/dissertation must be in accordance with that legislation and must be properly acknowledged. Further distribution or reproduction in any format is prohibited without the permission of the copyright holder.

ABSTRACT

Fouling and cleaning processes impact industrial production, in terms of economics, product quality, product safety, and plant efficiency. Therefore, optimisation of fouling and cleaning processes is a significant issue, and needs a good understanding of fouling and cleaning kinetics. Ideal monitors should determine the right time when a process run should stop and when a plant will be clean in order to improve the process efficiency.

This thesis investigated the fouling and cleaning behaviour of dairy fluids in a plate heat exchanger (PHE) and bench scale fouling rig, using whey protein concentrate (WPC) and WPC_m (with added minerals) as fluid models. Fouling and cleaning monitoring methods were also investigated as new ways to operate and control the processes. Experiments displayed that fouling increased with increasing protein concentration up to a limit of approx. β -Lg 0.3 wt. %. Increasing the flow rate from 100 to 150 l/h decreased the $\Delta(\Delta P)$ fouling rate for β -Lg concentrations of 0.1, 0.3 and 0.5wt.% by 34, 70 and 72.7%, respectively, due to the increasing of shear stresses at the heat transfer surface. Adding minerals to WPC has lowered the temperature at which β -Lg begins to denature. The differences in fouling behaviour of WPC and WPC_m had an effect on cleaning behaviour. Increasing the mineral content in WPC deposits leads to cleaning behaviour which differs completely from that of proteinaceous deposit as no pressure peak is observed.

Experiments have been conducted in a bench scale fouling rig and PHE to compare the deposit generated by both and also to investigate the effect of bulk temperatures of 70, 80 and 90°C and surface temperatures of 80, 89 and 98°C on fouling behaviour of the two model solutions WPC and WPC_m in terms of deposit thickness, weight and morphology. In general, the total amount of WPC deposition increased with increasing bulk and surface temperature. In contrast, for WPC_m, the increasing of deposit amount with temperature limited up ca.85°C, where the amount of deposit decreased afterwards. The bench scale fouling rig is able to follow the development of fouling in PHE quite closely. The morphology studies showed that the size of clumps increased with increasing concentration and temperature. In contrast, WPC_m deposit displayed a very fine structure with much smaller particulates compared to the WPC deposit.

Two novel monitoring devices have been developed to evaluate the cleaning process: a particle count technique and Peltier effect. The particle count technique was used to evaluate the removal of various whey protein deposits from the PHE, while the Peltier effect was used to measure the responsiveness of the device during the cleaning of two deposits: toothpaste and golden syrup. The particle count technique is a very sensitive tool. The removal of deposit could be detected by the Peltier effect the availability of images taken during the cleaning process providing useful information about the sensitivity of the Peltier device.

ACKNOWLEDGEMENTS

Praise be to Allah, Lord of the Heavens and the Earths, for enabling me to conduct this study. I pray to Him to accept this work and benefit me with it in this life and in the Hereafter.

My greatest gratitude and appreciation, undoubtedly, go to both of my supervisors, Peter Fryer and Phil Robbins for their invaluable supervision and guidance. Special thanks go to Kylee Goode for encouraging me at the middle of this project and paving the way for me during the course of carrying out some of the experiments. My debt to her is inexpressible for her time and great effort. I also owe profound thanks to Ibrahim Palabiyik, for his constant support and assistance.

I would also like to thank the Saudi Standards, Metrology and Quality Organisation and the Ministry of Higher Education for their financial support.

Heartfelt gratitude goes to my parents and all the members of my family, whose continuous encouragement was critical in completing this thesis. A very special "Thank You" goes to my wife, who kept me going when it was hard to do much work, and provided much needed support. Special thanks are also due to my beloved children, whose patience, love, and good nature have prevailed throughout. They were always a constant source of inspiration. They provided an enjoyable company and a break now and then during the write up process.

Moreover, I wish to acknowledge with gratitude the many direct and indirect contributions of my colleagues in the Department.

TABLE OF CONTENTS

| | |
|---|----------|
| LIST OF FIGURES | vii |
| LIST OF TABLES..... | xv |
| Nomenclature..... | xvii |
| CHAPTER 1: INTRODUCTION | 1 |
| 1.1 Fouling problem..... | 1 |
| 1.2 Dairy fouling..... | 2 |
| 1.3 Cleaning fouled surface | 3 |
| 1.4 Monitoring device..... | 5 |
| 1.5 Objectives of the study..... | 6 |
| CHAPTER 2: LITERATURE REVIEW..... | 7 |
| 2.1 Introduction..... | 7 |
| 2.2 Milk and its fouling..... | 10 |
| 2.2.1 Thermal stability of milk protein..... | 12 |
| 2.2.2 Mechanism of milk fouling | 14 |
| 2.2.3 Factors affecting milk fouling | 21 |
| 2.2.4 Use of whey protein concentrate (WPC) as a fluid model | 24 |
| 2.3 Cleaning dairy deposit | 25 |
| 2.3.1 Cleaning mechanism..... | 28 |
| 2.3.2 Effect of bulk parameters: temperature, chemical and flow rate..... | 32 |
| 2.4 Monitoring of fouling and cleaning | 36 |
| 2.4.1 Monitoring tools indicating surface fouling and cleaning..... | 39 |
| 2.4.2 Monitoring tools indicating fluid cleanliness | 44 |
| 2.5 Conclusions..... | 48 |

| | |
|---|----|
| CHAPTER 3: MATERIALS AND METHODS | 51 |
| 3.1 Introduction and aims | 51 |
| 3.2 Processing and cleaning fluid | 51 |
| 3.2.1 Soft water..... | 52 |
| 3.2.2 Whey protein concentrate (WPC35)..... | 53 |
| 3.2.3 WPC with minerals supplement (WPC _m)..... | 53 |
| 3.2.4 Cleaning chemicals..... | 53 |
| 3.2.5 Toothpaste and golden syrup deposits..... | 54 |
| Experimental equipment | 54 |
| 3.3 Plate heat exchanger | 54 |
| 3.4 The bench-scale fouling rig | 58 |
| 3.4.1 Test section | 63 |
| 3.5 Monitoring devices | 65 |
| 3.5.1 Online measurement | 65 |
| 3.5.2 Offline measurement | 67 |
| 3.5.3 Cleaning rig | 68 |
| 3.6 Operation of the PHE..... | 71 |
| 3.7 Operation of the bench-scale fouling rig | 73 |
| 3.8 Cleaning experiments (PHE) | 74 |
| 3.9 Deposit removal in the bench-scale cleaning rig: experimental procedure | 76 |
| 3.10 Analytical Techniques | 77 |
| 3.10.1 White-light scanning interferometer (WLI)..... | 78 |
| 3.10.2 Scanning electron microscope (SEM) | 78 |
| 3.11 Experimental error | 79 |
| 3.12 Minimising experimental error | 80 |
| 3.13 Heat transfer and pressure drop across the PHE..... | 80 |

| | | |
|---|---|------------|
| 3.13.1 | Heat transfer coefficient | 80 |
| 3.13.2 | Pressure drop | 86 |
| 3.14 | Conclusion | 87 |
| CHAPTER 4 : INFLUENCE OF PROCESS VARIABLES ON THE FOULING AND CLEANING BEHAVIOUR OF DAIRY DEPOSITS FORMED AT UP PASTEURASITION TEMPERATURE | | 88 |
| 4.1 | Introduction..... | 88 |
| 4.2 | WPC and its fluids deposits experimental profile..... | 89 |
| 4.3 | WPC and its fluids deposits fouling..... | 90 |
| 4.3.1 | Result and discussion from fouling experiments..... | 91 |
| 4.4 | Cleaning experiments profile..... | 104 |
| 4.4.1 | Result and discussion of cleaning experiments of WPC deposit..... | 106 |
| 4.4.2 | Result and discussion from cleaning experiments of WPC with adding minerals deposit..... | 118 |
| 4.5 | Conclusion | 124 |
| CHAPTER 5 : COMPARISON OF A LAB SCALE FOULING RIG TO GENERATE DEPOSITS SIMILAR TO A HEAT EXCHANGER | | 126 |
| 5.1 | Introduction..... | 126 |
| 5.2 | Details of the investigation | 127 |
| 5.3 | Results and discussion | 130 |
| 5.3.1 | Effect of β -Lg concentration and temperature on fouling rate | 130 |
| 5.3.2 | Effect of surface temperature on WPC deposit | 134 |
| 5.3.3 | Effect of surface temperature on WPC _m deposit | 136 |
| 5.3.4 | Effect of bulk temperature on WPC _m deposit..... | 137 |
| 5.3.5 | The evolution of deposit during fouling run..... | 140 |
| 5.3.6 | The evolution of pressure drop and heat transfer coefficient in PHE during fouling run..... | 143 |
| 5.3.7 | Deposit composition | 145 |

| | | |
|--|--|-----|
| 5.3.8 | Appearance of the deposits | 147 |
| 5.3.9 | Morphology of the deposits | 147 |
| 5.4 | Conclusion | 155 |
| CHAPTER 6 : INVESTIGATING CLEANING MEASUREMENTS IN A PLATE HEAT EXCHANGER (PHE) | | 157 |
| 6.1 | Introduction..... | 157 |
| 6.2 | Part A: Investigating cleaning measurements in a plate heat exchanger (PHE) | 159 |
| 6.2.1 | Fouling experiment procedure and conditions | 159 |
| 6.2.2 | Cleaning experiment procedure..... | 161 |
| 6.2.3 | Results and Discussion | 162 |
| 6.3 | Part B: The validation of using Peltier device technique on monitoring cleaning of two types of deposits | 183 |
| 6.3.1 | Cleaning experiments | 183 |
| 6.3.2 | Results and Discussion | 184 |
| 6.4 | Conclusion | 200 |
| CHAPTER 7: CONCLUSION AND FUTURE WORK | | 203 |
| 7.1 | Effect of process variable in fouling and cleaning..... | 203 |
| 7.2 | Bench scale fouling rig | 206 |
| 7.3 | Monitoring device..... | 208 |
| 7.4 | Contributions..... | 210 |
| 7.5 | Future work..... | 212 |
| APPENDIX : COMMISSIONING OF THE PHE | | 215 |
| A.1 | Operating procedure to achieve standard state of cleanliness at the PHE | 215 |
| A.2 | Characterisation of behavior under clean conditions..... | 215 |
| REFERENCES | | 229 |

LIST OF FIGURES

| | |
|--|----|
| Figure 2.1: Fouling distribution in an indirect heat exchanger operating on raw milk (Burton, 1994) | 12 |
| Figure 2.2: Schematic representation of the fouling mechanism during heating of whey protein and milk (Jeurnink et al., 1996)..... | 16 |
| Figure 2.3: Effect of Reynolds number on whey protein fouling on stainless steel surface for 60 min contact time; whey protein concentrate (WPC35), fluid inlet temperature 73°C and outlet temperature 83°C, oil inlet temperature 97°C and 95°C respectively (Gotham, 1990)..... | 19 |
| Figure 2.4: Two stages fouling mechanism; I induction, II fouling period (Jun and Irudayaraj, 2009). | 21 |
| Figure 2.5: Schematic diagram of the removal of milk deposit from a solid surface using NaOH, (Graßhoff, 1997). | 29 |
| Figure 2.6: Dependency of the stages of WPC deposit removal on the cleaning process parameters (Gillham, 1997)..... | 31 |
| Figure 2.7: Change in electrical resistance with time during fouling and cleaning process (Chen et al., 2004) | 43 |
| Figure 2.8: Turbidity profiles of cleaning toothpaste using two turbidity devices at different units: turbidity (FTU) and turbidity (ppm) (Cole et al., 2010). | 46 |
| Figure 3.1: Schematic diagram of the plate heat exchanger used in the whey protein fouling and cleaning. Letters P, Tc and FI denote pressure sensor, thermocouples and the flow meter respectively (Christian, 2004). | 55 |
| Figure 3.2: The window viewer displayed on the PHE data logging P.C throughout the fouling and cleaning experiments. Letters F, P, and T denote flow meter, pressure and thermocouples..... | 58 |
| Figure 3.3: Schematic diagram of the bench scale fouling rig. Letters C, F and T denote conductivity, flow meter and thermocouples. | 61 |
| Figure 3.4: Schematic diagram of plate heat exchanger, showing the connection of coupon rig at cooling outlet on the product flow side. Letters F , P, θ and T denote flow meter, Pressure , oil temperature and thermocouples. | 62 |

| | |
|---|----|
| Figure 3.5: The test section with all dimensions. | 64 |
| Figure 3.6: Peltier device (Thermoelectric, 2013)..... | 65 |
| Figure 3.7: Peltier device component (a) side view, (b) bottom view – modular, and (c) bottom view. | 66 |
| Figure 3.8: Peltier device in contact with heat sink with fan and fouled plate..... | 66 |
| Figure 3.9: Particles image on computer screen..... | 68 |
| Figure 3.10: Schematic diagram of the bench-scale cleaning rig. Letters C, T and V denote conductivity, thermocouples and the valve respectively. | 69 |
| Figure 4.1: Fouling behaviour for WPC in terms of pressure drop in PHE; β -Lg 0.3 wt.%, process flow rate 100 l/h, section 3 outlet temperature 95°C..... | 92 |
| Figure 4.2: Fouling behaviour for WPC according to heat transfer coefficient in terms of area (UA), β -Lg 0.3wt.%, process flow rate 100 l/h, section 3 outlet temperature 95°C... | 92 |
| Figure 4.3: Fouling behaviour in terms of pressure drop for the three β -Lg concentrations, process flow rate 100 l/h, section 3 outlet temperature 95°C..... | 94 |
| Figure 4.4: Fouling behaviour according to heat transfer coefficient in terms of area (UA) for the three β -Lg concentrations, process flow rate 100 l/h, section 3 outlet temperature 95°C..... | 94 |
| Figure 4.5: Fouling behaviour in terms of pressure drop for the three β -Lg concentrations, process flow rate 150 l/h, section 3 outlet temperature 95°C..... | 96 |
| Figure 4.6: Fouling behaviour according to heat transfer coefficient in terms of area (UA) for the three β -Lg concentrations, process flow rate 150 l/h, section 3 outlet temperature 95°C..... | 97 |
| Figure 4.7: Fouling rate in terms of rate of change in Biot number for the three β -Lg concentrations, process flow rate 100 l/h, section 3 outlet temperature 95°C. Error bars represent the standard deviation of the means of change rate in Biot number (n=6). | 98 |
| Figure 4.8: Fouling rate in terms of rate of change in Biot number for the three β -Lg concentrations, process flow rate 150 l/h, section 3 outlet temperature 95°C. Error bars represent the standard deviation of the means of change rate in Biot number (n=6). | 99 |
| Figure 4.9: Fouling rate in terms of rate of change in pressure drop for the three β -Lg concentrations, process flow rate 100 l/h, section 3 outlet temperature 95°C. Error bars represent the standard deviation of the means of change rate in pressure drop (n=6). | 99 |

| | |
|--|-----|
| Figure 4.10: Fouling rate in terms of rate of change in pressure drop for the three β -Lg concentrations, process flow rate 150 l/h, section 3 outlet temperature 95°C. Error bars represent the standard deviation of the means of change rate in pressure drop (n=6). | 100 |
| Figure 4.11: Fouling behaviour in terms of pressure drop at each section of PHE for WPC _{m/2} processed at flow rate 100 l/h, section 3 outlet temperature 95°C..... | 102 |
| Figure 4.12: Fouling behaviour according to heat transfer coefficient in terms of area (UA) at each section of PHE for WPC _{m/2} processed at flow rate 100 l/h, section 3 outlet temperature 95°C..... | 102 |
| Figure 4.13: Fouling behaviour in terms of pressure drop at section 2 for WPC _{m/2} processed at flow rate 100 l/h, section 3 outlet temperature 95°C. | 103 |
| Figure 4.14: Fouling behaviour according to heat transfer coefficient in terms of area (UA) at section 2 for WPC _{m/2} processed at flow rate 100 l/h, section 3 outlet temperature 95°C..... | 104 |
| Figure 4.15: Cleaning behaviour in terms of pressure drop for each section of the PHE for WPC (β -Lg 0.3%) processed at flow rate 100 l/h, section 3 outlet temperature 95°C and chemical concentration 0.5wt%, NaOH. | 107 |
| Figure 4.16: Cleaning behaviour according to heat transfer coefficient in terms of area (UA) for each section of the PHE for WPC (β -Lg 0.3%) processed at flow rate 100 l/h, section 3 outlet temperature 95°C and chemical concentration 0.5wt%, NaOH..... | 108 |
| Figure 4.17: Cleaning behaviour in terms of pressure drop for WPC at section 3, β -Lg (0.1, 0.3 and 0.5%), processed flow rate 100 l/h, chemical concentration 0.1wt% NaOH, and section 3 outlet temperature 95°C..... | 109 |
| Figure 4.18: Cleaning behaviour according to heat transfer coefficient in terms of area (UA) for WPC at section 3, β -Lg (0.1, 0.3 and 0.5%), processed flow rate 100 l/h, chemical concentration 0.1wt% NaOH, and section 3 outlet temperature 95°C..... | 110 |
| Figure 4.19: Cleaning behaviour in terms of pressure drop for WPC at section 3, β -Lg (0.1, 0.3 and 0.5%), processed flow rate 150 l/h, chemical concentration 0.1wt% NaOH, and section 3 outlet temperature 95°C..... | 111 |
| Figure 4.20: Cleaning behaviour according to heat transfer coefficient in terms of area (UA) for WPC at section 3, β -Lg (0.1, 0.3 and 0.5%), processed flow rate 150 l/h, chemical concentration 0.1wt% NaOH, and section 3 outlet temperature 95°C..... | 112 |
| Figure 4.21: Cleaning behaviour in terms of pressure drop for WPC at section 3, β -Lg 0.3%, processed flow rate 100 l/h, and section 3 outlet temperature 95°C..... | 113 |

| | |
|--|-----|
| Figure 4.22: Cleaning behaviour according to heat transfer coefficient in terms of area (UA) for WPC at section 3, β -Lg 0.3%, processed flow rate 100 l/h, and section 3 outlet temperature 95°C..... | 113 |
| Figure 4.23: Cleaning behaviour in terms of pressure drop for WPC at section 3, β -Lg 0.5%, processed flow rate 100 l/h, and section 3 outlet temperature 95°C..... | 115 |
| Figure 4.24: Cleaning behaviour according to heat transfer coefficient in terms of area (UA) for WPC at section 3, β -Lg 0.5%, processed flow rate 100 l/h, and section 3 outlet temperature 95°C..... | 115 |
| Figure 4.25: Cleaning behaviour in terms of pressure drop for WPC at section 3, β -Lg 0.3%, processed flow rate 150 l/h, and section 3 outlet temperature 95°C..... | 116 |
| Figure 4.26: Cleaning behaviour according to heat transfer coefficient in terms of area (UA) for WPC at section 3, β -Lg 0.3%, processed flow rate 150 l/h, and section 3 outlet temperature 95°C..... | 116 |
| Figure 4.27: Cleaning behaviour in terms of pressure drop for WPC at section 3, β -Lg 0.5%, processed flow rate 150 l/h, and section 3 outlet temperature 95°C..... | 117 |
| Figure 4.28: Cleaning behaviour according to heat transfer coefficient in terms of area (UA) for WPC at section 3, β -Lg 0.5%, processed flow rate 150 l/h, and section 3 outlet temperature 95°C..... | 117 |
| Figure 4.29: Cleaning behaviour in terms of pressure drop for WPC _{m/2} at all sections of PHE, β -Lg 0.3%, processed flow rate 100 l/h, and section 3 outlet temperature 95°C.... | 119 |
| Figure 4.30: Cleaning behaviour according to heat transfer coefficient in terms of area (UA) for WPC _{m/2} at all sections of PHE, β -Lg 0.3%, processed flow rate 100 l/h, and section 3 outlet temperature 95°C. | 120 |
| Figure 4.31: Cleaning behaviour in terms of pressure drop for WPC _m at all sections of PHE, β -Lg 0.3%, processed flow rate 100 l/h, and section 3 outlet temperature 95°C.... | 121 |
| Figure 4.32: Cleaning behaviour according to heat transfer coefficient in terms of area (UA) for WPC _m at all sections of PHE, β -Lg 0.3%, processed flow rate 100 l/h, and section 3 outlet temperature 95°C. | 121 |
| Figure 4.33: Cleaning behaviour in terms of pressure drop for WPC _{mx2} at all sections of PHE, β -Lg 0.3%, processed flow rate 100 l/h, and section 3 outlet temperature 95°C.... | 122 |
| Figure 4.34: Cleaning behaviour according to heat transfer coefficient in terms of area (UA) for WPC _{mx2} at all sections of PHE, β -Lg 0.3%, processed flow rate 100 l/h, and section 3 outlet temperature 95°C. | 123 |

| | |
|---|-----|
| Figure 5.1: Deposit thickness and weight formed at different bulk temperatures, surface temperature 98°C and β -Lg 0.6wt% for WPC solution..... | 131 |
| Figure 5.2: Deposit thickness and weight formed at different bulk temperatures, surface temperature 98°C, and β -Lg 1wt% for WPC solution..... | 132 |
| Figure 5.3: Deposit resistance (R_f/A) formed at different time, and bulk temperature 90°C. | 133 |
| Figure 5.4: Deposit thickness and weight formed at different surface temperatures 80, 89, and 98°C, bulk temperature 80°C, and β -Lg 0.6wt% for WPC solution..... | 135 |
| Figure 5.5: Deposit thickness and deposit weight formed for WPC _m (β -Lg 0.6wt.%) at bulk temperature 80°C, surface temperatures 80, 90 and 98°C..... | 136 |
| Figure 5.6: Deposit thickness and weight formed for WPC _m (β -Lg 0.6wt.%) at bulk temperatures 70, 80 and 90°C, and surface temperature 98°C..... | 138 |
| Figure 5.7: Deposit weight formed from WPC _m solution (β -Lg 0.6wt%) at bulk temperatures 70, 80 and 90°C, at surface temperature 98°C for coupon, and for PHE at section 3 outlet temperature 93°C and different deposit weights formed at sections 1, 2 and 3 of PHE..... | 139 |
| Figure 5.8: Fouling of WPC _m (β -Lg 0.6wt.%) at bulk temperature 93°C in all sections of PHE..... | 140 |
| Figure 5.9: Deposit thickness formed for WPC _m and WPC (β -Lg 0.6wt.%) at bulk temperatures 80 and 90°C respectively, and surface temperature 98°C..... | 141 |
| Figure 5.10: Deposit weight formed for WPC _m and WPC (β -Lg 0.6wt.%) at bulk temperatures 80 and 90°C respectively, and surface temperature 98°C..... | 142 |
| Figure 5.11: Fouling behaviour in terms of pressure drop for WPC and WPC _m , at section 3 outlet temperature 93°C, β -Lg 0.6%. | 143 |
| Figure 5.12: Pressure drop in PHE during fouling run by using WPC and WPC _m at section 3 outlet temperatures 82 and 93°C and β -Lg 0.6 and 1 wt.%. | 144 |
| Figure 5.13: Fouling resistance (R_f/A) in PHE during fouling run by using WPC and WPC _m at section 3 outlet temperatures 82 and 93°C and β -Lg 0.6 and 1 wt.% | 145 |
| Figure 5.14: White light interferometry of WPC at bulk temperature 70°C:(a) β -Lg 0.6wt%, (b) β -Lg 1wt%. | 150 |
| Figure 5.15: Scanning electron micrographs of WPC at bulk temperature 70°C :(a) β -Lg 0.6wt%, (b) β -Lg 1wt%. | 151 |

| | |
|--|-----|
| Figure 5.16: White light interferometry of WPC at bulk temperature 80°C:(a) β -Lg 0.6wt%, (b) β -Lg 1wt%..... | 151 |
| Figure 5.17: Scanning electron micrographs of WPC at bulk temperature 80°C :(a) β -Lg 0.6wt%, (b) β -Lg 1wt%..... | 152 |
| Figure 5.18: White light interferometry of WPC at bulk temperature 90°C: (a) β -Lg 0.6wt%, (b) β -Lg 1wt%..... | 152 |
| Figure 5.19: Scanning electron micrographs of WPC at bulk temperature 90°C: (a) β -Lg 0.6wt%, (b) β -Lg 1wt%..... | 153 |
| Figure 5.20: White light interferometry of WPC _m at bulk temperature 90°C, β -Lg 0.6wt%. | 153 |
| Figure 5.21: Scanning electron micrographs of WPC _m at bulk temperature 90°C, β -Lg 0.6wt%..... | 153 |
| Figure 5.22: Scanning electron micrographs of PHE deposit :(a) section 3 of PHE deposit of WPC _m , (b) section 2 of PHE deposit of WPC _m , (c) section 3 of PHE deposit of WPC, at bulk temperature 90°C and β -Lg 0.6wt%..... | 154 |
| Figure 6.1: Fouling behaviour in terms of pressure drop for WPC for each section of the PHE, section 3 outlet temperature 95°C..... | 163 |
| Figure 6.2: Fouling behaviour in terms of pressure drop for WPC for each section of the PHE, section 3 outlet temperature 140°C..... | 164 |
| Figure 6.3: Fouling behaviour in terms of pressure drop for WPC _m for each section of the PHE, section 3 outlet temperature 140°C..... | 165 |
| Figure 6.4: Cleaning behaviour in terms of pressure drop at section 3 for WPC deposit formed at 95°C..... | 166 |
| Figure 6.5: Cleaning behaviour in terms of pressure drop at section 3 for WPC deposit formed at 140°C..... | 167 |
| Figure 6.6: The remaining deposit once the pressure drop reached the nominal clean value (a) clean plate (b)..... | 171 |
| Figure 6.7: Cleaning behaviour according to heat transfer coefficient in terms of area (UA)at section 3 for WPC deposit formed at 95°C..... | 172 |
| Figure 6.8: Cleaning behaviour according to heat transfer coefficient in terms of area (UA) at section 3 for WPC deposit formed at 140°C..... | 172 |

| | |
|---|-----|
| Figure 6.9: The effect of temperature and chemical concentration on turbidity reading during cleaning of WPC deposit formed at 95°C..... | 174 |
| Figure 6.10: The effect of temperature and chemical concentration on turbidity reading during cleaning of WPC deposit formed at 140°C..... | 174 |
| Figure 6.11: The effect of temperature and chemical concentration on particles count during cleaning of WPC deposit formed at 95°C..... | 177 |
| Figure 6.12: The effect of temperature and chemical concentration on particles count during cleaning of WPC deposit formed at 140°C..... | 178 |
| Figure 6.13: Particles count and pressure drop during cleaning of WPC _m deposit at section 1 of PHE temperature 140°C..... | 181 |
| Figure 6.14: A typical particles size distribution and cumulative particles size (%) during cleaning of WPC deposit..... | 182 |
| Figure 6.15: Peltier device temperature readings with changes in flow rate..... | 186 |
| Figure 6.16: Peltier output power (%) readings with changes in flow rate..... | 186 |
| Figure 6.17: The effect of insulation layer on Peltier response in terms of Peltier temperature, heat sink 50°C and cleaning water 50°C..... | 187 |
| Figure 6.18: The effect of insulation layer on Peltier response in terms of output power (%), heat sink 50°C and cleaning water 50°C..... | 188 |
| Figure 6.19: The effect of using a fan on the Peltier temperature at heat sink temperature 60°C..... | 189 |
| Figure 6.20: The effect of using a fan on the Peltier output power (%) at heat sink temperature 60°C..... | 189 |
| Figure 6.21: Comparison of the response of the Peltier device on controlling one of the two surfaces temperatures..... | 190 |
| Figure 6.22: The resultant Peltier temperature when controlling the heat sink at 30, 35 and 40°C..... | 192 |
| Figure 6.23: Change in the Peltier temperature during cleaning of the tooth paste and golden syrup deposits by controlling heat sink temperature at 50°C..... | 193 |
| Figure 6.24: Change in output power (%) during cleaning of the tooth paste and golden syrup deposits by controlling heat sink temperature at 50°C..... | 194 |
| Figure 6.25: Images recorded during cleaning of toothpaste deposit by controlling heat sink temperature..... | 195 |

| | |
|---|-----|
| Figure 6.26: Images recorded during cleaning of the golden syrup deposit by controlling heat sink temperature..... | 196 |
| Figure 6.27: Changes in the heat sink temperature during cleaning of tooth paste by controlling the Peltier temperature. | 197 |
| Figure 6.28: Images recorded during cleaning of the tooth paste deposit by controlling the Peltier temperature..... | 198 |
| Figure 6.29: Change in the Peltier temperature during cleaning of tooth paste deposit at constant heat sink temperature of 40°C..... | 199 |
| Figure 6.30: Change in output power (%) during cleaning of the tooth paste deposit at constant heat sink temperature of 40°C..... | 199 |
| Figure A.1: Clean thermal conditions for the whole PHE. 1/UA vs 1/flow rate, at section 3 outlet temperature 95°C and flow rate range 50-150 l/h. | 224 |
| Figure A.2: Clean thermal conditions for sections 1, 2 and 3 of the PHE. 1/UA vs 1/flow rate, at section 3 outlet temperature 95°C and flow rate range 50-150 l/h. | 224 |
| Figure A.3: Clean hydraulic condition for each section of PHE for ranging flow rates from 50-150 l/h, at section 3 outlet pressure 10 kPa. | 226 |
| Figure A.4: Clean hydraulic condition for each section of PHE for ranging flow rates from 50-150 l/h, at section 3 outlet pressure 200 kPa. | 227 |
| Figure A.5: Clean hydraulic condition for each section of PHE for ranging flow rates from 50-150 l/h, at section 3 outlet pressure 400 kPa. | 227 |
| Figure A.6: Clean hydraulic condition for each section of PHE for ranging flow rate from 50-150 l/h, at section 3 outlet pressure 600 kPa. | 228 |
| Figure A.7: Clean hydraulic condition of the whole PHE; ranging flow rate from 50-150 l/h, and various pressure drops..... | 228 |

LIST OF TABLES

| | |
|--|-----|
| Table 2.1: Chemical composition of milk and WPC solution. Adapted from (Changani, 2000)..... | 11 |
| Table 2.2: Comparison of different detection methods together with their advantages and disadvantages..... | 48 |
| Table 3.1: Number of PHE plates involved in heat transfer in each section, and the heat transfer areas associated with the main sections of the PHE (Christian, 2004). | 85 |
| Table 4.1: Typical outlet temperature in each section at the thermally stabilised PHE and at flow rates of 100 and 150 l/h. | 91 |
| Table 4.2: Fouling rate in terms of change in pressure drop and Biot number (ΔBi) at section 3 of the PHE for WPC and at section 2 of the PHE for WPC _{m/2} , WPC _m and WPC _{m\times2} , process flow rate 100 l/h, β -Lg concentration 0.3wt.% , temperature 95°C. | 101 |
| Table 5.1: Composition of deposit removed from coupon rig, at flow rate 100 l/h. Note: compositions do not sum to 100% because of other species present. | 146 |
| Table 5.2: The roughness value for WPC _m and WPC deposit..... | 155 |
| Table 6.1: Swelling period during cleaning for WPC formed at 95°C..... | 168 |
| Table 6.2: Swelling period during cleaning for WPC formed at 140°C..... | 168 |
| Table 6.3: Time to clean according to: heat transfer coefficient in terms of area (UA), pressure drop and turbidity reading for WPC formed at 95°C. | 169 |
| Table 6.4: Time to clean according to: heat transfer coefficient in terms of (UA), pressure drop and turbidity reading for WPC formed at 140°C. | 170 |
| Table 6.5: Turbidity reading at the last stage of cleaning for WPC formed at 95°C. | 175 |
| Table 6.6: Turbidity reading at the last stage of cleaning for WPC formed at 140°C. | 176 |
| Table 6.7: The number of particles removed during cleaning process for WPC _m formed at 140°C..... | 180 |
| Table A.1: Typical outlet temperature in each section during clean operation of the PHE, at oil heater temperature 100°C and various flow rates (cooling flow rate 1 l/min). | 219 |
| Table A.2: Typical outlet temperature in each section during clean operation of the PHE, at oil heater temperature 100°C and various flow rates (cooling flow rate 2 l/min). | 219 |

| | |
|---|-----|
| Table A.3: Typical clean overall heat transfer coefficient in terms of area for each section at various flow rates (oil set to 100°C, cooling water flow rate 1 l/min). | 220 |
| Table A.4: Typical clean overall heat transfer coefficient terms of area for each section at various flow rates (oil set to 100°C, cooling water flow rate 2 l/min). | 220 |
| Table A.5: Typical clean overall heat transfer coefficient in terms of area for each section at various flow rates (oil set to 110°C, cooling water flow rate 1 l/min). | 220 |
| Table A.6: Typical clean overall heat transfer coefficient in terms of area for each section at various flow rates (oil set to 110°C, cooling water flow rate 2 l/min). | 221 |
| Table A.7: Typical clean overall heat transfer coefficient in terms of area for each section at various flow rates (oil set to 120°C, cooling water flow rate 1 l/min). | 221 |
| Table A.8: Typical clean overall heat transfer coefficient in terms of area for each section at various flow rates (oil set to 120°C, cooling water flow rate 2 l/min). | 221 |
| Table A.9: Typical clean heat balance for each section and the whole at various flow rates (oil set to 100°C, cooling water flow rate 1 l/min). | 222 |
| Table A.10: Typical clean heat balance for each section and the whole at various flow rates (oil set to 100°C, cooling water flow rate 2 l/min). | 222 |
| Table A.11: Typical clean heat balance for each section and the whole at various flow rates (oil set to 110°C, cooling water flow rate 1 l/min). | 222 |
| Table A.12: Typical clean heat balance for each section and the whole at various flow rates (oil set to 110°C, cooling water flow rate 2 l/min). | 223 |
| Table A.13: Typical clean heat balance for each section and the whole at various flow rates (oil set to 120°C, cooling water flow rate 1 l/min). | 223 |
| Table A.14: Typical clean heat balance for each section and the whole at various flow rates (oil set to 120°C, cooling water flow rate 2 l/min). | 223 |
| Table A.15: Clean pressure drop for each section of PHE, and whole PHE for flow rates ranging from 50-150 l/h, at section 3 outlet pressure 10 kPa. | 225 |
| Table A.16: Clean pressure drop for each section of PHE, and whole PHE for flow rates ranging from 50-150 l/h, at section 3 outlet pressure 200 kPa. | 225 |
| Table A.17: Clean pressure drop for each section of PHE, and whole PHE for flow rates ranging from 50-150 l/h, at section 3 outlet pressure 400 kPa. | 225 |
| Table A.18: Clean pressure drop for each section of PHE, and whole PHE for flow rates ranging from 50-150 l/h, at section 3 outlet pressure 600 kPa. | 226 |

Nomenclature

Abbreviations

| | |
|------------------|---|
| α -La | α -Lactalbumin |
| β -Lg | β -Lactoglobulin |
| CIP | Cleaning-in-Place |
| FTU | Formazine Turbidity Units |
| HTC | Heat Transfer Coefficient |
| MHFS | Micro-foil Heat Flux Sensor |
| NaOH | Sodium Hydroxide |
| PHE | Plate Heat Exchanger |
| SDV | Standard deviation |
| SEM | Scanning Electron Microscopy |
| R^2 | Coefficient of determination, ranging from 0 to 1, where 1 is a perfect fit to a trend line |
| UHT | Ultra-High Temperature |
| WLI | White-Light Scanning Interferometer |
| WPC | Whey Protein Concentrate |
| WPC _m | Whey Protein Concentrate with added minerals |

Symbols

| | | |
|--------------------|---|----------|
| a | Projected area of a single plate | m^2 |
| A | Total plate heat transfer area | m^2 |
| Bi | Biot Number | |
| ΔBi | Rate of change in Biot Number | h^{-1} |
| C | Chemical concentration | wt. % |
| C_p | Specific heat capacity | J/kg K |
| d | Diameter | m |
| d_e | Equivalent diameter | m |
| h_c | Film heat transfer coefficient for the processing stream | W/m^2K |
| h_h | Film heat transfer coefficient for the heating stream | W/m^2K |
| \dot{m} | Mass flow rate | kg/s |
| m | Constant | |
| n | Constant | |
| N | Number of plates in section of PHE | |
| Nu | Nusselt number | |
| P_1 | Inlet pressure | Pa |
| P_O | Outlet pressure | Pa |
| ΔP_f | Pressure drop across a section at the end of a fouling experiment | Pa |
| ΔP_s | Pressure drop across a section at the start of a fouling experiment | Pa |
| $\Delta(\Delta P)$ | Rate of change in pressure drop | Pa/h |
| Pr | Prandtl number | |
| R_f | Fouling resistance | m^2K/W |
| Re | Reynolds number | |
| \dot{Q} | Rate of heat transfer | W |
| Q | Process fluid flow rate | m^3/s |
| q | Heat flux | W/m^2 |
| T_b | Bulk temperature | K |
| $T_{h,in}$ | Temperature of heating fluid entering the PHE section | K |
| $T_{h,out}$ | Temperature of heating fluid exiting the PHE section | K |
| ΔT_{LM} | Log mean temperature difference | K |
| $T_{p,in}$ | Temperature of process fluid entering the PHE section | K |
| $T_{p,out}$ | Temperature of process fluid exiting the PHE section | K |
| T_s | Surface temperature | K |
| t | Time | s |
| U | Overall Heat transfer coefficient | W/m^2K |
| U_o | Clean Overall Heat transfer coefficient | W/m^2K |
| U_t | Overall Heat transfer coefficient at a given time | W/m^2K |
| UA | Overall Heat transfer coefficient in terms of area | W/K |
| UA_o | Clean Overall Heat transfer coefficient in terms of area | W/K |
| v | Flow velocity | m/s |
| x | concentration of β -Lg required in final solution | |
| x_p | Thickness of the plate | m |

| | | |
|---------------|------------------------------------|-------------------|
| y | Quantity of WPC powder required | kg |
| z | Quantity of soft water to be added | kg |
| ε | Constant | |
| γ | Constant | |
| λ_p | Thermal conductivity | W/m K |
| ρ | Density | kg/m ³ |
| μ | Viscosity | Pa s |

CHAPTER 1: INTRODUCTION

Fouling results from the accumulation of undesirable material on a surface, which is formed through the contact between the surfaces with fluid. The nature of these deposits is quite different, depending on fluid composition and operational conditions, and can be particulate, crystalline, corrosion, biological or a result of chemical reactions with the surface. In industry, the formation of deposits on surfaces is especially problematic in the heat transfer equipment due to the changes imposed on fluid temperature, thus, affecting the product quality and safety.

1.1 Fouling problem

Food fouling deposits on a heat transfer surface are formed as a result of the thermal instability of certain components in the products. The impact of fouling causes a severe problem in food industry that costs billions of pounds every year. For instance, in the dairy industry alone, fouling accounts for about 80% of the total production costs involved (Bansal and Chen, 2006). This high influence on the total operating costs may require minimising or delaying the fouling process of the equipment surface which consequently helps conserve energy and extend the operation of the equipment (Jun and Irudayaraj, 2009). According to Fryer et al. (1996), the study of fouling helps to understand the basic mechanisms. This understanding can lead to a more optimal potential to the development of new types of heat exchange that minimise fouling. Consequently, the costs of fouling effects could be reduced. Quality issues are equally important. As a matter of fact, many

times a shutdown is vital not only because of poor performance of a heat exchanger, but also due to a lot of concerns of product quality and/or contamination.

There are many effects of fouling which have a negative impact on production. Some of the key problems are listed below:

- i. Additional heating – due to the fouling layer behaving as a form of thermal insulation, maintaining the required temperature of the product needs greater heating as costs increase.
- ii. Additional pumping – the fouling layer narrows the channels and can also increase surface roughness, both of which increase the pressure drop in the process, whereby leading to greater pumping costs.
- iii. Shorter residence times – the narrowing of the channels increases average velocity; therefore, the product has on average a shorter residence time and, thus, does not gain as much heat treatment, which can impact product safety.
- iv. Reduced production rate – to combat (ii) and (iii), the production rate could be dropped; however, this will exacerbate the problems in (i) and have an economic impact as not as much product will be produced.

1.2 Dairy fouling

Milk must be microbiologically stable for safe human consumption. To ensure milk is free from potentially harmful microbes, it is thermally treated. Depending on the type of milk produced, it can be heated to pasteurisation temperature: 72°C or ultra-high temperature (UHT): 135 –142°C. Pasteurised and UHT milk are heat-treated before being dispensed into the container. Milk is composed of a number of thermally unstable components, such as proteins, fat, and minerals and, this complicates the study of dairy fouling.

Dairy fouling is a rapid process forcing the heat exchanger in the dairy to clean at least once a day to maintain production efficiency and keep the strict hygiene standards required in food processing. The deposits formed can be classified into two major types: type A formed at lower temperatures, consisting predominantly of denatured and unfolded aggregates of whey proteins and type B found at higher temperatures and containing noticeably more mineral salts, especially calcium phosphates (Burton, 1968, Changani et al., 1997, Bansal and Chen, 2006). The composition and structure of these deposits are very different; it which would be expected that the cleaning of these deposits might also varies. A better understanding of the fouling mechanism of these deposits could be useful in reducing operation down-time and improving cleaning processes.

1.3 Cleaning fouled surface

Cleaning can be defined as the removal of physical materials to return a system to the same pre-fouling conditions. Cleaning the deposit is also a time- and energy- consuming process of a substantial amount of water and chemicals. A typical dairy plant handling 75,000 gallons of milk per day could use up to 110 million gallons of water per year (Rausch and Powell, 1997). Rebello et al. (1988) estimates that water (23.9%) and cleaning chemicals (7.5%) were the highest contributors towards the cleaning expenses gained during deposit removal. Once the cleaning process is completed, the effluent needs to be processed or treated before reuse or disposals further add to the cost of production.

Cleaning is necessary both to remove fouled deposit and to control product quality and safety. It is necessary to understand the nature of the deposit that is to be removed in order to apply a suitable cleaning regime. Therefore, it is natural that cleaning has received considerable attention in the food sector, partly because of the frequent use of

a multi-purpose plant which uses the same equipment to process different materials; also, food deposits are quite likely to form and adhere firmly on the equipment surface.

Cleaning dairy deposits, which contain both proteins and minerals, is a complex process that involves interactions between surface, deposit and detergent. It is a multistage process, having many steps that may be controlled by shear stress, mass transfer, and chemical reaction. These cleaning stages could be described as follows:

- Diffusion of the cleaning solution from the bulk into deposit
- Chemical reactions start and the deposited materials are broken
- Dispersion of the deposit material into the cleaning solution by the shear action

The usual procedure for cleaning heat-treatment equipment in the dairy industry is the Cleaning in Place (CIP) system, so that dismantling of the equipment can be avoided. Industrial CIP systems are highly developed and automated. There are two types of CIP treatment in dairy processing (Timperley and Smeulders, 1987)

- Two-stage: first stage using alkali (commonly NaOH) and second stage using acid base (nitric or phosphoric), usually separated by a water rinse step (Romney, 1990). The alkaline is used first to remove the protein and fat deposits and expose the thin minerals layer which is then dissolved by the acid step.
- Single-stage: formulated detergent is used, which contains compounds to enhance cleaning, for instance sodium hydroxide, surface active and chelating agents.

It was noted that alkali and acid solution alone might not give sufficiently clean results. After the sodium hydroxide cleaning, the surface was still fouled at several spots, indicating that not all of the minerals deposits had been removed (Jeurnink and Brinkman, 1994).

1.4 Monitoring device

Monitoring fouling and the following cleaning processes are an essential process to ensure optimal performance through providing useful data for operational decisions to be made in food processing plants. Fouling is invisible from the industrial processing equipment, and thus can only be determined by methods such as measuring heat transfers (Bott, 1995, Lalande and Rene, 1988) or pressure drops (Burton, 1966, Fryer et al., 1997), which may not be sufficiently significant, especially in the case of thin fouling layers, to allow an operational decision making. It is therefore significant to use the correct method in order to determine the high standard of the cleanliness level achieved. During monitoring of the cleaning process, a significant proportion of particles are not visible to the naked eye. If small islands of remaining deposit are not detected, this may indicate that the monitoring tool used is not sensitive enough to detect the present deposit.

The definition of cleanliness will vary from sector to sector, for example, in the pharmaceutical industry, it refers to situations where a single microbe is catastrophic, and systems must be microbiologically clean. In food processing the system must be cleaned not only due to reductions in efficiency that result from fouling but also to remove deposits, which may be the source of microbial growth, and to avoid product cross-contamination at change-over.

The selection of monitoring technique depends on the goal of the work. If the main consideration is to monitor the development of deposit removal, a pressure sensor and particles count technique can be applied which are both suitable for industrial application. However, if the presence or absence of thin fouling layers is required to be detected, the Peltier device and acoustic methods are suitable.

The choice of feasible methods to monitor fouling and cleaning in a given application where a number of conditions should be considered can be extremely limited. Therefore, two novel monitoring devices have been developed to evaluate the cleaning process: particles count technique and Peltier device (see Chapter 6). The particles count technique was used to assess the removal of various whey protein deposits from the PHE, while the Peltier device was used to measure the responsiveness of the device during the cleaning of two deposits: toothpaste and golden syrup.

1.5 Objectives of the study

There are four specific objectives of this research:

- To investigate the effect of flow rate and β -Lg concentration on fouling behaviour for WPC and WPC with added minerals (calcium and phosphorus) at pasteurisation temperature 95°C.
- To investigate the effect of flow rate and chemical concentration on cleaning behaviour for WPC and WPC deposits with added minerals at pasteurisation temperature 95°C.
- To design and operate a lab scale fouling rig to generate deposits similar to those at a PHE and to investigate the effect of bulk and surface temperatures at 70, 80, and 90°C on the fouling behaviour of the two model solutions WPC and WPC_m in terms of deposit thickness, weight and morphology
- To examine a novel cleaning monitoring methods as new ways to operate, control and improve cleaning measurements in a heat exchanger.

CHAPTER 2: LITERATURE REVIEW

2.1 Introduction

Fouling in the dairy industry has been a problem since heat exchangers (HEs) were introduced for pasteurising and sterilising milk in the 1930s (Visser and Jeurink, 1997). Fouling on a heated surface during heating of milk is a complex process of deposit formation involving proteins, fat and minerals. The presence of a deposit decreased heat transfer coefficients, increased pressure drops and product losses and also offers places where microbial growth can occur. This leads to cleaning costs and a general environmental load.

A comprehensive understanding of the whole mechanism and underlying reaction between milk components that feature the fouling process is highly required. Both whey protein and calcium phosphate - the major components in milk fouling- form insoluble aggregates in the bulk as a result of their heat sensitivity. The majority of the published fouling studies deal mainly with protein deposit. Jeurink and De Kruif (1993) note that the temperature and pH of the product help unfold the protein chain which react with the similar or other types of protein to form aggregates and get adsorbed on the walls of the contact surface. Consequently, calcium and phosphate ions precipitate and add to the layers of adsorbed protein aggregates which results in a thick fouling layer, covering the heating surface (Belmar-Beiny et al., 1993).

Although whey proteins comprise only about 5% of the milk solids, they account for more than 50% of the fouling deposits in type A fouling which occur at temperatures between 75 and 110°C. Among the two major whey proteins: β -Lactoglobulin (β -Lg) and α -lactalbumin (α -La), the dominant one in heat-induced fouling is β -Lg due to its high heat sensitivity (Lyster, 1970, Lalande and Tissier, 1985, Gotham et al., 1992, Delaplace et al., 1994, Bylund, 1995). Minerals constitute less than 1% of milk, but they account for more than 70% of the fouling deposit in type B which take place at temperatures over 110°C.

It is widespread practice in dairy plants to shut down PHE operation once a day (at least) in order to clean the equipment (Fryer et al., 1996). As a result of fouling, frequent shut-down of the equipment for cleaning causes long plant operation while reducing product output. Cleaning the foulant is also a time-consuming and energy-intensive process that consumes a significant amount of water and chemicals. Plant downtime for a UHT plant can be in excess of 40% of the available production time (Pritchard et al., 1988). Optimisation of the cleaning cycle will yield reduced downtime, and costs for cleaning decreased environmental impact and increased plant flexibility. Cleaning in place (CIP) is an important and frequent unit operation applied throughout the food industry, particularly the dairy industry, where CIP is applied daily for most of the equipment.

CIP programmes are usually a single-stage or two-stage cleaning procedure. Two-stage cleaning used both acid and alkali, whereas single-stage cleaning uses formulated detergent containing wetting and other surface agent. Surfaces with no heat usually apply a single-stage process. Heated surfaces, where fouling is generally more severe, apply a two-stage alkali-acid procedure (Kane and Middlemiss, 1985, Grasshoff, 1989, Karlsson et al., 1998, Tamime, 2009).

Determining the right time to stop the fouling/cleaning process is crucial for the improvement in the efficiency of the whole unit with regards to energy saving, minimisation of production losses and wastewater treatment costs. Monitoring fouling and cleaning can provide useful information about the conditions of the deposits on the surfaces of the processing plant. Fouling can only be determined from parameter measurements, such as pressure drop and heat transfer coefficient, since it is usually invisible from the outside of the industrial processing equipment. However, these parameters may not be sensitive enough to detect the first attached fouling layers or accurately measure the cleaning status of the surfaces after CIP; others can be too expensive or technically difficult to be implemented in the field and operated by non-specialists (e.g. quartz crystal balance or photoacoustic spectroscopy) (Pereira *et al.*, 2006). Monitoring and validation of cleaning are equally significant, mainly for the process plant used for different products. Using a single method to meet all monitoring criteria seems to be implausible; combining various methods and switching between them is more practical (Wallhäußer *et al.*, 2012).

The aim of this chapter is to review the progress which has been made in the process of fouling and the factor that affects the formation of these deposits on the surface of dairy heat treatment equipment. The review also describes the cleaning of these deposits, and an overview is given of different monitoring methods to detect the fouling and cleaning processes which provide valuable indications for operational decision makers in food processing plants.

2.2 Milk and its fouling

Milk is a complex biological fluid (see Table 2.1), containing a number of thermally unstable components (e.g. proteins, fat, and minerals), which complicates the study of dairy fouling. Changani (2000) has provided a list of properties for milk and one of its products i.e. whey protein concentrate (WPC); this is reproduced in Table 2.1. From Table 2.1 it can be seen that most of the milk is water (87.6%), while about 6% is made of protein (which is sub-classed as casein, β -Lg and α -La). Minerals form less than 1% of milk, and fats form another 3.8% and are considered to be a precursor to deposit formation in milk fouling (Bylund, 1995). Of all these constituents of milk, the whey protein is the main foulant. Whey protein is composed of two sub-classes i.e. β -Lg and α -La. Out of these two sub-classes of the whey protein, the β -Lg is the most important and is studied extensively for protein deposits in standard WPC solution formed on heat exchangers in the dairy industry. For this reason quantity of β -Lg concentration has also been given in Table 2.1.

Generally milk fouling can be classed into two major types i.e. proteinaceous and mineral deposits, the former is also called Type A and the later Type B (Burton, 1968, Changani et al., 1997, Bansal and Chen, 2006).

Type A (proteinaceous) deposits are usually white, soft and spongy. In this type, fouling starts at temperatures between 75 and 110°C. The composition of these deposits is 50 to 70% protein, 30 to 40% minerals and 4 to 8% fats. At the lower end of the temperature range, most of the protein is denatured β -Lg, but a shift is found to predominantly casein at the top end (Tissier et al., 1984, Lalande and Tissier, 1985). Delaplace et al. (1994)

states that despite protein constituting only about 5% of the milk solid, it accounts for more than 50% of the fouling deposits in type A.

| Component | | Quantity in Milk (%) | Quantity in WPC* solution, of 0.3wt% β -Lg concentration (wt.%) |
|---------------|------------------------|----------------------|---|
| Water | | 87.6 | 98.1 |
| Protein Total | | 3.3 | 0.737 |
| Sub-Protein | | | |
| Caseins | | 2.5 | - |
| Whey Protein | β -lactoglobulin | 0.3 | 0.3 |
| | α -lactalbumin | 0.07 | 0.073 |
| Fat | | 3.8 | 0.073 |
| Carbohydrate | | 4.7 | 1.02 |
| Minerals | | | |
| | Na | 0.050 | 0.015 |
| | K | 0.150 | 0.050 |
| | Ca | 0.120 | 0.021 |
| | Mg | 0.012 | 0.003 |
| | P | 0.095 | 0.018 |
| | Fe | 0.00005 | |
| | Cu | 0.00002 | |
| | Zn | 0.00035 | |
| | S | 0.030 | |
| | Cl | 0.095 | 0.029 |

*WPC: whey protein concentrate

Table 2.1: Chemical composition of milk and WPC solution. Adapted from (Changani, 2000).

Type B (minerals) deposits are usually hard, brittle, granular in structure, and grey in colour. Here, fouling starts at temperatures above 110°C. The composition of these deposits is 70 to 80% minerals; mostly (calcium phosphate), 15 to 20% protein and 4 to 8% fats. Foster and Green (1990) found no distinct layers in the composition of type B, but protein was concentrated near the outside of the deposit. Lyster (1965) studied the mineral composition of the fouling deposit and noted that calcium and phosphorus

minerals typically formed 90% of the total mineral content of fouling deposits compared to only 30% of the mineral content in raw milk.

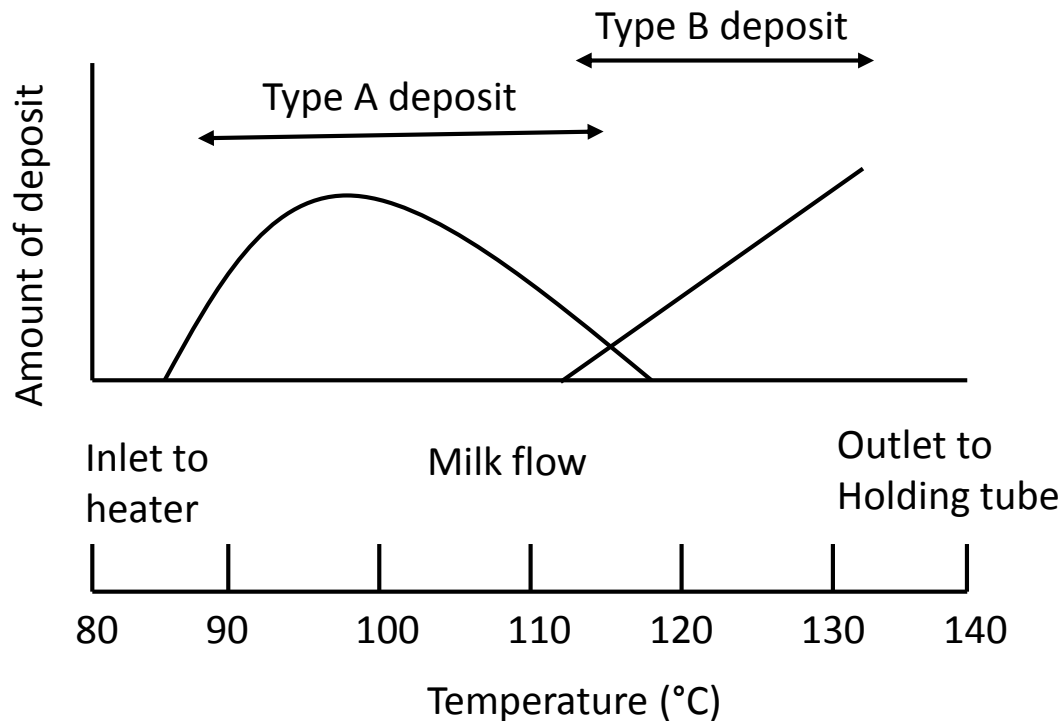


Figure 2.1: Fouling distribution in an indirect heat exchanger operating on raw milk (Burton, 1994)

Fat is the third main component present in milk and has been investigated by Mass et al. (1985) Foster et al. (1989) and Visser and Jeurnink (1997) in detail. They found that fats have little effect on fouling; however, (Lewis and Heppell, 2000) found that decreasing the pH leads to increase the amount of fats within the deposits.

2.2.1 Thermal stability of milk protein

Heating has a direct effect on the structure and functionality of protein in the food system. An understanding of the effects of heat on protein, i.e., denaturation and aggregation, might permit control of these phenomena. As mentioned earlier, the dominant protein in

heat-induced fouling: β -Lg has high heat sensitivity and, therefore, forms significant amounts of Type A deposits (Lyster, 1970, Lalande and Tissier, 1985, Gotham et al., 1992, Delaplace et al., 1994, Bylund, 1995).

The structure of β -Lg is irreversibly altered by denaturation and aggregation when heated above 70°C and these processes take place sequentially. During milk heating, the native proteins (β -Lg) first denature (unfold) and expose the core containing reactive sulphhydryl groups (SH). The denatured or unfolded protein molecules then react with disulphide bonds on other β -Lg molecules or other types of protein molecules and form aggregates (Jeurnink and De Kruif, 1993). The aggregates of β -Lg are entirely irreversible and the resulting aggregates are insoluble in water. β -Lg may form mixed aggregates with other proteins such as κ -casein (Sawyer, 1968). κ -caseins (another subtype of protein different from whey protein) are also resistant to thermal processing but do precipitate upon acidification (Fox, 1989, Visser and Jeurnink, 1997).

Corredig and Dalgleish (1996) found that the method of heat treatment affects markedly the rate and the degree of interaction of the whey proteins with the casein micelles. When milk was heated slowly by using indirect heating systems, approximately 80% of the denatured β -Lg was associated with the casein micelles (Smits and Brouwershaven, 1980, Corredig and Dalgleish, 1996). In contrast, when milk was heated rapidly by using direct heating systems, only about half of the denatured β -Lg and α -Lg became associated with the casein micelles. The interaction between casein micelles and denatured whey proteins changes the physical properties of the micelles and the milk in which they are suspended. The rest of the denatured whey protein remained in the milk serum as disulphide-bonded and hydro-phobically associated aggregates (Singh and Creamer, 1991, Oldfield et al.,

1998). Jeurnink (1992) examined the interaction of whey proteins with the micelles using turbidity techniques and reported that there was a parallel increase in both turbidity and denaturation of the whey proteins. Jeurnink and De Kruif (1993) observed increases in the viscosity of milk with heating, due to the association of whey proteins with the casein micelles. Anema and Li (2003) confirmed that the casein micelles in milk increase in size as a result of heat treatment.

The other main protein, α -La is also heat-labile and its contribution to the fouling process has been considered less important than β -Lg (Visser et al., 1997). The denaturation is 80–90% reversible after heating from 20 to 110°C, but the reversibility of α -Lg decreases with increasing temperature (Chaplin and Lyster, 1988). Being more surface-active than the native protein, the denatured form of α -La can be an active constituent of milk fouling deposits (Arnebrant et al., 1987).

2.2.2 Mechanism of milk fouling

It is necessary to understand the fouling mechanism that leads to its formation on heat transfer surfaces. For instance, if fouling is a bulk-controlled process, deposition may not be prevented by surface modifications. However, if fouling is a surface-controlled process, then the deposited species should be determined first in order to design a resistant surface to such a deposition (Changani et al., 1997).

There are two main views relating to the milk fouling process: First, fouling is controlled by a bulk homogeneous reaction process which is not influenced by mass transfer or a surface reaction process (Visser and Jeurnink, 1997). Second, mass transfer occurs between precursor generation in the bulk fluid and the thermal boundary layer. Further

evidence is sought to provide researchers with good understanding of the exact mechanism and the underlying chemical reactions, resulting in deposition.

2.2.2.1 Activation and transport of deposited species

Jeurnink et al. (1996) proposed a schematic representation of the fouling mechanism during the heating of whey protein and milk in a heat exchanger, as shown in Figure 2.2. The process can be described as follows: when a solution containing whey proteins comes into contact with a stainless steel surface at room temperature, a monolayer of protein immediately adsorbs on the surface. Since bulk fouling starts only at temperatures above 72°C, the first layer adsorbed at room temperature will not lead to an additional build-up of protein layers. As soon as the temperature of the solution reaches heat denaturation, initial particle aggregation in the bulk solution begins, and multilayer adsorption starts to form. The free SH groups, which become exposed at this temperature, are transported to the surface in order to react with the other deposited molecules most likely through the formation of a disulphide bond. Visser et al. (1997) suggested that not every collision with the surface leads to deposition because the reaction depends on the orientation of both the approaching molecule and the already deposited molecules. The deposition may be enhanced in the presence of calcium. Calcium phosphate may precipitate directly onto the stainless steel wall, which is thought to be partly driven by a large temperature difference between the bulk and its surface. In whey solution calcium phosphate may associate with β -Lg aggregation or when casein micelles are present; in the case of milk, calcium phosphate may also associate with casein micelles. In milk, the active β -Lg molecules may associate with κ -casein at the surface of the casein micelle and may entrap the micelles in the deposit, as seen in Figure 2.2.

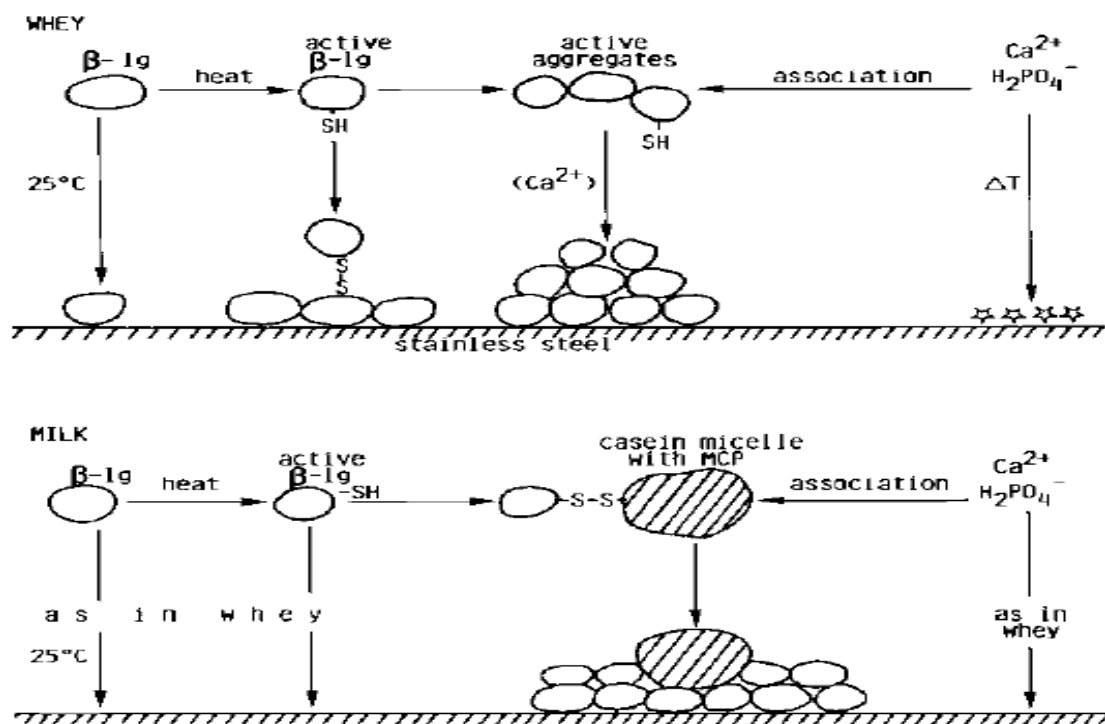


Figure 2.2: Schematic representation of the fouling mechanism during heating of whey protein and milk (Jeurnink et al., 1996).

The interaction between calcium and β -Lg has been extensively studied recently and it was established that calcium is able to influence β -Lg denaturation and aggregation mechanisms in three different ways, depending on the environmental conditions. Firstly, calcium can cause bridging between adjacent negatively charged groups (such as carboxylic groups) of β -Lg and leading to β -Lg aggregation. Secondly, ionic calcium takes part in the intra-molecular electrostatic shielding of β -Lg negative charges, which tends to lower electrostatic repulsion between protein molecules by hydrophobic bonds. Thirdly, calcium can induce specific conformational changes in the β -Lg tertiary structure, leading to local unfolding of β -Lg and exposition of its free thiol groups (Xiong, 1992, Jeyarajah and Allen, 1994, Simmons et al., 2007, O'Kennedy and Mounsey, 2009).

2.2.2.2 Rate determining step

According to Belmar-Beiny et al. (1993), fouling in heat exchanger surfaces depends on both surface and bulk processes. The deposition is a result of a number of stages. In the first stage, protein molecules are denatured and aggregated in the bulk. Then, the aggregated proteins are transported to the heat-transfer surface. Therefore, surface chemical reactions take place and, as a result, the proteins are incorporated into the deposited layer. The formed deposit layer is exposed to fluid shear stresses and, consequently, possible re-entrainment or removal of the deposits.

De Jong et al. (1992), Belmar-Beiny et al. (1993), and Schreier and Fryer (1995) proposed that the fouling process was not limited by mass transfer, but that it alternatively took place in the bulk and surface reactions. Moreover, Schreier and Fryer (1995) pointed out that the fouling rate was not dependent on the concentration of foulant in the fluid. Toyoda et al. (1994), on the other hand, considered that fouling is controlled by bulk and surface reactions as well as mass transfer.

If fouling involves both bulk and surface reactions, it will result from a series of stages:

- (i) Reaction in the fluid.
- (ii) Mass transfer to the surface.
- (iii) Surface reaction into the deposit.
- (iv) Possible transfer back to the bulk, i.e. re-entrainment.

The slowest process will probably be rate controlling. Belmar-Beiny et al. (1993) considered the following two cases:

- (i) If fouling is controlled by mass transfer, transfer of the reacting proteins to the wall is the slowest step. In this case the rate of deposition will be independent of temperature.

(ii) If fouling is controlled by surface processes, deposition will take place wherever the wall temperature is hot enough for protein denaturation and aggregation to occur; regardless of the bulk temperature deposition, there will be a function of the wall, but not the bulk temperature. If the controlling reaction for fouling occurs in the bulk, the denatured and aggregated protein could be generated either in the wall layer or throughout the fluid, depending on the temperature distribution. Further discussion of these factors is given in chapter 5.

To find out the main factor that contributes to the fouling process, Gotham (1990) studied fouling from WPC being deposited at the inner walls of a heated tube. The temperature of the tube surface was above the denaturation temperature of β -Lg ($T \geq 75^\circ\text{C}$). The temperature of the bulk started below this, but increased above the denaturation temperature of β -Lg along the tube. At the end of the experiment, the thickness of the deposit was observed to increase as the temperature increases along the tube; therefore, it was concluded that the fouling process is not controlled by mass transfer (Figure 2.3).

The amount of deposition of the foulants in the thermal boundary layer could differ, depending on the protein deposited whether it is aggregated or denatured. Delaplace et al. (1994) experimentally determined that only 3.6% of the denatured β -Lg was involved in the thermal boundary layer. Based on the assumption that only aggregated proteins caused deposition, Toyoda et al. (1994) modelled the milk fouling process. Similarly, Changani et al. (1997) pointed out that fouling takes place when the aggregated protein occurs next to the heated surface. Delaplace et al. (1997) believed that fouling by proteins can be controlled by the aggregation reactions of protein molecules. They also assumed that fouling can be reduced by macro-mixing in the plate heat exchanger (PHE).

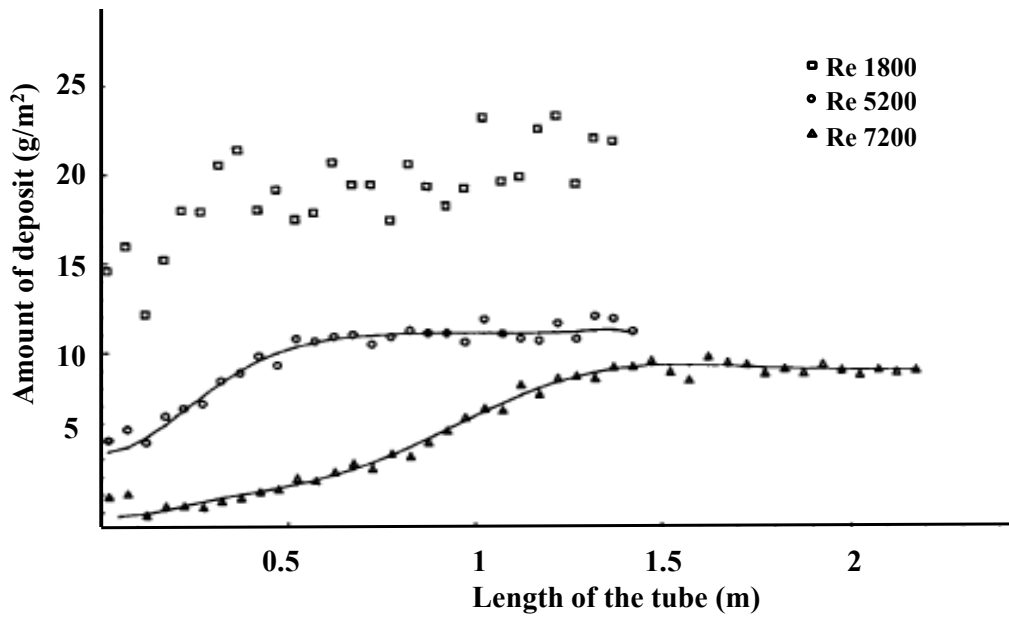


Figure 2.3: Effect of Reynolds number on whey protein fouling on stainless steel surface for 60 min contact time; whey protein concentrate (WPC35), fluid inlet temperature 73°C and outlet temperature 83°C, oil inlet temperature 97°C and 95°C respectively (Gotham, 1990).

Simmons et al. (2007) reported that denaturation is a strong function of temperature whereas, aggregation is a function of the applied shear field as well as the strength of the particle. According to Paterson and Fryer (1988) and Changani et al. (1997), fouling decreases with increasing velocity, the thickness of the laminar sub-layer decreases with increasing velocity and, consequently, the amount of foulant depositing on the heat transfer surface decreases.

2.2.2.3 Induction period

An induction period is time for the initial layer of fouling to deposit on the surface of stainless steel (Lewis and Heppell, 2000). During the induction period, the heat transfer and pressure drop do not change significantly (Figure 2.4). The latter changes when the

fouling period begins, resulting in an increase in pressure drop and reduction in heat transfer coefficient. The induction period represents a condition for forming the protein aggregates or insoluble mineral complexes before a noticeable amount of fouling is formed (Elofsson et al., 1996, Visser and Jeurink, 1997, De Jong et al., 1998). This time period differs between 1 and 60 minutes for tubular heat exchangers (De Jong, 1997). Yet, in plate heat exchangers, induction periods can be significantly shorter, due to higher turbulence (Belmar-Beiny et al., 1993).

The mechanism for the induction period involves the adsorption of protein and calcium phosphate onto the stainless steel (Delsing and Hiddink, 1983). The role of fat during the induction period has not been reported in the literature.

Hege and Kessler (1986) noted that during processing greater than one hour, where Type A deposit is initially formed, a high-mineral-containing sub-layer forms next to the heat transfer surface and is followed by a more spongy, proteinaceous layer, thus forming two distinct layers within the deposit (Fryer, 1989). This is caused by the diffusion of minerals through the deposits and crystallisation of insoluble calcium phosphate at the heat transfer surface (Fryer and Belmar-Beiny, 1991, Belmar-Beiny et al., 1993, Tissier and Lalande, 1986). Foster and Green (1990) argued that the proteinaceous layer and minerals build up at the same time. Belmar-Beiny et al. (1993) analysed the initial deposits adsorbed on the heating surface for 4 seconds and found that it had a high protein content rather than minerals.

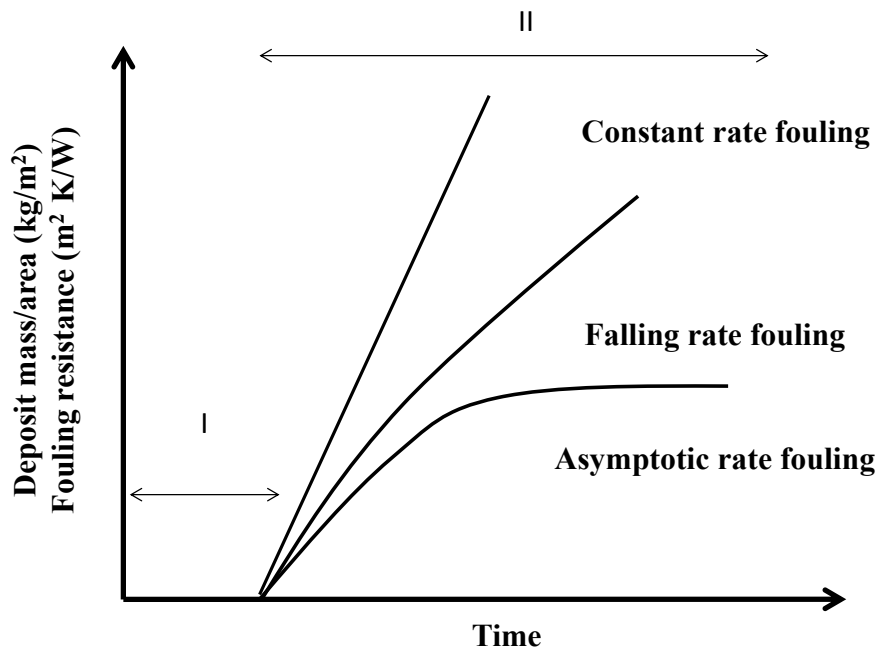


Figure 2.4: Two stages fouling mechanism; I induction, II fouling period (Jun and Irudayaraj, 2009).

2.2.3 Factors affecting milk fouling

A number of system variables (such as temperature, flow rate and product composition) affect the incidence of fouling on heat exchange surfaces. Attention to the magnitude of these variables, associated with all mechanisms of fouling, can minimise the effect of fouling problems.

2.2.3.1 Milk pH

Extensive studies have shown that there is an indirect effect of pH on fouling because it is related to both the denaturation process of protein and to the salt precipitation mechanism. A decrease in pH of milk, for instance, from, 6.8 to 6.4, results in a strong increase in deposition mostly due to the additional deposition of caseins (Skudder et al., 1986). A decrease in pH will also cause an increase in the concentration of ionic calcium, probably

owing to the dissolution of calcium phosphate from casein micelle and its increased solubility (Lewis and Heppell, 2000). Skudder et al. (1986) observed that a small increase in pH leads to increase processing time. In addition, casein micelle reaction rates with β -Lg increases at low pH (Corredig and Dalgleish, 1996). Fat present in milk has little effect on fouling; but, at higher acidity, casein micelles were shown to form aggregates with fats which may explain the increase in the fats amount within the deposit (Foster et al., 1989, Visser and Jeurink, 1997).

2.2.3.2 Pre-heating

A number of researchers have reported that preheating fresh milk prior to ultra-high temperature (UHT) processing results in lower extents of fouling. The amount of type A deposit was reduced after pre-holding, due to earlier denaturation of whey proteins, particularly β -Lg, such that the deposits that do result are predominantly minerals (type B) (Burton, 1968, Lalande and Tissier, 1985, Patil and Reuter, 1986, Mottar and Moermans, 1988). Bell and Sanders (1944) found that the amount of deposits can be minimised by pre-holding milk at 75°C for 10 minutes, and suggested that fouling was due to the denaturation of proteins as well as the decrease in solubility of milk salts with increasing temperature. Also, there is a reduction in the number of ionic calcium with preheating as calcium phosphate becomes associated with casein micelle (Lewis and Heppell, 2000). In contrast, Newstead et al. (1998) and Srichantra et al. (2006) found that relatively severe preheating (90°C for 120 seconds) increased the fouling rates for recombined, reconstituted and fresh milk. They associated this discrepancy in their findings to the differences in processing procedures used by different groups. Newstead et al. (1998) and Srichantra et al. (2006) pasteurised and homogenised milk prior to preheating, whereas Lalande and Tissier (1985) and Mottar and Moermans (1988) homogenised the raw milk

after preheating. Patil and Reuter (1986), on the other hand, did not homogenise the raw milk at all.

2.2.3.3 Flow velocity

Flow velocity is one of the most effective parameters on deposit formation in a heat exchanger, and high velocities may reduce deposit formation (Belmar-Beiny et al., 1993, Santos et al., 2003). According to Paterson and Fryer (1988) and Changani et al. (1997), the thickness of laminar sub-layer decreases with increasing Reynolds number; consequently, the amount of foulant depositing on the heat-transfer surface decreases. Belmar-Beiny et al. (1993) studied the effect of different types of fluids (laminar and turbulent) on deposition thickness. It was observed that a decrease in deposition thickness takes place with increasing turbulence. Rakes et al. (1986) found that higher flow velocities also promote deposit re-entrainment through increased fluid shear stresses. Fryer and Slater (1985) also stated that the shear stress created by the flow rate may bring about deposit removal. Simmons et al. (2007) noted that an increasing shear rate enhances the particle growth rate, owing to an increase in the number of particle collisions. Yet, the final particle size showed a complex behaviour with an increase in shear rate. Fryer and Slater (1985) confirmed that both the rate and amount of fouling decreased with increasing flow velocities in a tubular heat exchanger. However, an increase in the flow velocity tends to significantly increase the amount of deposit mass (Andritsos et al., 2002). They attributed that to the nature of calcium phosphate deposit: compact and adherent; which in turn leads to minimizing the removal process.

At higher flow rates, the deposits are more compact and smoother. It is more difficult to relate fouling to flow rate in plate heat exchangers because of complex geometries involved (Fryer et al., 1995).

2.2.3.4 Processing temperature

Temperature is undoubtedly the most important factor controlling fouling, either considering the absolute temperature, the temperature of the heat exchanger surface or the difference between both (Burton, 1968, Kessler and Beyer, 1991, Belmar-Beiny et al., 1993, Santos et al., 2003). Increasing the temperature causes higher fouling; beyond 110°C, the nature of fouling changes from type A to type B (Burton, 1968). In tubular heat exchangers, deposit formation increases with increasing both the surface and bulk temperature up to 100°C (Fryer, 1986, Hege and Kessler, 1986). Chen and Bala (1998) studied the effect of bulk and surface temperatures on fouling of the whole and skimmed milk, and also whey protein. They found that the surface temperature was the most significant factor in the initiation of fouling. No fouling was observed when the surface temperature was less than 68°C and the bulk temperature was 84°C.

2.2.4 Use of whey protein concentrate (WPC) as a fluid model

Whey protein concentrate (WPC) is utilised to simulate typical milk fouling formed at temperatures lower than 100°C, featuring minimal mineral involvement and the absence of casein as they are removed during the production of WPC.

Extensive studies on the fouling and cleaning mechanisms of milk deposits (Belmar-Beiny et al., 1993, Schreier et al., 1996, Changani et al., 1997, Robbins et al., 1999) established whey protein concentrate as a model dairy fluid over real fluids for a number of reasons, some of which are as follows:

- Reducing the variation of deposits among experiments.
- The difficulties of storage and the cost of using raw milk.
- Regular supply of WPC.

- The difficulty in controlling microbiological activity.

Robbins et al. (1999) proposed that WPC can be used to model milk fouling at pasteurisation temperatures. However, it has also been noted that the extension of the results to milk fouling above 120°C is not straightforward, owing to the difference in chemical composition (Davies et al., 1997, Robbins et al., 1999, Changani, 2000).

2.3 Cleaning dairy deposit

The rapid fouling of heat exchangers in the food industry compromises product quality and process efficiency, which leads to common interruptions for cleaning deposits to ensure consumer safety and ideal process operation.

Fryer and Asteriadou (2009) demonstrated a wide range of cleaning problems experienced in food and personal care product production:

- (i) Type 1 deposits: viscoelastic or viscoplastic fluids such as toothpaste, shampoo, gold syrup and yoghurt that can be removed by the action of water alone.
- (ii) Type 2 deposits: microbial and gel-like films such as biofilms and Turkish delight, removed in part by water and in part by chemicals.
- (iii) Type 3 deposits: solid-like cohesive foulants formed during thermal processing of a product such as whey protein deposits, cooked sweeten condensed milk (SCM), and starch. These products require chemical action for removal. The nature of the deposits will determine the type of cleaning chemical used (such as alkaline cleaning solutions to remove organic films and acidic solutions to remove mineral scales).

Traditionally, dairy CIP has been widely applied for the last 50 years to return the plant to a clean state (Stewart et al., 1996). During CIP, water and chemicals are circulated around

the plant for a prescribed time (Tamime, 2009). The period of circulation depends on the nature of the fouling deposits and the type of equipment being cleaned.

For milk fouling, cleaning of processing equipment is nearly always removed by hot alkaline solutions that break up the protein into water soluble units. Normally, 2% sodium hydroxide solution can be applied at temperatures of up to 85°C. Milk salts are simply detached by the use of a dilute mineral acid since most minerals are acid-soluble (Jeurnink and Brinkman, 1994, Grasshoff, 1996). The most common agent is nitric acid, typically, 0.5% at temperatures of up to 50°C, can be used for cleaning mineral deposits (SPX, 2012).

The nature of the deposit and local practice determines which cleaning solution is applied first; proteinaceous deposits are removed more effectively by first circulation of the alkali solution, but this might be reversed where a high mineral deposit is present. To examine the significance of the order of the two-stage process, Grasshoff (1996) used 0.65% nitric acid and 0.5% sodium hydroxide. He found that cleaning using acid before the caustic rinse was much more efficient than the caustic-acid procedure. It was suggested that the improvement obtained was due to the removal of minerals from the deposit matrix. Morison and Larsen (2005) cleaned two deposits, namely skimmed milk and whey protein, using two-stage cleaning, acid and sodium hydroxide. They found that the cleaning rates for the two-stage procedure were at least four times larger than with a single-stage cleaning and there was no longer a significant decrease in the cleaning rate at high concentrations of sodium hydroxide. The acid action is thought to result in a reduction in the viscosity; therefore, an increase in dissolution of the gel layer formed when caustic cleaning occurs. However, the maximum cleaning rate for whey protein deposits was found to be identical for both single- and two-stage cleaning. The optimal

sodium hydroxide concentration was (1%) which is higher for the two-stage procedure. This change in the optimum concentration was thought to be because of the presence of an acid which needed neutralisation. In contrast, SPX (2012) recommends not using acid before the alkaline cleaning when removing milk deposits, as acid will result in the subsequent removal of proteinaceous deposits to be more difficult.

Alkali and acid solution alone may not give sufficiently clean results. After the sodium hydroxide cleaning, the surface was still fouled at several spots, indicating that not all of the minerals deposits had been removed (Journink and Brinkman, 1994). These deposits were quickly removed by the subsequent acid cleaning. Timperley and Smeulders (1987) found that there was 25% w/w protein on the surface after cleaning with an alkali and once the cleaning stages were completed, residual calcium phosphate was still detected. The disadvantage of two-stages cleaning may be time-consuming, as it uses large amounts of water and may be insufficient to clean the surfaces completely (Timperley and Smeulders, 1987).

Jennings et al. (1957) found that removal of milk deposit improved drastically when specific cleaning agents were mixed i.e. alkaline cleaners and sequestering and wetting agents. Sequestering agents and surfactants (surface-active agents) are the major components in formulated detergents (single-stage cleaning) that can enhance the removal process. A typical sequestering application is the solubilisation of calcium and magnesium salts using EDTA (ethylenediaminetetra-acetic acid) to prevent precipitation by alkaline detergents, and may prevent re-deposition of fouling deposits (Kane and Middlemiss, 1985, SPX, 2012).

Single-stage cleaning typically requires only three steps: (1) rinsing (2) cleaning and (3) rinsing, compared with a minimum of five steps needed for two-stage cleaning: (1) rinsing

(2) alkali cleaning (3) rinsing (4) acid cleaning and (5) rinsing (Timperley and Smeulders, 1987).

Attempts to compare the single- and two-stage cleaning regimes showed that single-stage treatment is more economical due to reduction in rinsed water, energy consumptions and down time (Timperley and Smeulders, 1987, De Goederen et al., 1989). However, a single-stage cleaning chemical contains a mixture of chemicals that are potentially damaging to the environment.

2.3.1 Cleaning mechanism

The literature on cleaning is not as extensive as that on fouling. However, several studies have been performed on cleaning processes. In the food industry, cleaning studies have mostly focused on milk and its products, due to milk and its products having high consumption all over the world, as well as the high adhesive/cohesive strength of the fouling produced. It is necessary (i) to understand how deposits are removed from the heat transfer surfaces and (ii) to investigate the governing cleaning mechanisms, since they can decrease maintenance costs and production losses. Furthermore, a better understanding of cleaning could reduce contamination and downtime.

Graßhoff (1997) gave a schematic representation of the stages of whey protein deposit removal as shown in Figure 2.5.

The cleaning process takes place in three stages:

- (i) Swelling stage: an initial rapid swelling of the deposit was observed after contact with the alkaline solution, followed by the removal of the top layer of the swollen deposit as the diffusion process has not been completed for the whole deposit.

Then, a swelling of the remaining deposit layer occurs and at this stage the deposit is totally swelled.

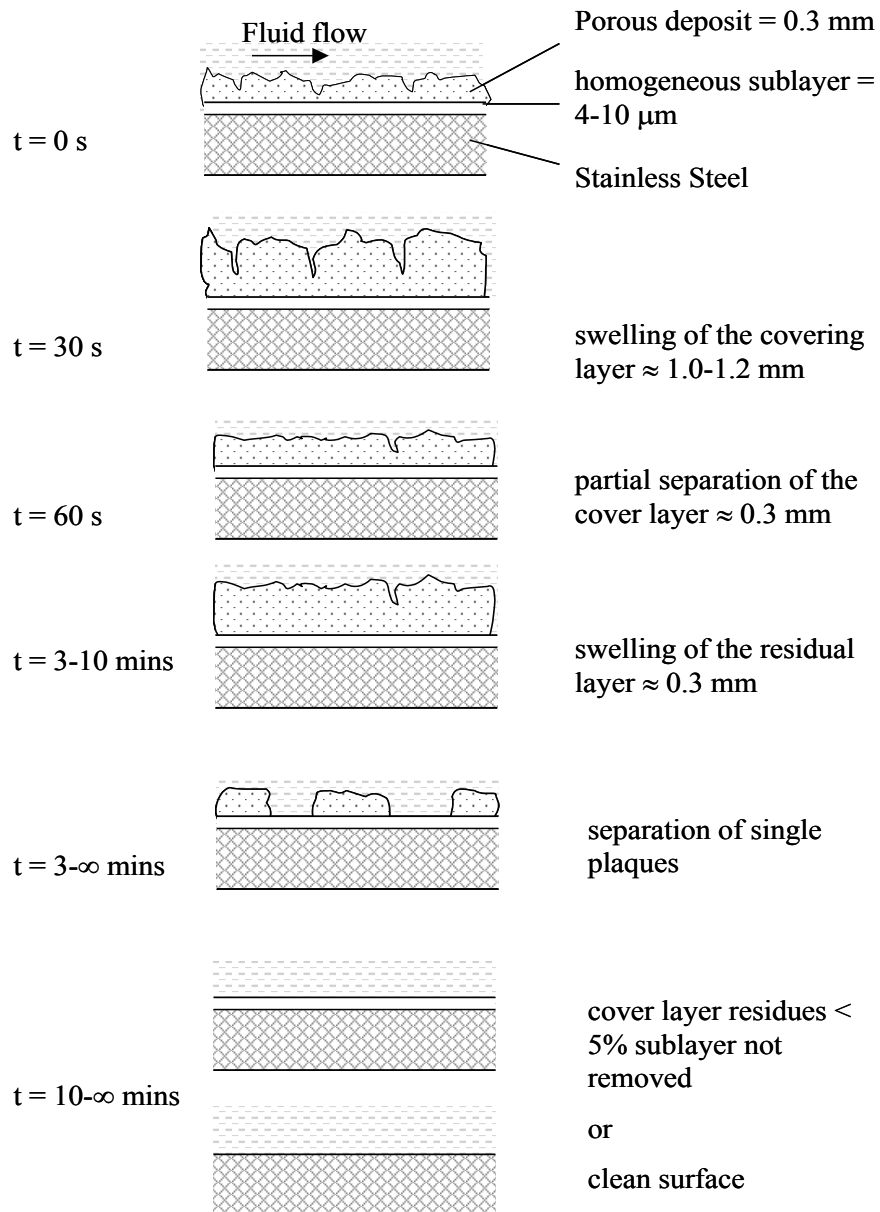


Figure 2.5: Schematic diagram of the removal of milk deposit from a solid surface using NaOH, (Graßhoff, 1997).

- (ii) Erosion: the remaining deposit attached to the metallic surface will break up and be removed in large pieces.
- (iii) Removal of mineral layer: after 10 minutes a mineral layer remained and was removed by acid cleaning.

Bird and Fryer (1991) reported that a whey protein deposit swelled after contacting with NaOH, followed by a break-up of the swollen deposit by removal of protein aggregates. After 20 minutes, only a layer of minerals remained.

Cleaning process results are usually presented in the form of cleaning rate curves (removal rate), as shown in Figure 2.6, involving three phases: (I) cleaning rate increasing and swelling of the deposit take place at the same time, (II) cleaning rate reaches its maximum, and (III) cleaning rate reduces slowly to zero, which represents the detachment of the residual deposit layer at the surface. These three distinct phases have been reported by many researchers during cleaning milk deposit (Graßhoff, 1997, Gillham et al., 2000, Tuladhar et al., 2000, Christian, 2004):

- (i) Swelling — alkali solution contacts the deposit and results in swelling, forming a high voidage-matrix-structure.
- (ii) Erosion — uniform removal of deposit by diffusion and shear stress forces. There could be a plateau region of the constant cleaning rate, which depends on the balance between swelling and removal.
- (iii) Decay — the swollen deposit strength was decreased to a level where shear controlled its removal.

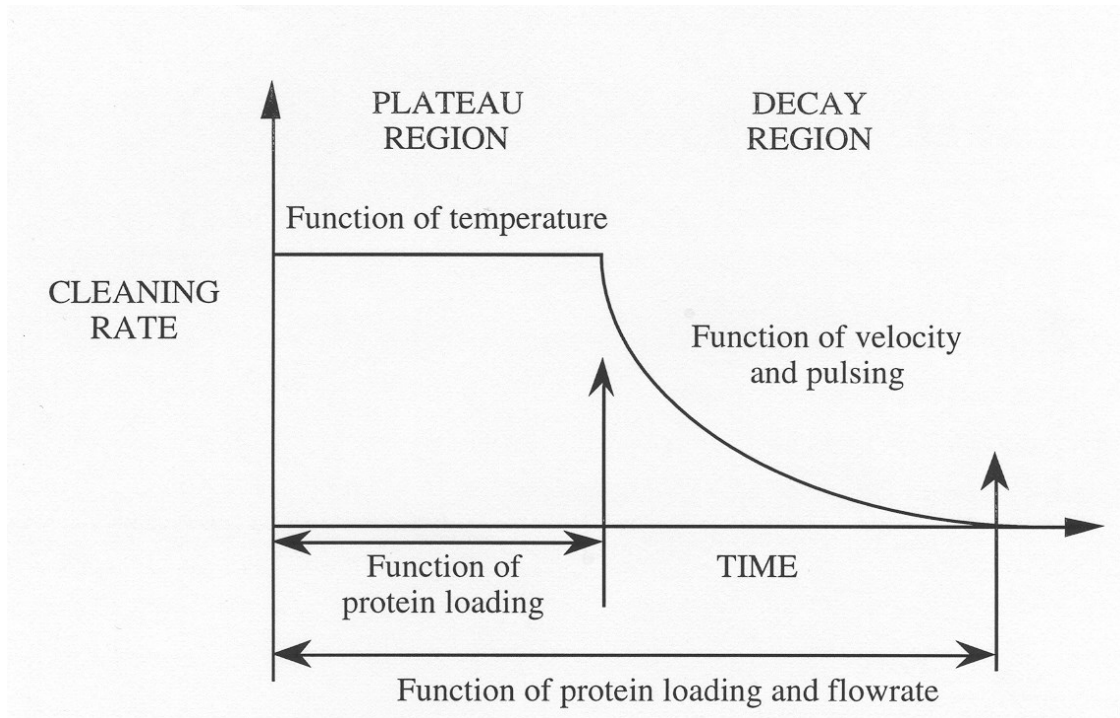


Figure 2.6: Dependency of the stages of WPC deposit removal on the cleaning process parameters (Gillham, 1997).

Changani (2000) and Christian (2004) found pressure values useful in aiding to determine the cleaning process, during cleaning of a pilot scale PHE. They observed the following steps in their studies:

- (i) An abrupt initial decrease in pressure drop (ΔP) when blockages from ports were removed
- (ii) Deposit swelling resulted in an increase in pressure drop
- (iii) Pressure drop decreased gradually to the clean value

Consequently, understanding the key steps in the cleaning mechanism is essential in order to find the right duration for every cleaning regime, formulation for the cleaning solution, and optimum cleaning process.

2.3.2 Effect of bulk parameters: temperature, chemical and flow rate

Mechanistic studies have shown that each stage shows different dependencies on operating parameters such as temperature, cleaning concentration, and flow rate (Graßhoff, 1997, Bird and Fryer, 1991). A combination of these parameters, which are interchangeable to a certain extent, must lead to effective removal of the deposits.

2.3.2.1 Fluid temperature

Temperature is a significant parameter, since increasing the temperature will affect the following:

- Increasing cleaning rate as a result of improved solubility.
- Faster diffusion and reaction altering the viscosity of the liquid.
- A thinner laminar boundary layer due to a higher Reynolds number.

Christian (2004) investigated the effect of temperature (30 to 70°C) on cleaning time. The temperature of the cleaning fluid influences the deposit removal process. Increasing the fluid temperature reduces the cleaning time. Under the conditions investigated, the swelling ratio (The maximum value of deposit resistance at swelling stage is divided by the value of deposit resistance at the beginning of the cleaning experiment) appears mainly to be controlled by the temperature: large swelling ratios are seen at the lowest temperature, even at the highest flow rate, suggesting that the deposit is insufficiently altered to allow rapid removal. The period of the decay stage significantly decreased when the deposit-liquid interface temperature exceeded 50°C. Above this temperature, little further influence on the length of the decay stage was observed. The effect of cleaning temperature is greater than that of flow; at all flow rates when the temperature was

increased from 30 to 70°C, the cleaning time decreases from more than 2000 seconds to less than 500 (Christian, 2004).

Mercadé-Prieto et al. (2008) found the diffusivity of NaOH in a protein gel layer at various temperatures (13 – 60°C). They have shown that the swelling ratio reduces with increasing temperature, while the penetration velocity of the NaOH increases. The cleaning rate during the uniform stage was most sensitive to the temperature of the deposit/solution interface (Gillham et al., 1999). However, the rate of cleaning during the decay phase has been found to be less dependent on temperature (Gillham et al., 1999, Tuladhar et al., 2002).

A number of researchers (Jennings, 1959, Gallot-Lavallee et al., 1984, Grasshoff, 1989, Fryer and Bird, 1994) have reported that the factor of cleaning rate improvement for every 10°C rise in temperature was found between 1.6-1.9 during cleaning milk deposits using sodium hydroxide solutions at temperatures of up to ca. 90°C.

Optimal temperatures have been confirmed for cleaning. Gallot-Lavallee et al. (1984) reported 65°C to be the optimum temperature for cleaning proteinaceous deposits. Hankinson and Carver (1968) stated an optimum temperature of 55°C for cleaning milk deposits by water alone, while using temperatures between 35 and 90°C. Jeurnink and Brinkman (1994) found that the optimal working temperature lies around 70°C. Too high temperature has been found to damage the apparatus (corrosion, gaskets) and lead to reactions of proteins in the deposits. This might cause the deposits to be harder to remove (Jeurnink and Brinkman, 1994).

2.3.2.2 Cleaning chemicals concentration

Cleaning is a multistage process primarily involving interaction between the cleaning components and the deposits. Cleaning begins with the deformation of the fouling by the reaction with the cleaning detergents (Graßhoff, 1997). Karlsson et al. (1998) concluded that cleaning is strongly influenced by deposit and surface characteristics together with the choice of cleaning agent.

Graßhoff (1997) reported that the driving forces are the chemistry of the cleaning agent and the physical influence of the fluid flow. For tenacious food fouling deposits, for instance milk, protein-based deposits, sodium hydroxide changes the structure of the deposit by breaking peptide bonds that helps the deposits be more soluble. Generally, hydrolysis of peptide bonds takes place actively at pH 12 to 13. Cleaning whey protein concentrate fouling layers with highly concentrated NaOH solutions markedly reduces the cleaning rate (Tuladhar et al., 2002). This phenomenon is particularly evident at pH values above 13.5 and at temperatures below 50°C. At pH > 13, the NaOH in the WPC gel is suggested to induce new intermolecular crosslinks that make the gels more alkali-resistant (Mercadé-Prieto and Chen, 2005).

Several studies have reported optimised chemical concentrations for the removal of proteinaceous deposits. Tuladhar et al. (2002) and Graßhoff (1997) found an optimum concentration of NaOH at around 0.5-1.0 wt%, whilst Bird (1992) found an optimum concentration of 0.5 wt% for sodium hydroxide, for the cleaning of proteinaceous deposits at 50°C. Fryer and Bird (1994) studied the effect of chemical concentration values of up to 2% on cleaning time. The authors found the optimum content of NaOH for cleaning to be at about 0.5%; at 2% NaOH, the cleaning rate declined. The authors thus forth suggested

that too high concentration of cleaning chemical can seal the surface and prevent deposit removal that may not be as susceptible to fluid shear.

Christian and Fryer (2006) investigated the influence of switching cleaning chemicals and water in short intervals rather than continuous application and demonstrated that the diffusion of hydroxide into the foulant and subsequent reaction played a critical role in determining the rate of cleaning.

2.3.2.3 Mechanical action

Cleaning rates are usually found to increase with increased mechanical action. The rate of cleaning under laminar flow conditions, i.e. <1.4 m/s, is not sufficient for commercial operation. As a result, flow velocities in the range of 1.5 to 2.1 m/s are generally used (SPX, 2012). However, Fryer and Bird (1994) showed that a velocity of 1.5 m/s is not necessary, as short cleaning times were found at a velocity of less than 0.6 m/s.

Mechanical action in a cleaning process is essential for removing the loosened deposits, splitting large deposit lumps into smaller ones, and preventing re-adherence of already loosened deposits (Graßhoff, 1997). The effect of fluid dynamics in removal of deposits is often described in terms of mass flow rate, Reynolds Number (Re), surface shear stress (τ) or flow velocity (v).

Graßhoff (1997) illustrated that the shear caused by fluid flow is much less than that caused by physical force. Shear forces produced by physical force for cleaning milk deposit are likely to reach more than 1250 N/m^2 , whereas the fluid flows through the plate heat exchanger only give shear forces up to 50 N/m^2 . To remove the particle or pieces of the deposit, fluid shear forces should be more than adhesion and cohesive forces of the deposit (Graßhoff, 1997). During cleaning, these deposit forces are weakened because of the effect of the cleaning chemical.

Flow pulsing is a technique for improving the cleaning rate through increasing shear rate and wall shear stress. Here it is not necessary for the maximum flow velocity to take place in the centre of the pipe. Gillham et al. (2000) stated that flow pulsing had the greatest influence on the uniform and decay stage. Cleaning rate behaviour in the uniform stage was more susceptible to pulse amplitude than pulsing frequency. The removal time per unit of protein coverage for steady flow at $Re = 9120$ is less than for pulsed flow cleaning at $Re = 1500$. Bode et al. (2007) indicated that when the amplitude of the flow pulse was larger or equal to the steady flow velocity, the cleaning time is reduced during removal of WPC deposit, from approximately 25 to 10 minutes. This change was attributed to the effect of temporary flow reversal.

Jennings et al. (1957) suggested that the existence of a threshold Re of 25,000 for cleaning a pipe surface of dry milk deposit before an increase in Re resulted in an increased cleaning rate. Gillham et al. (1999) investigated the removal of WPC deposit by 0.5 wt% NaOH and found that the removal time varied significantly even at low Re ($500 \leq Re \leq 2000$) and was much less sensitive to Re at higher values of up to 5000.

Timperley and Smeulders (1987) concluded that the removal time of a deposit in a PHE decreased with an increasing flow velocity, with the greatest reduction occurring upon increasing the flow velocity from 0.2 to 0.5 m/s. Christian (2004) and Tuladhar et al. (2002) concluded that an increase in Re was only beneficial to cleaning time at low temperature and concentration.

2.4 Monitoring of fouling and cleaning

The success of food and beverage manufacture relies fundamentally on producing products with reliable quality and consumer safety. Poor hygiene can be a result of fouling

layers building up in a plant. Thus, ensuring good cleaning performance is vital in maintaining plant hygiene and product quality. Fouling layers on process surfaces also increase the cost of production by increasing the energy load required to heat the surface and pump material. CIP measurement and control are fundamental for ensuring hygiene and efficiency on a daily basis. Processes used to establish and run CIP operations include (Goode, 2012):

- (i) *Validation* – determining the right method of cleaning and setting it as a standard; it is done before implementation of a new method and after alterations in an existing operation and should always be up to date.
- (ii) *Verification* – are the results correct and accepted? Checks the system behaves in the predetermined and expected way; after validation.
- (iii) *Monitoring* – continuous monitoring of specific points of a process determining if the process is under control; after verification.

Finding a monitoring tool which could display the onset and build-up of fouling would be useful to determine the right time to stop the production process and begin the cleaning operations. This monitoring information will improve the plant efficiency in terms of energy saving, minimising product losses, and maximising process efficiency.

Monitoring fouling and cleaning can provide valuable indications for making operational decisions in the food industry. Being invisible from outside the industrial processing equipment, fouling can only be determined by techniques such as measuring heat transfers or pressure drops, which may not be sufficiently significant, especially in the case of small local deposits, to allow making an operational decision. Therefore, an optimal monitoring method should have the potential to measure the extent of deposit formation and indicate

its location accurately. Using the same monitoring tool to monitor the cleaning process would be highly beneficial to display when the fouling film had been completely removed. In the industry, this information must be obtained online, *in situ*, non-destructively, and in real time reproducibly and automatically.

Some of the essential criteria for any good monitoring process are listed as follows (Withers, 1996, Pereira et al., 2006):

- The sensor should be non-invasive.
- It should be accurate for detecting the build-up of deposits.
- It must have the potential of online application.
- Being a portable sensor is required in order to be used at different sites throughout the plant.
- Sufficient robustness is also necessary to withstand the different industrial plant conditions involved in the process plant.
- The hygienic design of a sensor is considerably important to avoid the microbiological growth.
- Easy to use by non-specialists.

Typically, a mixture of online and offline CIP tools is used for monitoring and verification. Offline techniques tend to be used to verify the process, for example, routine titration of cleaning chemicals and microbial enumeration of rinse waters, whereas online techniques are used to monitor the process to ensure they remain within pre-determined set points, for example, temperature, conductivity and flow rate of CIP fluids.

2.4.1 Monitoring tools indicating surface fouling and cleaning

2.4.1.1 Pressure drop

Building up of fouling films during the processing of many liquid food products causes two direct effects on the liquid flow:

- (i) It increases the roughness of the surface in contact with the liquid.
- (ii) It reduces the mean square area in a flow channel.

These effects can be identified by measuring the pressure drop of the liquid through the PHE, as these effects lead to pressure drop at a constant flow rate.

Measurement of pressure drop (ΔP) across a system has been used to indicate fouling and cleaning. ΔP is defined as: $\Delta P = P_1 - P_0$ where P_1 and P_0 are inlet and outlet pressures. ΔP increases during fouling and decreases during cleaning generally. During cleaning of a plate heat exchanger (PHE), Fryer et al. (2006) illustrated an initial increase in pressure drop due to deposit swelling in contact with the cleaning fluid. Further rinsing decreased the pressure drop as the deposit was removed. This effect has been well characterised in pulsed-flow cleaning by Christian and Fryer (2006) and Gillham et al. (2000). Robbins et al. (1999) and Changani (2000) also used pressure drop across a PHE to characterise the fouling of milk and whey protein fouling. As the PHE running time increased, the pressure drop also increased in the UHT section, indicating fouling.

The advantage of this monitoring tool is to avoid excessive pressure and, therefore, heat exchanger damage. The disadvantages of the method are that they are usually not sensitive enough to detect the onset of fouling and that the place of fouling remains unidentified (Wallhäußer et al., 2012).

2.4.1.2 Temperature and heat transfer

The build-up of a deposit on a surface introduces an additional resistance to heat transfer, with product temperature dropping through the heat exchanger, which can be assessed if the heat flux and wall and fluid temperatures are known. The heating media temperature may be increased in order to fix the product outlet temperature.

Heat transfer coefficient (U) in a PHE is defined as: $U = \frac{\dot{Q}}{A\Delta T_{LM}}$, where \dot{Q} is the rate of

heat transfer between the hot and cold fluids, A is the area of the heat transfer surface, and ΔT_{LM} is the log-mean temperature difference calculated from the inlet and outlet temperatures. Robbins et al. (1999) measured U in a PHE during milk and whey protein heating. As the operational time increased, U decreased in the UHT section, indicating

fouling. Fickak et al. (2011) related $U \approx \frac{\dot{Q}}{A(T_s - T_b)}$, where \dot{Q} is the power input, A is the

area of the heat transfer surface, T_s is the surface temperature, and T_b is the bulk fluid temperature. They used U to indicate the fouling and cleaning of different concentrations of whey protein gel on a heated rod. 2, 4 and 6 wt.% whey protein were seen to foul similarly but clean differently.

2.4.1.3 Heat flux sensor

Micro-foil heat flux sensors (MHFS) have been used previously to monitor the change in heat transfer coefficient (HTC) during fouling (Zelver et al., 1985, Christian, 2004, Aziz, 2008). During cleaning, as the insulating deposit layer is removed, the heat transfer across the surface increases. MHFS has been used to monitor the change in HTC during cleaning of whey protein fouled pipes (Gillham et al., 2000); data obtained from the MHFS was

compared to the protein removal rate. It was found that heat recovery did not occur in the same way as mass removal during cleaning. Christian (2004) and Aziz (2008) have reported that MHFS can detect the removal of an insulating layer from a surface, however, the exact end-point and, therefore, the time to clean are difficult to determine. The thermal resistance of deposits and their effective thermal conductivity was measured *in situ* using a novel technique based on a heat flux sensor by Davies et al. (1997).

Tuladhar et al. (2002) used dynamic gauging for thickness measurements in association with heat flux sensors to monitor the process of swelling and removal of thin, soft, fouling films of whey protein by alkaline CIP *in situ*, in real time. Both sensors were capable of exhibiting the three cleaning stages.

The disadvantage of using heat flux is that it is not sensitive enough to detect the thin layer of a milk deposition of less than 0.1 or 0.2 mm (Truong et al., 2002).

Goode et al. (2010) used a heat flux sensor to determine U during the cleaning of yeast from a non-heated surface. Truong et al. (2002) positioned a heat flux sensor at the outlet of a direct steam injection heater in a milk plant to monitor U during fouling of the non-heated surface. U can be used to determine a deposit (or fouling) resistance. (R_f) is defined as: $R_f = \frac{1}{U_o} - \frac{1}{U_t}$, where U_o is at a clean system and U_t is at a given time. As cleaning time increases, R_f decreases.

2.4.1.4 Ultrasound and vibrational methods

Acoustic parameters alter as fouling takes place and can be measured by the following common techniques:

- Transmission utilises one transducer a transmitter and a second as a receiver.
- Pulse echo uses one transducer to do both the pulsing and the receiving.

Merheb et al. (2007) used normal-beam ultrasonic through-transmission to monitor the evolution of the acoustic power and the delay of the acoustic waves in PHE during fouling and cleaning, comparing them to pressure drop and the mass of wet weight of the deposit in each plate. The results show that power and delay decreased strongly with fouling, depending on the mass of wet deposits in each section.

The formation and removal of three types of deposit: calcium phosphate solution, calcium phosphate with whey protein, and whey protein alone were monitored by mechatronic surface sensor (MSS) for validation by Pereira et al. (2006). The MSS consisted of an actuator (piezoelectric ceramic) and an acceleration sensor attached to the stainless steel plate, (on the face, which is not in contact with the liquid flowing inside the duct). The actuation element makes the stainless steel vibrate. This vibration is then captured by the sensor. The MSS was capable of monitoring the build-up and cleaning the deposit accurately. The damping factor varied with elasticity of the fouling layer, making it possible to differentiate between different layers. Since whey protein has a more elastic structure than the calcium phosphate layer, it presented a higher damping factor. These findings were confirmed by Pereira et al. (2008) when they used organic/inorganic deposit and attached/sedimented deposits.

In addition, an MSS was also used to detect the end cleaning point of hair shampoo removal on a stainless steel plate by Pereira et al. (2009). Different cleaning conditions were used with increasing cleaning temperatures from 31 to 51°C and flow velocities from 0.14 to 0.47 m/s. The validation of MSS to monitor the cleaning end point was assessed by visual inspection, spectrophotometry, and contact angle measurements. The MSS detected the cleaning end-point correctly with different cleaning conditions, resulting in different cleaning rates.

2.4.1.5 Electrical resistance measurement

Chen et al. (2004) developed an online monitor to determine the extent of fouling and cleaning on a surface using electrical resistance measurements. Two electrodes within the test section measure the electrical resistance of the fouling built up and cleaning process between the electrodes. The fouling experiment was carried out at a bulk temperature of 62°C and three different surface temperatures of 88, 98 and 115°C. At the beginning of the fouling runs, an induction period was observed and was shortened when the surface temperature increased. For the cleaning experiment, an initial dramatic drop in the electrical resistance was observed once the cleaning solution contacted the fouling deposit formed at the surface temperature at 96°C, due to the fact that NaOH solution is a strong conductive medium (see Figure 2.7). This drop in the electrical resistance for deposit formed at a surface temperature of 115°C was not very abrupt compared to that formed at a surface temperature of 96°C, as a more porous layer was generated at a lower temperature (96°C).

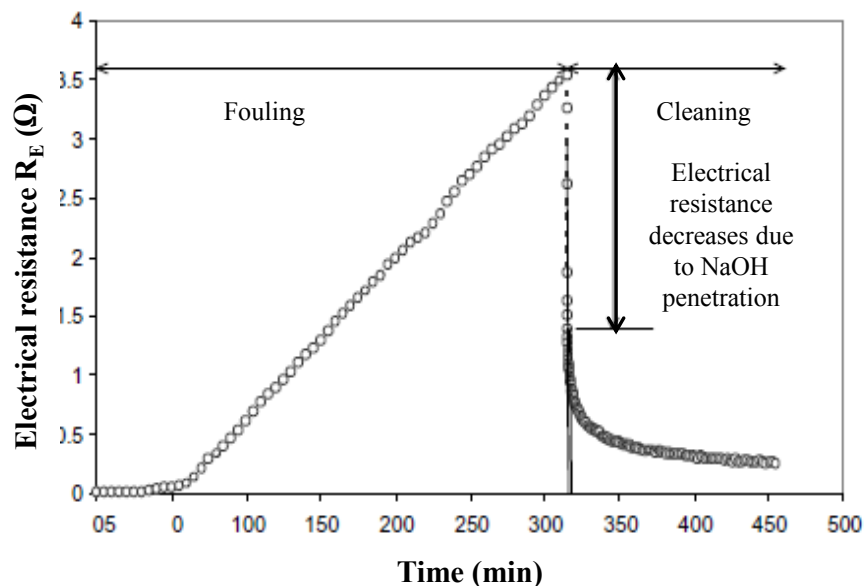


Figure 2.7: Change in electrical resistance with time during fouling and cleaning process (Chen et al., 2004)

Electrical monitors are highly sensitive to detect the thin layers as well as the fouling thickness. A disadvantage is the invasive implementation of the electrodes (Wallhäußer et al., 2012).

2.4.1.6 Proximity gauging technique

Tuladhar et al. (2000) developed a proximity gauging system using a siphon technique for measuring various thicknesses (0 to 1000 μm) of butter, sticky foam and whey protein deposit. The gauge had an accuracy of $\pm 20 \mu\text{m}$ for a deposit thickness of 500 to 1000 μm . Fouling/cleaning experiments established that the proximity gauging technique has a significant potential to detect the onset of fouling layer and the cleaning end point, particularly when combined with other techniques. The limitation of using this gauge is the possible damage or distortion of the deposits being studied.

Tuladhar et al. (2002) also used dynamic gauging to study swelling and removal of whey protein deposit. It was able to detect the removal of the deposit with an accuracy of 10 μm .

2.4.2 Monitoring tools indicating fluid cleanliness

Conductivity can be used to indicate product-water interfaces in nonchemical cleaning. Fickak et al. (2011) measured conductivity during water rinsing of a heated rod fouling with HIWPG (heat-induced whey protein gel). The conductivity was seen to increase from 380 to 1200 $\mu\text{S}/\text{cm}$ in the first 100 to 200 s and decrease thereafter to 200 $\mu\text{S}/\text{cm}$ in around 1000 s. The decrease in conductivity was a smooth slope. Van Asselt et al. (2002) also measured conductivity during cleaning of a dairy evaporator with chemicals. An increase in conductivity during chemical phases and a decrease during water phases was

seen. Conductivity was only observed when the phase was changed from water to alkali in the cleaning procedure.

A technique based on the amount of light scattered by particles in the cleaning solution - called a turbidity meter - was used by Fickak et al. (2011) at the outlet of the fouled rod during water rinsing. The fouled rod was rinsed until 0.5–1 NTU (Nephelometric Turbidity Units) was reached, whereby indicating drinking water quality. The turbidity increased to approximately 28 NTU in the first 200 s and decreased thereafter. At 1200 s, however, the turbidity value increased from 3 to 7 NTU before decreasing further. The turbidity profile contained numerous jagged peaks. Turbidity measurement may be more sensitive than conductivity measurement. Van Asselt et al. (2002) measured online and offline turbidity during cleaning of a dairy evaporator revealing different profiles. For example, online turbidity revealed peaks, whereas offline turbidity revealed no peaks. The application of an on-line turbidity sensor resulted in a more sensitive measurement than the current off-line version, as the sensor is monitoring in real-time. Cole et al. (2010) used a turbidity meter to monitor the cleaning of tooth-paste over time. Two peaks were observed: the first peak occurred due to core removal, and the second peak occurred due to film removal (Figure 2.8). The pipe was termed cleaned when the turbidity reading reached 4 ppm, which corresponded to less than 0.2% deposit by weight. A disadvantage of the turbidity sensor is its sensitivity to foam, which influences the values of the measurements, as stated by Van Asselt et al. (2002). They also measured calcium ion concentration online and offline during cleaning of a dairy evaporator. The online calcium -sensor was less sensitive than the offline method, as no calcium was measured during the cleaning phase when the pH-level was above 8, although enough calcium was available.

Moreover, the online calcium sensor cannot yet be applied in dairy processing due to restrictions of pH and robustness.

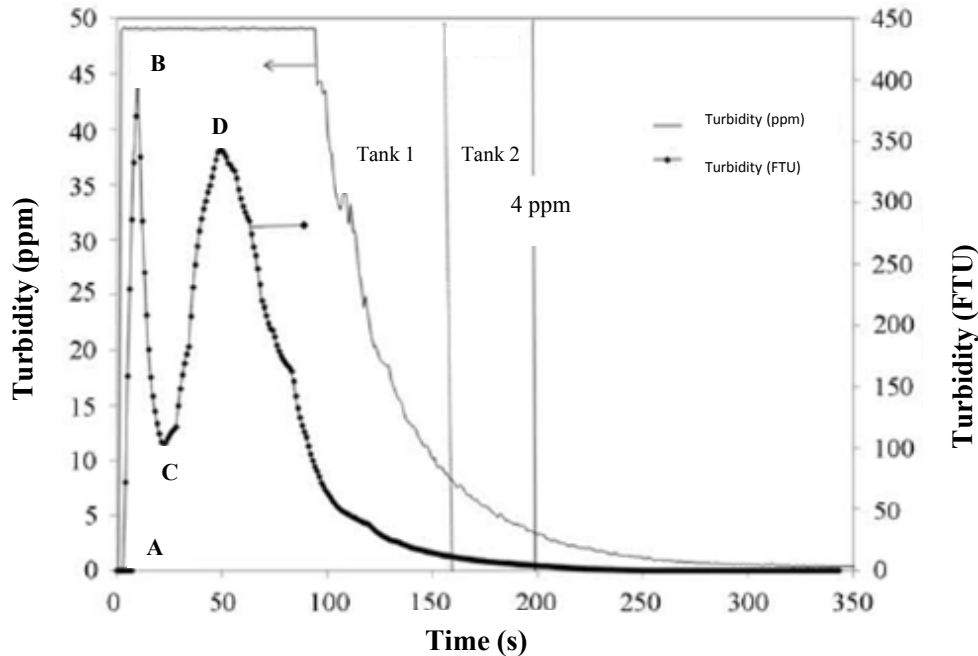


Figure 2.8: Turbidity profiles of cleaning toothpaste using two turbidity devices at different units: turbidity (FTU) and turbidity (ppm) (Cole et al., 2010).

Du et al. (2010) demonstrated a new method for offline measurement of a number of particles in the nano-size range in different suspensions. They found that the suspension concentration and the particle size effect of the accuracy of the counting process of particle number can be controlled by reduced sample concentration. Malvern Instruments (Malvern, UK) have commercially available technologies that could be used to monitor particle sizes and counts online during CIP.

Martin et al. (2013) used spectroscopic measurements and turbidity to detect the end-point for cleaning toothpaste. This study concludes that the online spectral measurement can be used only to discriminate between soils, while the turbidity probe was capable of indicating a cleaning end-point.

Winqvist et al. (2005) described the use of a voltammetric ‘electronic tongue’ integrated into a dairy process line. The measurement technique consists of a series of electrodes implanted in a surface. A measurement series is based on successive voltage pulses of gradually changing amplitude between the base potential applied and the current continuously measured. A difference in current was observed between the process stream, water, alkali, and acid, although the investigation back to the clean state was not presented. The authors concluded that the ‘dirtiness’ of the solutions could be distinguished by the tongue.

Table 2.2 gives an overview about various monitoring methods to detect the progress of fouling and cleaning processes. Depending on a single method to detect the fouling and cleaning processes seems not to be practical. Therefore, combination of various methods can be more advantageous to enhance both detection stability and the probability to determine the exact place of fouling, as well as an overall value (fouling presence and absence). Accordingly, in chapter 6, two novel monitoring devices have been developed to evaluate the cleaning process: a particle count technique and Peltier device. The particle count technique was used to evaluate the fluid cleanliness, while the Peltier device was used to evaluate the surface cleaning (local monitor).

| Monitoring Methods | Advantages | Disadvantages |
|--|---|--|
| Pressure drop | - Usually measured - Caution of excessive | - Not very sensitive - Fouling place unknown |
| Temperature | Usually measured | -Not very sensitive -Thin layers not monitored -Fouling place unknown |
| Heat transfer coefficient method | Flow/temperature usually measured | - Not very sensitive - Fouling place unknown |
| Micro-foil heat flux sensors (MHFS) | -Local monitor - High ability to follow the progress of cleaning process | - difficulty in defining the cleaning end-point |
| Ultrasound and vibrational measurement | -Local monitor -Non-invasive -Very sensitive to material changes | -Very sensitive to temperature -Highly sensitive to bubbles of air or vapour in the fluid - Scattering can occur |
| Electrical resistance | -Very sensitive to thin layers -Fouling thickness Determinable | -Invasive -Distortion of the deposit due to contact Inapplicable for non-conducting materials |
| Proximity gauging | -Local monitor - Very sensitive to material Changes. | -Distortion of soft deposits can happen which may affect the removal time. |
| Conductivity | Discriminating between phases (water-alkali) | Not sensitive to follow the progress of cleaning process in the last stage |
| Turbidity | Very sensitive to follow the development of cleaning process | - The sensitivity is affected by the measuring of foam -The exact cleaning end-point is difficult to determine |
| spectroscopic measurements | Discriminating between soil | Not sensitive to follow the progress of cleaning process |
| electronic tongue | High ability to distinguish the degree of 'dirtiness' | -Non-hygienic - less ability to follow the cleaning process |

Table 2.2: Comparison of different detection methods together with their advantages and disadvantages.

2.5 Conclusions

In the dairy industry, an undesirable deposit, mainly consisting of proteins and minerals, is formed on the heating surface. The impact of this deposit in the dairy plants is an issue of primary concern. The frequent interruptions due to fouling lead to significant periods of

equipment downtime and reduced process efficiency. Cleaning the foulants is also uneconomic in terms of water, energy and chemicals used. Determining the right time to end the fouling/cleaning process is crucial information that could be used to improve the efficiency of the whole process.

A number of authors have extensively investigated the phenomena of fouling with a particular regard to the dairy industry. As discussed in section 2.2.2.2, the exact fouling mechanisms and underlying chemistry are still not well understood. However, there is general agreement that the deposition is a result of a number of stages. In the first stage, protein molecules are denatured and aggregated in the bulk. Then, the aggregated proteins are transported to the heat-transfer surface. Therefore, surface chemical reactions take place and, as a result, the proteins are incorporated into the deposit layer. The formed deposit layer is exposed to fluid shear stress forces; consequently, there is possible re-entrainment or removal of the deposits.

The literature on cleaning is not as extensive as that on fouling. However, several studies have been conducted on the cleaning process. In food industry, most cleaning studies have been concerned with milk and milk products, due to both the high consumption of the product throughout the world and the high adhesive/cohesive strength of the fouling produced. It is necessary to understand how deposit is removed from the heat transfer surface and the controlling processes involved, since it can help in optimising the overall cleaning process.

During the last decade, different fouling and cleaning monitoring has been assessed in order to optimise production cycles, increase the product quality, and reduce environmental load. Not many monitoring devices can be said to be feasible for current industrial applications. Some are not sensitive enough to detect the first attached layers,

such as pressure drop measurements; others can be too expensive or technically difficult to be implemented in the industrial processes and be operated by non-specialists. For this reason, there is a need for smart monitoring devices and optimised cleaning procedures accordingly.

CHAPTER 3: MATERIALS AND METHODS

3.1 Introduction and aims

This chapter describes the materials and equipment used to study the effect of process parameters on build-up of fouling and monitoring the removal of deposits in order to improve cleaning monitoring.

The main equipment used in this work:

- (i) A pilot scale plate heat exchanger (PHE).
- (ii) Fouling rig.
- (iii) Monitoring techniques such as turbidity and particles count.
- (iv) Cleaning rig involving Peltier device.

The pilot scale PHE was used to:

- (i) Study fouling and cleaning behaviour.
- (ii) Monitor the cleaning process.
- (iii) Pre-heat the WPC and WPCm before the fouling rig.
- (iv) The following sections describe the fouling, cleaning and monitoring processes in detail.

3.2 Processing and cleaning fluid

Soft water was used throughout this work to thermo-hydraulically stabilise the PHE before carrying out fouling or cleaning experiments. A two-stage cleaning regime was applied in the PHE: firstly, sodium hydroxide (NaOH) was used to remove proteinaceous

deposit; secondly, P3-horolith V based on nitric acid was applied to remove mineral deposit. Four different types of material have been investigated with respect to their fouling or cleaning behaviour: WPC, WPC with minerals, tooth-paste, and golden syrup.

3.2.1 Soft water

Soft water was used to establish datum thermo-hydraulic conditions in the PHE. Soft water was also used to dissolve the whey protein concentrate (WPC) powder and cleaning solution used for the desired concentration. Water softening methods mainly rely on the removal of calcium and magnesium from water, which tend to precipitate out as adherent solids on the surfaces of pipes, especially on the hot heat exchanger surfaces.

The softener contains resin beads which hold sodium ions. When hard water passes through the beads inside the softener, the beads attract and hold the calcium and magnesium ions in exchange for sodium. After this ion exchange process, the water leaving the softener is soft. Once the resin bed is loaded with calcium and magnesium ions, it must be cleansed (or regenerated) so that it can continue to soften water. The salt in storage tank mixes with water to wash the resin beads. The brine solution loosens the hardness minerals which have built up on the resin beads; then the system backwashes and flushes the hardness minerals away. By using soft water instead of tap water, it was ensured that only negligible amounts of minerals or organic material were added to the system under test; thus, fouling from these materials from the water was negligible. The softener was purchased from GM Autoflow, connected directly to the mains, and operated up to 1.4m³/h at a pressure of 600 kPa. The hardness level of the water was checked regularly every two weeks by using water hardness test kit.

3.2.2 Whey protein concentrate (WPC35)

Whey protein concentrate powder was provided by Carberry Milk Products, Ireland, and contained 35 wt.% proteins (19.8% β -lactoglobulin (β -Lg)), and 2.6% α -lactalbumin (α -La). The mineral content in the original powder was less than 5% of total dry weight. The powder used was WPC35, which was named because it nominally contained 35 wt.% in protein. Whey protein concentrate (WPC) powder is produced by separation of whey protein from fresh liquid cheese, whey, and is widely available at a low cost. As a result of this manufacturing process fat, and casein (and associated minerals) are removed from the raw milk after pasteurisation, leaving lactose, whey proteins and serum Ca and P in solution.

3.2.3 WPC with minerals supplement (WPC_m)

As mentioned above, a considerable amount of minerals has been removed during the production of WPC; the extent of this loss is dependent on the processes involved and also the degree of concentration of the product. Since the majority of milk fouling occurred at pasteurisation temperature, it becomes essential to add minerals to whey protein concentrate to simulate milk fouling (Christian et al., 2002).

3.2.4 Cleaning chemicals

The chemicals used in experiments presented in this work were two-stage cleaning solutions: sodium hydroxide 30 wt.% aqueous solution to clean the proteinaceous deposit supplied by VWRI, and P3-horolith V based on nitric acid to remove mineral deposit supplied by Ecolab Ltd. P3-horolith V comprised 30-50% nitric acid and 2-5% phosphoric acid.

Cleaning solution (NaOH) was prepared by diluting the original cleaning liquid with soft water. The following formula was used to prepare the cleaning solution:

$$\text{Volume of cleaning solution (l)} \quad x = \frac{C(\text{wt.}\%) \times z}{\rho(30\% - C(\text{wt.}\%))} \quad \text{Equation 3.1}$$

Where C (wt.%) is the desired concentration of the cleaning solution (NaOH) used, ρ is the density of the original cleaning liquid (kg/m^3), and z is the mass of soft water used for dilution (kg).

3.2.5 Toothpaste and golden syrup deposits

Two types of model deposit were used to validate the Peltier device: toothpaste and golden syrup. The toothpaste used was supplied by GSK (Brentford, UK), while Golden syrup was bought from an Aldi supermarket. The reason behind this selection is to observe the sensitivity of Peltier device to the different cleaning behaviour of deposit that has different rheological properties (see section 6.3).

Experimental equipment

3.3 Plate heat exchanger

Instrumental PHE was used throughout this work, with a schematic of this being shown in Figure 3.1. The PHE was a TR10 model designed by APV Baker Ltd., Derby, and constructed at AEA Technology, Harwell. It has previously been used by Schreier (1995) and Changani (2000) to study the fouling of WPC solution at UHT temperature, and described in detail.

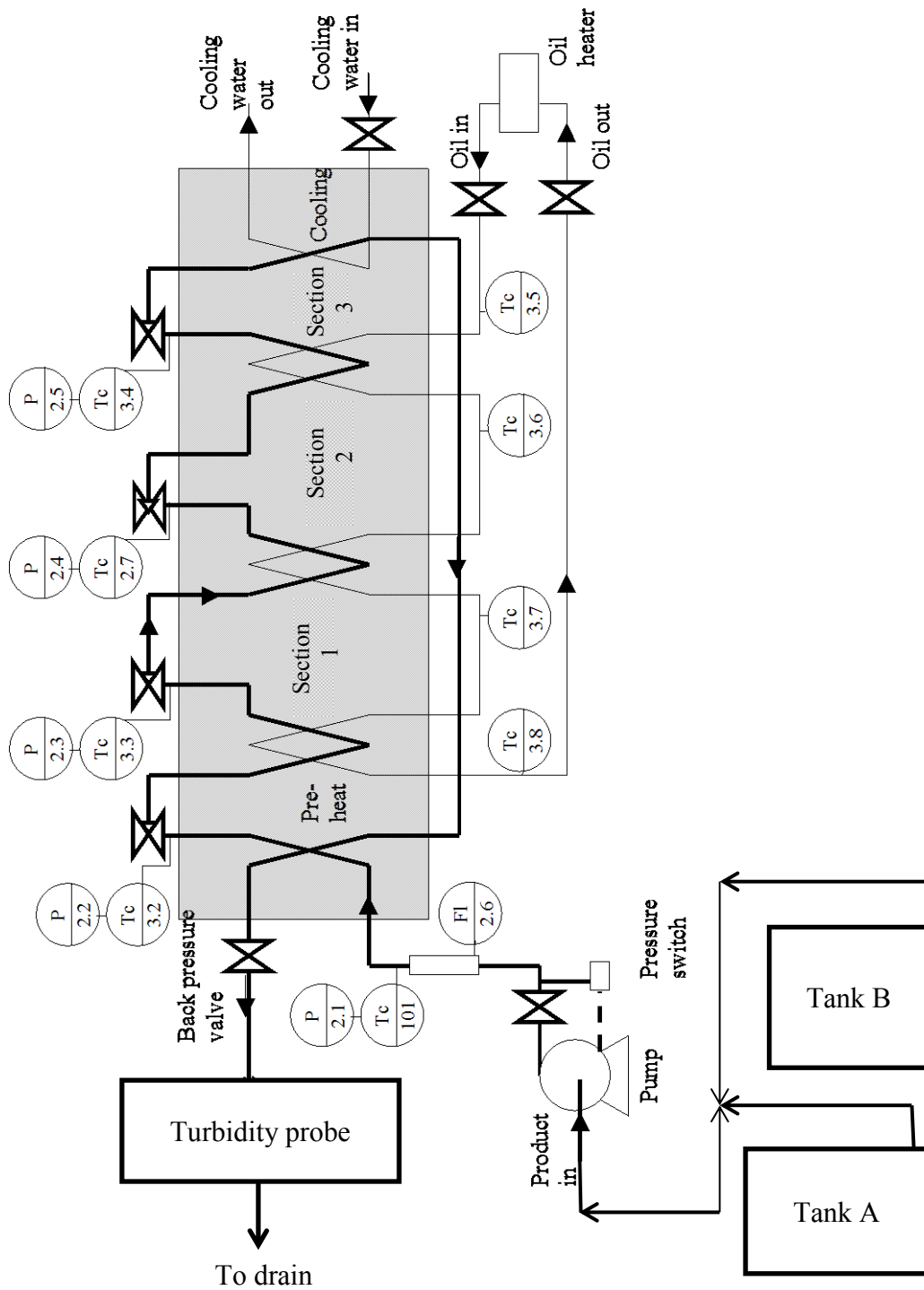


Figure 3.1: Schematic diagram of the plate heat exchanger used in the whey protein fouling and cleaning. Letters P, Tc and FI denote pressure sensor, thermocouples and the flow meter respectively (Christian, 2004).

The PHE was divided into five sections: the pre-heat section, sections 1, 2 and 3, followed by the cooling section. These sections were separated by an end-plate and they were connected to one another by ½" BSP stainless steel pipes.

Each plate had a troughed chevron design to induce a high degree of turbulence, thus maximising heat transfer. The plates were 0.6 mm thick and made from AISI 316 stainless steel and the plate separation was approximately 2 mm. The plates and ports connecting the pipes were sealed using peroxide cured paraclip gaskets.

The PHE was capable of processing 210 l/h of fluid at temperatures of up to 180°C. The maximum allowable operating pressure was 750 kPa, with PHE being shut down by an automatic safety system once pressure reached 750 kPa.

Figure 3.1 shows the overall layout of the equipment used in the operation of the PHE, which included:

- A positive displacement pump, Mono Pump, (Type PLF20211R5/s, supplied by Mono Pumps Ltd., Manchester), with a variable speed electronic drive that allows accurate flow control.
- A backpressure regulator valve (supplied by APV Baker Ltd., Derby) located at the product outlet to adjust the system pressure and prevent nucleate boiling, which promotes fouling for temperature greater than 100°C.
- Over-pressurisation of the PHE was prevented by the installation of a pressure switch, which was just downstream of the pump and set to 750 kPa. If the switch was tripped, then power to the pump controller was cut.
- An 18 kW oil heater (model 18-20), supplied by Conair Churchill Ltd., Uxbridge, was used to provide the heating to the PHE. The oil pump was designed to deliver

the oil at up to 200°C, 400 kPa and 5 l/min. The oil used was Thermia Oil B, supplied by Shell U.K. Ltd., Manchester.

- Two large open plastic tanks (400 and 200 L) were used to contain the fluids required for the fouling and cleaning experiments. The tanks were connected to the feed pump of the PHE, via a 3-way diverter valve (Capper, Birmingham), with a reinforced hose of 1½" in diameter. Tank A had an approximate capacity of 400 litres and was used to hold the soft water used for the thermal stabilising of the system. Tank B had a capacity of approximately 200 litres and was used to hold WPC solution or cleaning chemicals.

It was possible to monitor temperatures and pressures at the inlet/outlet of each section as well as the flow rate of process and heating fluids:

- K-type thermocouples (RS Components Ltd.) were put inside the pipes connecting each section rather than on the surface of the pipe.
- Pressure transducers manufactured by Keller AG, Germany, were welded into the connecting pipes so that they were directly in the flow path.
- A non-intrusive electromagnetic flow meter on the product side, supplied by Krohne Measurement and Control Ltd., Wellingborough (model number IFC080), was connected in-line. An oil side flow meter was supplied by Universal Flow Monitors, Inc., USA.

All of the monitoring devices were connecting to the data acquisition unit and assembly by Bioscience Workshop, University of Birmingham.

All plant sensors gave outputs in the form of a 4-20 mA signal, a standard format used in the industry for the transmission of plant data over a distance. The data acquisition read the 4-20 mA signals and converted them to engineering unit outputs (Figure 3.2).

These sensors were capable of monitoring the extent of fouling and cleaning across each section of the PHE separately and as a whole, through the change in pressure drop and heat transfer coefficient in terms of area (UA).

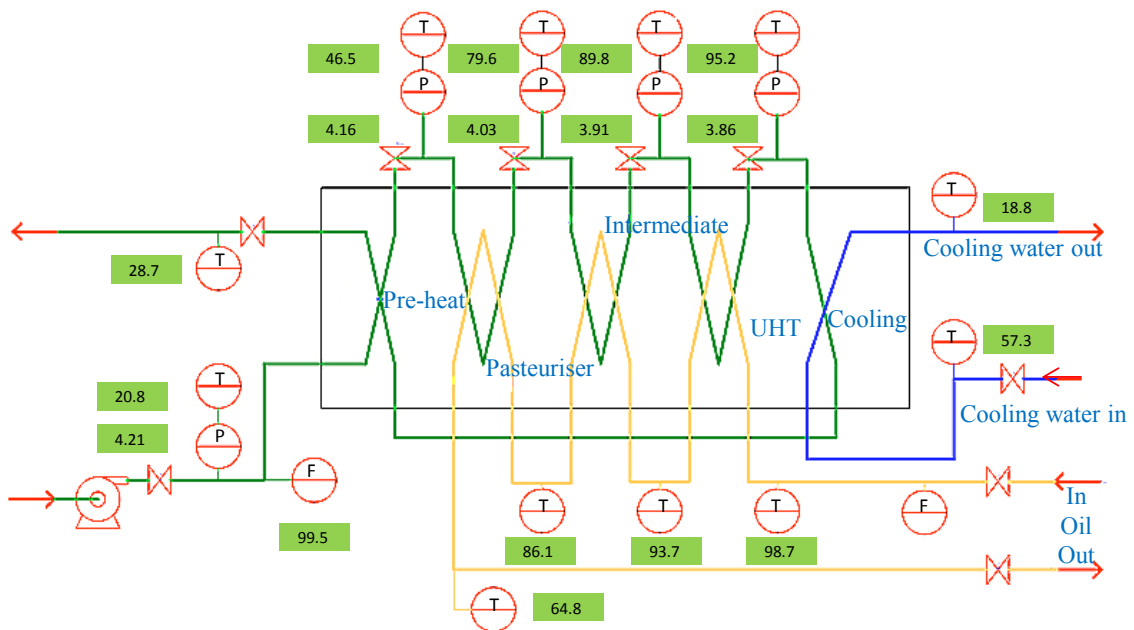


Figure 3.2: The window viewer displayed on the PHE data logging P.C throughout the fouling and cleaning experiments. Letters F, P, and T denote flow meter, pressure and thermocouples.

3.4 The bench-scale fouling rig

A schematic of the bench scale fouling rig is shown in Figure 3.3. The rig consists of two tanks: (i) a 70 l capacity for WPC solution or the alkaline cleaning solution and (ii) 70 l capacity for soft water used to establish thermal equilibrium. The tanks were connected to

the rig by three-way valves and interconnecting silicone tubing, enabling easy substitution of differently sized tanks. The 1.5 kW centrifugal (SolidC-1, Alfa Laval, Denmark), flow transmitter (TE67A3, Alfa Laval, Denmark), conductivity meter (LMIT08, Ecolab, Germany), and temperature probes (LMIT08, Ecolab, Germany) were connected by 1” stainless steel tubing. The stainless steel tank used to heat the product was constructed by engineers at the School of Chemical Engineering, University of Birmingham (size: 800 mm h; 560 mm D). The tank was fitted with three 3 kW heating elements (RS Components, Corby) and a stainless steel coil (16.5 m L; 10 mm D; 1 mm wall thickness) immersed in the tank for product to flow through. The tank was filled with water, which was stirred (RW20, IKA Labortechnik, Germany) and heated to the desired temperature using a controller (808, Eurotherm, Rugby). The heated tank was connected to the rig by flexible silicone tubing. The fouling rig is of a modular design for ease of construction, maintenance and maximum operational flexibility. Each probe and manual valve is connected to the surrounding pipe work by clamp ferrules and tri-clamps. The manual valves were positioned either side of the test piece, the by-pass and at the outlet to allow isolation of individual rig sections and to divert flow accordingly. There are two key modes of operation:

- (i) Single pass through the test section.
- (ii) Circulation through the test section back to the product/chemical tank.

In these experiments, a single pass through the test section was selected to ensure the same percentage of denatured protein entered the test section. Therefore, the fouling rig was connected to the cooling section outlet port of the PHE to be able to monitor the pressure drop in section 3 during the fouling experiment. Reinforced silicone tubing,

secured with hose clips, was used to connect these two sections and to allow processed WPC solution to pass through the test section before sending the fluid to the drain as seen in Figure 3.4.

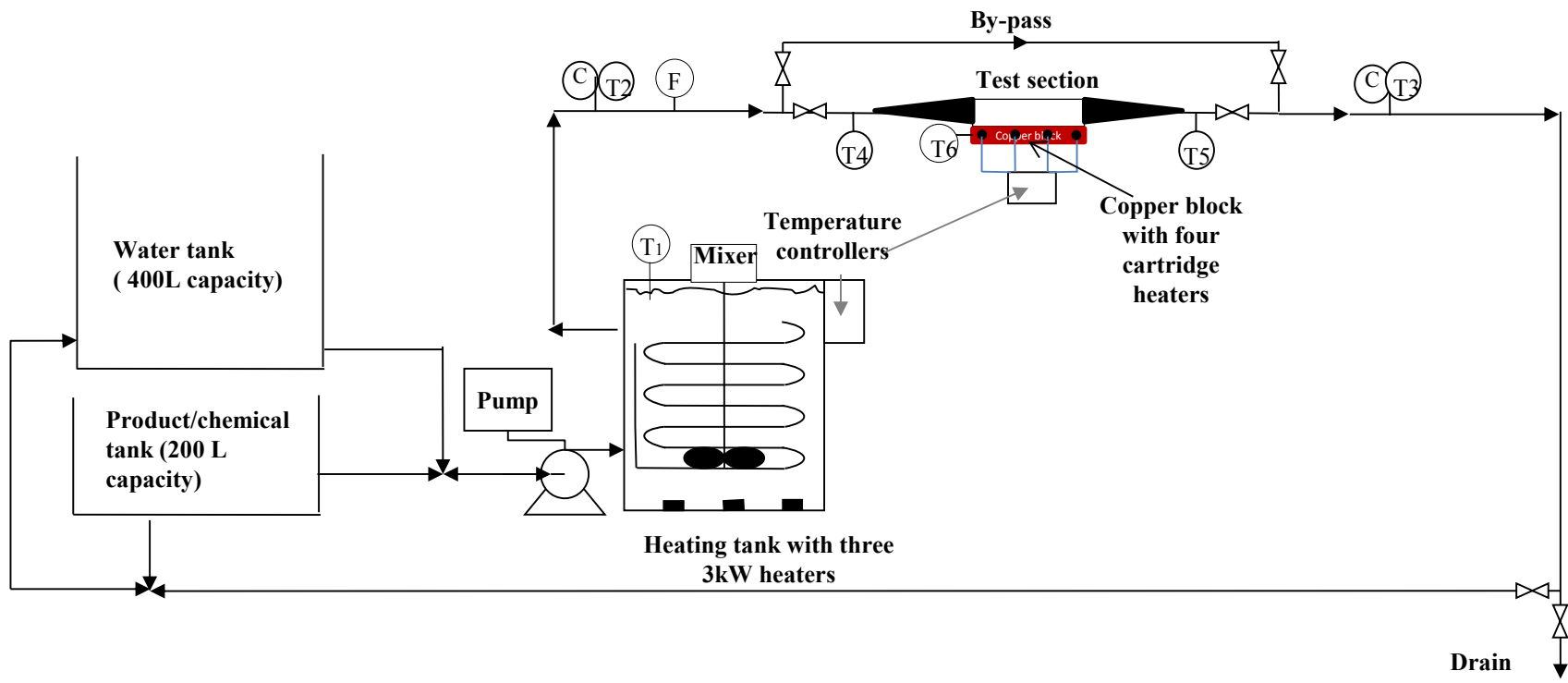


Figure 3.3: Schematic diagram of the bench scale fouling rig. Letters C, F and T denote conductivity, flow meter and thermocouples.

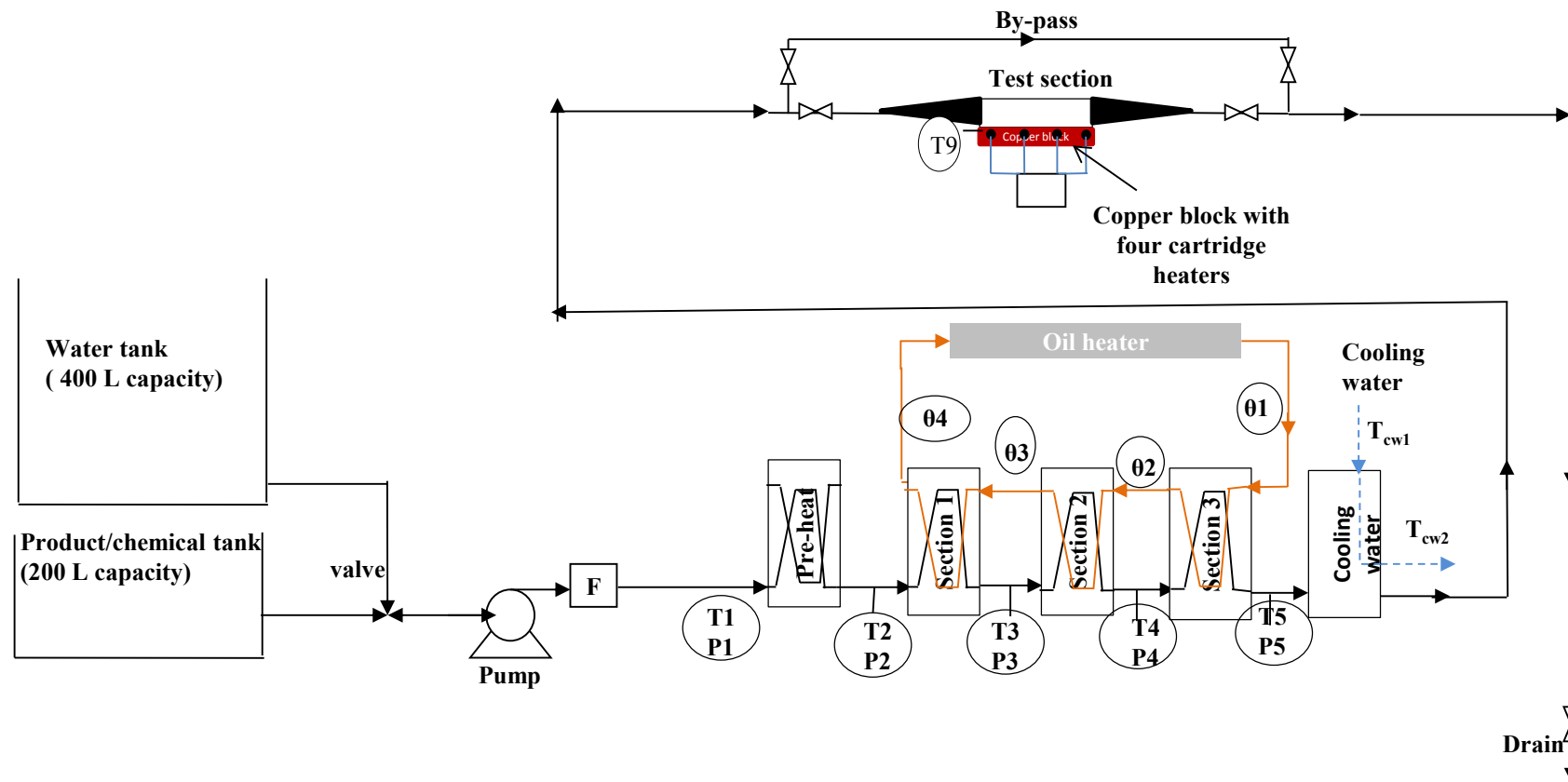


Figure 3.4: Schematic diagram of plate heat exchanger, showing the connection of coupon rig at cooling outlet on the product flow side. Letters F , P, θ and T denote flow meter, Pressure , oil temperature and thermocouples.

3.4.1 Test section

The test section and its dimensions are shown in detail in Figure 3.5. The test section was made by the university's Biosciences Workshop (Birmingham, UK). The fouling test section was designed to house 12 stainless steel coupons to capture the fouling deposits. The base of each coupon is in contact with the heated copper block, and the face of each coupon is in contact with the fluid flow. The copper block houses four 300 W cartridge heaters (10 mm D, 150 mm L, RS components) designed to heat the block up to 100°C. The block also houses a temperature probe connected to a controller (west 2300), which, in turn, is connected to the cartridge heaters. The block is insulated to contain as much heat as possible.

The outer walls are made of aluminium and are the only non-removable feature. They are fixed in place by screws into the copper block and sealed with sealant to prevent leakage. The coupons are held in place by a stainless steel frame. The frame has 12 square holes cut to house the coupons so that each coupon face is flushed with the frame face, giving a continuous surface in contact with the fluid flow. The coupon frame fits flush to the two outer walls of the rig and are held in place by the test section assembly. The inner wall frame is positioned on top of the coupon frame fitting flushing to the fixed outer walls forming the inside wall of the duct, and is made of stainless steel. This is because steel offers better corrosion resistivity compared to other metals, for example, aluminium when sodium hydroxide is present. The glass is positioned on top of the inner frame, and the top frame (which supports the test section) is positioned on top of the glass. Both the inner frame and top frame house O-rings to seal the system when assembled. The top frame is fixed in place by 12 screws into the outer walls. Both ends of the test section are attached to a stainless steel end plate welded to a duct reducer (from 3" to 1") to connect to the rest

of the system. The size of the end plate matches the cross-section size of the test section once assembled. Each end plate is held in place to the test section by 10 screws. The fouling rig used in conjunction with a plate heat exchanger (PHE) via the outlet port of the PHE. Reinforced silicone tubing, secured with hose clips, was used to connect these two sections and to send the processed WPC solution to the drain.

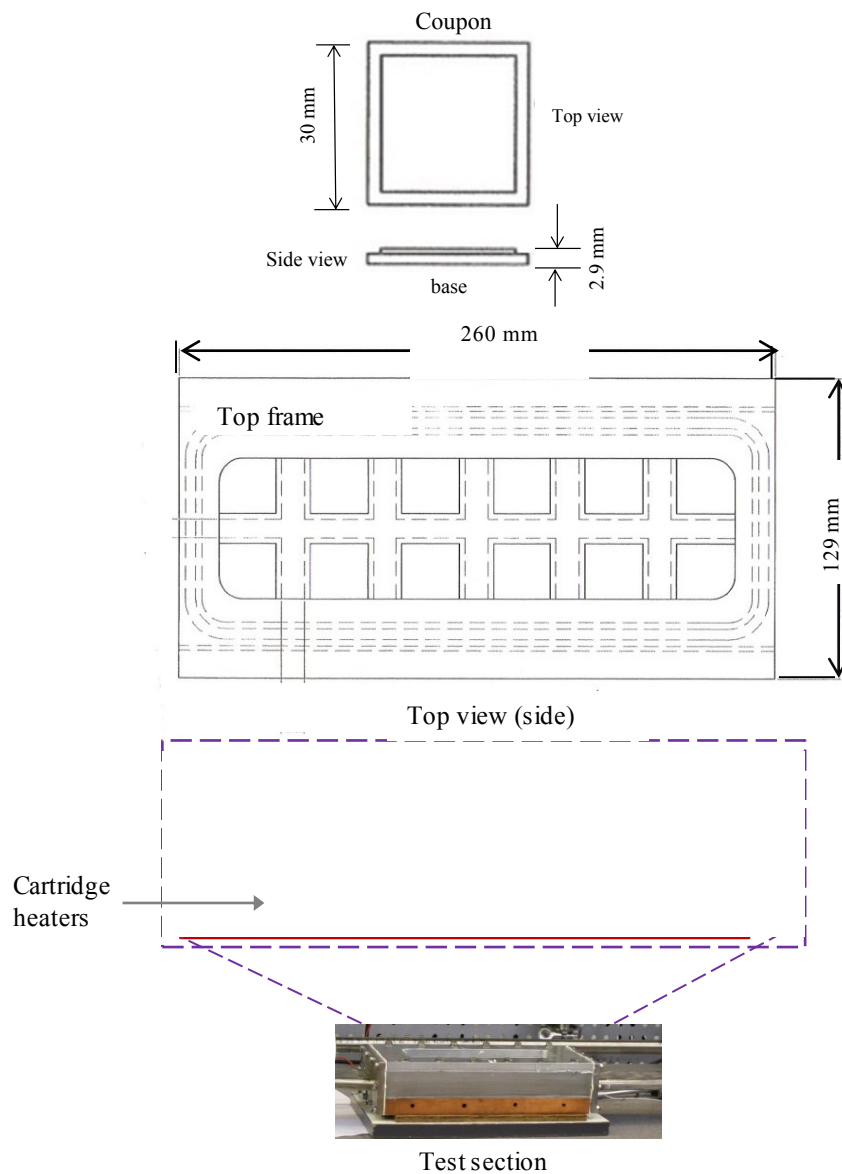


Figure 3.5: The test section with all dimensions.

Between experiments the disks were treated by a standard protocol to ensure the surfaces are totally free of any protein or other dirt; they were swabbed with sodium hydroxide solution and left for at least 10 minutes. Then the disks were rinsed repeatedly in water at 50°C and left to dry.

3.5 Monitoring devices

3.5.1 Online measurement

3.5.1.1 Peltier device

A Peltier device is used to create a heat flux between the junctions of two different types of material. The device has two sides; one side of the device is heated to a temperature greater than the other side (Figure 3.6).

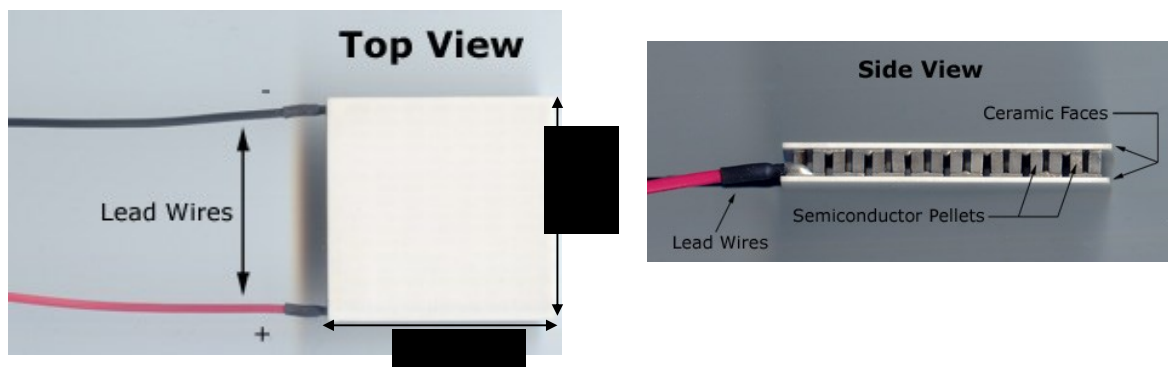


Figure 3.6: Peltier device (Thermoelectric, 2013).

A circular plate made of stainless steel (AISI 316, diameter 64mm) was used to hold the Peltier device (37.9W (3.9A) part number (ET-127-10-13-RS)). A square-shaped cavity was made in the middle of a circular plate to allow Peltier to slot in; then Peltier was fixed in place by a cubic copper metal with two screws, as seen in Figure 3.7. Another Two

screw holes were made in a circular plate to place the heat sink with a fan attached to the top of the Peltier device (Figure 3.8).

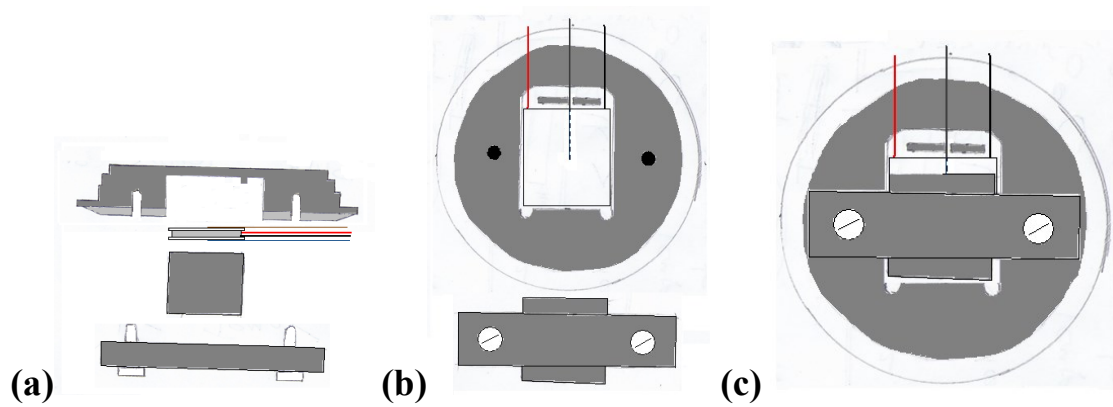


Figure 3.7: Peltier device component (a) side view, (b) bottom view – modular, and (c) bottom view.

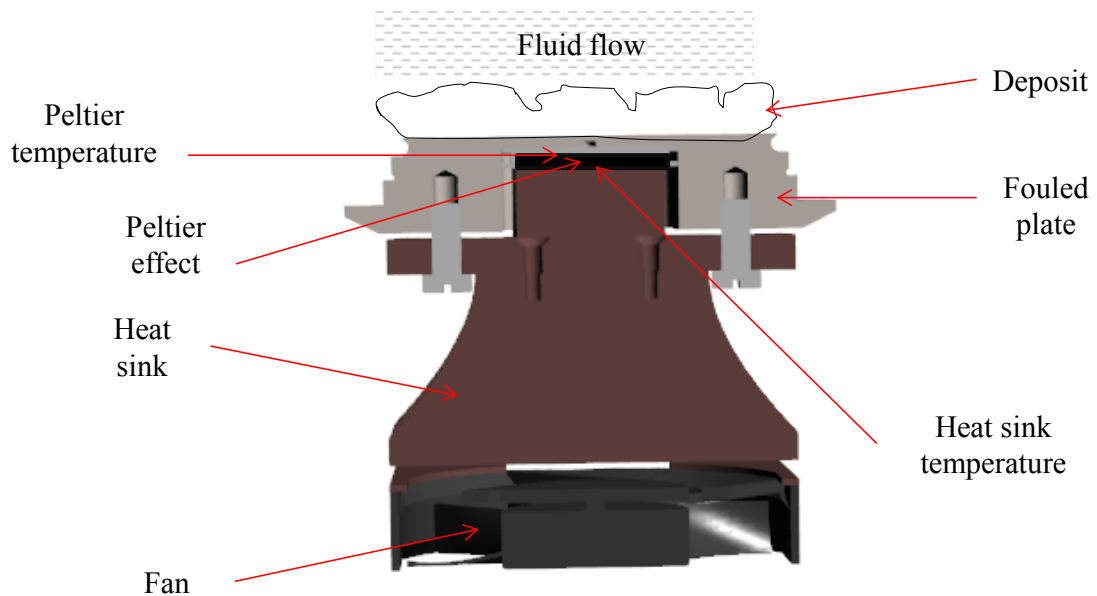


Figure 3.8: Peltier device in contact with heat sink with fan and fouled plate.

The Peltier has two surfaces: the one next to the fouled plate has been named the Peltier surface, and the one above the heat sink has been named the heat sink surface. Two thermocouples were placed on both sides of the Peltier. A temperature controller was used to control the temperature of the Peltier surface to the selected temperature. A thin, continuous film of thermal paste was applied to both sides of the Peltier. A small amount of pressure was applied to the Peltier, with the device being slid back and forth, left and right, to ensure a tight fit and to remove any air layers in between the connecting sides.

3.5.1.2 Turbidity meter

Turbidity is the measure of the amount of light scattered by particles in a sample. A beam of light passes through a sample containing suspended particles. The particles interact with the light and cause its scatter. The Kemtrak sensor was used in this experiment, which measures the Formazin turbidity unit (FTU). This is a non-descript measure of scattered light at 90° to the light source. Scattered light was calculated by the manufacturer by multiplying the calibration constant by the detector current, as provided by the Kemtrak user guide.

3.5.2 Offline measurement

3.5.2.1 Measurement of nano particles

A nano particles measuring device (NanoSight LM10 system) was used for measuring the number of nano-particles in discharged cleaning solution during the cleaning of PHE.

This method is based on a laser-illuminated microscopical technique in which the nano particles are tracked and visualised individually by a computer-controlled camera, making the particles directly measurable. When particles pass through the laser beam, their image

appears as bright spots moving rapidly on the computer screen. The particles number in the cleaning solution equals the spot number on the computer screen. In this instrument, many parameters can be adjusted to control the light captured from the particles, with final images obtained always showing similar intensity light spots for particles of different sizes, as seen in Figure 3.9.

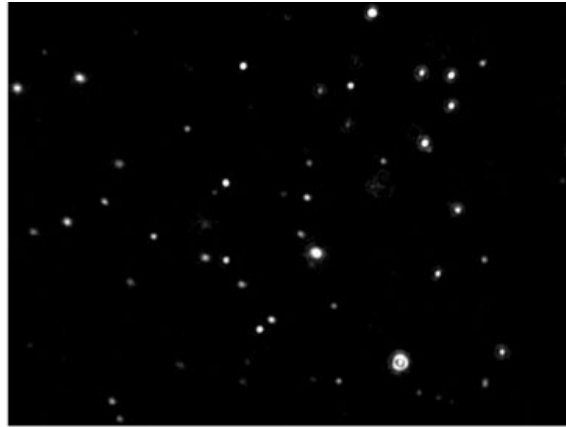


Figure 3.9: Particles image on computer screen.

The video was recorded by a digital camera for 10s at three frames per second for each measurement. For each frame in the video, the particle number was counted directly by their scattered light spots from the laser-illuminated ion, which was a direct count of the particles in the sample. The scattered beam volume for measurement in this instrument was calculated to be 1.41×10^{-7} ml.

3.5.3 Cleaning rig

Detailed description of the cleaning rig construction used in this work has been reported by Aziz (2008) and Christian (2004) presented in Figure 3.10. The rig was modified by replacing the flow channels and the test sections. The modified flow channel was an AISI

316 stainless steel tube with a diameter of 1 inch and 2 mm thickness and was installed horizontally. The modified rig has three main parts: fluids reservoir, heating system and flow channel. All the apparatuses were connected by reinforced silicone tubing (25 mm diameter).

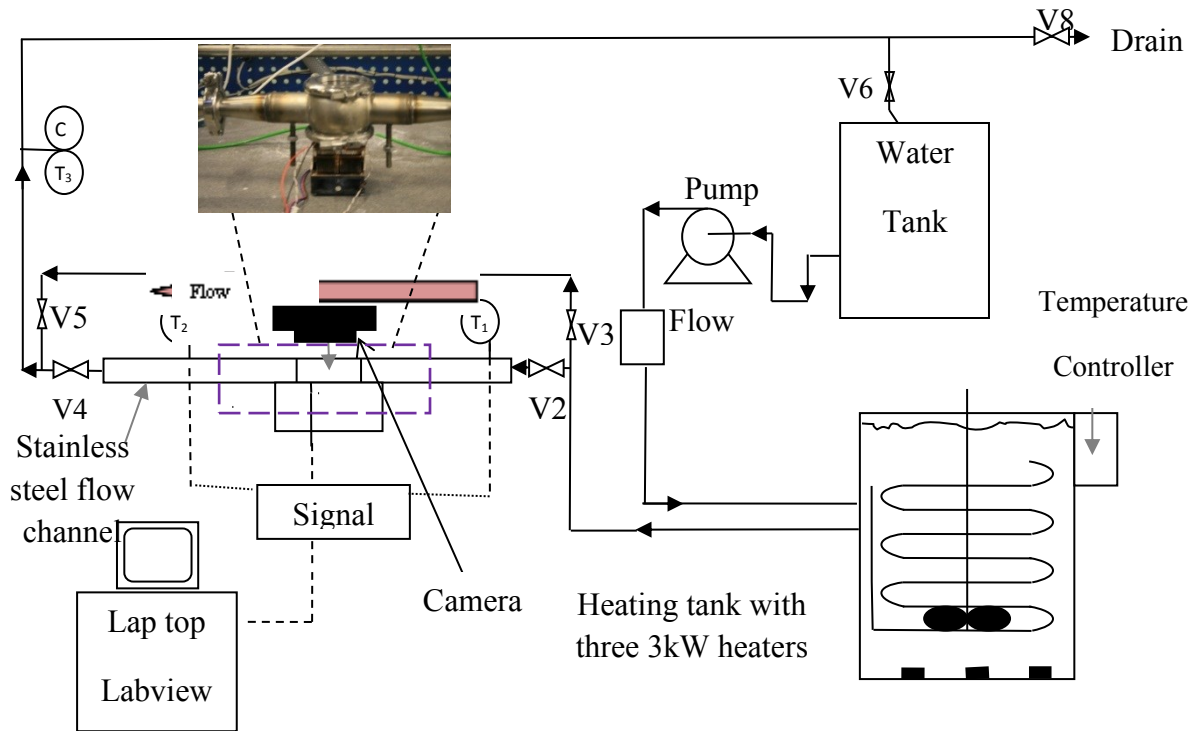


Figure 3.10: Schematic diagram of the bench-scale cleaning rig. Letters C, T and V denote conductivity, thermocouples and the valve respectively.

For the fluids reservoir, a 55 litre tank containing soft water was needed for cleaning of the two deposits; toothpaste and golden syrup. A 25 mm reinforced rubber tubing and a three-way diverting valve (Industrial Pipeline Supplies Ltd, Birmingham) were used to link both of the tanks and to change the input source. Liquid from the tank was pumped to the heating system by the chemically resistant centrifugal pump (SolidC-1, Alfa Laval, Denmark, 1.5 kW), and its flow rate was controlled by the fine needle control valve (Hoke International, Middlesex). Before entering the test section, the water was passed through a

heating tank (constructed at the university from stainless steel). The system comprises a tank (height 800 mm and diameter 560 mm) and a coil tubing (length 16.5 m, 1 mm wall thickness, 10 mm diameter) (both of which are made of stainless steel), three 3 kW heating elements (RS Components, Corby), a temperature controller (808, Eurotherm, Rugby), and an electric overhead stirrer (RW20, IKA Labortechnik, Staufen, Germany). The heating tank was always filled with soft water and must reach the indication level. If not, the heating elements will not activate (as a safety measure). During heating, the heating elements heated the fluid to achieve the desired temperature while the fluid was stirred to ensure uniform temperature inside the tank. This externally-heated fluid then heated up fluid inside the coil which came from the reservoir. A temperature controller was used to adjust the temperature inside the heating tank to ensure the outlet temperature was at the set point. The soft water was allowed to enter the flow channel (1 inch diameter). The pipe flow channel was made from AISI 316 stainless steel with 2 mm thickness. The inlet and outlet of the flow channel were tapered and connected to the stainless steel piping using a clamp. Several parts of the apparatus were attached to the channel: a test section, K-type thermocouples of 2 mm diameter (RS Components, Corby), a small lab jack, digital camera (Canon EOS 30D, Japan), light control box, and data logging system. The test section containing the Peltier device was circular in shape, had a diameter of 64 mm and height of 49 mm, and was positioned near the middle of the flow channel (400 mm inlet and 300 mm outlet lengths). The Peltier device was in fixed contact with the reverse side of the fouled circular disk throughout the experiments. Underneath the fouled plate were the Peltier device and the two thermocouples. One thermocouple was located between the upper surface of the Peltier device and the lower surface of the fouled plate, while the other thermocouple was next to the lower surface of

the Peltier device. The two thermocouples attached to the Peltier surfaces were plugged into a temperature controller and information was continuously recorded by the Lab view software. The software also displays the output power and controls the direction of the current, which allows for setting the temperature of either the Peltier surface or the heat sink surface.

The fouled plate was fitted into the test section of the flow channel. The fouled plate was visible through the glass section at the top of the channel; this was fixed to the circular channel with a clamp. K-type thermocouples were placed at the inlet and outlet of the flow channel to measure the fluid temperature. Reading from the latter thermocouples and the flow rate were collected by a signal conditioning unit and was recorded by Labview software (both manufactured by National Instruments, Newbury). Cleaning was recorded by a digital camera, power output (%) and the temperature measurements of the both Peltier surfaces. After entering the flow channel, fluid was then directed to the drain.

3.6 Operation of the PHE

Two tanks (A- 400 l and B- 200 l) were used in the fouling experiments. Tank A contained soft water, and Tank B was used to prepare the whey protein solution. Sodium chloride was added to Tank A to ensure correct functioning of the process side flow meter. Whey protein powder (WPC35) was added to Tank B to the level required to make up the specified WPC concentration; an electric mixer was lowered into it. The quantity of WPC powder required for an experiment was calculated according to the following equation:

$$x = \frac{0.198 y}{z + y} \qquad \text{Equation 3.2}$$

Where x is concentration of β -Lg required in final solution (wt.%), y is WPC powder and z the weight of the soft water to be added both in kg, the value of 0.198 arises from the β -Lg content of WPC powder.

An electronic mixer was used to ensure the WPC solution was homogeneous. The blades of the mixer were lowered so that they were completely wetted by the water. The mixer was turned on and the powder added gradually to the soft water while continuously mixing. This prevented the formation of lumps, which could block the PHE or cause excessive local fouling. The minerals were also added after the WPC powder using the same technique. After approximately 20 minutes, the mixer was switched off, removed and wiped clean. The WPC solution was left for a minimum of 30 minutes to de-aerate.

The product pump was started to draw soft water, and the flow rate adjusted. If the flow rate reading was unstable, more salt was added to the soft water to give sufficient conductivity at the electromagnetic flow meter. When water had passed through the whole system, the pump of the oil heater was switched on. After 5 minutes of water and oil at room temperature flowing through the system, the oil heater set point was adjusted to the desired temperature and the heater was turned on. The cooling water (from tap water lines) was turned on and adjusted to give the desired temperature across the PHE; a small change in cooling water flow rate controls the temperature of the process fluid that heats the preheat section and, therefore, influences the temperature profile across the PHE. The backpressure valve was adjusted to give 400 kPa at the section 3 outlet in order to maintain the accuracy of the pressure reading and to ensure that the process fluid remained as liquid at temperatures in excess of 100°C. The pressure required was determined by using the standard steam tables (Perry and Green, 1984).

The system was left for 2 hours and forty minutes to reach thermal stability. The last 10 minutes were recorded (recording interval was 1 seconds) to prove that thermal stability was achieved before starting either the fouling or cleaning experiment. This point was defined as the change in exit temperatures of sections 1, 2 and 3 was 0.2°C ; thus, heat flux through each of these sections was constant.

At a known time, the flow was diverted to draw from the tank containing WPC solution. Fouling runs lasted as per the specification of each experiment. As soon as the fouling experiment was started, the soft water tank was refilled so that there was enough water available for the subsequent cleaning run. At the end of the fouling experiment, the diverter valve was switched to pump soft water through the PHE in order to reach the thermal equilibrium for a cleaning run.

3.7 Operation of the bench-scale fouling rig

The PHE was used to heat up the WPC solution to the desired temperature before entering the test section. The fouling experiment protocol was similar to section 3.6 up until the initiation of the experiment. In the fouling rig, WPC solution was sent to the test section and sent afterwards to the drain. The test section's heater was switched on and the desired surface temperature was set before 30 minutes of starting the fouling experiment. The heater reached the set temperature within 5 minutes, depending on the bulk temperature and the selected surface temperature. There was a decrease in temperature by ca. 3°C between the outlet of the cooling section in PHE and the inlet of the test section. The experiment lasted for 80 minutes, and the flow rate was set at 100 l/h for all experiments. At the end of the fouling run, the test section and the oil heaters were switched off, but the

flow was maintained until the entire PHE was below 50°C, after which the oil and the product flow pumps were both switched off.

The fouling rig was carefully disconnected by initially removing the bolts from both end plates and then removing the bolts from the top frame. The glass and the inner wall frame were removed carefully. Using a chiselled screwdriver, the stainless steel frame was prised from coupons and placed in a moulded plastic tray. Approximately 5 ml of soft water was put in the tray to keep the deposit wet. Then the bottom of each coupon was dried by a paper towel, weighed, and the thickness of each side of the deposit formed was measured on the micromanipulation rig detailed by Liu et al. (2002).

The test section was cleaned by removing all the removable parts and submerging them in the cleaning solution to soak for approximately 30 minutes. A bottlebrush was used to clean any deposits left; afterwards, all sections were rinsed thoroughly to remove any cleaning chemicals. The wall and the bottom of the test sections were cleaned by cleaning solution, removing any deposit using a paper towel.

3.8 Cleaning experiments (PHE)

Cleaning of the PHE directly followed the fouling run. The system conditions were altered to the predetermined cleaning conditions. Therefore, the cooling water was switched off, the oil heater set point was altered, and the product flow rate was changed if necessary. The thermal stability in the cleaning run was achieved rapidly in an hour and a half as the cooling water was off.

While the PHE was stabilising at the new cleaning experimental setting, the tank containing WPC solution was drained and cleaned using water and weak detergent. The tank was then filled with soft water to an appropriate level to produce the desired final

concentration of the cleaning chemicals for the cleaning run. Extreme care was taken to wear the appropriate glove and facial protection, since there was a risk of burns from the cleaning solution (which was 30% sodium hydroxide). Once the PHE achieved thermal equilibrium, the sampling interval was set to 1 second. After 10 minutes of sampling, the diverter valve was switched so that the pump could draw the cleaning solution from the tank and pump it through the PHE and out to the drain. Cleaning was terminated very rapidly (<5 minutes) in some cleaning conditions. The pressure drop across each section of the PHE and turbidity probe was closely monitored during the cleaning experiment, with the cleaning run lasting for 80 minutes. If the WPC_m was used during the fouling run, a water rinse step for 1 minute was used before introducing the nitric acid solution at a concentration of 1 wt.% to clean the remaining mineral deposits. In the particle count analysis, 13 samples of the cleaning fluid were taken during the cleaning process, at the outlet of the PHE to represent cleaning behaviour of the three types of deposit. It was assumed that no dissolution of the particles occurred during transport from the surface to the PHE outlet. Samples were held in ice until the time of testing, which was conducted the same day to quench any reaction that may change particle count or size. Samples were diluted to the point where particles were easy to count (approximately 40 particles (in 1.41×10^{-7} ml)).

At the end of the cleaning run, the diverter valve was switched back to its previous position so that the pump now pumped soft water through the PHE to remove any remaining cleaning solution. At the same time the cooling water was switched on at full tape pressure and the oil heater was switched off; the flow was maintained until the entire PHE was below 50°C, when the oil and the product flow pumps were both switched off.

3.9 Deposit removal in the bench-scale cleaning rig: experimental procedure

Two types of deposit were used, namely tooth paste and golden syrup. The reason behind this selection is to measure the effect of cleaning time of the two deposits on the response of the Peltier (see section 2.3). As discussed earlier in section 2.3, the two deposits could be removed by flow of water action alone. The general preparation procedure carried out for the removal of both of these deposit types is detailed below.

A known mass ($7\text{g} \pm 0.2\text{g}$) of toothpaste or ($4\text{g} \pm 0.4\text{g}$) golden syrup was spread evenly over the fouled plate, inserted in the circular channel, and joined together by a clamp. A small lab jack was used to level the test section. The water bath temperature was set at 3°C above the desired flow temperature of the cleaning/rinsing water. The 70 l tank was filled with soft water along with the pipes attached to the pump so that the pump did not run dry. The digital camera and light box were placed facing the fouling test and the sampling rate was set to 3 minutes and 30 seconds for both fluids, i.e. tooth paste and gold syrup. The flow rate was set to the desired rate, and the flow was directed to run through a bypass route until thermal equilibrium was achieved. The data logger was turned on and the temperature of either the Peltier surface or heat sink was selected. The Peltier and fan were run approximately 15 minutes before the commencement of the cleaning to achieve the desired set point. When the desired temperature was achieved at the heating tank, the pump was started to circulate the water in the tank containing soft water until achieving the desired temperature. When all the instruments achieved their desired temperatures, the pump was turned off and the valve arrangement was altered in such a way to allow the flow through the test section. The camera was turned on; time and sample rate were recorded so that images could be compared to the Peltier readings. Afterwards, cleaning was initiated again by restarting the pump.

Deposit removal was a random process; the force of water alone could remove the entire deposit. Soft water was passed through the system until it was seen that no deposit remained at the surface. The plate was therefore termed 'clean' when either the entire deposit had been removed or when the small, seemingly irremovable islands of deposit remained as the Peltier readings become steady.

At the end of each experiment data logging was stopped and the camera was turned off. Before the pump was turned off, the flow rate was set to the desired value for the next experiment. The test section was disassembled and prepared for the next experiment. Between experiments, pictures from the camera and data files from the Peltier device could be downloaded at any time or after the experiment had been completed.

The assembly protocol for the test section is as follows:

Firstly, the coupons were placed at the test section, and the coupon frame built in grooves held the coupons in place. The inner wall frame is placed on top of the coupon frame, and silicon grease was applied at the frame edge to prevent any leakage during fouling and cleaning experiments. The glass plate was placed at the top of the inner wall frame, and the top frame was tightened with bolts. The end plate was tightened in place with bolts at the very end. The PHE and test section are now ready to be cleaned by chemical solutions and prepared for the next fouling experiment.

3.10 Analytical Techniques

Two analytical techniques, namely white-light scanning interferometer (WLI) and scanning electron microscopy (SEM), were used to characterise the deposits formed at the PHE and the test section (holding the coupons). To study the deposit morphology, both the PHE and fouling rig were dismantled after each run, and the recovered deposits were

dried and prepared for WLI and SEM analysis. Analytical technique results for WPC deposits will be discussed in Chapter 5.

The characterisation techniques used in this work have been described in the following sections in more detail.

3.10.1 White-light scanning interferometer (WLI)

A white-light scanning interferometer (Omniscan Microxam 2) is a measuring method to chart the surface morphology of an object. To achieve this, the light is collimated from the light source and split into two beams i.e. reference and measurement beams. The reference beam is reflected from a reference mirror, while the measurement beam is reflected from the object being measured. During the vertical scan, the interference patterns are captured by the video camera while the software analyses the topographical structure of the sample. The interferometer also offers the ability to produce quantitative values for surface roughness without contacting the surface or damaging it.

3.10.2 Scanning electron microscope (SEM)

The SEM (Philips XL30) is a microscope that uses electrons instead of light to form an image. The SEM also has much higher resolution than a white-light scanning interferometer; closely spaced specimens can be magnified many times more. The use of electromagnets rather than lenses by the SEM allows much more control in the degree of magnification, and resolution better than one nanometer is usually achievable. A specimen is required to be completely dry, since the specimen chamber is at a high vacuum. Samples are sputter-coated with gold before examination in the microscope.

3.11 Experimental error

All measuring devices were checked before the experimental work was commenced with instrumental accuracy being tested on a regular basis.

The individual sources of error from monitoring devices are listed and discussed below.

- K-type thermocouples ($\pm 1^\circ\text{C}$ accuracy) used in the PHE, fouling rig, bench scale cleaning experiments, and the Peltier were checked at the beginning of a set experiments with ice water.
- Pressure transducers had an error of ± 2 kPa, and any pressure drop had a maximum error of 4 kPa.
- The flow meter readings in the oil side flow of the PHE were correct to $\pm 5\%$.
- The flow meter in the product flow of the PHE was accurate to $\pm 0.03\%$. The Rotameter used for cooling water had an accuracy of 1%.
- WPC composition varies with different batches of the same nominal material; this was not quantified.
- The volume of soft water used was generated and measured by a volumetric meter attached to the soft unit and is considered to be accurate within a range of 1%.
- The accuracy of weighing scales used to prepare WPC solution and to weigh the mass deposit was 10 g and 10 mg, respectively.
- The overall error in UA is 3.16% (including the error in temperature 1% and the standard deviation of UA 3% (see Appendix)).
- The overall error in ΔP is 2.83% (including the error in pressure sensor 0.4% and the standard deviation of ΔP 2.8% (see Appendix)).

3.12 Minimising experimental error

A number of steps were taken to try to minimise those errors:

- All measuring devices were checked before the commencement of the experiments.
- All thermocouples were put inside the pipes instead of mounting them on the pipe surface.
- Experiments were repeated at least twice in order to understand the potential variation in the results.
- All monitoring devices were allowed to achieve thermal stability before the commencement of experiments.
- Values for heat transfer coefficient and heat balance were periodically checked to ensure sensor accuracy and experimental repeatability.

3.13 Heat transfer and pressure drop across the PHE

Heat transfer coefficient and pressure drop were discussed earlier in Section 2.4 as methods of monitoring fouling and cleaning. The data generated for the heat transfer coefficient and pressure drop using soft water were later compared with the data from the fouling and cleaning experiments (see Chapter 4 and 6).

3.13.1 Heat transfer coefficient

The overall heat transfer coefficient (U) is a measure of the ease of heat transfer between two fluid streams which have a difference in bulk temperature (ΔT). It is defined in terms of:

$$q = UA\Delta T \quad \text{Equation 3.3}$$

q is the local heat flow (W), A is the heat transfer surface area (m^2), and U is the overall heat transfer coefficient based on that area ($\text{W}/\text{m}^2\text{K}$). The overall heat transfer coefficient involves (i) the resistance to convection heat transfer for the heating medium and water, and (ii) the resistance to the heat transfer wall. The clean overall heat transfer coefficient (U_o) can be calculated from

$$\frac{1}{U_o A} = \frac{1}{Ah_h} + \frac{x_p}{A\lambda_p} + \frac{1}{Ah_c} \quad \text{Equation 3.4}$$

where h_h and h_c are film heat transfer coefficient for heating and process fluid (water) respectively ($\text{W}/\text{m}^2\text{K}$), x_p is the thickness of the plate (m), and λ_p is thermal conductivity of the plate ($\text{W}/\text{m K}$). The fouling adds an insulated layer to the heat transfer surface. The fouled overall heat transfer coefficient can be calculated as:

$$\frac{1}{UA} = \frac{1}{Ah_h} + \frac{x_p}{A\lambda_p} + \frac{1}{Ah_c} + \frac{R_f}{A} \quad \text{Equation 3.5}$$

Where R_f is the fouling resistance ($\text{m}^2 \text{K}/\text{W}$).

It is obvious from equation 3.5 that the higher the film coefficients, the greater effect the fouling resistance will have on the overall coefficient.

The heat transfer correlation for a fluid flow past a solid surface is expressed in a dimensionless form:

$$Nu = \gamma Re^n Pr^{0.4} \quad \text{Equation 3.6}$$

Where γ and n are correlation constants with values specific to each PHE system and Re is defined as:

$$Re = \frac{\rho v de}{\mu} \quad \text{Equation 3.7}$$

Where ρ is the density of the process fluid (kg/m^3), v is the velocity of the process fluid (m/s), de is the equivalent diameter (m), and μ is the viscosity of the process fluid (Pa.s).

Pr groups process fluid physical properties:

$$Pr = \frac{C_p \mu}{k} \quad \text{Equation 3.8}$$

Where C_p is specific heat capacity at constant pressure (J/kg K), k is thermal conductivity of the fluid (water) (W/m K).

Based on the corrugation design, n varies and is generally determined experimentally (Hewitt *et al.*, 1994). Equivalent results can be obtained for n . Schreier (1995) and Changani (2000) found that $n=1$ gave the best fit to their data.

In practice it is very difficult to measure the individual film heat transfer coefficients, h_h and h_c ; here, U_o was calculated using plant measurements. The clean heat transfer coefficient U_o was characterised for constant heating fluid flow rates as a function of the water flow rate. Under these circumstances, the two terms on the right-hand side of the equation (3.9) remain constant; the heating fluid flow rate and temperature do not alter,

and the geometry of the exchanger does not change. However, change in the average water side fluid velocity will change heat transfer coefficient h_c . Equation 3.4 thus becomes:

$$\frac{1}{U_o A} = const + \frac{1}{A h_c} \quad \text{Equation 3.9}$$

h_c will be proportional to Q , where Q is the process fluid (water) flow rate (m^3/s). The Equation 3.6 can be written as:

$$\frac{h_c de}{k} = \gamma \left(\frac{\rho v de}{\mu} \right)^n \left(\frac{\mu C_p}{k} \right)^{0.4} \quad \text{Equation 3.10}$$

From Equation 3.10:

$$\varepsilon = \gamma \frac{k}{de} \left(\frac{\rho de}{\mu A} \right)^n \left(\frac{\mu C_p}{k} \right)^{0.4} \quad \text{Equation 3.11}$$

Equation 3.6 and Equation 3.9 can be manipulated to give:

$$\frac{1}{U_o A} = const + \frac{1}{\varepsilon A Q^n} \quad \text{Equation 3.12}$$

Thus, a plot of $1/AU_o$ versus $1/Q$ should yield a straight line of slope $1/\varepsilon$ and an intercept of $(1/A h_h + x_p / A \lambda_p)$; it was found that a value of $n=1$ yielded the best straight line fit (see Figure A.1 and Figure A.2, Appendix).

For these experiments, U_o was calculated for both sections of the PHE. The general design equation for a heat exchanger is:

$$U = \frac{q}{A\Delta T_{LM}} \quad \text{Equation 3.13}$$

q is the rate of heat transfer between the hot and cold fluid (W), A is the total plate heat transfer area (m^2), and ΔT_{LM} is the log mean temperature difference (K). To determine U in each section, q , A and ΔT_{LM} are calculated from the next three equations

$$q = m C_p \Delta T \quad \text{Equation 3.14}$$

Where m is the mass flow rate (kg/s) for both processes and heating fluid, C_p is specific heat capacity (J/kg K); ΔT is fluid inlet and outlet temperature difference (K), and q is for both the process and heating fluids. The heat transfer surface area can be calculated from:

$$A = Na \quad \text{Equation 3.15}$$

Where N is the number of plates in each section of PHE, a is the projected plate area of a single plate (m^2) calculated by multiplying the width by the length of the plate involved in heat transfer. Table 3.1 gives the calculated plate heat transfer area for each section of PHE.

| Section of PHE | Number of plates involved in heat transfer | Total Heat Transfer Area (A) for each section (m ²) |
|----------------|--|---|
| Pasteuriser | 7 | 0.427 |
| Intermediate | 5 | 0.305 |
| UHT | 5 | 0.305 |

Table 3.1: Number of PHE plates involved in heat transfer in each section, and the heat transfer areas associated with the main sections of the PHE (Christian, 2004).

The log mean temperature difference is given by:

$$\Delta T_{LM} = \frac{[(T_{h,in} - T_{p,out}) - (T_{h,out} - T_{p,in})]}{[(T_{h,in} - T_{p,out}) / (T_{h,out} - T_{p,in})]} \quad \text{Equation 3.16}$$

Where $T_{h,in}$ and $T_{h,out}$ are the temperatures of heating fluid entering and exiting the PHE section (K), $T_{p,in}$ and $T_{p,out}$ are the temperatures of process fluid entering and exiting the PHE section (K).

A heat balance for each of the PHE sections was calculated as follows:

$$\dot{q} = \left[\dot{m} C_p \Delta T \right]_{product} = \left[\dot{m} C_p \Delta T \right]_{oil} \quad \text{Equation 3.17}$$

Therefore, the percentage of heat transfer, or heat balance, would be:

$$\text{Heat Balance} = \frac{\left[\dot{m} C_p \Delta T \right]_{product}}{\left[\dot{m} C_p \Delta T \right]_{oil}} \times 100 \quad \text{Equation 3.18}$$

3.13.2 Pressure drop

The formation of deposits on the heat transfer surfaces causes an increase in pressure drop due to the decrease in the hydraulic diameter of the flow during fouling of heat exchanger ducts, as according to Chenoweth (1987), more heat exchangers are taken out of service because of excessive pressure drop than because of reduced heat transfer.

The instrumentation of the PHE used here enables pressure drops to be monitored for each of the sections of the PHE, as well as the PHE as a whole. Pressure drop was calculated using the following equation:

$$\Delta P = P_I - P_O \quad \text{Equation 3.19}$$

Where ΔP is the pressure drop across a section or the whole of PHE (kPa), P_I and P_O are the inlet and outlet pressure (kPa). The change in pressure drop ΔP is monitored. In a plate heat exchanger in turbulent conditions, the pressure drop is related to the flow velocity as follows:

$$\Delta P \propto v^m \quad \text{Equation 3.20}$$

m is dependent upon corrugation design but often has the value of 1.9 (Hallstroem et al., 1981).

To test the accuracy and repeatability of plant measurement such as temperature, flow rate and pressure sensor, a number of preliminary experiments were undertaken on the PHE using soft water. During the preliminary experiments, the heat transfer coefficients and the pressure readings in each section of the PHE were recorded, and the heat balance (from

Equation 3.18) in each section of the PHE was calculated (see Appendix for more details).

3.14 Conclusion

This chapter gives details of the configuration and operation of pilot-scale PHE, and the fouling rig designed to be placed in-line after section 3 of the PHE to foul stainless steel coupons. The procedure to return the PHE to a clean state following fouling the PHE after fouling has been given.

Monitoring fouling and cleaning processes has become an important issue to optimise production cycles, increase the quality of the final product, and reduce environmental impacts. Two monitoring techniques were described: particle counts and the Peltier device were used to detect the cleaning end-point. The particles count technique can be used to monitor the removal of proteinaceous deposit from PHE off-line under different flow, temperature and chemical regimes, and the validity can be quantified by monitoring other parameters UA, ΔP and turbidity. The Peltier device is located in contact with the fouled plate; the bench-scale cleaning rig can be used to monitor the cleaning of two types of deposit *in situ* and in real time. The end-points determined by the Peltier device were confirmed by images from a digital camera throughout the experiments.

CHAPTER 4 : INFLUENCE OF PROCESS VARIABLES ON THE FOULING AND CLEANING BEHAVIOUR OF DAIRY DEPOSITS FORMED AT UP PASTEURISATION TEMPERATURE

4.1 Introduction

Chapter 3 detailed the experimental procedures to test temperature and pressure measurements as a means for the development of monitoring of fouling and cleaning in the PHE rig. The clean thermal conditions must be adequately specified to check and confirm the repeatability of experiments and, therefore, check if similar fouling is obtained (see Appendix).

Fouling and cleaning processes can be affected significantly by small changes in fluid composition. Since WPC lack of mineral, adding minerals back to WPC to the same level as milk may change the rate, extent and composition of the deposit (Christian and Fryer, 2002). Minerals may precipitate directly on the stainless steel wall or they may contribute to a deposit via precipitation on depositing protein aggregates. It is remarkable that increasing the calcium concentration of the milk led to an increase in the deposition and lower heat stability (Roefs and Kruif, 1994).

Cleaning milk and other dairy products deposits cannot be removed by water alone. Therefore, it is common practice in the dairy industry to run CIP (see section 2.3). Removal of dairy deposits is influenced by a variety of factors, such as temperature, fluid

flow, chemical concentration and chemical type. Cleaning chemicals produce a deposit with an open structure that is more susceptible to fluid shear, and are henceforth removed from the system. In this chapter, the balance between chemical and physical factors required to remove proteinaceous dairy deposit is investigated. The fouling and cleaning behaviour of WPC and WPC with added minerals (calcium and phosphorus) at pasteurisation temperature (95°C) under different conditions (flow rate, β -Lg concentration and cleaning concentration) has been investigated. In all fouling figures time = 0 second refers to the time where the diverter valve was switched to draw from WPC solution tank.

4.2 WPC and its fluids deposits experimental profile

Chapter 2 showed that fouling from milk and milk products is a complex process, resulting from processes occurring both near the heat transfer surface and in the bulk of the fluid flow, and that fouling is a function of many variables such as β -Lg concentration, minerals concentration, temperature, and flow rate. Due to natural fluctuations in milk composition throughout the year (Burton, 1994), three different concentrations of β -Lg and minerals were used to investigate the effect of chemical composition change (β -Lg and minerals concentration) upon the fouling and cleaning behaviour (see Table 2.1, chemical composition of milk and WPC solution). Accordingly, four types of fluids were prepared and tested in these experiments: WPC, WPC_m, WPC_{m/2}, and WPC_{m x 2}. WPC refers to fluid made with WPC powder alone, and the latter three refer to WPC solutions with calcium and phosphorus contents the same as milk, half that of milk and twice that of milk, respectively.

(i) Experimental conditions for WPC were:

- Concentration of β -Lg (0.1, 0.3, 0.5%)
 - Flow rate (100, 150l/h)
- (ii) Experimental conditions for WPC_m , $WPC_{m/2}$ and $WPC_{m \times 2}$ were,
- One flow rate of 100l/h
 - One concentration of β -Lg 0.3%

Two materials were identified that could be used to increase calcium and phosphorus levels in WPC. The following materials were used:

- $CaCl_2 \cdot 2H_2O$ Calcium Chloride Dehydrate
- NaH_2PO_4 Anhydrous Monobasic Sodium Phosphate

These were chosen as they:

- have a high degree of solubility in water
- minimise the presence of other materials that could influence fouling behaviour
- are safe to handle.

The fouling experiments were carried out following the procedure described in section 3.6, and applying the appropriate processing conditions.

4.3 WPC and its fluids deposits fouling

All of the WPC fluid experiments were carried out in the pilot scale PHE using pasteurisation processing temperatures. Six experiments were carried out under the same conditions to assess the repeatability of the fouling process. The initial temperature distribution across the sections of the PHE for the process fluid for the two flow rates, i.e. 100 and 150 l/h, under thermally stable conditions is presented in Table 4.1. Each fouling run for all four model fluids was one hour. During the fouling experiments, temperature

across each section changed due to the fouling build-up of deposit on PHE surfaces; however, the outlet temperature was maintained at 95°C. Type A deposit were observed for the four model fluids in sections 2 and 3 of PHE.

| Flow rate (l/h) | Temperature (°C) | | | | Fluid type |
|-----------------|------------------|-----------|-----------|-----------|------------|
| | Pre-heat | Section 1 | Section 2 | Section 3 | |
| 100 | 46.4 | 79.6 | 89.7 | 95.3 | Water |
| | 64.9 | 86.0 | 93.6 | 98.5 | Oil |
| 150 | 53.2 | 69.4 | 82.0 | 95.5 | Water |
| | 60.8 | 76.7 | 89.7 | 103.5 | Oil |

Table 4.1: Typical outlet temperature in each section at the thermally stabilised PHE and at flow rates of 100 and 150 l/h.

4.3.1 Result and discussion from fouling experiments

Figure 4.1 and Figure 4.2 present the fouling profiles obtained during build-up of the WPC deposit at a β -Lg concentration of 0.3 wt.%, in terms of changes in pressure drop and in overall heat transfer coefficient in terms of Area (UA) with time. The extent of fouling significantly increases with temperature, therefore giving the greatest amount of fouling in section 3 of the PHE.

These results suggest that the remarkable increase in pressure drop and reduction in UA are due to deposition of denatured and aggregated proteins formed in the bulk of the fluid. In contrast to the significant fouling in section 3 for all experiments, the pressure drop and the heat transfer coefficient remain constant in section 1 and 2 of the PHE, demonstrating that fouling is not taking place to a measurable level. They may firstly refer that at these temperatures the denatured whey protein in the bulk is more likely to react with another denatured protein in the bulk than with that on the surface (Simmons et al., 2007)

secondly, they may refer to the fact that a low amount of protein reacted in sections 1 and 2 of the PHE due to low temperature.

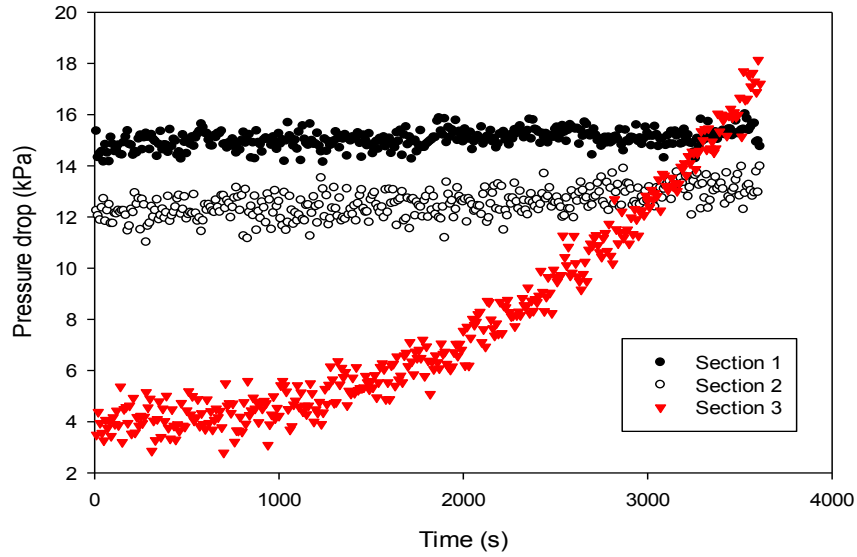


Figure 4.1: Fouling behaviour for WPC in terms of pressure drop in PHE; β -Lg 0.3 wt.%, process flow rate 100 l/h, section 3 outlet temperature 95°C.

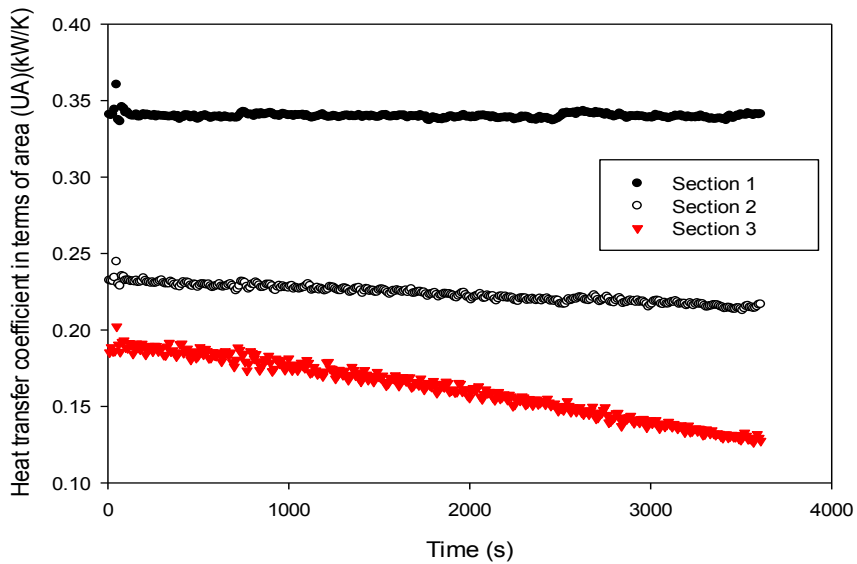


Figure 4.2: Fouling behaviour for WPC according to heat transfer coefficient in terms of area (UA), β -Lg 0.3wt.%, process flow rate 100 l/h, section 3 outlet temperature 95°C.

4.3.1.1 β -Lg concentration

Figure 4.3 and Figure 4.4 present pressure drop and overall heat transfer coefficient with time for the three trials at β -Lg concentration (0.1, 0.3 and 0.5wt.%), each lasting up to one hour. Two phases of fouling phenomena were observed during fouling experiments: (i) an induction period occurred at the beginning of the experiments in which the overall pressure drop was close to the value of the cleaning state. This period lasted for approximately 900 seconds and was followed by (ii) a fouling period in which the changes in pressure drop became different for each β -Lg concentration. Fast increases observed for the trials at β -Lg concentrations of 0.3 and 0.5 wt. % were due to the large amount of reacted protein adhered at the PHE surfaces. Excessive fouling narrowed the PHE exchanger channels; these, in turn, increased the average velocity, causing the pressure drop increase exponentially. There was no measurable fouling at β -Lg concentration of 0.1wt.%. This may be due to the small amount of protein reacted.

Figure 4.4 shows the evolution of overall heat transfer coefficient in terms of area UA with time for the three β -Lg concentrations. The two fouling phases were also observed during fouling experiments. The overall heat transfer coefficient in terms of area UA was nearly constant for the first 900 seconds, and then decreased linearly with time. These results were in good agreement with those obtained by Delaplace et al. (1994), Robbins et al. (1999) and Changani (2000).

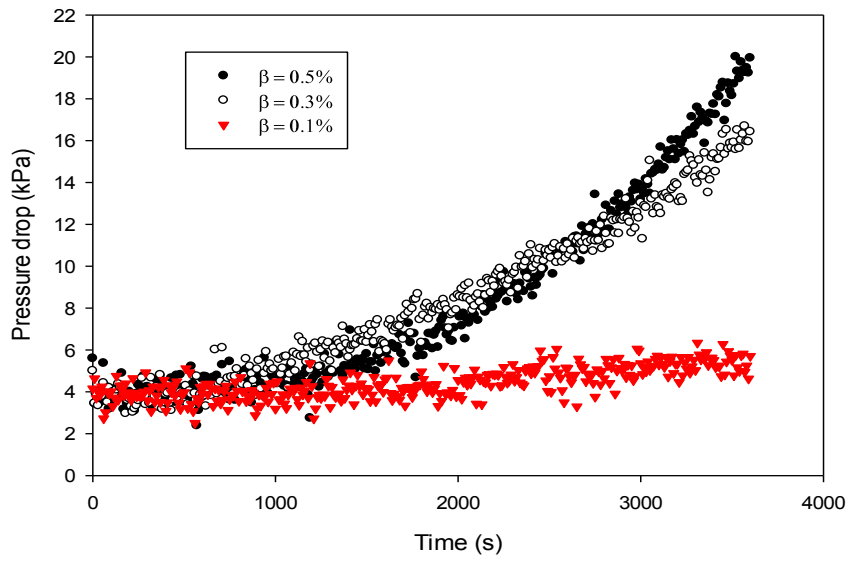


Figure 4.3: Fouling behaviour in terms of pressure drop for the three β -Lg concentrations, process flow rate 100 l/h, section 3 outlet temperature 95°C.

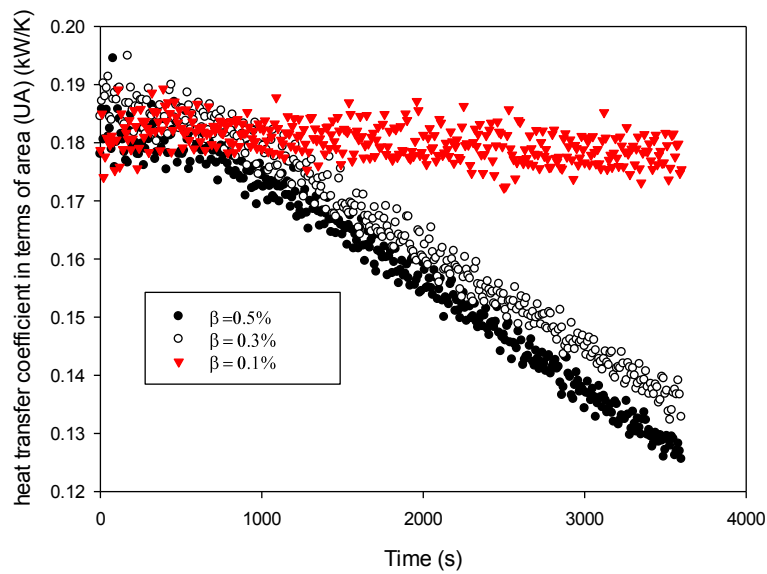


Figure 4.4: Fouling behaviour according to heat transfer coefficient in terms of area (UA) for the three β -Lg concentrations, process flow rate 100 l/h, section 3 outlet temperature 95°C.

The fouling rate for each section of PHE was compared and calculated in terms of pressure drop and Biot number, as follows:

$$\Delta(\Delta P) = \frac{(\Delta P_f - \Delta P_s)}{t} \quad \text{Equation 4.1}$$

$$\Delta Bi = \frac{[\frac{1}{UA} - \frac{1}{U_o A}] \times U_o A}{t} \quad \text{Equation 4.2}$$

Where ΔP_f is pressure drop across a section at the end of a fouling experiment (Pa), ΔP_s is pressure drop across a section at the start of a fouling experiment when the PHE is clean and thermally stable (Pa), and t is the duration of the fouling experiment (h). The fouling rates in terms of pressure drop [$\Delta(\Delta P)$] and Biot number (ΔBi) for the three concentrations are discussed below.

The fouling rates are compared for each β -Lg concentration at section 3 of the PHE in Figure 4.7 and Figure 4.9. β -Lg concentration at 0.5% showed the highest fouling rate [$\Delta(\Delta P) = 13.56$ Pa/h, $\Delta Bi = 0.453/h$], followed by β -Lg concentration (0.3%) [$\Delta(\Delta P) = 12.4$ Pa/h, $\Delta Bi = 0.434/h$]; finally, the fouling rate was much lower than the two latter β -Lg concentrations (0.3 and 0.5 wt.%) [$\Delta(\Delta P) = 1.76$ Pa/h, $\Delta Bi = 0.0426/h$]. Increasing the β -Lg concentration considerably increased the fouling rate effectively from β -Lg concentration 0.1 to 0.3wt.% However, small increased in ΔP was observed when β -Lg increased from 0.3 to 0.5wt.%. This result confirms the findings of Gotham (1990) who found that the increase of fouling, in tubular heat exchanger, with increasing protein concentration could be limited up to 3.75wt%. The plateau at 3.75% was explained in terms of fouling becoming controlled by the amount of protein in the laminar sub layer. It

was difficult to measure the fouling in sections 1 and 2, as the fouling at these sections was not significant. Overall, it is clear that a relatively small change in β -Lg concentration can give significant changes in fouling behaviour.

4.3.1.2 Effect of increased flow rate and β -Lg concentration on fouling behaviour

Figure 4.5 and Figure 4.6 show the effect of increasing the process fluid flow rate from 100 l/h to 150 l/h on the fouling behaviour of the three β -Lg concentrations, i.e. 0.1, 0.3 and 0.5wt.%. Increasing the flow rate alters the temperature profile across the sections of the PHE. As mentioned earlier, Table 4.1 shows that higher temperatures were achieved much later in the PHE at 150 l/h compared to 100 l/h.

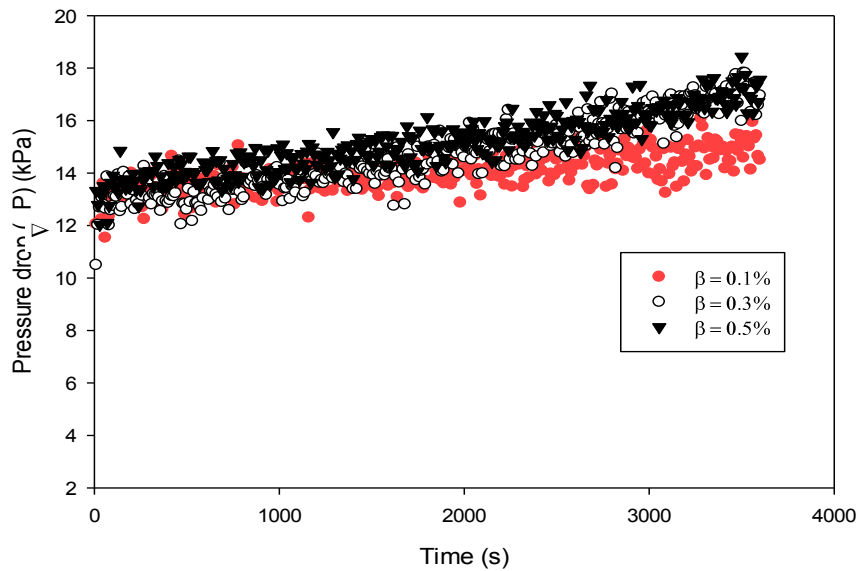


Figure 4.5: Fouling behaviour in terms of pressure drop for the three β -Lg concentrations, process flow rate 150 l/h, section 3 outlet temperature 95°C.

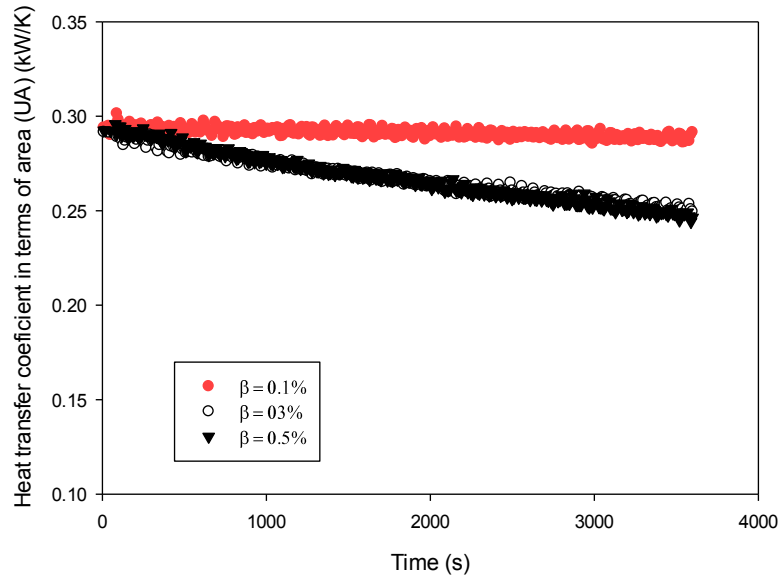


Figure 4.6: Fouling behaviour according to heat transfer coefficient in terms of area (UA) for the three β -Lg concentrations, process flow rate 150 l/h, section 3 outlet temperature 95°C.

Figure 4.7 to Figure 4.10 show that increasing the flow rate from 100 to 150 l/h decreased the fouling rate in terms of rate of change in ΔBi decreased with increasing flow rate for β -Lg concentrations 0.1, 0.3 and 0.5wt.% by 8.5, 66, and 60 %, respectively. Similarly, the fouling rate in terms of rate of change in $\Delta (\Delta P)$ for β -Lg concentrations 0.1, 0.3 and 0.5wt.% decreased by 34, 70 and 72.7%, respectively. There was very little distinction in $\Delta (\Delta P)$ and ΔBi between β -Lg concentrations 0.3 and 0.5 wt.%. Fryer (1986) and Belmar-Beiny et al. (1993) observed that a decrease in deposit thickness took place with increasing turbulence in tubular heat exchanger. Higher flow velocities promote deposit re-entrainment through increased fluid shear stresses, and the deposit can become more compact and smoother. Simmons et al. (2007) also found that the final size of the aggregates is considerably smaller, ranging from 20 to 60 μm as opposed to 90–120 μm at the lower shear rate (111s^{-1}) for the experiments where the temperature changed from 75

to 90°C after 20 minutes. However, Changani (2000) found that increasing the flow rate from 100 to 150 l/h increased both the $\Delta(\Delta P)$ and ΔBi fouling rate by more than two. This may be due to Changani's use of high temperatures in her experiments at 140°C, and similar results were reported by Simmons et al. (2007). They found that the dependence of the final aggregate size on shear rate decreased with increasing temperature, as the aggregates produced at higher temperatures were more resistant to shear.

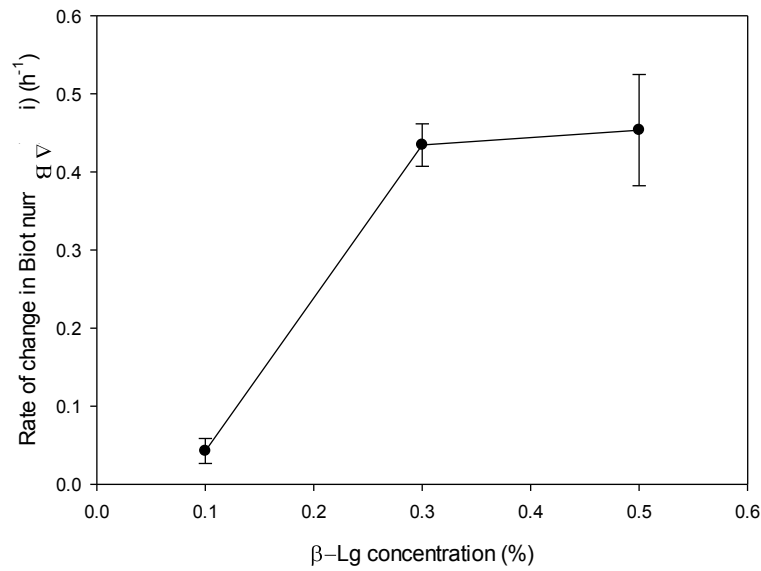


Figure 4.7: Fouling rate in terms of rate of change in Biot number for the three β -Lg concentrations, process flow rate 100 l/h, section 3 outlet temperature 95°C. Error bars represent the standard deviation of the means of change rate in Biot number (n=6).

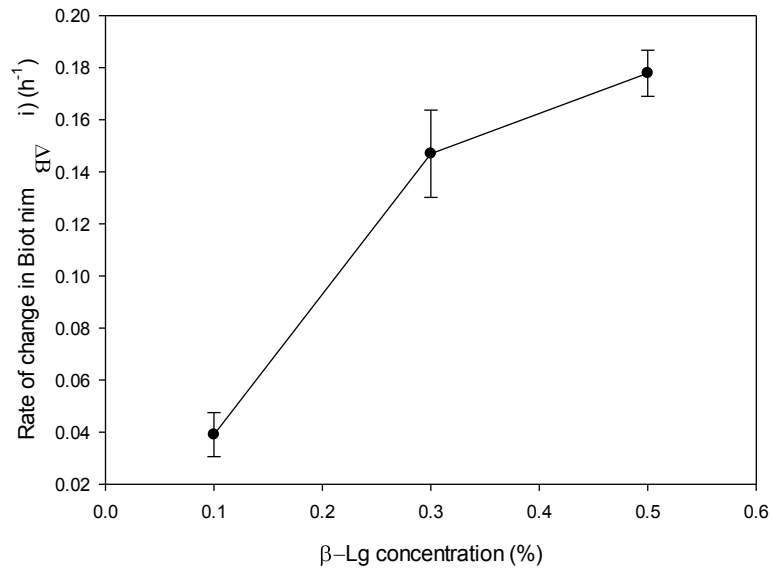


Figure 4.8: Fouling rate in terms of rate of change in Biot number for the three β -Lg concentrations, process flow rate 150 l/h, section 3 outlet temperature 95°C. Error bars represent the standard deviation of the means of change rate in Biot number (n=6).

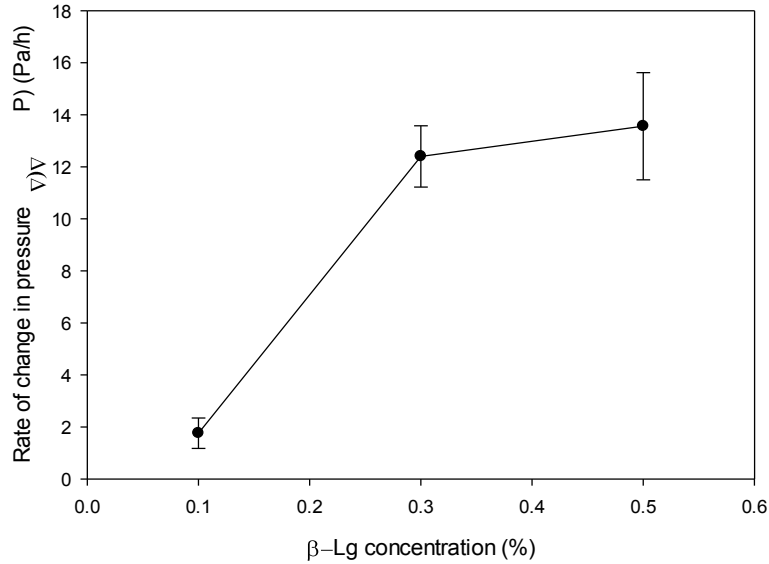


Figure 4.9: Fouling rate in terms of rate of change in pressure drop for the three β -Lg concentrations, process flow rate 100 l/h, section 3 outlet temperature 95°C. Error bars represent the standard deviation of the means of change rate in pressure drop (n=6).

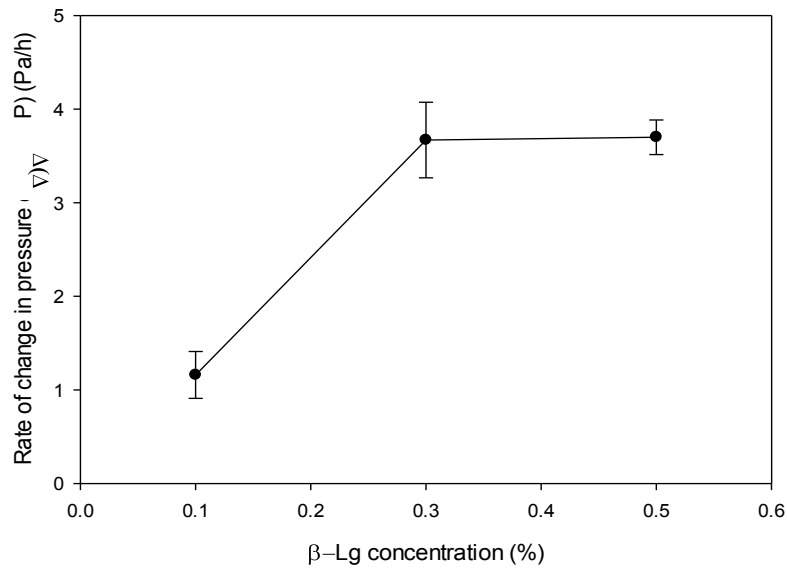


Figure 4.10: Fouling rate in terms of rate of change in pressure drop for the three β -Lg concentrations, process flow rate 150 l/h, section 3 outlet temperature 95°C. Error bars represent the standard deviation of the means of change rate in pressure drop (n=6).

4.3.1.3 Fouling behaviour of WPC with added minerals

Owing to WPC being low in minerals, adding calcium and phosphorus to the same level as present naturally in the whole milk may alter fouling and cleaning behaviour. As mentioned in section 4.2, four types of fluid were used in this work: WPC, WPC_m, WPC_{m/2} and WPC_{m_x2}. β -Lg concentration 0.3wt.% was used since it had the same concentration as found in milk and because of the importance of this protein in dairy fouling. Each fluid was processed at 100 l/h and carried out twice.

Figure 4.11 and Figure 4.12 show the fouling behaviour in terms of ΔP and UA for individual sections of the PHE. Generally, fouling was reduced by the addition of minerals to WPC; the fouling in section 3 of PHE became negligible when minerals were added. However, the three model fluids appear to foul mainly in section 2, with very little

fouling observed in section 1, as the added minerals reduced the heat stability of whey protein. The fouling rates in terms of both $\Delta(\Delta P)$ and ΔBi showed that fouling was considerably greater for WPC than for the three modified fluids as seen in Table 4.2. The fouling rate in terms of ΔBi for WPC_{mx2} was lower than the other three fluids. In contrast, $\Delta(\Delta P)$ was slightly higher than the rest of the three modified fluids. The decrease in ΔBi could indicate a deposit exhibiting different thermal conductivity properties due to compositional differences.

Adding the calcium and phosphate to WPC slowed the fouling rate as the solubility of calcium and phosphate salts decreases with increasing temperature and lowers the overall fouling rate. Altering the composition of the deposit gives more fouling at a much lower temperature (Jeurnink and De Kruif, 1995).

| Fluid type | $\Delta(\Delta P)$ (Pa/h) | ΔBi (h^{-1}) |
|-------------|---------------------------|--------------------------|
| WPC | 12.40 | 0.4343 |
| $WPC_{m/2}$ | 3.66 | 0.1336 |
| WPC_m | 3.65 | 0.1106 |
| WPC_{mx2} | 3.97 | 0.0709 |

Table 4.2: Fouling rate in terms of change in pressure drop and Biot number (ΔBi) at section 3 of the PHE for WPC and at section 2 of the PHE for $WPC_{m/2}$, WPC_m and WPC_{mx2} , process flow rate 100 l/h, β -Lg concentration 0.3wt.% , temperature 95°C.

Previous experiments using milk showed that most of the fouling occurred at temperatures less than 110°C with the fouling rates being much lower than WPC (Robbins et al., 1999). This behaviour resembles the fouling behaviour of WPC with added minerals. Therefore,

a simple chemical change in WPC solution can produce a material that has a fouling behaviour closer to that of milk.

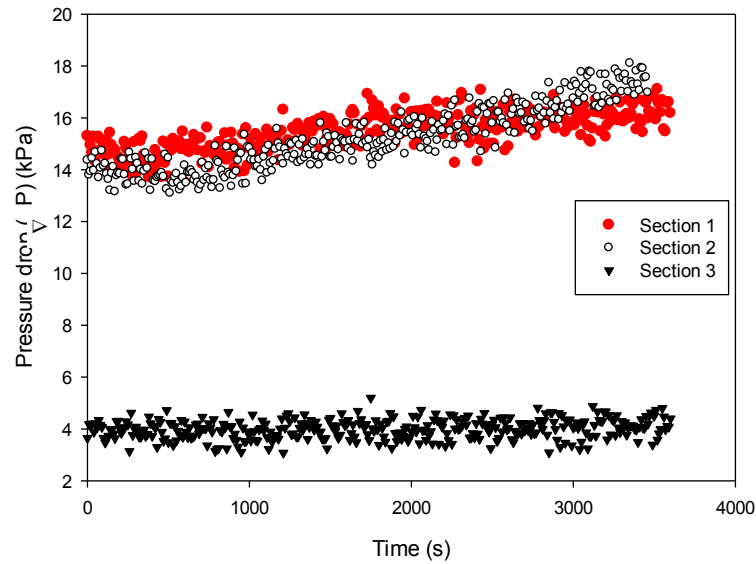


Figure 4.11: Fouling behaviour in terms of pressure drop at each section of PHE for WPC_{m/2} processed at flow rate 100 l/h, section 3 outlet temperature 95°C.

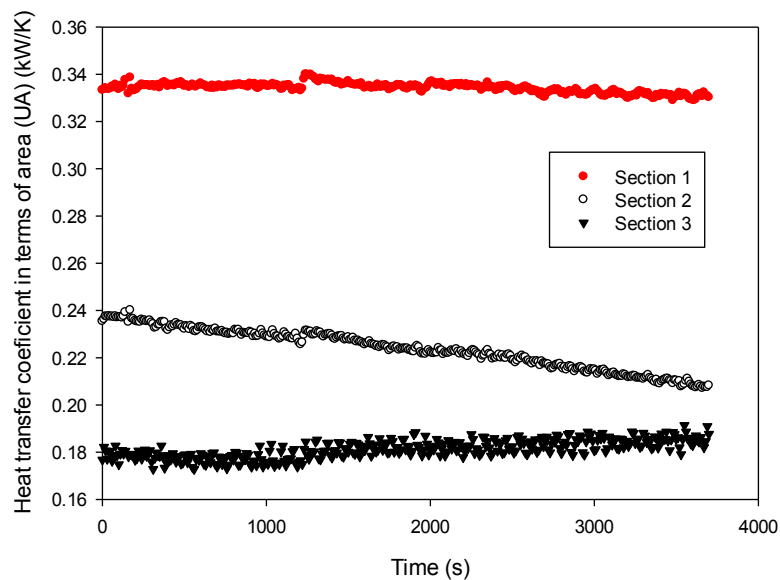


Figure 4.12: Fouling behaviour according to heat transfer coefficient in terms of area (UA) at each section of PHE for WPC_{m/2} processed at flow rate 100 l/h, section 3 outlet temperature 95°C.

Figure 4.13 and Figure 4.14 show no difference in fouling behaviour in terms of pressure drop between the three modified fluids at temperature below 95°C. However, the fouling behaviour in terms of UA revealed that the solution with twice the amount of calcium and phosphates than true milk gave a slightly lower UA than the other fluids.

It was noted that during the preparation of WPC with added minerals, the pH of the solution changed from 6.5 to 5. Thus, the changes observed by the addition of calcium and phosphorus salts might also be due in part to the change in pH. It is clear that adding calcium and phosphate salts (with the decline in pH) lowers the fouling rate and changes the composition of the deposit to give extensive fouling at much lower temperature, as discussed in section 2.2.3.1. For WPC, significant fouling did not start until the temperature was greater than 90°C. However, for WPC with added minerals, extensive fouling occurred at temperature less than 90°C.

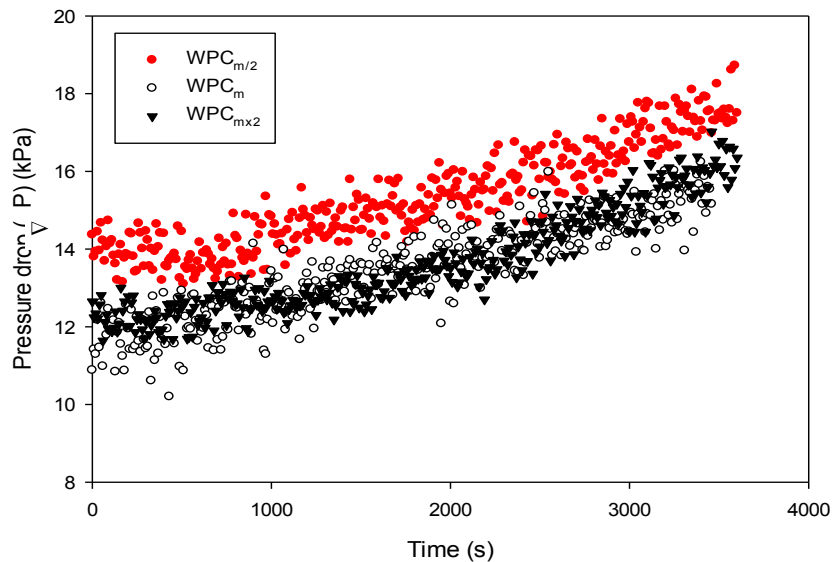


Figure 4.13: Fouling behaviour in terms of pressure drop at section 2 for WPC_{m/2} processed at flow rate 100 l/h, section 3 outlet temperature 95°C.

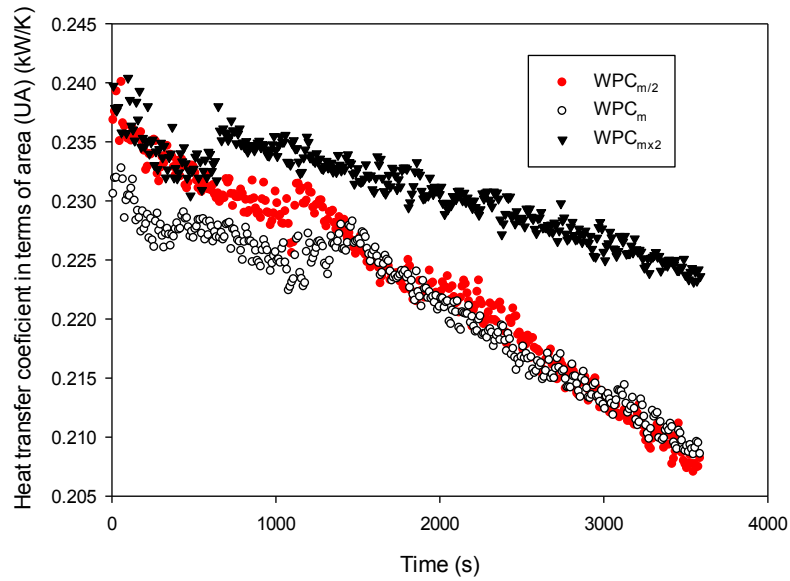


Figure 4.14: Fouling behaviour according to heat transfer coefficient in terms of area (UA) at section 2 for $WPC_{m/2}$ processed at flow rate 100 l/h, section 3 outlet temperature 95°C.

4.4 Cleaning experiments profile

It has been noted earlier in section 3.2 that deposits formed by milk and other dairy products cannot be removed by water alone. Therefore, two cleaning solutions were used: alkaline cleaning solutions to mainly remove proteinaceous deposits, and the acidic solutions to remove mineral deposits. The cleaning behaviours of deposits produced at pasteurising temperature of 95°C for WPC and the three modified fluids have been compared to one another. For investigating the effect of cleaning conditions on removal, the combined influence of the following conditions was studied:

- (i) Experiment conditions for cleaning WPC deposits are:
 - Chemical concentration (including 0.1, 0.5 and 1.0 wt% NaOH).
 - Flow rate (100, 150 l/h).

- Cleaning temperature (95°C at the outlet of section 3).
- (ii) Experiment conditions for cleaning WPC with adding mineral (WPC_{m/2}, WPC_m and WPC_{m×2}) deposits are:
- Chemical concentration (0.5wt% NaOH and P3-horolith V based on nitric acid 1wt.%).
 - Flow rate (100 l/h).
 - Cleaning temperature (95°C at the outlet of section 3 of the PHE).

The experiments were carried out in two halves: firstly, the PHE was fouled using one of the four fluids; secondly, the deposit was cleaned. During the deposit formation, experimental conditions were kept as similar as possible between experiments in order to replicate the deposits in composition and quantity, hence reducing the experimental error in the cleaning processes.

Each cleaning experiment was carried out following the procedures discussed in section 3.8, and applying the appropriate processing conditions. At the end of each fouling experiment, flow was diverted to draw from the soft water tank. The cooling water was switched off and the PHE was thermally stabilised for the appropriate cleaning conditions. After a minimum of 10 minutes of thermal stability, data recording was initiated, time recorded, and the flow diverted from the soft water to the cleaning chemical tank to initiate the commencement of the cleaning of the deposit. The progress of cleaning was followed by recording plant pressure and temperature readings at each section of the PHE. Once the pressure drop reading had reached the clean state and remained at these values for at least 10 minutes, the PHE was considered clean. Flow was diverted to draw from the soft water tank again, with the PHE being cooled down as described in section 3.8. If

the WPC with added minerals was deposited in PHE, the cleaning by acid solution was only applied after the application of the alkaline solution, which lasted till the pressure drop reading achieved the clean state and remained at these values for at least 10 minutes.

4.4.1 Result and discussion of cleaning experiments of WPC deposit

The effect of changing one of the two process variables, i.e. flow rate and chemical concentration, was investigated for WPC deposit individually to establish an optimum cleaning chemical concentration for pasteurisation deposit in a pilot scale PHE. The model fouling fluids developed in the previous sections were also used to investigate the cleaning behaviour of these fluids at a cleaning temperature of 95°C.

Typical changes in pressure drop and overall heat transfer coefficient in terms of area (UA) with time recorded during standard PHE cleaning experiments are given in Figure 4.15 and Figure 4.16 for the individual sections. From Section 4.3.1.1, it can be observed that the extent of WPC fouling significantly increases with temperature, therefore giving the greatest amount of fouling in section 3 of the PHE; as a result, most of the changes in pressure drop during cleaning arise from section 3 too. Small changes in pressure drop are observed in section 2, although to a significantly less extent than section 3. No change in pressure drop occurs in section 1, suggesting that there is insignificant fouling in this section. Throughout this discussion, time $t = 600$ seconds refers to the time where the diverter valve was switched to draw cleaning chemicals from the tank used as the datum point, since the PHE did not allow time of entry of the cleaning chemical into an individual section of PHE to be determined. A lag time of ca. 105 seconds occurs before the cleaning solution reaches section 3. The pressure drop and the heat transfer coefficient in terms of area (UA) are steady during this time. Typical changes in pressure

drop and UA recorded during standard PHE cleaning experiments are given in Figure 4.15 and Figure 4.16 for the individual sections of PHE. Most of the change in pressure drop and UA of the whole PHE during cleaning arises from changes in the section 3; the majority of deposit is in this section. Small changes are observed in the section 2, although to a significantly less extent than section 3. No change in pressure drop and UA occur in the section 1, suggesting there is insignificant fouling in this section.

Upon contact with cleaning chemical the deposit swells, whereby increasing the pressure drop by nearly a factor of four in the case shown in Figure 4.15. The pressure drops for section 3 then decreases to a steady clean value (ΔP) of ca. 4 kPa. The extent of swelling and the time taken to reach the clean value are a function of process conditions such as cleaning solution and flow rate.

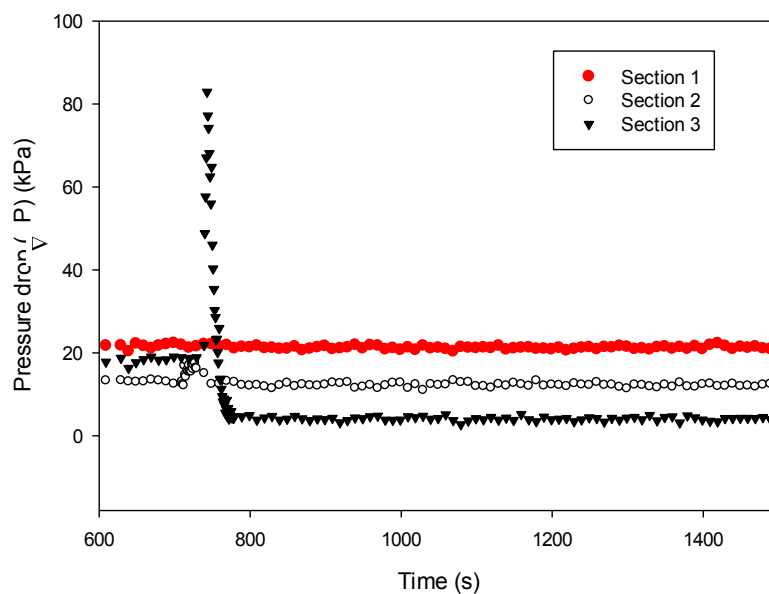


Figure 4.15: Cleaning behaviour in terms of pressure drop for each section of the PHE for WPC (β -Lg 0.3%) processed at flow rate 100 l/h, section 3 outlet temperature 95°C and chemical concentration 0.5wt%, NaOH.

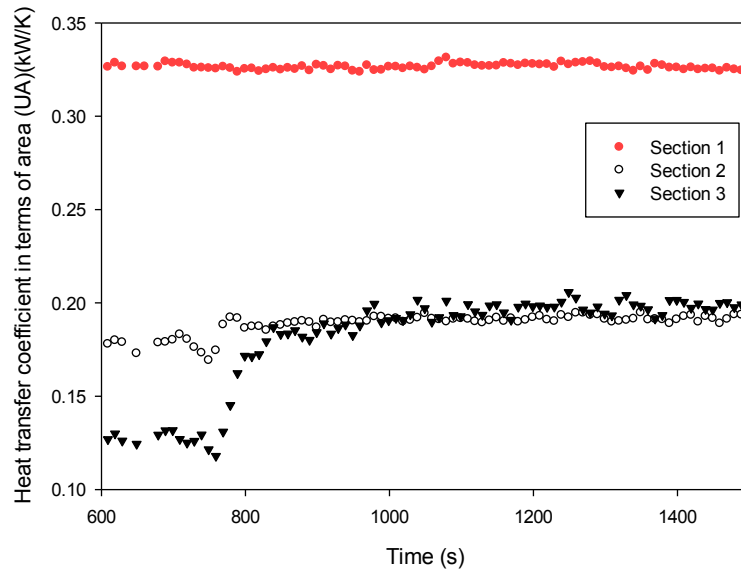


Figure 4.16: Cleaning behaviour according to heat transfer coefficient in terms of area (UA) for each section of the PHE for WPC (β -Lg 0.3%) processed at flow rate 100 l/h, section 3 outlet temperature 95°C and chemical concentration 0.5wt%, NaOH.

Figure 4.16 shows a typical thermal recovery profile obtained during cleaning of the PHE. An initial reduction in heat transfer coefficient in terms of area (UA) was observed due to swelling of the deposit in contact with the cleaning chemical. A minimum of UA was observed in each case before the UA recovery rapidly increased until achieving a steady value for the clean system.

4.4.1.1 Effect of process parameters

Usually, cleaning time is short when chemical concentration or flow rate is high; if not, a combination of process parameters such as flow rate and chemical concentration is needed to enhance the cleaning process (as discussed in section 2.3.2). Therefore, to shorten the cleaning time, (i) increasing chemical concentration and (ii) increasing flow rate are required. The influence of each parameter on the cleaning behaviour is discussed below.

4.4.1.1.1 Flow rate

Cleaning rates are usually found to increase with an increased flow rate. Two different flow rates were investigated: 100 and 150 l/h. Figure 4.17 to Figure 4.20 show the effect of the cleaning flow rate for two WPC deposits produced at the fouling flow rate (100 and 150 l/h), and β -Lg (0.1, 0.3 and 0.5%) on cleaning time has been investigated. Figure 4.17 shows that the ΔP for the deposit produced at β -Lg 0.5wt% was higher than other β -Lg concentrations (0.1 and 0.3wt.%). This was due to the greater degree of fouling and, therefore, a thicker deposit that results at higher β -Lg concentration; ΔP stays high for a considerable time. It also shows two peaks in ΔP suggesting swelling of the deposit of β -Lg 0.3 and 0.5wt. %. Changes in ΔP was more difficult to discern at β -Lg 0.1wt.% than the other sections as insignificant fouling at this concentration.

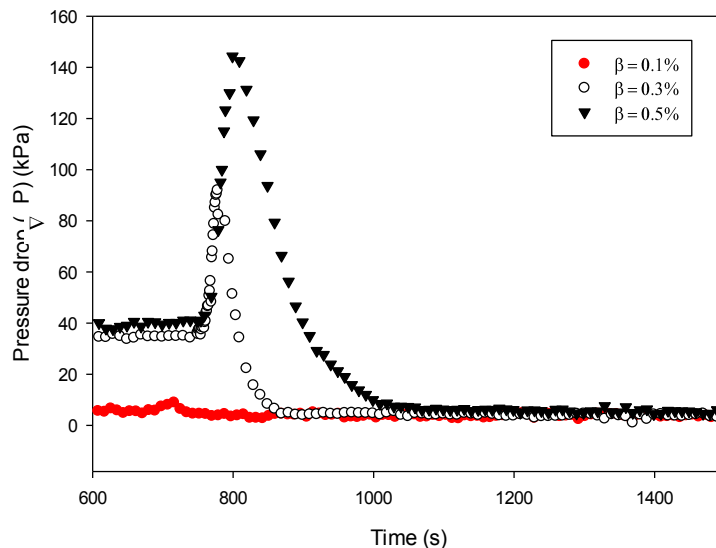


Figure 4.17: Cleaning behaviour in terms of pressure drop for WPC at section 3, β -Lg (0.1, 0.3 and 0.5%), processed flow rate 100 l/h, chemical concentration 0.1wt% NaOH, and section 3 outlet temperature 95°C.

Cleaning behaviour in terms of UA was mirrored to that of ΔP as seen in Figure 4.18. Upon contact with the cleaning solution two reductions in UA were occurred after 780 sec., which corresponded to the point at which the ΔP reached a maximum value for two deposit formed at β -Lg 0.3 and 0.5wt.% . As there is very little fouling for deposit formed at β -Lg 0.1wt. %, significant changes were not expected.

The time to clean for β -Lg 0.5% in terms of ΔP was much lower than UA, 8 and 14 minutes, respectively.

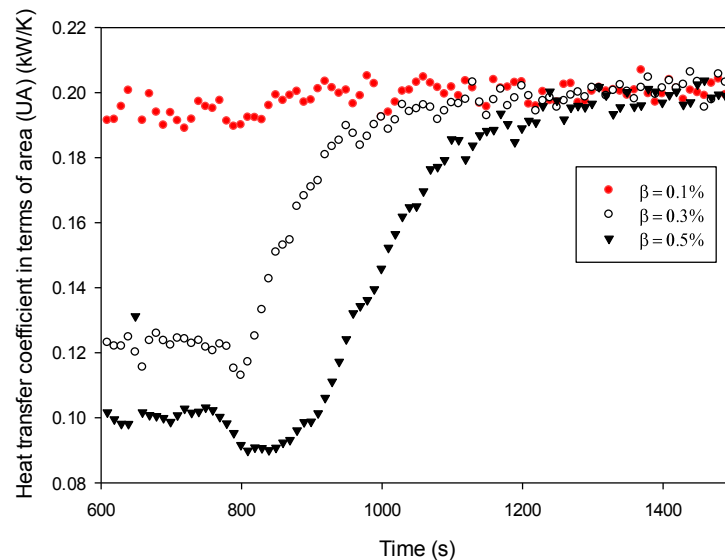


Figure 4.18: Cleaning behaviour according to heat transfer coefficient in terms of area (UA) for WPC at section 3, β -Lg (0.1, 0.3 and 0.5%), processed flow rate 100 l/h, chemical concentration 0.1wt% NaOH, and section 3 outlet temperature 95°C.

The influence of the high fluid flow on the deposit cleaning profile, at 95°C, is shown in Figure 4.19 and Figure 4.20. Large swelling was occurred for the deposit formed at β -Lg 0.5%, followed by the deposit formed at β -Lg 0.3%, and finally the deposit formed at β -Lg 0.1% at flow rate 150 l/hr. ΔP at the start of these experiments was much lower (ca. 20 kPa) than the deposit formed at 100 l/h (ca. 40 kPa). However, a reverse trend was

observed, i.e. a large increase in the ΔP at flow rate 150 l/h. Although the flow rate was high (150 l/h), the WPC deposit formed at flow rate 150 l/h showed higher resistance to removal. This may suggest that the deposit produced at a high flow rate during the fouling process was more compact. The time to clean in terms of pressure drop for deposit formed at β -Lg 0.5% and flow rate 150 l/h was considerably long compared to deposit formed at flow rate 100 l/h 5600 and 480 seconds respectively. These results show clearly how the changing in the fouling process flow rate can affect the rate and extent of the cleaning process.

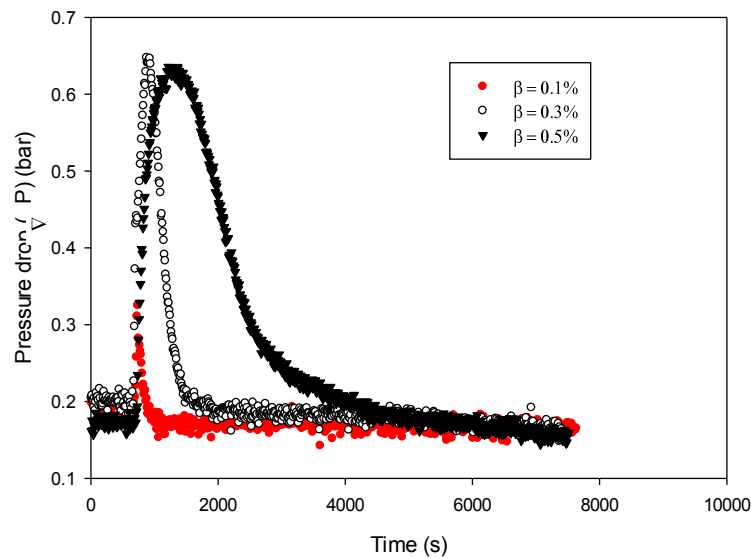


Figure 4.19: Cleaning behaviour in terms of pressure drop for WPC at section 3, β -Lg (0.1, 0.3 and 0.5%), processed flow rate 150 l/h, chemical concentration 0.1wt% NaOH, and section 3 outlet temperature 95°C.

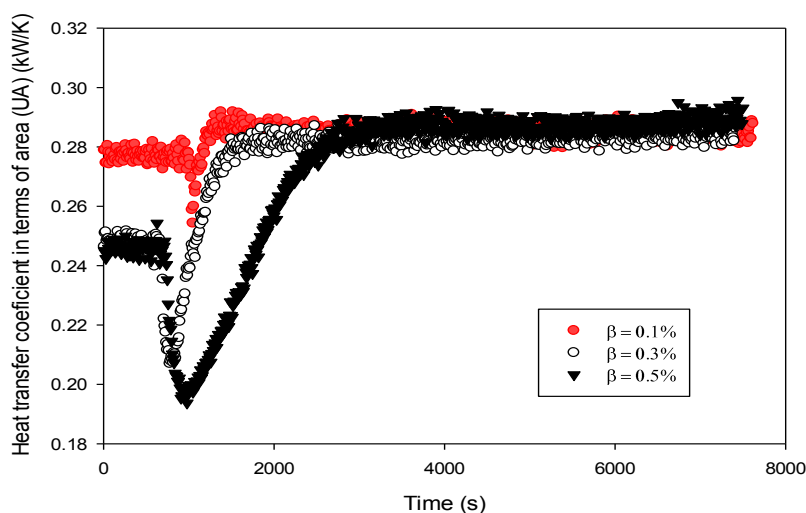


Figure 4.20: Cleaning behaviour according to heat transfer coefficient in terms of area (UA) for WPC at section 3, β -Lg (0.1, 0.3 and 0.5%), processed flow rate 150 l/h, chemical concentration 0.1wt% NaOH, and section 3 outlet temperature 95°C.

4.4.1.1.2 Chemical concentration

Cleaning profiles at different chemical concentrations are shown in Figure 4.21 to Figure 4.28. The behaviour of the cleaning profiles is similar to that found by previous authors studying WPC deposit removal on a PHE produced at UHT temperature (Changani (2000) and Christian and Fryer (2006)). Generally, increasing the cleaning solution from 0.1 to 1wt.% NaOH narrows the pressure drop peak, i.e cleaning times decrease. Beyond a clean chemical concentration of 0.5 wt.% NaOH this reduction in cleaning time was less apparent. It is likely that at concentrations greater than 0.5 wt.% the deposit is changed so that it is less susceptible to fluid shear (as discussed in 2.3.2.2); this can be seen in Figure 4.21 and Figure 4.22. At all β -Lg concentrations and flow rates, increasing cleaning solution from 0.5 to 1 wt% NaOH does not significantly change the cleaning time and behaviour. At this level of NaOH concentration, chemical influence is expected to be stronger than fluid flow, so different levels of flow do not give much effect on cleaning time. These results suggest that the optimum concentration for the cleaning of

why protein deposit clearly exists around 0.5 wt% NaOH at section 3 outlet temperature 95°C. This optimal concentration has been reported by Bird (1992) and Tuladhar et al. (2002) as discuss in section 2.3.2.2.

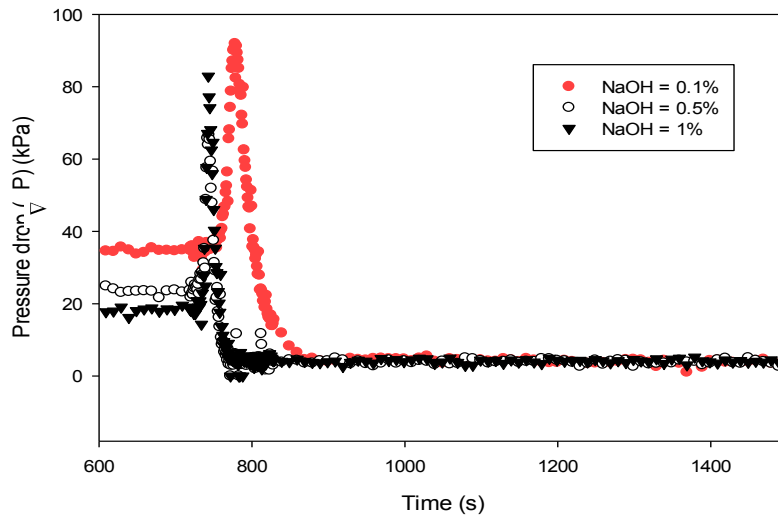


Figure 4.21: Cleaning behaviour in terms of pressure drop for WPC at section 3, β -Lg 0.3%, processed flow rate 100 l/h, and section 3 outlet temperature 95°C.

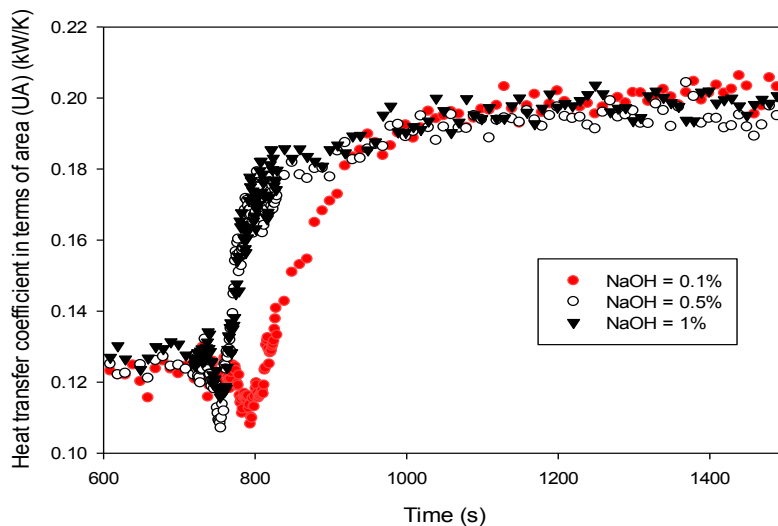


Figure 4.22: Cleaning behaviour according to heat transfer coefficient in terms of area (UA) for WPC at section 3, β -Lg 0.3%, processed flow rate 100 l/h, and section 3 outlet temperature 95°C.

The cleaning time for the deposit produced at β -Lg 0.3wt.%, β -Lg 0.5wt.%, and flow rate 100 l/h is similar at cleaning solution concentration 0.5 and 1wt.%NaOH (see Figure 4.23 and Figure 4.24). However, the cleaning time with respect to recovery of pressure drop decreased drastically from 2100 to 300 seconds (86%) when β -Lg decreased from 0.5 to 0.3wt.% at cleaning concentration 0.1% NaOH and flow rate 100 l/h, but after chemical concentration 0.5wt.% NaOH, the cleaning time do not change significantly (see Figure 4.21 and Figure 4.23) .

The cleaning time in terms of pressure drop decreased drastically from 5600 to 1585 seconds (72%) when β -Lg decreased from 0.5 to 0.3wt.% at cleaning concentration 0.1% NaOH and flow rate 150 l/h; this can be seen in Figure 4.25 and Figure 4.27.

Cleaning behaviour with respect to recovery of UA was mirrored that of ΔP . Generally, the time to clean in terms of UA is longer than ΔP . At lower flow rate 100 l/h, the cleaning time in terms of UA decreased drastically from 2170 to 970 seconds (55%) when β -Lg decreased from 0.5 to 0.3wt.% at cleaning concentration 0.1% NaOH (see Figure 4.22 and Figure 4.24). The cleaning time in terms of UA decreased rapidly from 3000 to 1100 seconds (63%) when β -Lg decreased from 0.5 to 0.3wt.% at cleaning concentration 0.1% NaOH and flow rate 150 l/h; this can be seen in Figure 4.26 and Figure 4.28. Since the minimum chemical concentration changed with a change in flow rate and β -Lg concentration, the rate and the extent of cleaning were affected. Although higher chemical concentration would make removal of the deposit from the PHE even more rapid, there is clearly no advantage in an excessively high cleaning chemical concentration; such a fluid will have high cost, will cause greater corrosive damage and will be more difficult and expensive to dispose of.

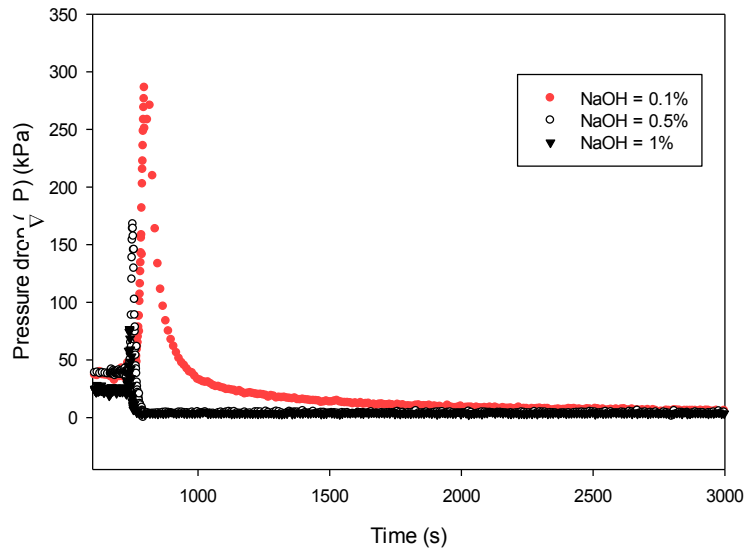


Figure 4.23: Cleaning behaviour in terms of pressure drop for WPC at section 3, β -Lg 0.5%, processed flow rate 100 l/h, and section 3 outlet temperature 95°C.

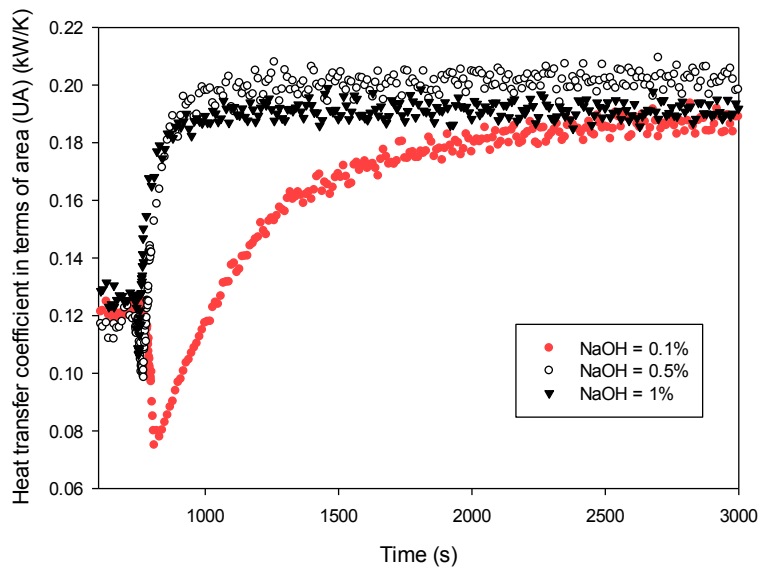


Figure 4.24: Cleaning behaviour according to heat transfer coefficient in terms of area (UA) for WPC at section 3, β -Lg 0.5%, processed flow rate 100 l/h, and section 3 outlet temperature 95°C.

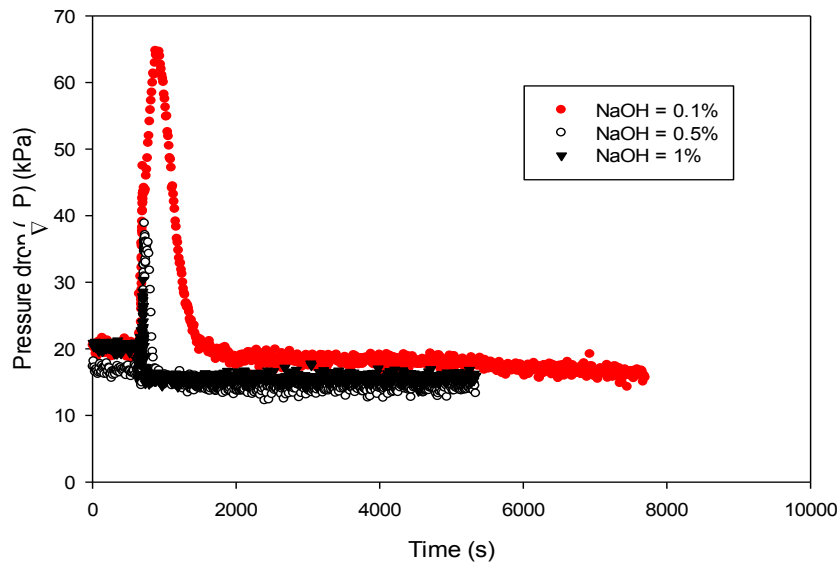


Figure 4.25: Cleaning behaviour in terms of pressure drop for WPC at section 3, β -Lg 0.3%, processed flow rate 150 l/h, and section 3 outlet temperature 95°C.

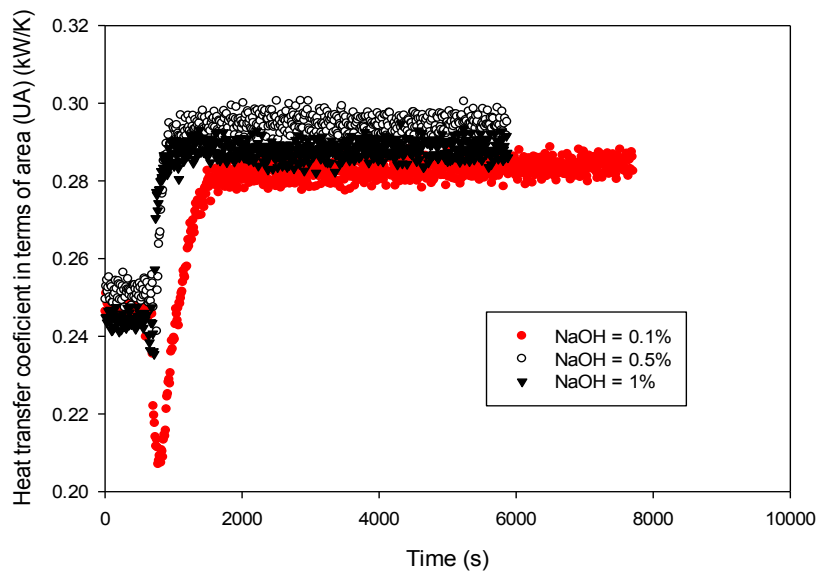


Figure 4.26: Cleaning behaviour according to heat transfer coefficient in terms of area (UA) for WPC at section 3, β -Lg 0.3%, processed flow rate 150 l/h, and section 3 outlet temperature 95°C.

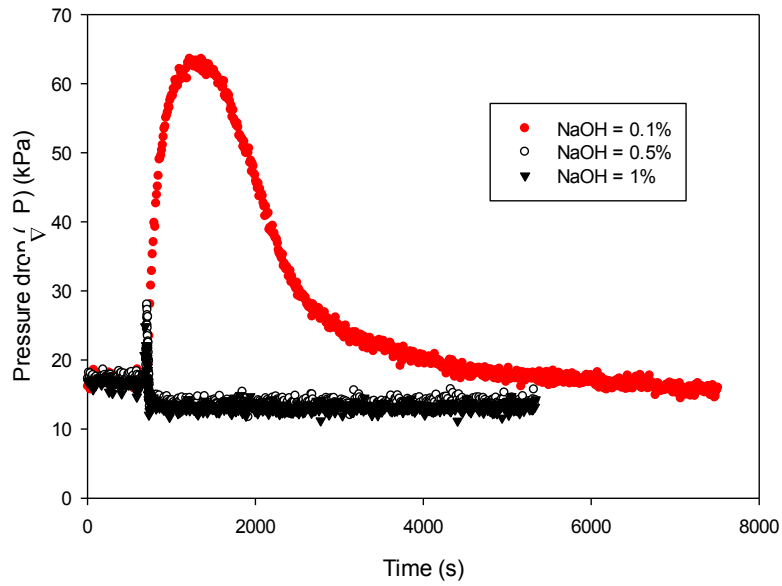


Figure 4.27: Cleaning behaviour in terms of pressure drop for WPC at section 3, β -Lg 0.5%, processed flow rate 150 l/h, and section 3 outlet temperature 95°C.

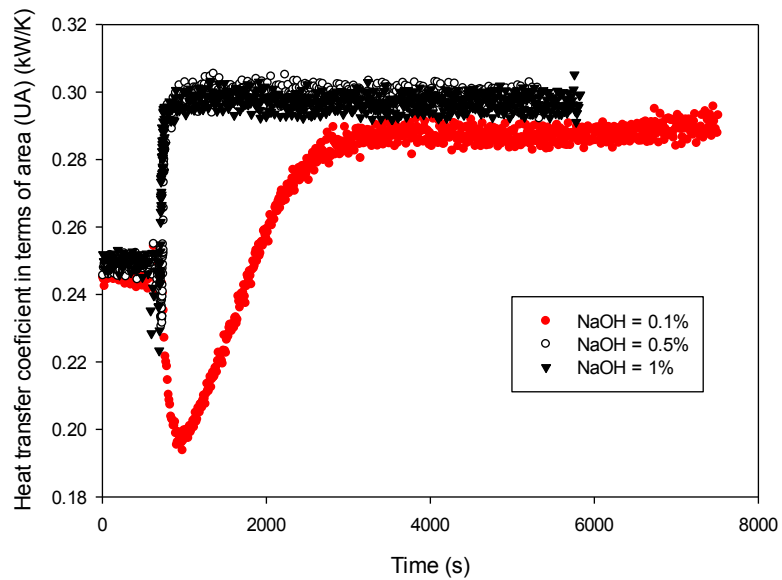


Figure 4.28: Cleaning behaviour according to heat transfer coefficient in terms of area (UA) for WPC at section 3, β -Lg 0.5%, processed flow rate 150 l/h, and section 3 outlet temperature 95°C.

4.4.2 Result and discussion from cleaning experiments of WPC with adding minerals deposit

Figure 4.29 to Figure 4.34 give cleaning profiles obtained during removal of the WPC deposit in terms of (a) changes in pressure drop and (b) changes in overall heat transfer coefficient in terms of area (UA) with time. Section 2.2.4 notes that WPC is deficient in minerals and adding calcium and phosphorus salts to WPC it has proven possible to change the fouling behaviour to be similar to milk fouling behaviour. Therefore, the cleaning of WPC with adding minerals has shown different behaviour from cleaning behaviour of WPC. Most of the change in pressure drop during cleaning arises from changes in section 2; the majority of deposit is in this section. Slight changes are observed in section 1, although to a significantly less extent than section 2. No change in pressure drop occurs in section 3, suggesting there is insignificant fouling in this section.

- At low mineral content ($WPC_{m/2}$), the cleaning behaviour resembles cleaning behaviour of WPC as seen in Figure 4.29. It shows a very large peak in ΔP (25 kPa above the fouled condition) in section 2, and then declined rapidly to a clean state. No change in pressure drop occurs in the section 1 and 3, suggesting there is insignificant fouling in these sections.

There was no change in ΔP when acid rinse was introduced in all sections of PHE, suggesting that the remaining minerals deposit cannot be detected by a pressure drop sensor.

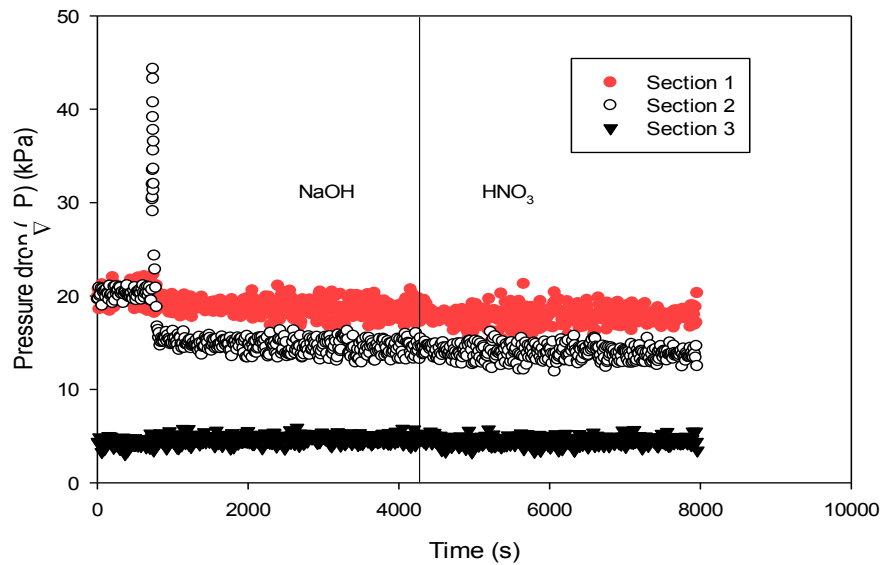


Figure 4.29: Cleaning behaviour in terms of pressure drop for $WPC_{m/2}$ at all sections of PHE, β -Lg 0.3%, processed flow rate 100 l/h, and section 3 outlet temperature 95°C .

Figure 4.30 shows fouling behaviour in terms of UA in all sections of the PHE. The trends for the tree section mirror the observation of fouling behaviour with respect to ΔP discussed above. Initially, there was a small decline in UA, at section 2, which started around the time of the start of the decline in ΔP from the peak maximum. Then UA rose again to the value under a clean state and settled there until the cleaning with 1wt. % acid was introduced at 4200 seconds, which allowed the remaining mineral deposit to be removed. However, a slight increase in UA at section 1 when acid rinse was introduced; with no change in UA at section 3, it suggested no significant fouling in this section.

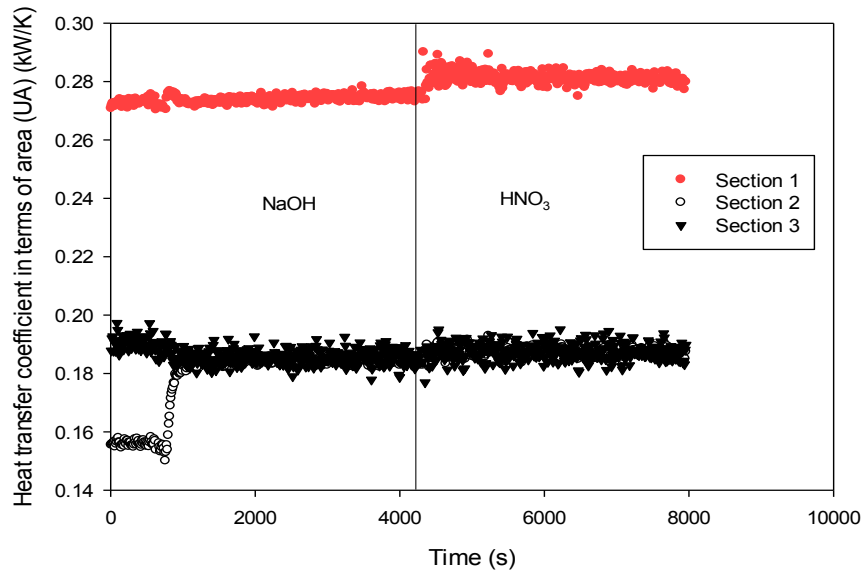


Figure 4.30: Cleaning behaviour according to heat transfer coefficient in terms of area (UA) for $WPC_{m/2}$ at all sections of PHE, β -Lg 0.3%, processed flow rate 100 l/h, and section 3 outlet temperature 95°C.

- For cleaning WPC_m deposit, although ΔP at the start of the cleaning experiment for section 2 was higher than that for $WPC_{m/2}$, the pressure peak was smaller (11 kPa above the fouled condition) than that for $WPC_{m/2}$. That was evident of the change of cleaning behaviour with increasing minerals in WPC solution. Initially, there was a rapid increase in ΔP similar to cleaning behaviour of $WPC_{m/2}$ deposit. It then dramatically declined in ΔP to above the level of the clean state, and ΔP remained constant during alkaline cleaning; as can be seen in Figure 4.31. This indicated that section 2 was still unclean. When acid solution was introduced, there was an abrupt decline to the clean state observed for ΔP . For UA at section 2, two increases in UA values were observed at the time of introducing sodium hydroxide and acid solution as shown in Figure 4.32.

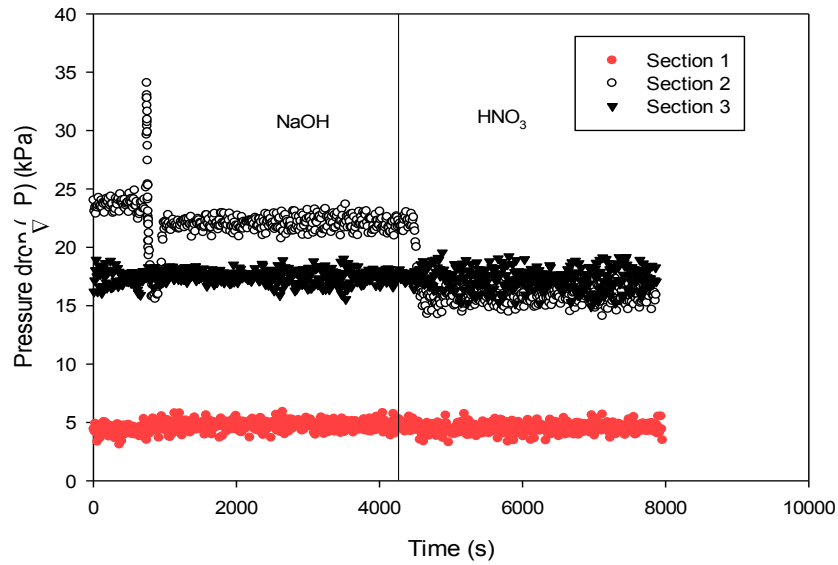


Figure 4.31: Cleaning behaviour in terms of pressure drop for WPC_m at all sections of PHE, β -Lg 0.3%, processed flow rate 100 l/h, and section 3 outlet temperature 95°C.

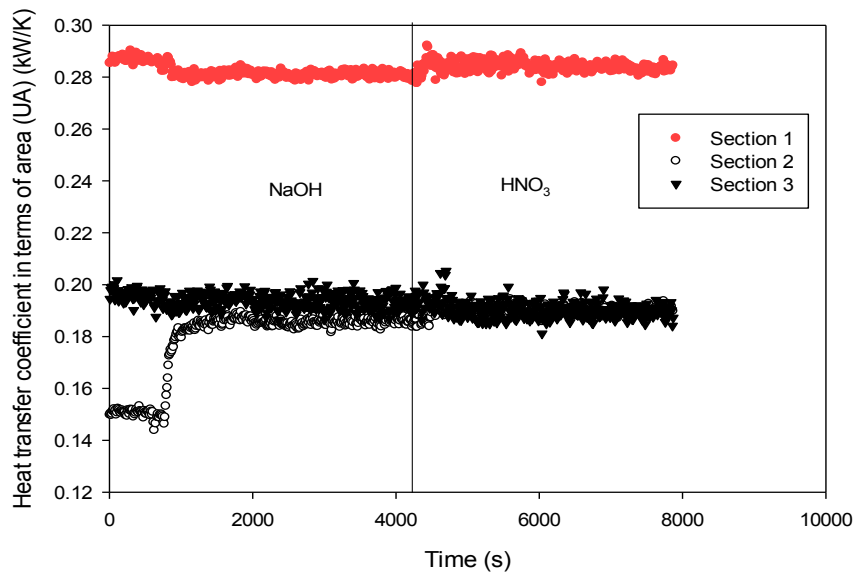


Figure 4.32: Cleaning behaviour according to heat transfer coefficient in terms of area (UA) for WPC_m at all sections of PHE, β -Lg 0.3%, processed flow rate 100 l/h, and section 3 outlet temperature 95°C.

At section 1 there was a slight increase in ΔP during cleaning with sodium hydroxide. Pressure remained constant and then abruptly decreased when the cleaning with acid was introduced, as shown in Figure 4.31. This behaviour was reported by Jeurnink and Brinkman (1994) who observed that, during cleaning protein deposit in tubular heat exchanger and evaporator, the contact of the acid cleaning solution with the protein in the deposit layer did not result in swelling. This may be due to the bonds within the deposit being stronger or more numerous than the attachment of the deposit to the stainless steel. This behaviour was also proven by UA in Figure 4.32. There was a small decline in UA around the time of the start of increases in ΔP , keeping steady till the cleaning with acid solution is commenced. This indicates that the protein is entrapped in the calcium phosphate matrix (see Table 5.1). No noticeable changes are observed in ΔP and UA at section 3 suggesting no measurable fouling occurred in that section.

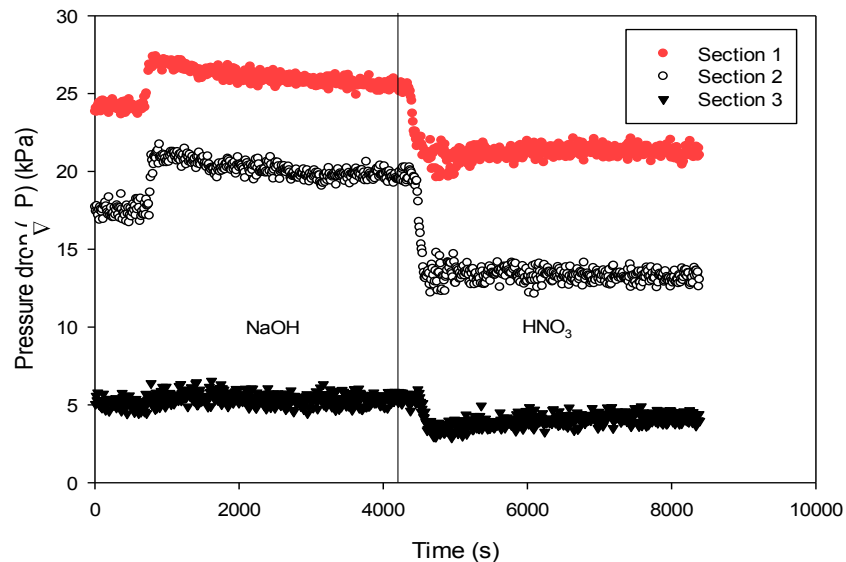


Figure 4.33: Cleaning behaviour in terms of pressure drop for WPC_{mx2} at all sections of PHE, β -Lg 0.3%, processed flow rate 100 l/h, and section 3 outlet temperature 95°C.

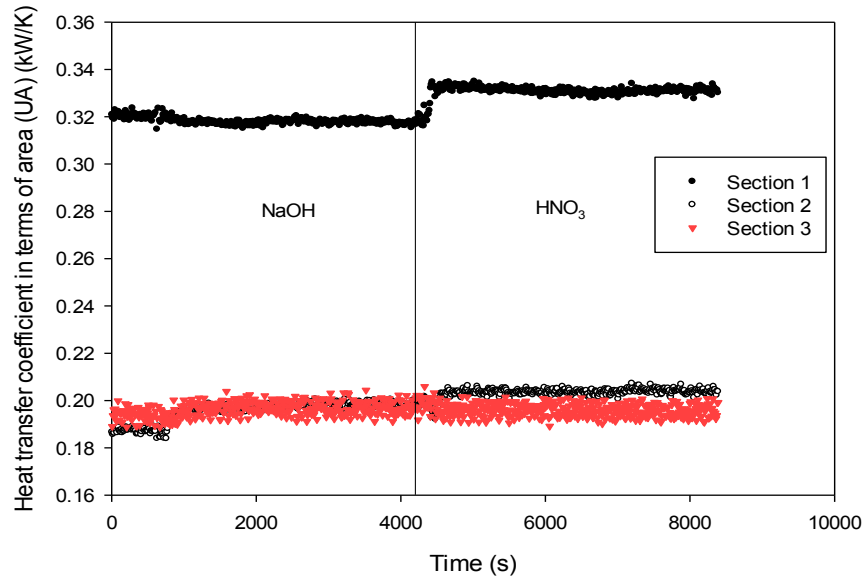


Figure 4.34: Cleaning behaviour according to heat transfer coefficient in terms of area (UA) for WPC_{mx2} at all sections of PHE, β -Lg 0.3%, processed flow rate 100 l/h, and section 3 outlet temperature 95°C.

- For cleaning WPC_{mx2} deposit, upon contact with cleaning chemicals the deposit swells in all sections of PHE, increasing the pressure drop to a certain amount and settling at that point as shown in Figure 4.33. UA in section 1 shows a slight decrease during alkaline cleaning. This suggested that the minerals present within the protein matrix are dominant and cannot be removed by NaOH solution alone. There were two increases in UA value in section 2 as a result of alkaline cleaning and acid cleaning as shown in Figure 4.34. Section 3 shows slight changes in ΔP and UA which indicate that the section starts to foul more noticeably with increasing minerals in WPC solution. Therefore, two increases in UA value in section 3 as a result of alkaline cleaning and acid cleaning.

4.5 Conclusion

Experiments have been conducted to quantify the effects of changing β -Lg concentration on the fouling process. Processing WPC solution at different β -Lg concentrations results in a proteinaceous deposit (see Table 5.1) only in section 3 of the PHE, as the extent of fouling increased with increasing temperature. However, no fouling was observed at β -Lg 0.1%, suggesting that the amount of reacted protein was insignificant. The fouling rate increased significantly with increasing β -Lg concentration from 0.1% to 0.3%, and then the fouling rate increased slightly when β -Lg increased to 0.5%. As the flow rate increases, the total amount of fouling decreases, as a result of increasing shear rate and decreasing the residual time in PHE for the whey protein solution.

The extent of deposits formed depends on the product processed and the processing conditions. Altering the composition of the WPC solution has a significant influence on the fouling profiles observed (as mentioned in section 3.2.3). Adding calcium and phosphorus salts back to WPC has lowered deposition temperature. The majority of fouling has occurred at temperature less than 90°C. No significant fouling was measured across section 3 of the PHE. The fouling rate of WPC with added minerals was considerably lower than WPC. These differences in deposit chemistry had a measurable effect on the cleaning process behaviour.

Cleaning experiments have been conducted for the four fluid models over a range of chemical concentrations and flow rates, using the PHE. Initial increases in pressure drop and decreases in heat transfer can be seen, due to swelling of deposit. Increasing in heat transfer follows the subsequent removal of the deposit from the heat exchanger surface as well as pressure drop change. Significantly different cleaning times arose for the different conditions investigated: chemical concentration and flow rate. In all cases, increasing the

concentration from 0.1 to 0.5 wt% has a significant effect on the time to clean of each flow rate. There was no significant effect on cleaning time when chemical concentration increased from 0.5 to 1% (NaOH). Therefore, a chemical concentration optimum at 0.5 wt.% at section 3 outlet temperature 95°C is found. The WPC deposit formed at 150 l/h appeared to be hard to remove at 0.1% NaOH, suggesting that the deposit was compact. However, increasing the chemical concentration to 0.5% NaOH was sufficient to clean the PHE at that condition within 5 minutes.

Cleaning of WPC and WPC with adding mineral deposit has shown that very different behaviour is seen. In general, decreasing the mineral content to be added to WPC solution leads to cleaning behaviour similar to WPC deposit without the addition of minerals. The cleaning behaviour of WPC_{m/2} is similar to cleaning behaviour of WPC deposit without the addition of minerals, as the minerals added were little. Sodium hydroxide (NaOH) can remove part of the deposit when minerals are added to WPC to the same level as milk and the remaining mineral deposit can be removed by acid solution.

CHAPTER 5 : COMPARISON OF A LAB SCALE FOULING RIG TO GENERATE DEPOSITS SIMILAR TO A HEAT EXCHANGER

5.1 Introduction

Fouling and cleaning are costly operational issues for a manufacturing plant especially in the food and beverage industry. This is due to the heating of multiple process steps to develop flavour, structure and to kill microbes detrimental to product quality and safety (Fryer and Robbins, 2005). Any non-production activity in a manufacturing plant is considered a monetary loss. Due to the drive for continuous production, access to the plant for non-routine investigation is often restricted with only narrow time frames being allocated for on-plant investigations. Unfortunately, this often means data acquired from online investigation is limited or inconclusive. For this reason there is clear merit in investigating fouling and cleaning phenomena at the bench scale rather than the production scale. Bench scale investigations can be conducted offline (separate to production), whereby minimising cost, time and risk to product quality and safety. Therefore, obtaining lab scale findings with direct application to an industrial plant is crucial to plant optimisation and innovation. Literature detailing the application of small scale findings to an industrial plant is scarce.

Chapter 4 has noted that the plant measurements used, i.e. pressure sensor and heat transfer coefficient, were capable only of quantifying the fouling globally. It was not practical to dismantle the PHE to measure the fouling in each plate. The rig used in the

experiments of this chapter was intended to facilitate controlling surface temperature and quantifying fouling locally, together with easy assembling and dismantling during experimental work.

The mechanism of deposit formation is not well understood (Jun and Irudayaraj, 2009). The literature in section 2.2.2.2 indicates that deposit formation results from a combination of mass transfer, surface and bulk temperature. Knowledge of the role of surface and bulk temperature in deposit formation might well help reduce both deposit formation during processing of heat sensitive fluids and aid development of cleaning strategies.

The aim of this work is to (i) present a lab scale rig designed to create fouling similar to a heat exchanger, and (ii) investigate the effect of bulk and surface temperatures at 70, 80, and 90°C on the fouling behaviour of the two model solutions WPC and WPC_m in terms of deposit thickness, weight and morphology. The hope is that scale-up rules can be developed using a model foulant. WPC and WPC_m with added minerals are used here as a model fouling fluid similar to other studies (Changani, 2000, Christian et al., 2002). This small-scale rig could be used to determine fouling innovations directly applicable to industry produced at reduced cost and time.

5.2 Details of the investigation

Section 3.4 describes an experimental procedure by which proteinaceous dairy deposits are formed from heated WPC solution on a stainless steel coupon. A bench-scale fouling rig is described in section 3.4, with the operating procedure being given (section 3.7). A series of fouling experiments on the WPC and WPC_m deposits were carried out in the

bench-scale fouling rig. The surface, bulk temperature and β -Lg concentration are investigated. In these experiments, β -Lg was increased to 0.6 wt.%, due to the variation of WPC composition, which consequently leads to the small amount of fouling at 0.3wt.% compared to that obtained in the fouling experiments under similar conditions (see Chapter 4). Also, the temperature was selected at 90°C, instead of 95°C, due to the removal of the pipe that connects the cooling section outlet to the preheat section which in turn reduces the outlet preheat temperature.

The experimental conditions are given below. The combined influence of the following conditions was studied:

Experiment conditions for WPC are:

- Concentration of β -Lg (0.6, 1%).
- Flow rate (100 l/h).
- Bulk temperatures (70, 80 and 90°C).
- Surface temperature (98°C).

Experiment conditions for WPC_m are:

- Concentration of β -Lg (0.6%).
- Flow rate (100 l/h).
- Bulk temperatures (70, 80 and 90°C).
- Surface temperature (98°C).

Experiment conditions for surface effect of WPC are:

- Concentration of β -Lg (0.6%).

- Flow rate (100 l/h).
- Bulk temperatures (80°C).
- Surface temperatures (80, 89 and 98°C).

Experiment conditions for surface effect of WPC_m are:

- Concentration of β -Lg (0.6%).
- Flow rate (100 l/h).
- Bulk temperature (80°C).
- Surface temperatures (80, 89 and 98°C).

To design equipment, it is necessary to understand fouling reactions, and where they occur within the equipment (Belmar-Beiny et al., 1993). It may be possible that one process controls the fouling rate over a range of temperatures and WPC concentrations. If surface reaction contributes to fouling, deposition will be a function of wall temperature. But if the fouling takes place in bulk, then the amount of fouling should increase with increasing bulk temperature.

The PHE was used here to heat up the WPC solution to the desired temperature before entering the test section. The test section's heater was switched on and the desired surface temperature was set at 30 minutes before starting the fouling experiment. Once fouling solution was prepared and the PHE was thermally stabilised, the flow was diverted from soft water to draw from the fouling solution tank, i.e. to commence the fouling experiment. The progress of fouling was followed by recording the plant measurements: pressure and temperature. At the end of fouling experiments, the flow was diverted again

to draw from the soft water tank, and the PHE was cooled down (as described in section 3.7).

Once the PHE was cooled down and all associated equipment was turned off, the test section was dismantled (see section 3.7). The fouled coupons were removed, weighed, and the thickness of the deposit formed was measured by the micromanipulation rig, detailed in Liu et al. (2002).

The whey protein solution here was not recirculated in order to be able to control the residence time of the protein solution at high temperature and to eliminate the possibility of fouling from material that had already passed through the system.

5.3 Results and discussion

5.3.1 Effect of β -Lg concentration and temperature on fouling rate

It was mentioned earlier in section 2.2.3.4, that fouling increased significantly when the temperature in the turbulent core of the fluid exceeded that at which the protein becomes thermally unstable, suggesting that deposition was occurring from material formed in the turbulent core (Obeng and Hoare, 1988). In this work, the experiments were conducted in which the WPC solution concentration was 0.6 wt% and 1 wt%, at a constant surface temperature of 98°C, and bulk temperatures of 70, 80 and 90°C. Figure 5.1 shows the effect of WPC solution concentration and bulk temperatures on the amount of protein deposition. It can be seen that the total amount of deposition increases with increasing both the bulk temperature and WPC solution concentration even at bulk temperature 70°C. This could be due to high surface temperature applied (98°C). According to Fryer and Belmar-Beiny (1991), the denaturation of native proteins in heat exchangers starts

only at bulk temperature above 70°C. At β -Lg 0.6wt%, a slight increase in deposit thickness and weight was observed, due to an increase in bulk temperature from 70 to 80°C. However, as bulk temperature increased to 90°C, the amount of deposit, in terms of deposit thickness and weight, from the turbulent core increased sharply by 3.4 times. These results suggest that the sudden increase in fouling is due to deposition of denatured or aggregated proteins formed in the bulk of the fluid. Simmons et al. (2007) reported that 8% of the whey protein in Couette apparatus have denatured after 10 minutes at 70°C compared with 70% at 80°C and 100% at 90°C.

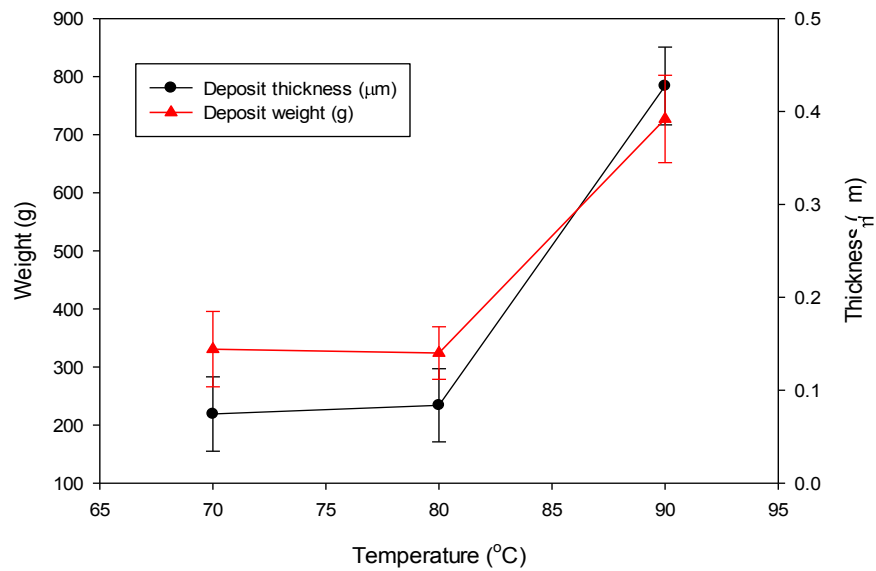


Figure 5.1: Deposit thickness and weight formed at different bulk temperatures, surface temperature 98°C and β -Lg 0.6wt% for WPC solution.

Figure 5.2 illustrates how the increases of β -Lg to be 1wt.% affect the fouling rate. It can be seen that the total amount of deposition in both thickness and weight increased linearly with increasing temperature. The presence of additional β -Lg greatly increased the rate of

reaction of the total β -Lg in WPC solution. As can be observed from the description of the results above, more highly concentrated (β -Lg 1 wt.%) whey protein solutions fouled more quickly than the less concentrated whey protein solution (β -Lg 0.6 wt.%). The possible explanation for this is that increasing the whey protein concentration of the solution results in an increase of the number of β -Lg molecules in the solution and increasing the driving force of mass transfer of the fouling species towards the wall. The rate for the aggregation is expected to be strongly influenced by the protein concentration.

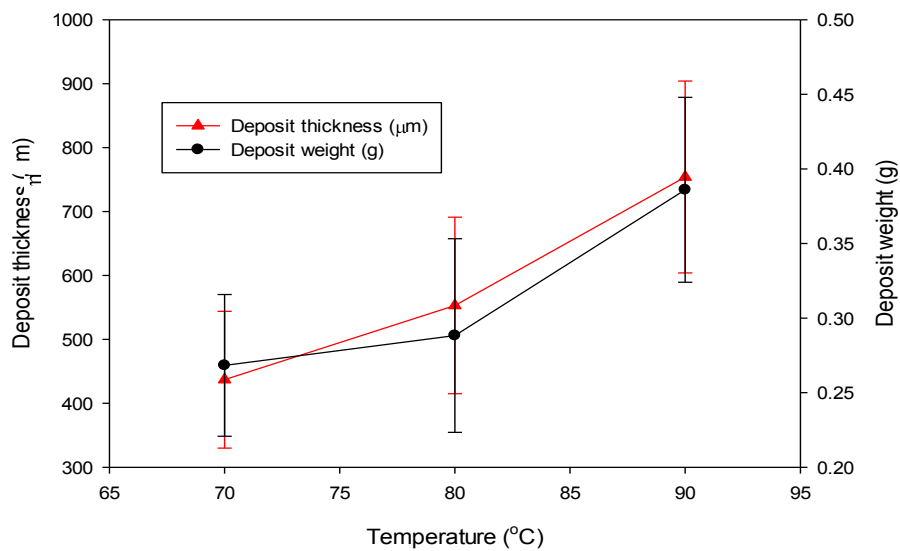


Figure 5.2: Deposit thickness and weight formed at different bulk temperatures, surface temperature 98°C, and β -Lg 1wt% for WPC solution.

At high β -Lg concentrations, the rate for the aggregation is observed to increase due to the more frequent interactions among protein intermediate species (Roefs and Kruif, 1994, Hoffmann and van Mil, 1997). It was found that increasing fluid bulk whey protein concentration leads to faster build-up of fouling. Therefore, the increase of the fouling rate was more than double at 70 and 80°C, as shown in Figure 5.1 and Figure 5.2. The

additional β -Lg markedly influenced the kinetics of interaction of the whey proteins. However, no change in deposit thickness or weight between the two β -Lg concentrations (0.6 and 1wt.%) at bulk temperature of 90°C was observable. Visser and Jeurink (1997) reported that at higher concentrations and temperature, the deposits became so voluminous that all extra material deposited would be entrained with the fluid and prevent adhesion. Furthermore, at deposit thickness of ca. 780 μm , there may be no effect of surface temperature on the fouling process as coupons were covered by thick deposit. This result confirms the findings of Gotham (1990) who found that the increase of fouling, in tubular heat exchanger, with increasing protein concentration could be limited up to 3.75wt%. The plateau at 3.75% was explained in terms of fouling becoming controlled by the amount of protein in the laminar sub-layer.

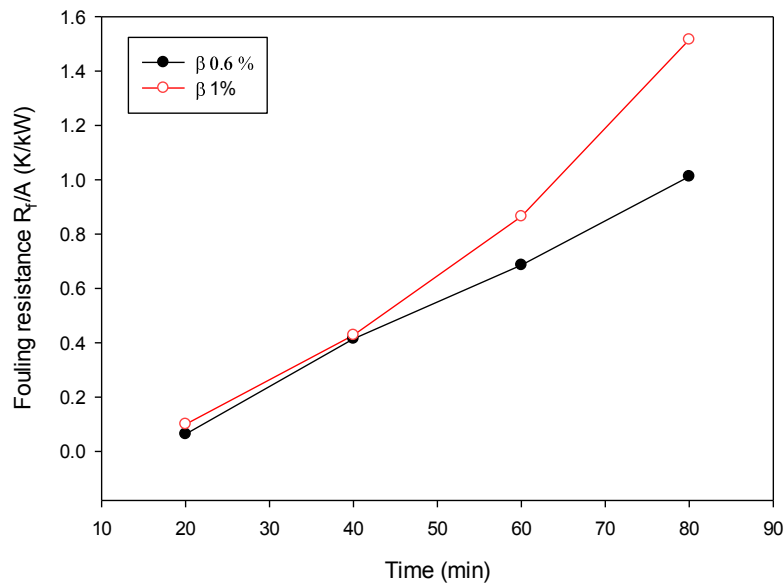


Figure 5.3: Deposit resistance (R_f/A) formed at different time, and bulk temperature 90°C.

In PHE, there was an insignificant fouling at both bulk temperatures; 70 and 80°C as the surface temperature here was not as high as fouling rig 81.5 and 89°C, respectively. However, at section 3 outlet temperature 93°C, with the increment of β -Lg concentration to 1wt%, the fouling resistance R_f/A increased by 50% (from 1.012 to 1.515 K/kW), as seen in Figure 5.3. This may be due to the large size of the heat transfer area of section 3, compared with the test section of the fouling rig which, in turn, increased the probability of foulant to adhere at lower temperature within section 3 with increasing of β -Lg concentration to 1%.

5.3.2 Effect of surface temperature on WPC deposit

It has been suggested that the fouling reaction is a heterogeneous one, where fouling occurs due to aggregation of proteins already attached to the wall with protein in the fluid at the solid-liquid interface (Lalande and Rene, 1988). As mentioned earlier in section 2.2.2.2, If a surface reaction is responsible for fouling, the amount of fouling should depend primarily on the wall temperature. Therefore, the experiments were conducted in which the surface temperature was varied 80, 89, and 98°C, whilst keeping bulk fluid temperature constant at 80°C.

It can be seen from Figure 5.4 that the change in wall temperature is responsible for the sudden increase in deposit formation. As the surface temperature increases, the amount of fouling increases linearly. The increase from the low to medium surface temperature, i.e. 80 to 89°C, at constant bulk temperature investigated, has the greatest effect on deposition. The deposit thickness formed at these temperatures increased by more than six-fold (from 39 to 155 μm), compared to the deposit thickness formed at surface temperature of 98°C, as shown in Figure 5.4.

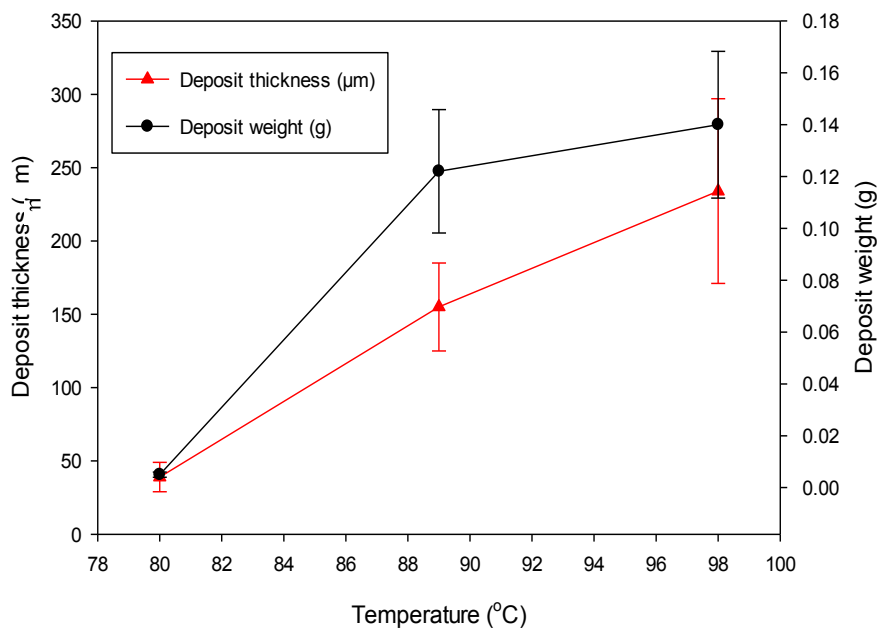


Figure 5.4: Deposit thickness and weight formed at different surface temperatures 80, 89, and 98°C, bulk temperature 80°C, and β -Lg 0.6wt% for WPC solution.

At surface temperature 98°C, the increment in deposit thickness was less than 1.5 times to 234 μm . These results suggest that the change in protein reaction rates is due to an increase of surface temperature. In addition to the important contribution of wall temperature to the deposition of fouling, as mentioned earlier (see Figure 5.1), although the bulk temperature was 70°C, which is under the temperature for denaturation of protein, the thickness of the deposit was high (219 μm) at surface temperature 98°C. This result indicated that at low bulk temperature (80°C \leq), protein aggregates on the coupon surface were susceptible to the surface temperature. This is in accordance with a previous study (Chen and Bala, 1998), where the effect of surface and bulk temperatures was investigated on fouling of milk components onto a stainless steel probe; it was found that the surface temperature was the most important factor in initiating fouling. When the

surface temperature was less than 68°C, no fouling was observed, even though the bulk temperature was up to 84°C.

5.3.3 Effect of surface temperature on WPC_m deposit

Section 4.4.2 has demonstrated the role of minerals in the fouling process. Adding calcium and phosphorus salts to WPC has lowered the excessive deposition temperature to less than 90°C. According to Jeurnink and De Kruif (1995), either increasing or decreasing the calcium concentration in milk leads to lower heat stability and to more fouling in comparison with normal calcium concentration.

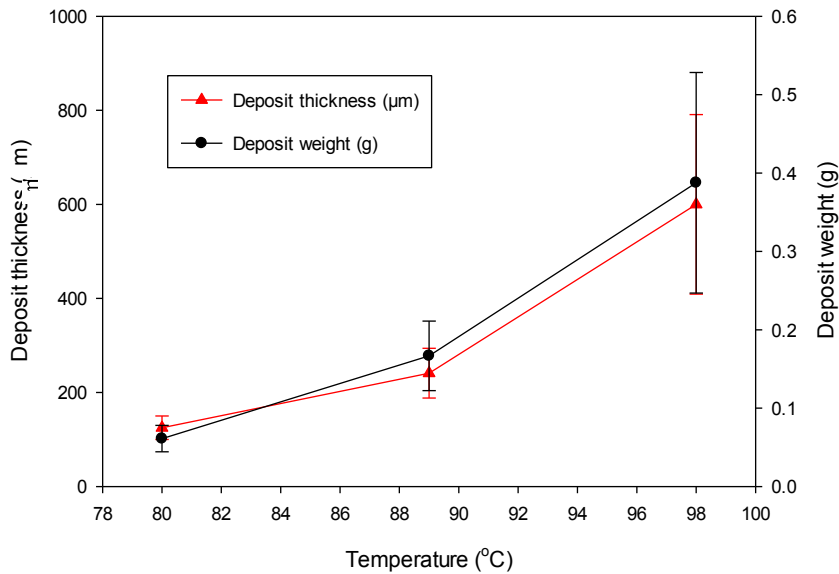


Figure 5.5: Deposit thickness and deposit weight formed for WPC_m (β-Lg 0.6wt.%) at bulk temperature 80°C, surface temperatures 80, 90 and 98°C.

Figure 5.5 shows the amount of deposit formed after 80 minutes for the following conditions: bulk temperature 80°C, and surface temperatures 80, 89, and 98°C. The amount of deposit formed was significantly higher than the deposit formed from WPC

solution, as the addition of minerals enhances deposition by reducing the heat stability of protein (Foster et al., 1989, Xiong, 1992, Corredig and Dalgleish, 1996, De Jong et al., 1998). This is consistent with a study carried out by Daufin et al. (1987) who found that this deposit forms rapidly after less than 10 min. It can also be seen that the total amount of deposition increases with increasing the surface temperature, effectively at surface temperature 98°C. Here the increase in surface temperature from 89 to 98°C has the greatest influence on the fouling deposition. This may refer to the fact that the minerals in the bulk promote aggregation of β -Lg and, in turn, enhance the deposition with increasing surface temperature. Belmar-Beiny et al. (1993) and Xiong (1992) found that on the heating surface, calcium forms bridges between adsorbed protein and the protein aggregates formed in the bulk, and these then adhere to the surface. Thus, the lowered deposition temperature would also be expected. The combined influence of surface and bulk temperature is evident in increasing mineral deposition by 2.5 times at surface temperature between 89 and 98°C. In contrast, during WPC deposition at surface temperature between 89 and 90°C, the contribution of bulk temperature on fouling was less effective as the amount of reacted protein at 80°C is small.

In PHE, insufficient deposit was formed for measurement at bulk temperature 80°C for WPC, as no noticeable change in pressure drop or heat transfer coefficient occurred. Expectedly, the deposit resistance for WPC_m deposit is significantly high (1.27K/kW) at section 3 of PHE, as a result of the higher mineral deposition at bulk temperature 80°C.

5.3.4 Effect of bulk temperature on WPC_m deposit

The solubility of calcium phosphate decreases with heating. The calcium ions present in milk influence the denaturation temperature of β -Lg, promote aggregation by attaching to

β -Lg, and enhance the deposition by forming bridges between the proteins adsorbed on the heat transfer surface and aggregates formed in the bulk (Xiong, 1992, Changani et al., 1997, Christian and Fryer, 2002). Robbins et al. (1999) reported that milk did not produce a deposit between 100 and 120°C. However, a heavy fouling occurred in the pasteuriser section of the PHE.

To evaluate the influence of bulk temperature on the fouling process, several bulk temperatures (70, 80 and 90°C) at a constant surface temperature of 98°C were tested.

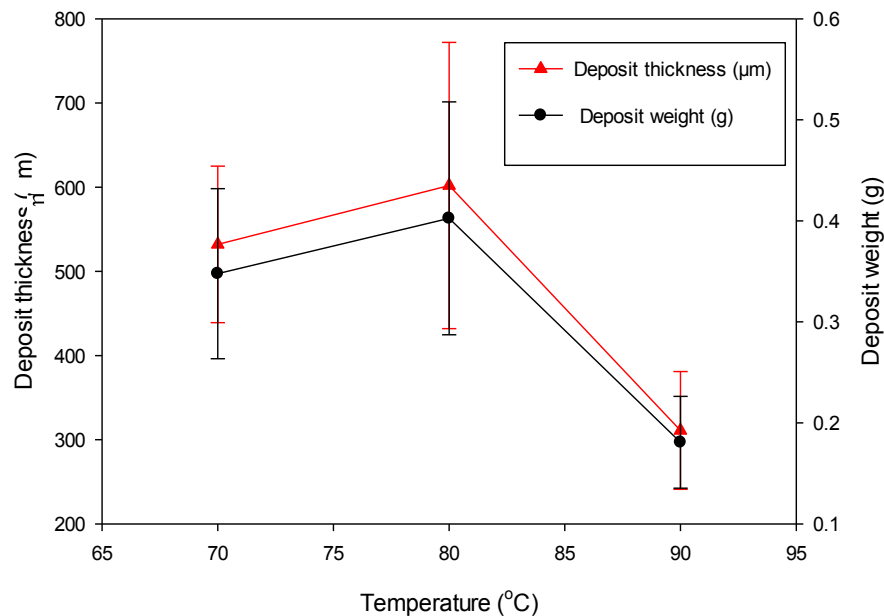


Figure 5.6: Deposit thickness and weight formed for WPC_m (β -Lg 0.6wt.%) at bulk temperatures 70, 80 and 90°C, and surface temperature 98°C.

The amount of deposit formed after 80 minutes at those bulk temperatures and at constant surface temperature 98°C is presented in Figure 5.6. An increase in deposition to its maximum was seen when the bulk temperature increased from 70 to 80°C, followed by a dramatic decrease in deposit thickness which was observed at bulk temperature 90°C.

This decrease may be due either to a complete reaction in the bulk, to the formation of material which does not adhere or to protein hydrolysis noted by (Creamer and Matheson, 1980).

In PHE, although the surface temperature was changed in each plate, the same trend as fouling in the coupon was observed, as shown in Figure 5.7 and Figure 5.8. Section 3 of PHE consists of three product plates.

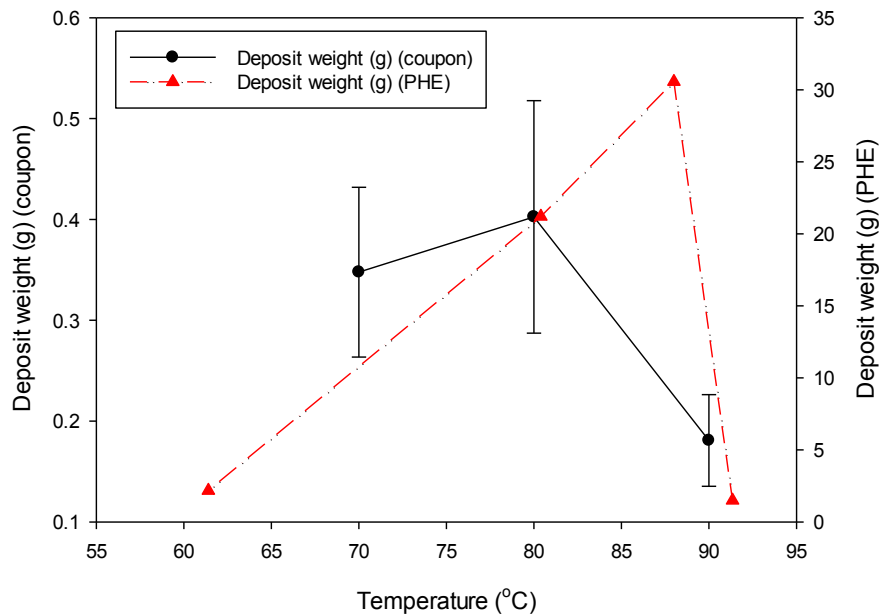


Figure 5.7: Deposit weight formed from WPC_m solution (β -Lg 0.6wt%) at bulk temperatures 70, 80 and 90°C, at surface temperature 98°C for coupon, and for PHE at section 3 outlet temperature 93°C and different deposit weights formed at sections 1, 2 and 3 of PHE.

The first and second plates held an excessive fouling, the bulk temperature was varied between 81 and 89°C, and the deposit weights were 25.1 and 21.2g, respectively. However, the amount of fouling was considerably lower in the third plate, where the bulk temperature was varied between 89 and 93°C and the deposit weight was 2.18g. In

general, the amount of fouling deposited in the bench scale fouling rig is similar to that in PHE. Thus, the bench scale fouling rig is able to follow the development of fouling in PHE quite closely in terms of relative amounts of deposit.

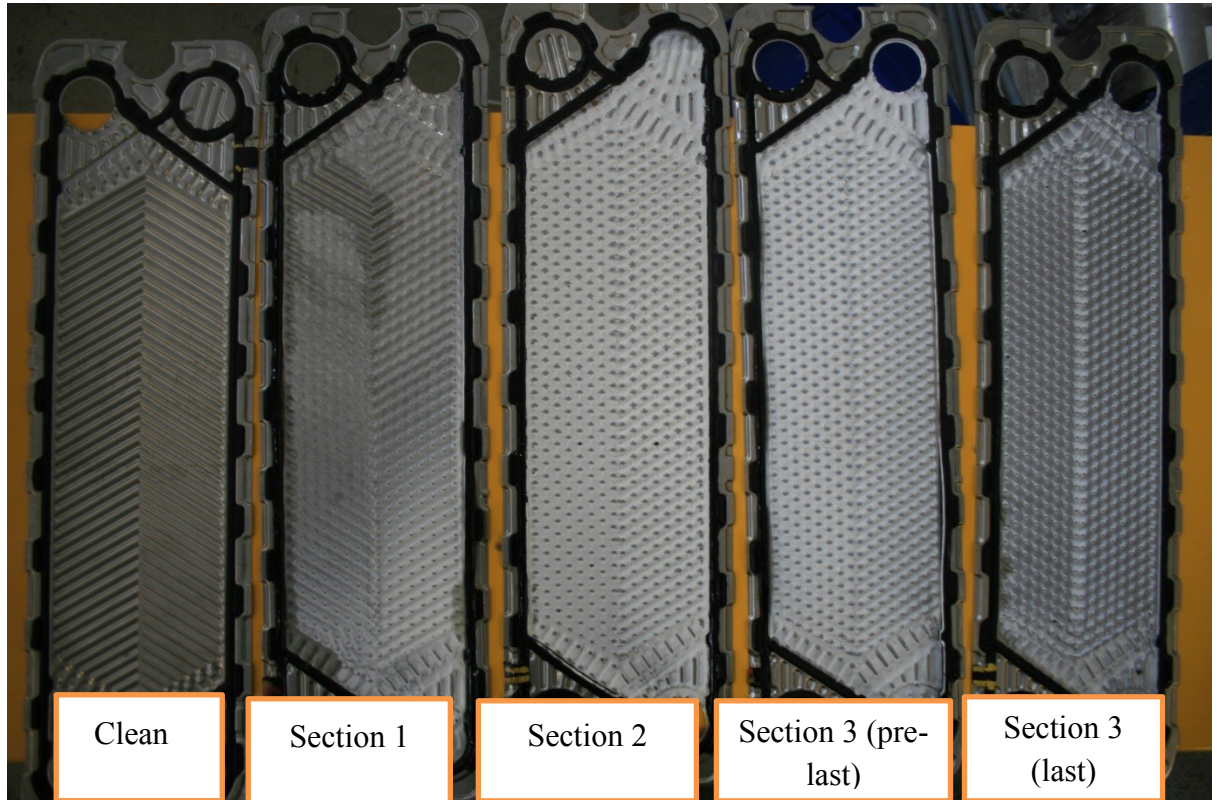


Figure 5.8: Fouling of WPC_m (β -Lg 0.6wt.%) at bulk temperature 93°C in all sections of PHE.

5.3.5 The evolution of deposit during fouling run

Experiments were carried out using two types of solution: WPC and WPC_m at bulk temperatures 80 and 90°C, respectively, and surface temperature 98°C to compare the fouling rate for the two deposits. As a large amount of deposit occurred at these two bulk temperatures (80 and 90°C) for WPC_m and WPC deposits, they were selected to investigate the evolution of deposit during the fouling run.

Figure 5.9 shows that the overall fouling rate in terms of deposit thickness for WPC_m was lower compared to the fouling rate of WPC. This is consistent with a study carried out by Changani (2000) who found that adding minerals to WPC, produced at 140°C, has slowed the fouling rate compared to WPC with no minerals added. The maximum fouling rate for WPC occurred in the first 40 minutes, followed by a decrease in the fouling rate. In contrast, the fouling rate for WPC_m is fairly constant over the fouling run. 70% of the deposit thickness for WPC and WPC_m can be achieved in the first 40 minutes and 60 minutes respectively. The initial WPC layer formed after 20 minutes did not cover the coupon entirely and did not seem to adhere firmly to the coupon. However, the initial WPC_m layer covered the coupon completely and the structure of the deposit layer was more compact.

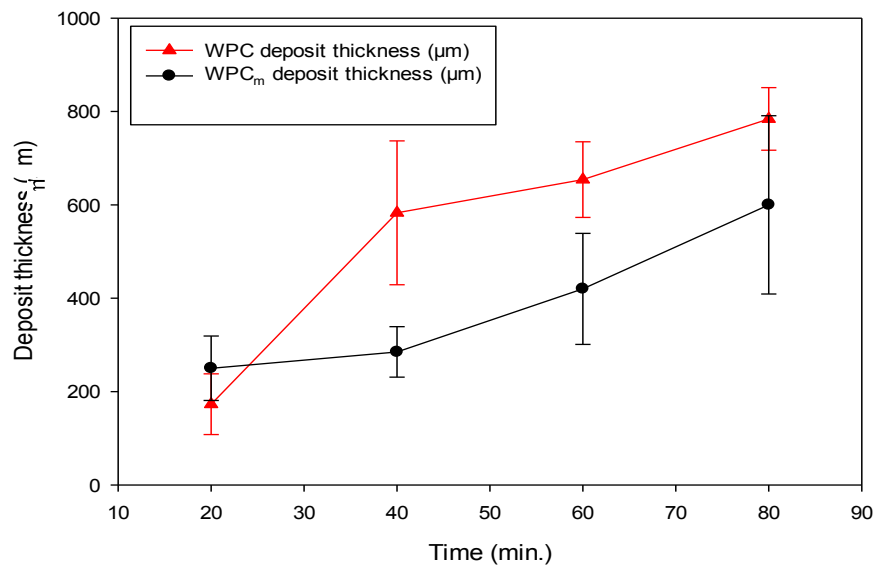


Figure 5.9: Deposit thickness formed for WPC_m and WPC (β -Lg 0.6wt.%) at bulk temperatures 80 and 90°C respectively, and surface temperature 98°C.

Figure 5.10 shows that 75% of deposit formed at the beginning of 40 minutes for WPC deposit, while WPC_m deposit developed fairly constant over the fouling run. These findings underline the fact that the initial deposition behaviour is the result of surface effect.

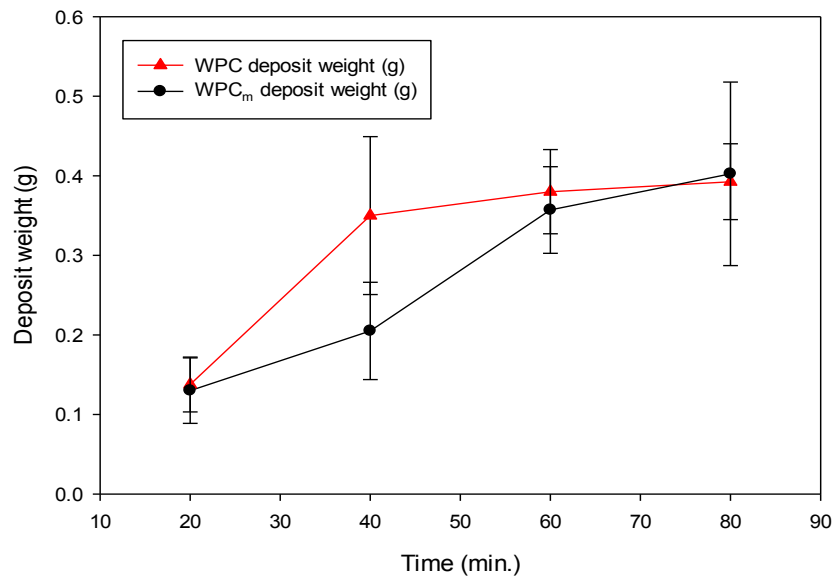


Figure 5.10: Deposit weight formed for WPC_m and WPC (β -Lg 0.6wt.%) at bulk temperatures 80 and 90°C respectively, and surface temperature 98°C.

In PHE, the fouling rate for WPC_m is higher than that for WPC, but the fouling rate for both solutions is fairly constant over the fouling run, as shown in Figure 5.11. This is due once again to at low bulk temperature ($90^{\circ}\text{C} \leq$), the WPC_m gave heavy fouling as added minerals lowered the heat stability of β -Lg. While the WPC started to foul excessively at section 3 of PHE at latter temperature, observations made on opening the plate pack confirmed that there was heavy fouling starting from the last plate of PHE at temperature range 89 to 93°C.

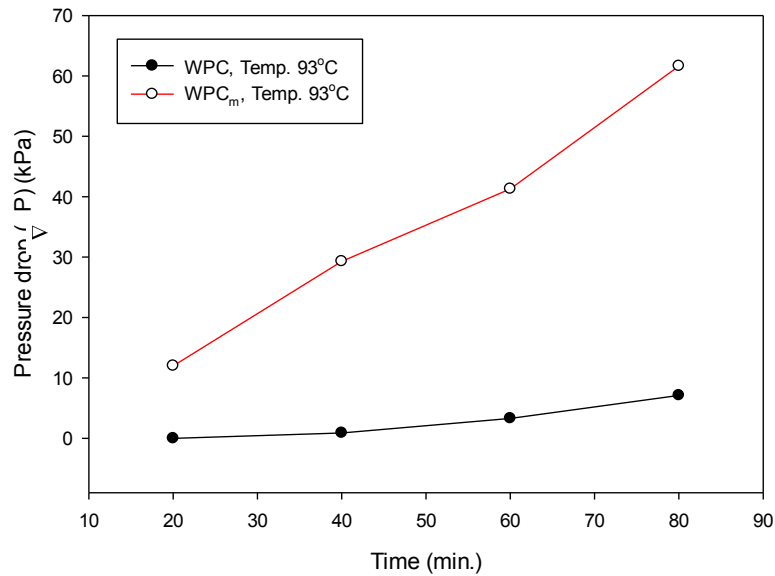


Figure 5.11: Fouling behaviour in terms of pressure drop for WPC and WPC_m, at section 3 outlet temperature 93°C, β -Lg 0.6%.

5.3.6 The evolution of pressure drop and heat transfer coefficient in PHE during fouling run

As fouling proceeds, the reduction in size of flow channels resulted in an increase in pressure drop and decrease in conductivity of the wall over the heat exchanger. Increasing the temperature and whey protein concentration resulted in higher fouling. The mineral added to WPC solution lowered the denaturation temperature of β -Lg. An induction period is seen for the formation of the protein aggregates or insoluble mineral complexes before noticeable amounts of deposits are formed, as seen in Figure 5.12 and Figure 5.13. In general, the amount of deposits increases with time, β -Lg (%) concentration and process temperature. As can be observed from later figures, more highly concentrated (β -Lg 1 wt.%) whey protein solutions fouled more quickly than the less concentrated (β -Lg 0.6 wt.%) ones. This could be due once again to the fact that increasing the whey protein

concentration of the solution results in an increase of the number of β -Lg molecules in the solution, which, in turn, leads to increasing the driving force of mass transfer of the fouling species towards the wall. The most significant change in pressure drop (ΔP) and heat transfer coefficient (R_f/A) was seen when WPC_m solution was used at section 3 outlet temperature 93°C . The fouling rate in terms of pressure drop for WPC_m at temperature 93°C was considerably greater than the other fluids treated at different conditions by six-folders from 60 to 10 kPa, respectively. As seen in Figure 5.12, the results of other fluids treated at different conditions were quite close to each other. However, observations made on opening the plate pack confirmed that there was heavy fouling at the first two plates at section 3 of PHE and little deposit was observed at the third plate at section 3 of PHE, as seen in Figure 5.8. Therefore, the reason for the large change in pressure drop (ΔP) and fouling resistance (R_f/A) was that these measurements give a global measurement of fouling over section 3 of PHE.

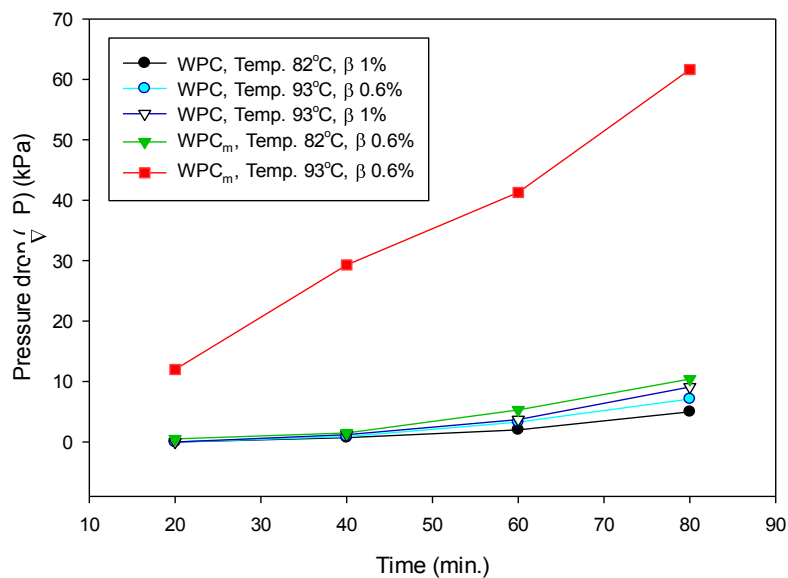


Figure 5.12: Pressure drop in PHE during fouling run by using WPC and WPC_m at section 3 outlet temperatures 82 and 93°C and β -Lg 0.6 and 1 wt.%.

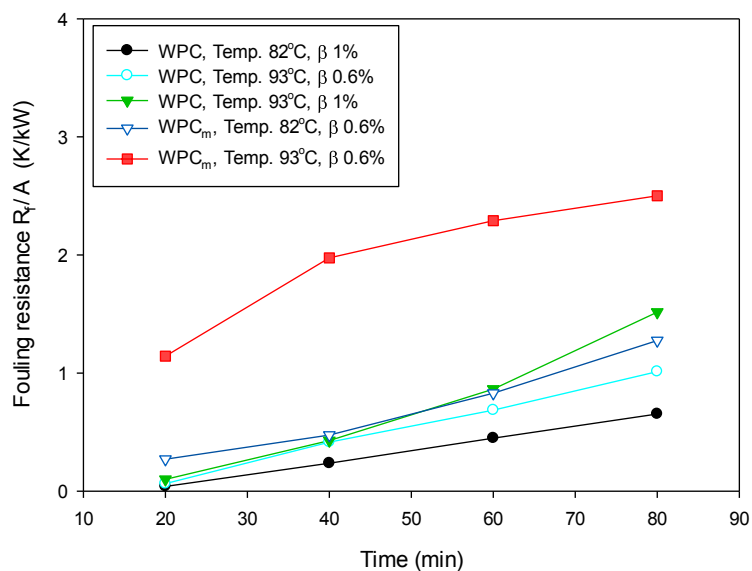


Figure 5.13: Fouling resistance (R_f/A) in PHE during fouling run by using WPC and WPC_m at section 3 outlet temperatures 82 and 93°C and β -Lg 0.6 and 1 wt.% .

5.3.7 Deposit composition

Samples of deposits were removed from coupons at different process temperatures of 70, 80 and 90°C and at times 20, 50 and 80 minutes, respectively, for both WPC_m and WPC runs and analysed for protein, calcium (Ca) and phosphorus (P) (Analytichem, Birmingham). Table 5.1 shows the results of this analysis, expressed as %w/w: (other components present in the deposits such as ash, fat, lactose, water, and other carbohydrates are not included here). Table 5.1 shows that for the WPC formed at 90°C and 80 minutes, the deposit contains 76%w/w protein; whilst the WPC deposit at 90°C and 40 minutes also showed a high protein content of 67%w/w, it was less than that observed for WPC at 80 minutes. The amount of mineral fouling was much less than that of protein for both deposits at 90°C; for the WPC at 80 minutes, the amount of mineral fouling was <0.7%w/w of the deposit, while this figure was 0.73%w/w for the WPC at 40

minutes. The WPC_m deposit at 90°C also showed a high protein content of 47%w/w, which was less for WPC at 80 minutes. Expectedly, the amount of mineral fouling of WPC_m deposit at 90°C was much more (11%w/w) than that of both WPC deposits at 90°C, and there was a predominance of Ca over P. This result differs from that reported in literature for milk deposit formed at pasteurisation temperature and discussed in section 2.2 where the composition of milk deposit is 50 to 70% protein, 30 to 40% minerals.

| Bulk temperature (°C) | Model fluid | Fouling run (min) | Calcium (%) | Phosphorus (%) | Protein (%) |
|-----------------------|------------------|-------------------|-------------|----------------|-------------|
| 70 | WPC _m | 80 | 5.92 | 3.26 | 56.2 |
| 80 | WPC _m | 20 | 21.35 | 10.37 | 27.9 |
| | | 50 | 4.95 | 2.96 | 54.1 |
| | | 80 | 7.62 | 4.17 | 49.9 |
| 90 | WPC _m | 80 | 7.07 | 3.90 | 46.7 |
| 90 | WPC | 40 | 0.52 | 0.17 | 76.4 |
| 90 | WPC | 80 | 0.47 | 0.26 | 66.8 |

Table 5.1: Composition of deposit removed from coupon rig, at flow rate 100 l/h.
Note: compositions do not sum to 100% because of other species present.

A significant difference among the composition of the deposit formed from WPC_m fluid at different fouling runs (20, 50, and 80 minutes) was observed. Deposit formed after 20 minutes showed a very high mineral content (32%w/w) with protein composition 28%. However, the protein content increased significantly with time to 54%w/w, while the mineral fouling decreased significantly with Ca and P to less than 10% after 50 minutes. At the end of the fouling run (80 minutes), a slight decrease in protein to 50% corresponds

to a slight increase in mineral content to 12%. This may suggest that the mineral deposition in the beginning of the experiment may enhance the protein deposition by forming a bridge between the protein absorbed in the surface and aggregates formed in the bulk (Xiong, 1992, Changani et al., 1997, Christian and Fryer, 2002).

The composition of the WPC_m deposit formed at different temperatures of 70, 80 and 90°C showed a decrease in protein content of 56%, 50% and 47%, respectively, while there was a slight difference in mineral content of 9%, 12% and 11%, respectively.

5.3.8 Appearance of the deposits

At the end of each fouling run, the test section was opened and each coupon examined for deposit. WPC deposits produced at bulk temperature 90°C were cream in colour and fluffy in nature, adhered only weakly to the metal surface and could be easily removed. It was observed that the thickness of the fouling layer was not uniform along the coupon surface. However, at the bulk temperatures of 70 and 80°C, the fouling layers became more compact and adhered strongly on the surface of stainless steel.

WPC_m deposits produced at bulk temperatures 70, 80 and 90°C were off-white in colour and fouled evenly on the surface. The structure of the deposit layer became more compact and adhered strongly on surface.

5.3.9 Morphology of the deposits

The aim was to see whether the coupon deposits were representative of deposits obtained from PHE sections under similar temperature conditions.

Samples of deposits were removed from the test section (coupons) and from each section of the plate heat exchanger for both WPC_m and WPC runs. Coupon deposit was obtained at bulk temperatures of 70, 80 and 90°C, and surface temperature 98°C, while PHE deposit was obtained at section 3 outlet temperature 93°C. As shown in Figure 5.14 (a) and (b), a WLI image for β -Lg 0.6wt% and 1wt% at bulk temperature 70°C, illustrated that the structure of both deposits consisted of small clumps of aggregates comprising smaller aggregates of 1-2 μ m in size. Deposit formed at β -Lg 1wt% consisted of agglomerates of protein bigger than deposits formed at β -Lg 0.6wt%. Figure 5.15 (a) and (b) showed an SEM image, with a higher magnification (1500) than WLI, for deposits mentioned above; a similar structure was observed to that by WLI. It is clear that at high protein concentration β -Lg 1 wt% contains larger aggregate sizes than with lower protein concentration β -Lg 0.6 wt%. These observations are consistent with those of Mleko (1999) who reported that increasing the protein concentration results in increasing the aggregate size of the whey protein. A fair difference between the roughness of the deposit formed from both β -Lg concentrations was found by WLI (see section 3.10.1). The roughness of deposit formed at β -Lg 0.6wt% (21.9 μ m) showed less roughness than deposits formed at β -Lg 1wt% (33.4 μ m), as shown in Table 5.2.

Figure 5.16 (a) and (b) a WLI for β -Lg 0.6wt% and 1wt% at bulk temperature 80°C, the structure of deposit formed at β -Lg 1wt% shows an amorphous structure with no discernible aggregates. Cracking is clearly visible at higher β -Lg (1 wt.%) and probably occurred as the sample was dried. All coupons were drip dried in the laboratory after experiments. In contrast, the deposit formed at β -Lg 0.6wt%, showed a similar structure to the deposit formed at β -Lg 1wt% and bulk temperature of 70°C; agglomerates of protein aggregates. Figure 5.17 (a) and (b) shows an SEM image for deposits mentioned

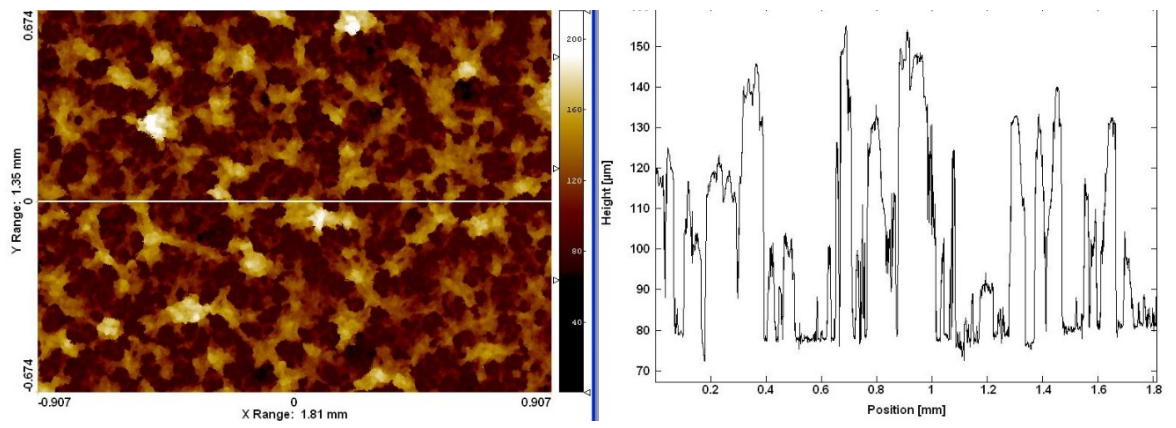
above. A similar structure was observed to that by WLI. The picture becomes a little clearer and shows what appears to be a more fluffy or cauliflower-like deposit on top at β -Lg 0.6 wt.%, followed by a more compact deposit at β -Lg 1 wt.%. This deposit nature has often been observed by other researchers in tubular heat exchanger (e.g., Burton (1968) and Davies et al. (1997)). A slight difference was also observed between the roughness of the deposit formed at both β -Lg concentrations used. The roughness of the deposit formed at β -Lg 0.6wt% (24.8 μ m) was lower than the deposit formed at β -Lg 1wt% (31 μ m), as shown in Table 5.2.

Figure 5.18 (a) and (b) a WLI for β -Lg 0.6wt% and 1wt% and at bulk temperature 90°C, the structure of both deposits show no discernible aggregates. Cracking is clearly visible at both β -Lg 0.6 and 1 wt.% as the deposit became thicker. Figures 20 (a) and (b) shows an SEM image for deposits mentioned above and an amorphous structure with no discernible aggregates, which is effectively the deposit formed at β -Lg 1wt%. The roughness of deposits formed at β -Lg 1wt% (14.4 μ m) was lower than the deposit formed at β -Lg 0.6wt% (18.2 μ m), as shown in Table 5.2.

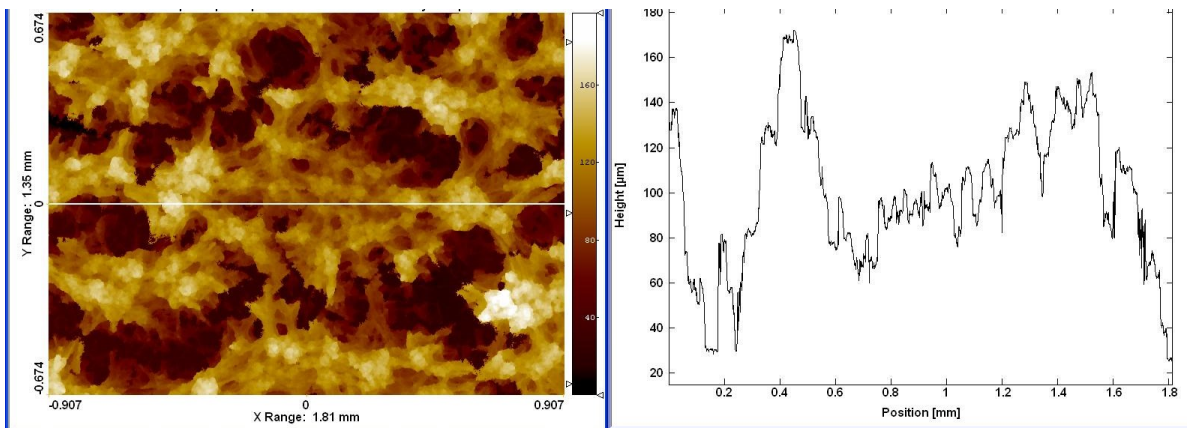
Figure 5.20 (a) and (b) of a WLI images for WPC_m at bulk temperature 90°C shows a very fine structure with much smaller particulates than in the WPC deposit, which is very distinct from closed. The roughness of these deposits was the lowest among the coupon deposits, as shown in Table 5.2.

In PHE, the structure of WPC deposit for section 3 is similar to that of WPC_m deposit for section 2. It shows a rough, open structure and fluffy structure of deposits reported extensively in the literature for deposits produced at a lower temperature typical of a pasteurisation plant (e.g., Gotham (1990)). The deposits consist of a structure of

agglomerates containing aggregates of 5 μm in size, while the structure of WPC_m deposit for section 3 consists of small clumps of 10 μm aggregates comprising smaller aggregates of 1-2 μm in size, as shown in Figure 5.22. Table 5.2 shows the roughness value of deposit at different conditions. In general, the roughness value for WPC_m deposit is lower than WPC deposit. These trends can easily be observed from the even surface of the WPC_m deposits.

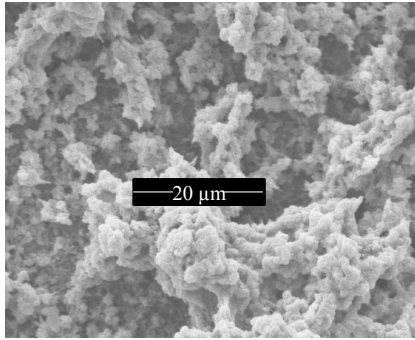


a)

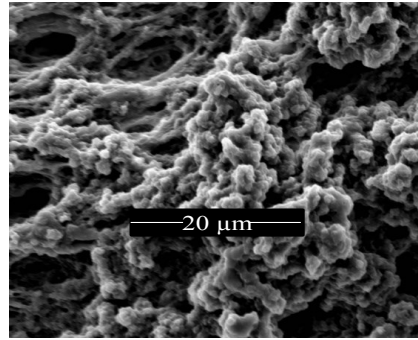


b)

Figure 5.14: White light interferometry of WPC at bulk temperature 70°C:(a) β -Lg 0.6wt%, (b) β -Lg 1wt%.

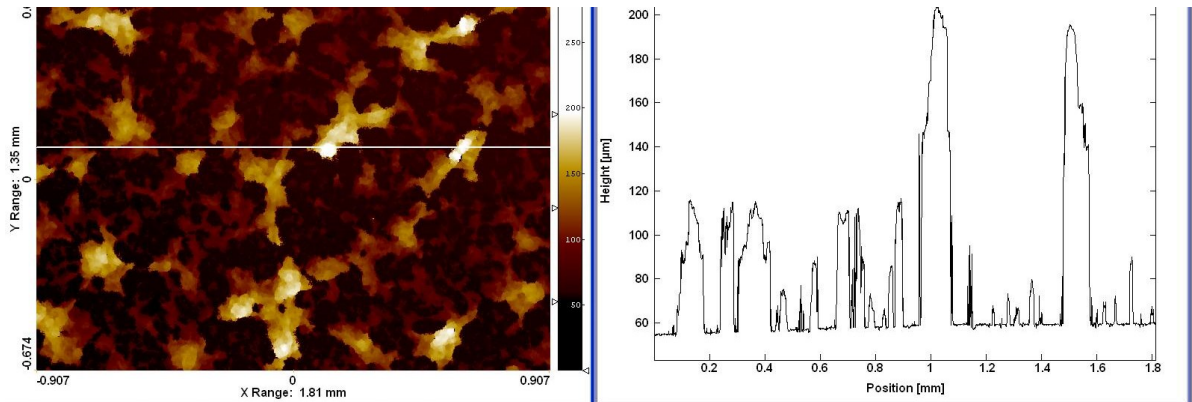


a)

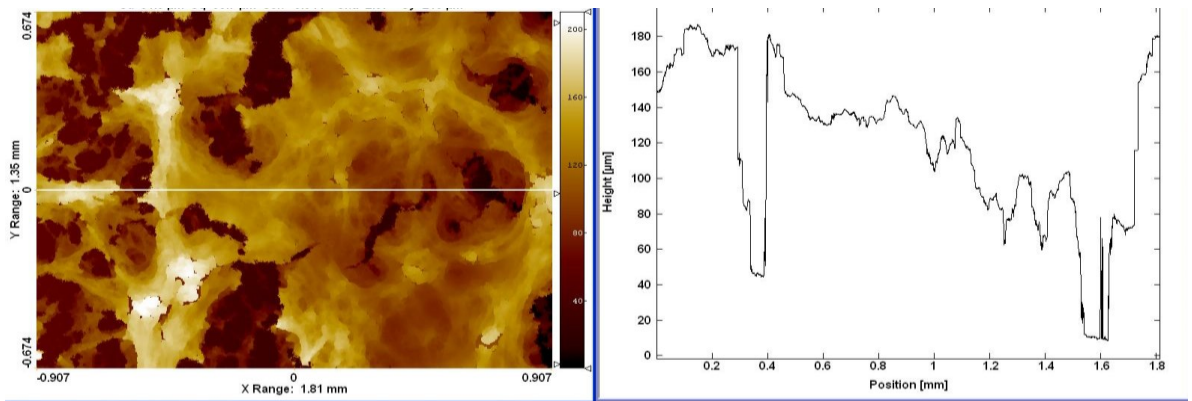


b)

Figure 5.15: Scanning electron micrographs of WPC at bulk temperature 70°C :(a) β -Lg 0.6wt%, (b) β -Lg 1wt%.

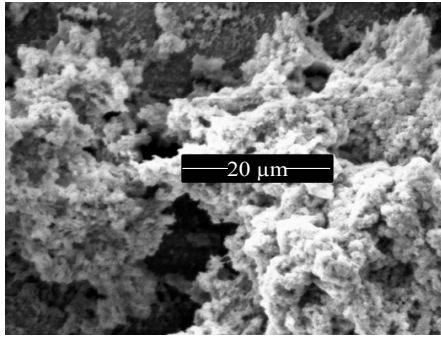


a)

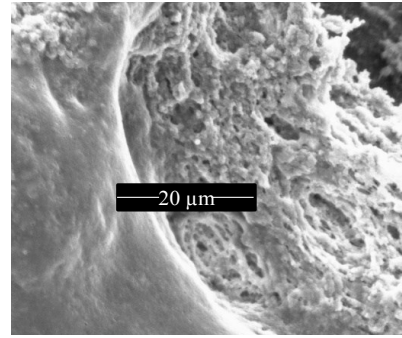


b)

Figure 5.16: White light interferometry of WPC at bulk temperature 80°C:(a) β -Lg 0.6wt%, (b) β -Lg 1wt%.

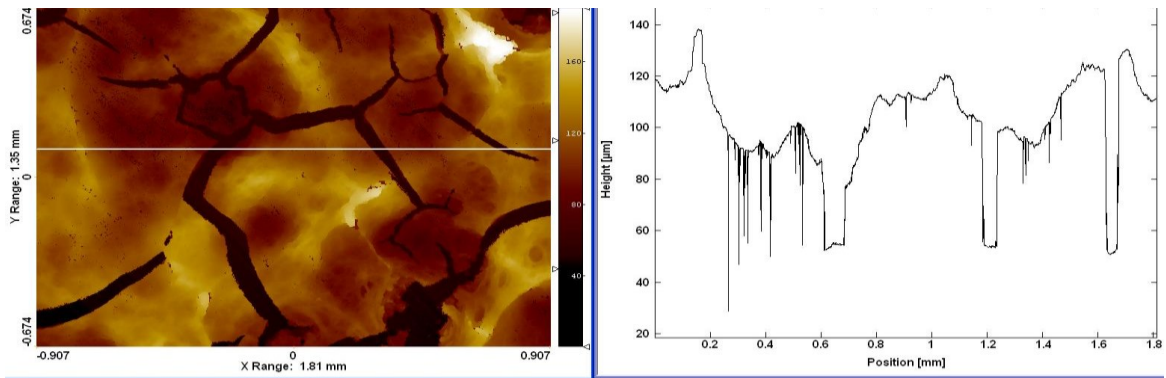


a)

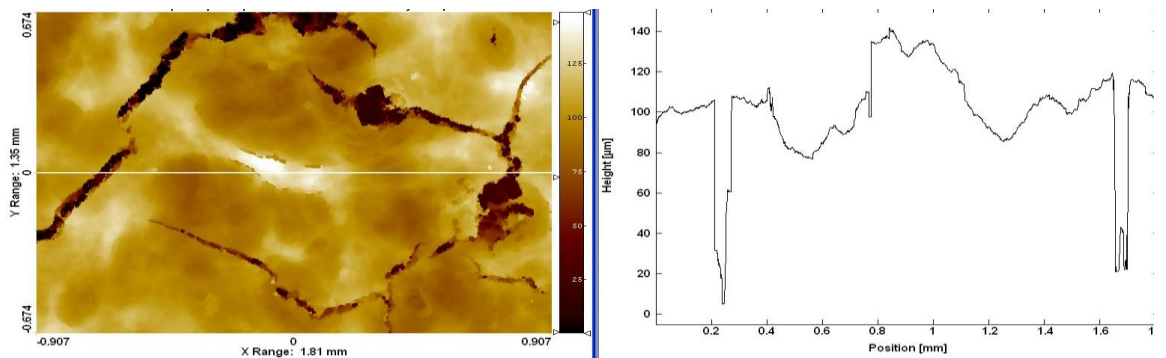


b)

Figure 5.17: Scanning electron micrographs of WPC at bulk temperature 80°C : (a) β -Lg 0.6wt%, (b) β -Lg 1wt%.



a)



b)

Figure 5.18: White light interferometry of WPC at bulk temperature 90°C: (a) β -Lg 0.6wt%, (b) β -Lg 1wt%.

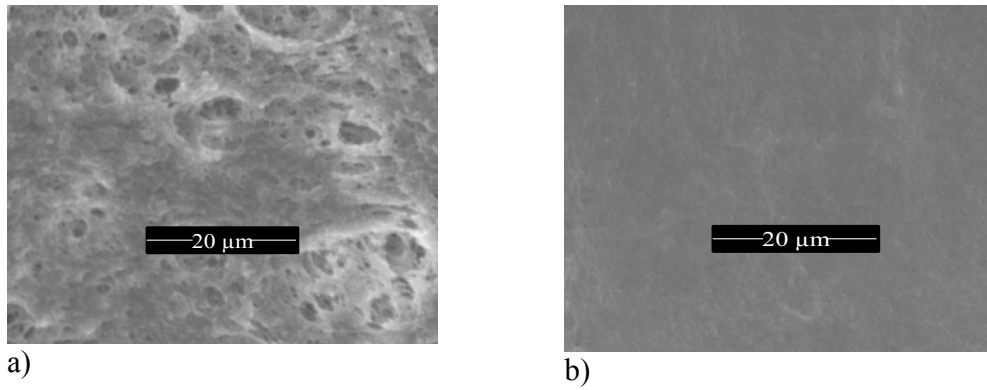


Figure 5.19: Scanning electron micrographs of WPC at bulk temperature 90°C: (a) β -Lg 0.6wt%, (b) β -Lg 1wt%.

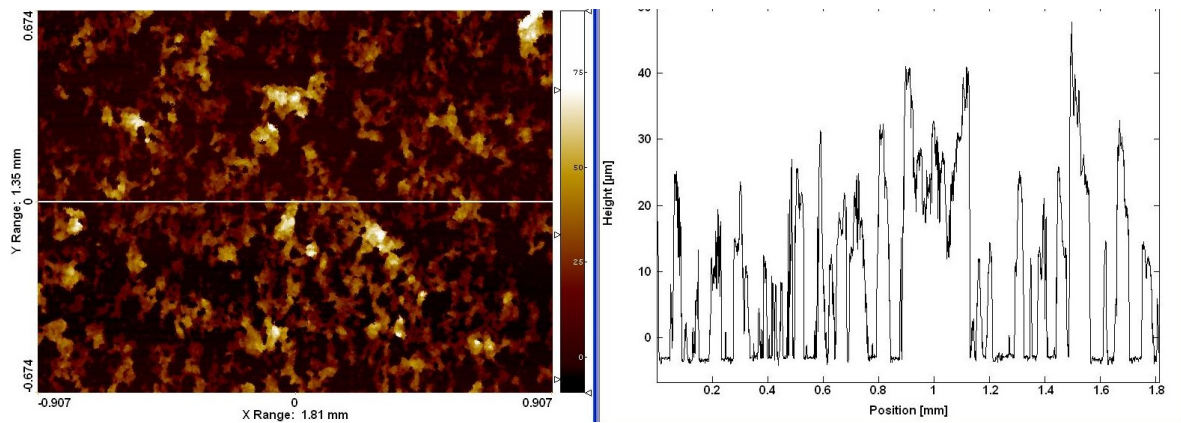


Figure 5.20: White light interferometry of WPC_m at bulk temperature 90°C, β -Lg 0.6wt%.

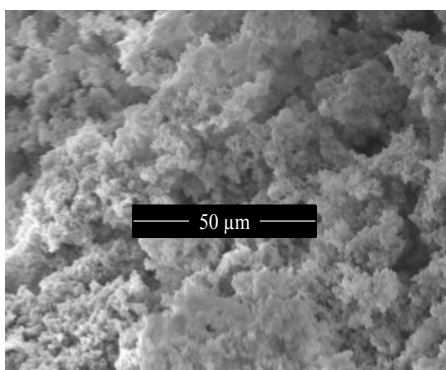
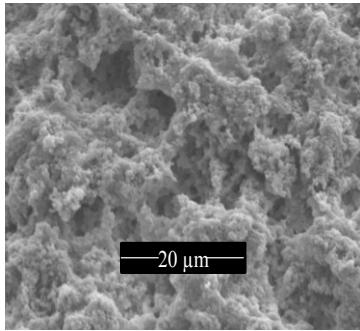
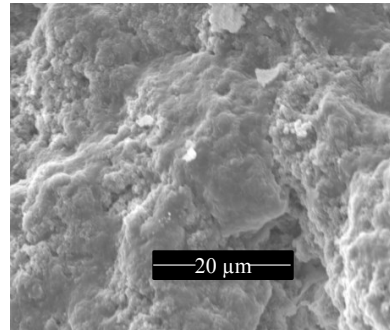


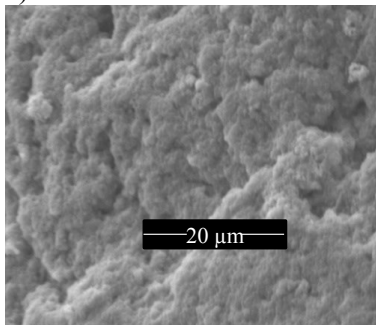
Figure 5.21: Scanning electron micrographs of WPC_m at bulk temperature 90°C, β -Lg 0.6wt%.



a)



b)



c)

Figure 5.22: Scanning electron micrographs of PHE deposit :(a) section 3 of PHE deposit of WPC_m, (b) section 2 of PHE deposit of WPC_m, (c) section 3 of PHE deposit of WPC, at bulk temperature 90°C and β -Lg 0.6wt%.

| Bulk temperature(°C) | β -Lg (wt.%) | Fouling surface | Roughness (μm) | Solution model |
|----------------------|--------------------|-----------------|-----------------------------|------------------|
| 70 | 0.6 | coupon | 21.9 | WPC |
| 70 | 1 | coupon | 33.4 | WPC |
| 80 | 0.6 | coupon | 24.8 | WPC |
| 80 | 1 | coupon | 31 | WPC |
| 90 | 0.6 | coupon | 18.2 | WPC |
| 90 | 1 | coupon | 14.4 | WPC |
| 90 | 0.6 | coupon | 12.2 | WPC _m |
| 90 | 0.6 | PHE (section3) | 10.2 | WPC |
| 90 | 0.6 | PHE (section1) | 3.6 | WPC _m |
| 90 | 0.6 | PHE (section2) | 6 | WPC _m |
| 90 | 0.6 | PHE (section3) | 1.4 | WPC _m |

Table 5.2: The roughness value for WPC_m and WPC deposit.

5.4 Conclusion

Experiments were conducted to generate deposits similar to those generated at the heat exchangers in the industry. The effects of bulk and surface temperatures at 70, 80 and 90°C on fouling behaviour of the two model solutions (WPC & WPC_m) on deposit thickness, weight and morphology were quantified and presented. The total amount of WPC deposition increased with a temperature increase. Deposition from WPC_m increased with increasing temperature up to ca. 80°C, and decreased with increasing temperature afterwards. The reason for different fouling responses to temperature for each fluid was

associated with their respective chemistry. Adding minerals to WPC solution reduced pH, which, in turn, lowered the heat stability of whey protein. The surface temperature was the most important factor in initiating WPC fouling. At a low surface temperature of 80°C or lower, no fouling was observed; however, for WPC_m, fouling was observed even at a surface temperature and bulk temperature of 70°C. The morphology data showed significant differences in the composition of the deposits formed at different temperatures. The roughness data for WPC_m deposit was lower than the WPC deposit. The bench scale fouling rig is able to follow the development of fouling in PHE quite closely in terms of relative amounts of deposit.

CHAPTER 6 : INVESTIGATING CLEANING MEASUREMENTS IN A PLATE HEAT EXCHANGER (PHE)

6.1 Introduction

Monitoring the cleaning process ensures product quality and can potentially be used to reduce environmental impact by reducing the rejects and chemicals used. The desired level of cleanliness varies from sector to sector. To determine which monitoring/cleaning method suits a given application, many factors must be considered. These include (i) type of deposits to be monitored, (ii) level of cleanliness that must be monitored, (iii) accuracy required, (iv) speed of measurements, and (v) cost of the measurement (Kanegsberg and Kanegsberg, 2011). Determining the right time to end the cleaning procedures is essential in improving the efficiency of the process.

As discussed in section 2.4 several types of monitors used previously to study fouling and cleaning was examined. The critical part of optimising a cleaning process would be the incorporation of cleaning measurements into the process schedule; at present, cleaning times are set automatically and are not changed in operation. If measurements made during cleaning could be used to determine the end-point of cleaning with high confidence, it would be possible to develop some form of a process control strategy which could minimise the cleaning cost (Yang et al., 2008). This approach can be successful if measurements are robust, inexpensive and known to be representative of the system.

Fouling and cleaning are usually not visible from outside the industrial processing equipment and, therefore, can only be ascertained from their effects, such as by measuring heat transfers (Bott, 1995, Lalande and Rene, 1988) or pressure drops (Burton, 1966, Delaplace et al., 1994, Fryer, 1989), which in the case of small, local deposits may not be significant enough to allow an operational decision to be made. Pressure drop and heat transfers, where used in chapters 4 and 5, are usually not sensitive enough to detect the first attached layers or accurately assess the cleaning status of the surfaces after cleaning PHE. Therefore, two novel tools have been developed to evaluate the cleaning process: particles count technique and Peltier device. The particles count technique was used to assess the removal of various whey protein deposits from the PHE, while the Peltier device was used to measure the responsiveness of the device during the cleaning of two deposits: toothpaste and golden syrup. The Peltier device located in contact with the fouled plate, within the bench-scale cleaning rig, has been characterised in chapter 3.

This chapter has been divided into two parts. The aim of the first part is to investigate the cleaning behaviour of a PHE by conventional and novel measurement techniques. Conventional measurements are pressure drop and heat transfer coefficient in terms of area (UA), novel online and offline turbidity and particle count, respectively. Two model fluids were investigated: WPC deposit formed at outlet section 3 temperature 95°C and 140°C and WPC_m (with minerals) produced at outlet section 3 temperature 140°C, at flow rate 100 l/h. Two temperatures (70°C and 50°C) and two chemical concentrations of NaOH were 0.3% and 1%.

The aim of the second part is to (i) measure the sensitivity of the Peltier device during removal of deposit, (ii) compare the thermal behaviour of the Peltier device to visual

analysis (images) of the deposits remaining on the plate surface, and (iii) optimise the setup of the Peltier device.

6.2 Part A: Investigating cleaning measurements in a plate heat exchanger (PHE)

Four methods of monitoring are applied; pressure drop sensor, heat transfer coefficient, turbidity probe and particles count technique to investigate the response of each monitoring methods under cleaning three types of deposit: WPC deposit formed at 95°C, WPC deposit formed at 140°C, and WPC_m deposit with additional minerals formed at 140°C. The structure of deposit is affected by temperature and chemical composition. This influences the ease of removal of deposits during the cleaning procedures. At higher temperatures, most whey protein has denatured, with aggregation being due to covalent bonding between SH groups, while at lower temperatures agglomerates of native form are made via weaker van der Waals forces (Gotham, 1990, Simmons et al., 2007). At higher concentrations of minerals, the structure of the deposit layer becomes more compact (De Jong, 1997).

6.2.1 Fouling experiment procedure and conditions

All of these experiments were carried out in PHE described in section 3.6 using flow rate 100 l/h and at two temperatures (95 and 140°C). The PHE was brought to being thermally stabilised and left for 10 minutes by using soft water. Then the flow was diverted to draw from the product tank. For the two deposits formed from WPC at 95°C and 140°C, the fouling experiments were stopped when pressure drop at section 3 of PHE reached 17 kPa to prevent the turbidity meter from reaching the maximum value of 550 FTU and also to prevent the product pump from tripping during the cleaning stage.

The experimental conditions for the three types of deposit are listed below:

- Whey protein concentrate (WPC) processed at 140°C.
 - (i) The temperature at section 3 of PHE inlet and outlet was 132°C and 140°C respectively.
 - (ii) WPC solution concentration was 0.2%.
 - (iii) The length of the experiment was 40 minutes.

- Whey protein concentrate with added minerals (WPC_m) processed at 140°C.
 - (i) The temperature at section 3 of PHE inlet and outlet was 132°C and 140°C respectively.
 - (ii) WPC solution concentration was 0.2%.
 - (iii) The length of the experiment was 40 minutes.

- Whey protein concentrate (WPC) processed at 95°C.
 - (i) The temperature at section 3 of PHE inlet and outlet was 88°C and 95°C respectively.
 - (ii) WPC solution concentration was 0.6%.
 - (iii) The length of the experiment was 50 minutes.

These different types of deposit were selected because they display different cleaning behaviours which in turn enable to assess the monitoring devices. Also, β -Lg at 0.2 wt.% was used for fouling at 140°C, as higher β -Lg than 0.2 wt.% gives such heavy fouling to the extent that the pressure increased to 750 kPa within 12 minutes and so the pressure switch would be tripped to the power to the process pump and thus terminating the fouling experiment.

6.2.2 Cleaning experiment procedure

Nine different experiments were carried out to determine the cleaning behaviour of the three deposits, using the particles count technique, and repeated twice. Two cleaning solutions were used in cleaning experiments, depending on the nature of fouling deposit: sodium hydroxide was used to clean WPC deposit at 1 wt.% and 0.3 wt.% concentration strength and P3-horolith V based on nitric acid was used to clean mineral deposit as sodium hydroxide alone cannot remove this type of deposit. In all cleaning experiments, the end of cleaning was determined as the point where the pressure drop and turbidity meter reading become zero and the number of particles reached the minimum value of approximately 10 particles. The cleaning experiment protocol was as follows: after the fouling experiment, the PHE was brought to thermal equilibrium at the desired process temperature in one hour using soft water at flow rate 100 l/h, and then the flow was diverted to draw from the sodium hydroxide tank until the pressure drop values decreased to the cleaning point. If the WPC_m was used during a fouling run, a water rinse step for 1 minute was used before introducing nitric acid solution at concentration 1 or 0.3 wt. % to clean the remaining mineral deposit. During the experiment, 13 samples of the cleaning fluid were taken, during the cleaning process, at the outlet of the PHE for particle count analysis to represent cleaning behaviour for the three types of deposit. It was assumed that no dissolution of the particles occurred during transport from the surface to the PHE outlet. Samples were held in ice until the time of testing on the same day to quench any reaction that may change particle count or size. Samples were diluted to the point where particles were easy to count (approximately 40 particles (in 1.41×10^{-7} ml)). Measurement of the cleaning solution by particle count and turbidity was hoped to increase the accuracy of the end point of cleaning measured by pressure drop. For monitoring cleaning by the

particles count and turbidity meter, time $t = 0$ second refers to the time where the diverter valve was switched to draw cleaning chemicals while for monitoring cleaning by pressure sensor and heat transfer coefficient in term of area (UA), time $t = 600$ seconds refers to the time where the diverter valve was switched to draw cleaning chemicals.

6.2.2.1 Cleaning experiment procedure

The cleaning conditions for the three types of deposit are listed below.

- Whey protein concentrate deposit (WPC):
 - (i) Two cleaning temperatures (50°C, 70°C).
 - (ii) Two cleaning concentrations (1 wt.%, 0.3 wt.%).
 - (iii) The length of the experiment was 80 minutes.

- Whey protein concentrate with added minerals (WPC_m):
 - (i) One cleaning temperature at 50°C.
 - (ii) One sodium hydroxide concentration of 1 wt.%.
 - (iii) One P3-horolith V based on nitric acid concentration 1 wt.% (HNO₃).
 - (iv) The length of the experiment was 115 minutes.

6.2.3 Results and Discussion

6.2.3.1 Fouling results

Milk is a complex biological fluid (see Table 2.1), containing a number of thermally unstable components (e.g., proteins, fat, and minerals); this complicates the study of dairy fouling. Two types of deposits are formed when milk undergoes heat treatment: type A is

high in protein content and forms at process temperatures of 85–110°C, and type B is mainly composed of minerals, mostly calcium phosphate, and forms at process temperatures of 110-140°C (Burton, 1968). These differences in physical properties of the different deposits may affect cleaning processes, which, in turn, affects the monitoring process.

Figure 6.1 to Figure 6.3 show the fouling behaviour in terms of pressure drop for the three types of deposit. As the temperature rises, the deposit formation rate increases rapidly with both surface and bulk temperatures. The fouling deposit formed at section 3 outlet temperature of 95°C occurred only in section 3 of PHE (88 to 95°C), whereas a thin fouling layer was observed in section 2 when PHE was dismantled.

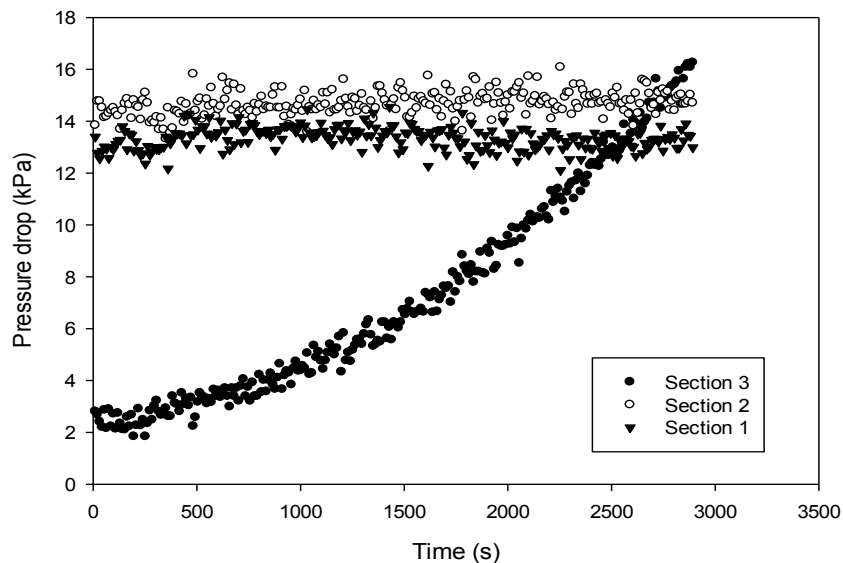


Figure 6.1: Fouling behaviour in terms of pressure drop for WPC for each section of the PHE, section 3 outlet temperature 95°C.

Although the deposit formed at 140°C was low in whey protein concentration (β -Lg 0.2wt.%), the fouling rate was high. The maximum fouling occurred in section 3, some

fouling was observed in section 2, and the least amount of fouling was not detectable by ΔP in section 1, as shown in Figure 6.2.

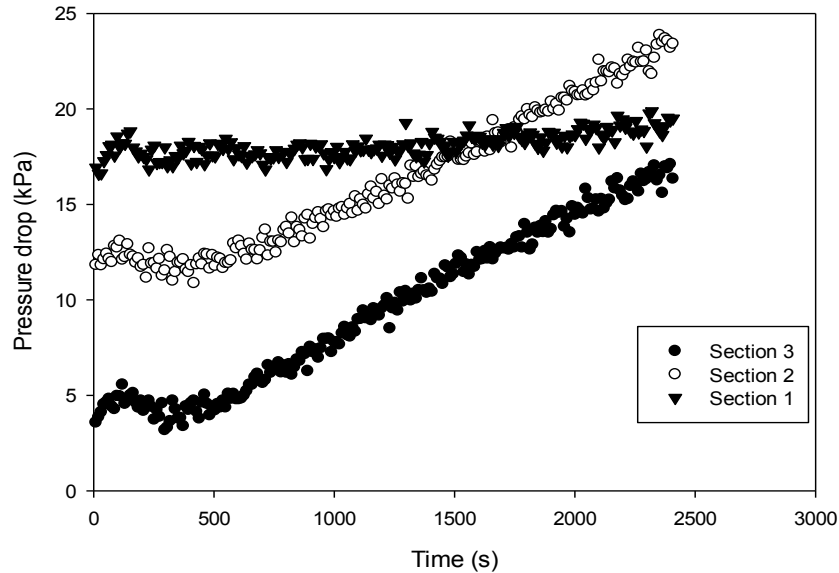


Figure 6.2: Fouling behaviour in terms of pressure drop for WPC for each section of the PHE, section 3 outlet temperature 140°C.

The effect of adding minerals to WPC can be seen in the fouling rate behaviour of the individual section of the PHE, as seen in Figure 6.3. Adding minerals lowers the fouling rate. Section 1 fouled the most from WPC_m with little or no fouling in the section 2 and 3 of PHE. Robbins et al. (1999) proposed that reduction in protein fouling at higher temperature is due to the increase in aggregate size. High shear forces in the PHE will tear the deposits from the wall or prevent adhesion.

The fouling experiments were terminated when the pressure drop reached 17 kPa at section 3 of PHE for both WPC deposits formed at 140°C and 95°C.

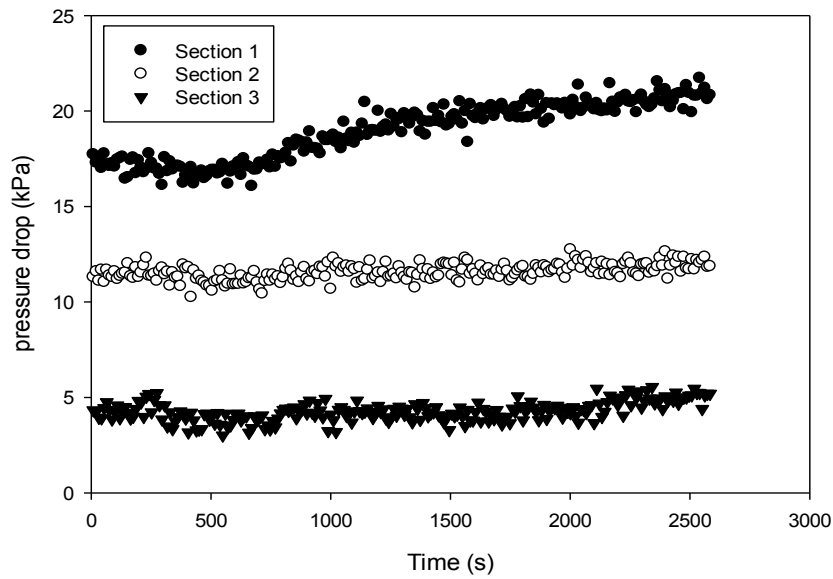


Figure 6.3: Fouling behaviour in terms of pressure drop for WPC_m for each section of the PHE, section 3 outlet temperature 140°C .

6.2.3.2 Cleaning results

The cleaning behaviour of three types of deposit was assessed by using four monitoring methods: pressure drop, heat transfer coefficient, turbidity probe, and particles count technique.

6.2.3.2.1 Monitoring fouling removal vs pressure drop

A typical cleaning curve for a WPC deposit is given in Figure 6.4 and Figure 6.5. Deposit swelling can be occurred initially formed as a result of protein contacting the cleaning solution (NaOH). Deposits formed at 95°C and 140°C were removed from the surfaces of PHE by using one single stage (NaOH). However, WPC_m was removed from PHE by using two stages of cleaning involving alkaline solution followed by acid solution. This process of cleaning shows one pressure peak when the proteinaceous deposit has been contacted with alkaline solution. However, although no pressure peak was observed

during cleaning of the remaining minerals deposit, an abrupt pressure drop was only observed which coincided with introducing nitric acid to remove the remaining minerals.

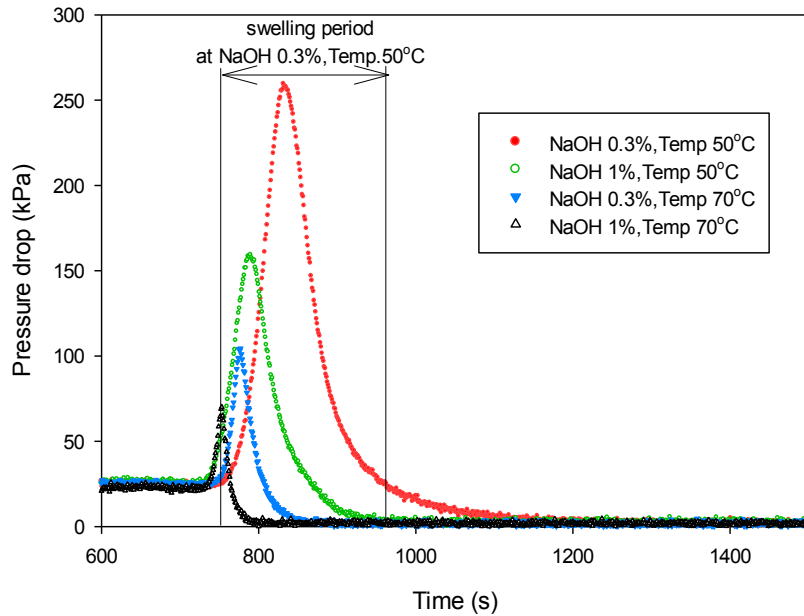


Figure 6.4: Cleaning behaviour in terms of pressure drop at section 3 for WPC deposit formed at 95°C.

The pressure peak and swelling period are a function of the type of deposit, cleaning temperature and cleaning solution concentration. Increasing the cleaning temperature and cleaning concentration decreases the pressure peak and swelling period. This is in accordance with previous studies (Tuladhar et al., 2002, Christian, 2004) where the increase in cleaning temperature, coupled with the NaOH %, led to a larger decrease in cleaning time during cleaning WPC deposit in coupons. Generally the swelling period decreases with increasing fouling temperature with the exception of 50°C, NaOH 1wt% when the swelling of deposit was produced at 95°C took longer by 10 seconds.

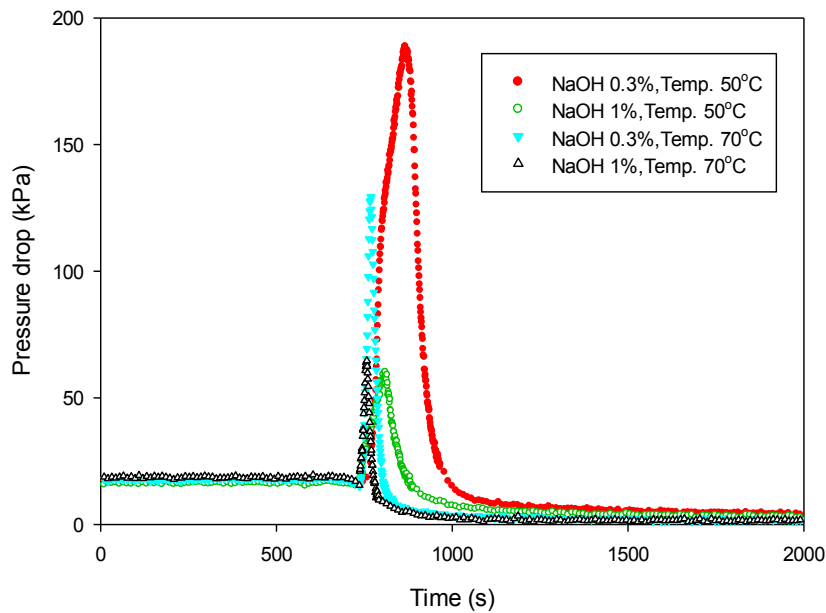


Figure 6.5: Cleaning behaviour in terms of pressure drop at section 3 for WPC deposit formed at 140°C.

For the WPC deposit formed at 140°C (see Figure 6.5), the swelling period and pressure peak decreased by 45% and 68% respectively when the cleaning solution (NaOH) concentration was increased from 0.3 wt.% to 1 wt.% and at a cleaning temperature of 50°C, as shown in Table 6.1 and Table 6.2. Similarly, the swelling period and pressure peak decreased by 33% and 37% respectively when the cleaning solution (NaOH) concentration was increased from 0.3 wt.% to 1 wt.% at a cleaning temperature of 50°C for the WPC deposit formed at 95°C. This increase in pressure peak and reduction in the swelling period for deposit produced at 95°C, compared to WPC deposit formed at 140°C, may refer to the nature of the deposit formed at the lower temperature of 95°C being soft and spongy in structure (Changani et al., 1997, Bansal and Chen, 2006).

| Temperature (°C) | 50 | | 70 | |
|------------------------------------|------|-----|------|-----|
| Cleaning concentration (NaOH %) | 0.3 | 1 | 0.3 | 1 |
| Pressure drop (ΔP) (kPa) | 2.55 | 1.6 | 1.05 | 0.8 |
| Swelling period (sec.) | 195 | 130 | 45 | 30 |

Table 6.1: Swelling period during cleaning for WPC formed at 95°C.

| Cleaning temperature (°C) | 50 | | 70 | |
|------------------------------------|------|-----|------|------|
| Cleaning concentration (NaOH %) | 0.3 | 1 | 0.3 | 1 |
| Pressure drop (ΔP) (kPa) | 1.88 | 0.6 | 1.29 | 0.65 |
| Swelling period (sec.) | 220 | 120 | 60 | 45 |

Table 6.2: Swelling period during cleaning for WPC formed at 140°C.

At higher temperatures the reaction between the cleaning solution and deposit is rapid; and the deposits are removed quickly, resulting in a smaller swelling period. Therefore, the swelling period and pressure peak decreased by 29 % and 50 % respectively when the cleaning solution (NaOH) concentration was increased from 0.3 wt.% to 1 wt.% at a cleaning temperature of 70°C, for the WPC deposit formed at 140°C. Consequently, the swelling period and pressure peak decreased by 37% and 25% respectively when the cleaning solution (NaOH) concentration was increased from 0.3 wt.% to 1 wt.% at a cleaning temperature of 70°C for, the WPC deposit formed at 95°C, as seen in Table 6.1 and Table 6.2. Increases in cleaning temperature cause reductions in pressure peak,

swelling period and the duration of each stage. This finding is consistent with the work by Tuladhar et al. (2002) and Christian (2004).

The time to clean in terms of pressure drop for both WPC deposits formed at 140°C and 95°C shows considerable differences. In general, the time to clean deposits formed at 140°C took much longer than the deposits formed at 95°C, as seen in Table 6.3 and Table 6.4. This may be due to further denaturation of proteins, resulting in a deposit that is harder to clean.

| Temperature (°C) | 50 | | 70 | |
|---|------|-----|-----|------|
| Cleaning concentration (NaOH %) | 0.3 | 1 | 0.3 | 1 |
| Time to clean (ΔP) (sec.) | 770 | 510 | 335 | 255 |
| Time to clean (UA) (sec.) | 1200 | 910 | 630 | 610 |
| Time to clean (turbidity reading) (FTU) | 2045 | 975 | 855 | 1035 |

Table 6.3: Time to clean according to: heat transfer coefficient in terms of area (UA), pressure drop and turbidity reading for WPC formed at 95°C.

As discussed earlier in section 2.3.2.1, several authors have attributed the rise of cleaning temperature to reduction of time needed for cleaning (including (Hankinson and Carver, 1968, De Goederen et al., 1989, Fryer and Bird, 1994)) during cleaning WPC deposit in tubular heat exchanger and coupon.

For deposits formed at 140°C (see Table 6.4), the rise in cleaning temperature from 50°C to 70°C at a cleaning solution (NaOH) concentration of 0.3 wt.% decreased the time for

cleaning by 76 %. Similarly, for the deposit formed at 95°C, the increasing of cleaning temperature from 50°C to 70°C, at a cleaning concentration of 0.3 wt.% (NaOH) decreased the time to clean by only 26%. The contribution of temperature is more important at a lower concentration of 0.3 wt.% NaOH, where the time to clean decreases more noticeably with an increase in temperature than at a higher concentration of 1wt% (see Table 6.3 and Table 6.4). Cleaning experiments, for deposit produced at 140°C, at the lower temperature of 50°C involved significantly longer cleaning times, with a ca. 4.2 times increase compared to 70°C at 0.3 wt% NaOH. The deposit produced at high temperature can be removed from the surface with much greater difficulty. This behaviour may refer to the hard structure of the deposit formed at 140°C.

| Temperature (°C) | 50 | | 70 | |
|--|------|------|------|------|
| Cleaning concentration (NaOH %) | 0.3 | 1 | 0.3 | 1 |
| Time to clean (ΔP) (sec.) | 2570 | 2225 | 610 | 390 |
| Time to clean (UA) (sec.) | 740 | 750 | 435 | 380 |
| Time to clean (turbidity reading) (FTU) | 1840 | 1160 | 1945 | 2430 |

Table 6.4: Time to clean according to: heat transfer coefficient in terms of (UA), pressure drop and turbidity reading for WPC formed at 140°C.

The plate pack was opened once the pressure drop had reached the clean value in section 3 of PHE; small patches of fouling can be observed with translucent white colour, and the texture was viscous as shown in Figure 6.6. This result indicated that the pressure sensor cannot detect the small layer of fouling.

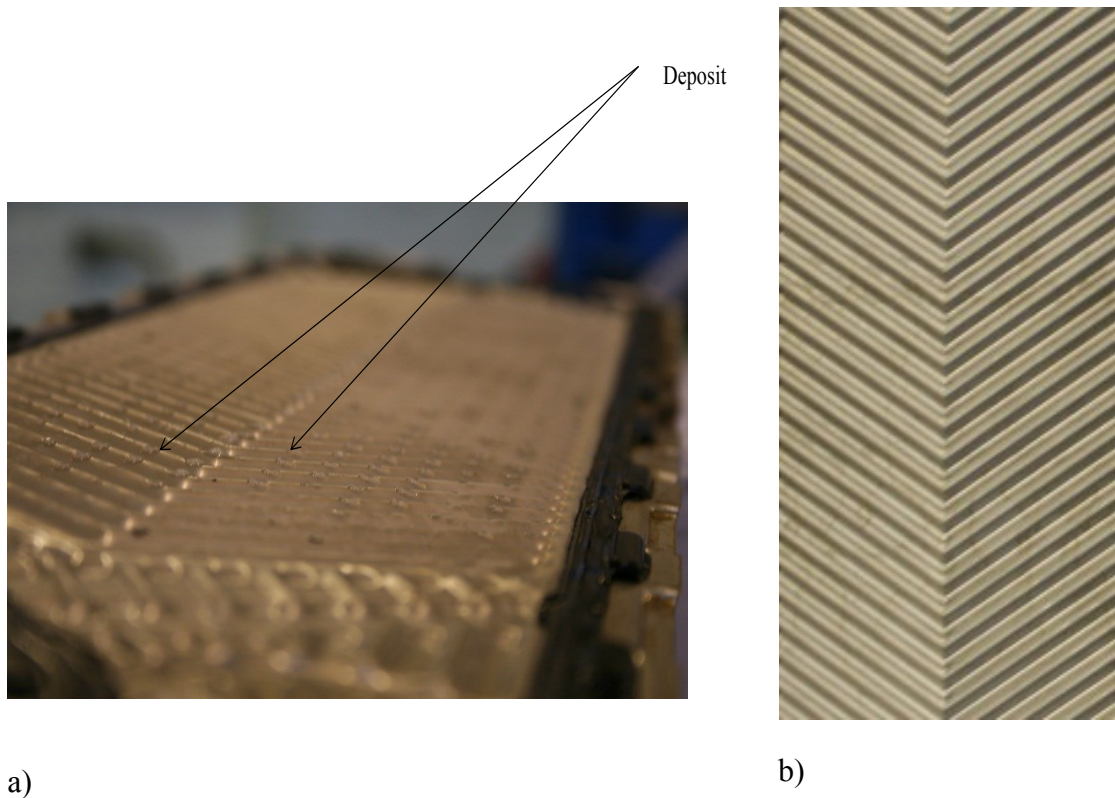


Figure 6.6: The remaining deposit once the pressure drop reached the nominal clean value (a) clean plate (b).

6.2.3.2.2 Monitoring fouling removal vs heat transfer coefficient

The heat recovery during removal of WPC deposits shows similar trends under all conditions. Although the fouling experiment for both deposits formed at 95°C and 140°C was terminated when the pressure drop reached 17 kPa, the initial heat transfer coefficients were 0.12 kW/K and 0.17 kW/K respectively.

A typical cleaning curve (heat transfer coefficient vs. time) is given in Figure 6.7 and Figure 6.8. There is an initial reduction in heat recovery in each case due to swelling of the deposit before the heat transfer coefficient in terms of area UA recovers back and continues to increase until it achieves a final steady value.

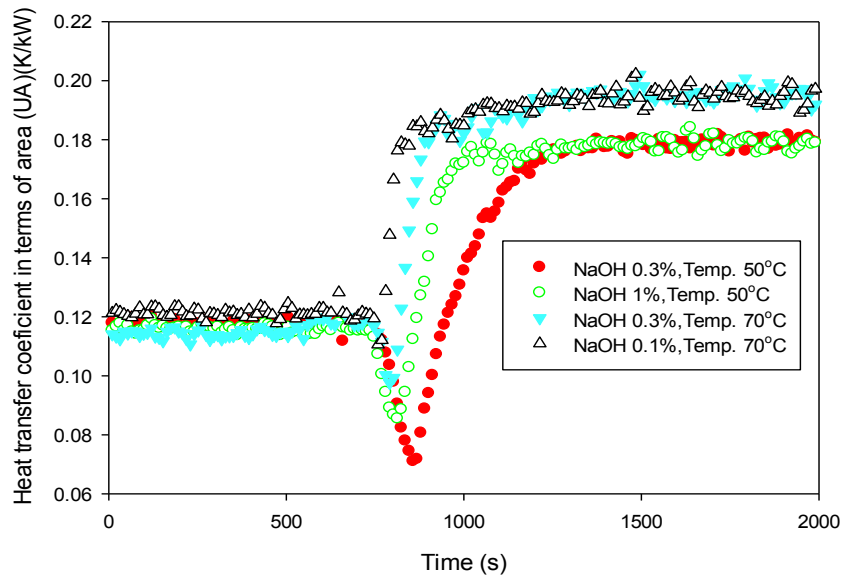


Figure 6.7: Cleaning behaviour according to heat transfer coefficient in terms of area (UA) at section 3 for WPC deposit formed at 95°C.

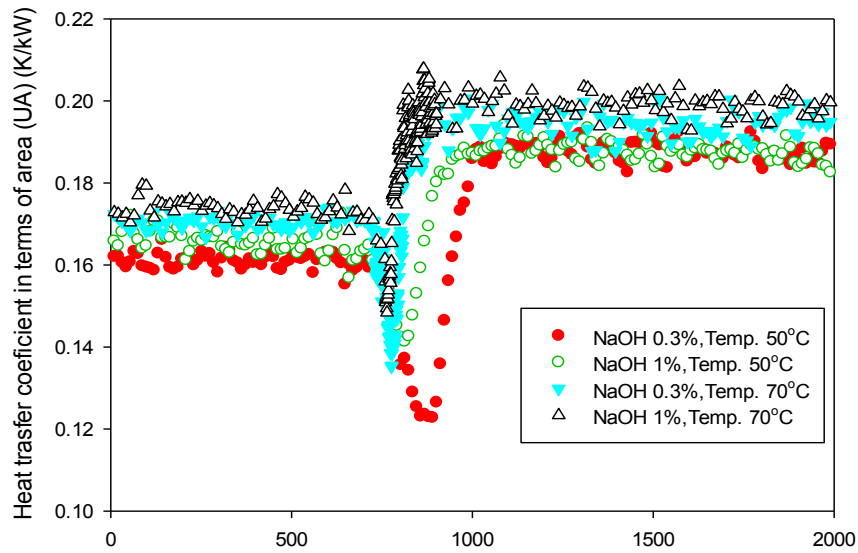


Figure 6.8: Cleaning behaviour according to heat transfer coefficient in terms of area (UA) at section 3 for WPC deposit formed at 140°C.

The heat transfer coefficient in terms of area UA became narrower as the concentration of cleaning chemical and cleaning temperature was increased, i.e. cleaning times decreased. In general the time to clean in terms of heat recovery for the deposit formed at 95°C was longer than the deposit formed at 140°C. This may refer to the greater reduction in UA during fouling for deposit formed at 95°C compared to those at 140°C. While the maximum reduction in the time to clean in terms of heat recovery for each deposit at different cleaning conditions was 49% for both deposits, it was 85% and 67% in terms of pressure drop for deposit produced at 140 and 95°C, respectively, as seen in Table 6.3 and Table 6.4. These results may imply that this measurement cannot detect the remaining small fouling layer and that it does not respond well to the change in cleaning conditions. Thus, there is an advantage to pressure drop measurement to detect the cleaning end point over heat transfer coefficient.

6.2.3.2.3 Monitoring fouling removal vs turbidity

Turbidity was determined online using a turbidity probe during cleaning experiments. The turbidity probe was located directly in the exit pipe of the PHE. Figure 6.9 and Figure 6.10 show the effect of temperature and cleaning concentration on removing deposit in terms of turbidity during cleaning. The cleaning behaviour monitored by the turbidity probe was mirrored in the cleaning behaviour during pressure drop monitoring. The data in those figures show at 0.3 wt. % NaOH that an increase in temperature tends to decrease turbidity more quickly (more so at 70 than 50°C). At 50°C a decrease in turbidity is quicker at 1 wt. % NaOH than at 0.3 wt. % NaOH. When cleaning temperature rose to 70°C, the pressure drop and turbidity reading achieved clean values earlier, within the first 12 minutes. The turbidity profile suggests that more deposit is removed at a higher temperature and higher chemical solution, which was the case.

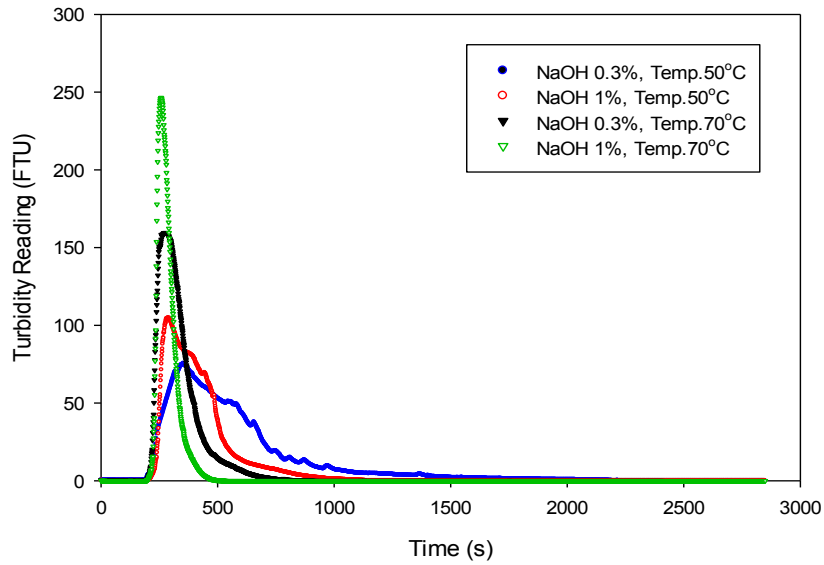


Figure 6.9: The effect of temperature and chemical concentration on turbidity reading during cleaning of WPC deposit formed at 95°C.

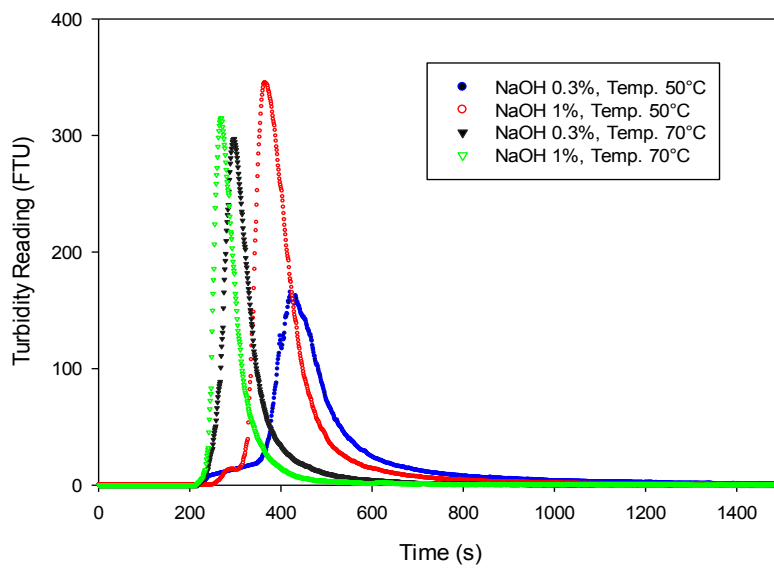


Figure 6.10: The effect of temperature and chemical concentration on turbidity reading during cleaning of WPC deposit formed at 140°C.

The cleaning time and duration of each cleaning stage are longest at low temperatures and chemical concentration. Table 6.5 and Table 6.6 show the reading of the turbidity probe at

the last stage of cleaning for the two WPC deposits cooked at 95°C and 140°C. When pressure drop reached the cleaning value and lasted for 10 minutes at a cleaning temperature of 50°C and 0.3 NaOH% for deposit produced at 95°C, the turbidity meter did not confirm that PHE was clean and reported a value of 4.2 FTU. This may indicate that the turbidity could detect the removal of a small amount of deposit. However, if the turbidity reading reaches 0 reading, this does not indicate that the PHE is clean, as the turbidity probe could only measure the turbidity of fluid which has dissolved deposit, not surface-bound deposit. It is evident that during thermal stability with water prior to cleaning, the turbidity probe showed 0 despite the existence of deposit on the PHE surface.

| Temperature (°C) | 50 | | | | | | 70 | | | | | |
|-------------------------|-----|------|------|-----|-----|-----|-----|-----|-----|-----|-----|------|
| | 0.3 | | | 1 | | | 0.3 | | | 1 | | |
| Turbidity reading (FTU) | 10 | 1 | 0 | 10 | 1 | 0 | 10 | 1 | 0 | 10 | 1 | 0 |
| Time (sec.) | 760 | 1855 | 2045 | 515 | 850 | 975 | 450 | 730 | 855 | 270 | 730 | 1035 |

Table 6.5: Turbidity reading at the last stage of cleaning for WPC formed at 95°C.

The cleaning rate at the last stage of cleaning for the WPC deposit formed at 140°C is lower than the WPC deposit formed at 95°C, which was confirmed also by pressure drop data, as seen in Table 6.5 and Table 6.6. This may refer once again to the hard structure of the WPC deposit formed at 140°C. Increasing the fluid temperature increased the cleaning

rate for all the conditions investigated, resulting in a quicker removal of the deposit and a narrower peak of turbidity reading.

| Temperature (°C) | 50 | | | | | | 70 | | | | | |
|---------------------------------|-----|------|------|-----|------|------|-----|-----|------|-----|-----|------|
| Cleaning concentration (NaOH %) | 0.3 | | | 1 | | | 0.3 | | | 1 | | |
| Turbidity reading (FTU) | 10 | 1 | 0 | 10 | 1 | 0 | 10 | 1 | 0 | 10 | 1 | 0 |
| Time (sec.) | 595 | 1210 | 1840 | 650 | 1135 | 1160 | 355 | 710 | 1945 | 270 | 610 | 2430 |

Table 6.6: Turbidity reading at the last stage of cleaning for WPC formed at 140°C.

The plate pack was only opened when both the turbidity reading and pressure drop achieved clean values as in some conditions, such as, at a cleaning temperature of 50°C and concentration of 0.3 wt.% NaOH for the deposit formed at 140°C, turbidity readings reached 0 while pressure was still decreasing. Section 3 of PHE was visually clean, and the surface did not give a greasy feeling to clean fingers when they were rubbed on the surface.

6.2.3.2.4 Monitoring fouling removal vs particles count technique

Figure 6.11 and Figure 6.12 show the effect of temperature and cleaning concentration in removing deposits in terms of particles count during cleaning. In general, the phenomenon of removing particles from PHE by using the particles counting technique is similar to a turbidity meter. Since there is a difficulty of setting the sampling time less than 30 seconds, the maximum number of whey protein particles removed from PHE does not

show the real maximum number of particles. For instance, at 70°C and 0.3 wt. % NaOH for deposit produced at 95°C, the maximum particles removed were 16000, while at 1 wt. % NaOH were 8000 particles as shown in Figure 6.11 and Figure 6.12 .

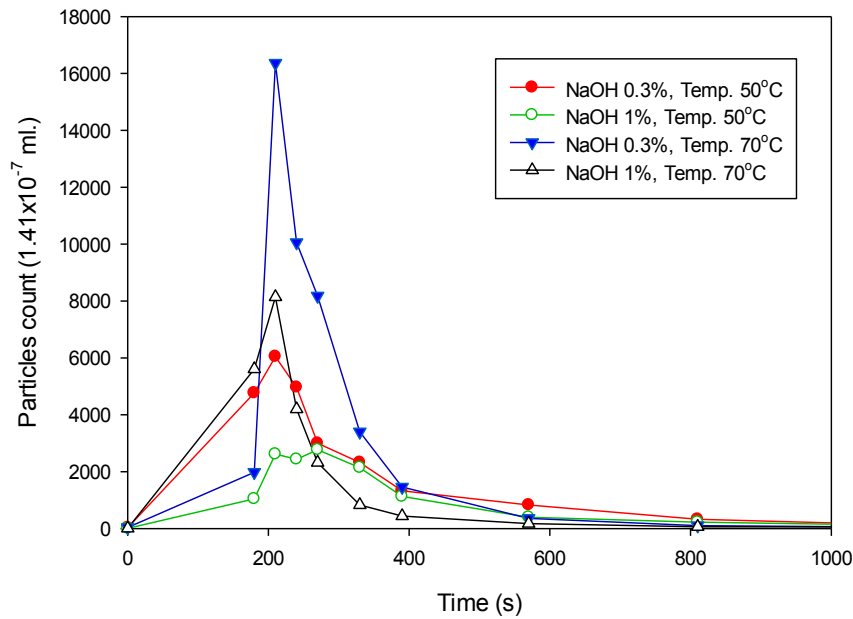


Figure 6.11: The effect of temperature and chemical concentration on particles count during cleaning of WPC deposit formed at 95°C.

At 1 wt. % NaOH and 70°C the maximum particles removed should be more, but due to the sampling time being 30 seconds, the maximum particles were missed in this case. The maximum number of particles at low temperature can be achieved at a later time compared to those at high temperature. For example, at 1wt. % NaOH and 70°C for deposit formed at 140°C, the maximum particles removed were achieved at ca. 300 sec. while at 0.3wt. % NaOH and 50°C, those removed were achieved at ca. 500 sec. This may be due to the swelling of WPC deposit in contact with NaOH not releasing significant amounts of deposit until extensive swelling has occurred.

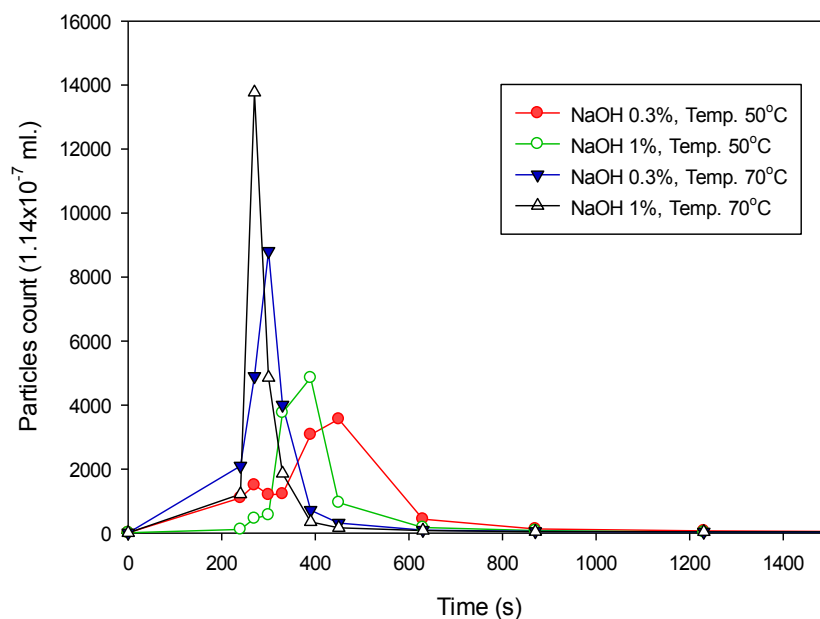


Figure 6.12: The effect of temperature and chemical concentration on particles count during cleaning of WPC deposit formed at 140°C.

A clear view for temperature effect on cleaning time is shown in Figure 6.11 and Figure 6.12. The results show cleaning times for every cleaning condition and show a reduction in cleaning time with a temperature increase. Low temperature and chemical concentration give rise to the greatest decay time, as can clearly be observed, i.e. at 50°C and 0.3 wt. % NaOH. High cleaning temperature results in a quicker removal of the deposit and a narrower peak of the particles reading.

The time to clean PHE by using this technique may exceed 50 minutes, as this tool can detect particles invisible to the naked eye. The initial number of particles before introducing the cleaning chemical was fewer than 13 particles in 1.41×10^{-7} ml. At all cleaning conditions, the number of particles dropped to fewer than 35 particles after the first 30 minutes. The minimum number of particles observed at the end of the cleaning

process (80 minutes) was 5 particles in 1.41×10^{-7} ml. The particles count is a very sensitive technique for detecting any particles passing through the PHE.

6.2.3.2.5 Monitoring removal of the WPC_m deposit

Two-stage cleaning was used in these experiments. Whey protein deposit is initially removed by NaOH for 50 minutes, and then an acid step was introduced to remove minerals remaining on the surface.

Figure 6.13 shows the behaviour of WPC_m particles removed from the PHE during cleaning time. Initially, the particles removed were very high in the first 5 minutes when the deposit contacted with the cleaning solution, and then the particle removal rate gradually decreased until achieving the clean value of fewer than 20 particles after approximately 30 minutes as seen in Table 6.7. The increasing in pressure drop after ca. 600 sec. may be due to the blockage in PHE, as no particles have been removed. In this stage the pressure drop has not indicated the cleaning value yet, and cleaning by nitric acid was introduced to clean the remaining mineral deposits. Another abrupt pressure drop coincides with an increase in particle count removal, which made the pressure drop return to the clean status.

Similar to the turbidity probe, the disadvantage of the particles count method is that it can only detect the deposit in the fluid.

| Time (min.) | No. particles in (1.41×10^{-7} ml) |
|--------------------------------------|--|
| Cleaning with NaOH | |
| 0 | 20 |
| 3 | 60 |
| 3.5 | 10750 |
| 4 | 6500 |
| 4.5 | 2850 |
| 5 | 5500 |
| 6 | 6250 |
| 7.5 | 3600 |
| 10 | 700 |
| 14 | 175 |
| 20 | 51 |
| 30 | 20 |
| 50 | 10 |
| Cleaning with HNO₃ | |
| 56.5 | 32 |
| 57 | 327 |
| 57.5 | 550 |
| 58 | 2004 |
| 60 | 68 |
| 63 | 22 |
| 73 | 8 |
| 113 | 5 |

Table 6.7: The number of particles removed during cleaning process for WPC_m formed at 140°C.

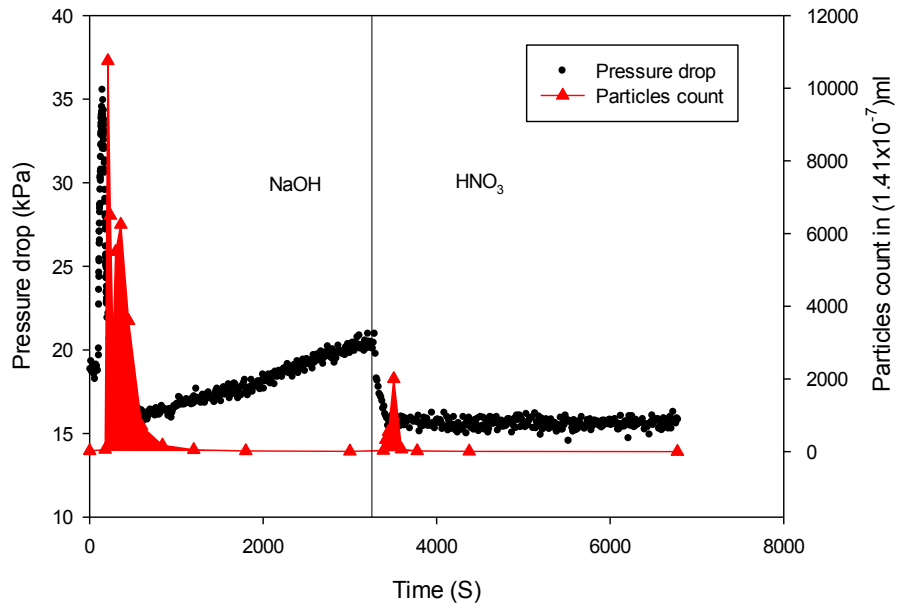


Figure 6.13: Particles count and pressure drop during cleaning of WPC_m deposit at section 1 of PHE temperature 140°C.

6.2.3.2.6 Particle size distribution

A typical particle size distribution for whey protein deposit during cleaning is given in Figure 6.14. The mean particle size is 177 nm \pm 15 nm, with 50% of particle size being less than 163nm \pm 13.6 nm, and 90% of particle size being less than 287 nm \pm 33nm.

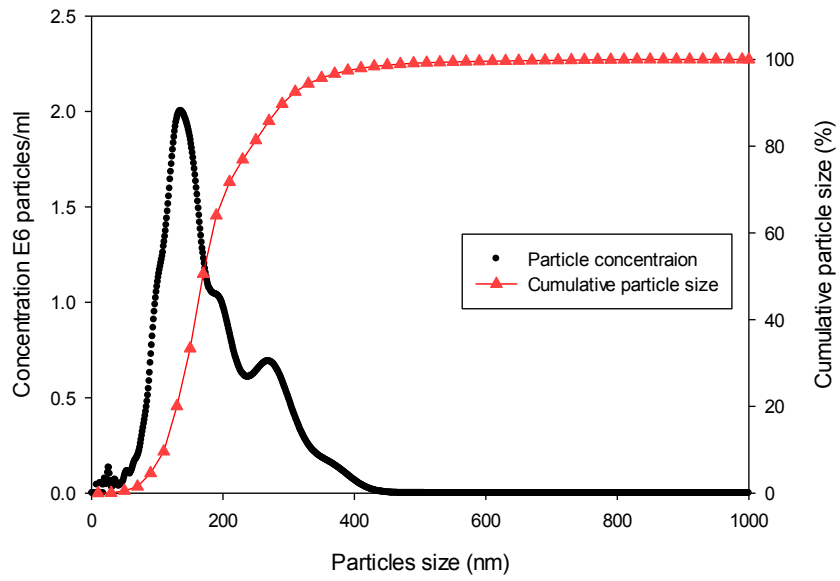


Figure 6.14: A typical particles size distribution and cumulative particles size (%) during cleaning of WPC deposit.

6.3 Part B: The validation of using Peltier device technique on monitoring cleaning of two types of deposits

The turbidity and particle count techniques cannot detect the deposit removal, if there is no any deposit present in the effluent water, unless the chemical concentration and cleaning temperature were sufficient to remove all the deposits from the surface and flow them in the cleaning fluid to be measured. In this part, a preliminary work was conducted to investigate the possibility of using a Peltier device as a novel monitoring method in cleaning studies. This technique is a fully integrated on-line monitoring system, *in situ* and in real time, providing information about the change of Peltier temperature and output power (%) during the cleaning of deposits. Peltier is used to create a heat flux between the junctions of two different types of materials. The device has two sides; one side of the device is heated to a temperature greater than the other side. Throughout this section, the side of the Peltier next to the fouled plate is called the Peltier surface, and the side next to the heat sink is called the heat sink surface. When a DC Voltage is applied to the device, a difference in temperature will build up between the two sides, which bring heat from one side to the other so that one side gets cooler while the other gets hotter. Reversing the polarity will result in reversed hot and cold sides. The aims of this part are to measure the response of the Peltier device during the removal of deposit and to optimise the setup of the Peltier device.

6.3.1 Cleaning experiments

Two types of deposit were used, namely tooth paste and golden syrup. The difference in the cleaning behavior between the two deposits was remarkably different. The reason behind this selection is to observe the sensitivity of the Peltier device to the different

removal situations. The two deposits could be removed by flow of water action alone. Cleaning was monitored from the recovery of the temperature, output power (%) and the visual analysis (images) of the deposits remaining on the plate surface.

A bench scale cleaning rig, as described in Section 3.5.3, is used because its thermal and hydraulic conditions are well defined. While the heater tank reached the desired temperature, the pump was started to circulate the water in the tank containing soft water until achieving the desired temperature (see section 3.9). A known mass of toothpaste or golden syrup was spread evenly over the fouled plate, inserted in the circular channel and joined together by a clamp. The camera was turned on; time and sample rate were recorded so that images could be compared with the Peltier readings. Afterwards cleaning was initiated again by restarting the pump. Throughout this discussion, time $t = 0$ refers to time where the pump was initiated to draw water from the water tank and pump it through the test section.

6.3.2 Results and Discussion

Peltier device has been used in the experiments that follow to monitor the cleaning process by the change in temperature and output power (%). It has been observed that as the insulating deposit layer is removed during cleaning, the temperature and output power (%) of Peltier across the surface change. The cleaning behaviour of the tooth paste and golden syrup was compared based on the data obtained from the Peltier as well as the images taken from the camera. However, due to the square shape of the Peltier in comparison with the circular shape of the fouled plate, only ca. 28% of the fouled plate was detected by the Peltier.

There are many variables in the Peltier device which should be set to monitor the cleaning process in the best possible way. These are surfaces of the Peltier device, temperature of the surfaces to be set and the operation of the fan. A large amount of time was spent to investigate the optimum operation of the Peltier in cleaning experiments. Since the use of Peltier for cleaning deposits has not been reported previously, the main objective of this chapter is to investigate the response of the Peltier device during cleaning.

6.3.2.1 Flow diagnoses

The response of the Peltier device on cleaning the rig was investigated by flowing water across the clean plate at the following conditions: water flow temperature of 50°C, heat sink temperature set to 35°C and at different flow rates. Four different flow rates of water were used through the test section, i.e. 6 L/min, 9.4 L/min, 12.7 L/min, and 16.2 L/min which give a flow velocity at the middle of fouled plate of 0.032, 0.050, 0.067, and 0.086 m/s respectively. For the first 5 minutes, the flow rate was set to 6 L/min and allowed to achieve a steady state. After achieving a steady state, this flow rate was kept for 10 minutes. After every 10 minutes, the flow rate was increased from 9.4 L/min to 16.2 L/min, followed by a reduction in the flow rate. As shown in Figure 6.15, the Peltier temperature showed a slight change with changing flow rates. Initially, a sharp increase in Peltier temperature was observed at the first 200 seconds, and then it levelled off with a changing flow rate and fluctuated within $\pm 3^\circ\text{C}$. This behaviour was also proven by output power (%) in Figure 6.16. There was a rapid increase in output power (%) around the starting time of increasing the temperature of Peltier. Then, there was a considerable noise on the Peltier device reading in terms of output power (%), but the trend in the Peltier device can still be observed.

Cleaning profiles in the present study show less response to the change of flow rate, compared with MHFS used to investigate different types of deposit found by Bird (1992), Gillham (1997), Christian (2004), and Aziz (2008).

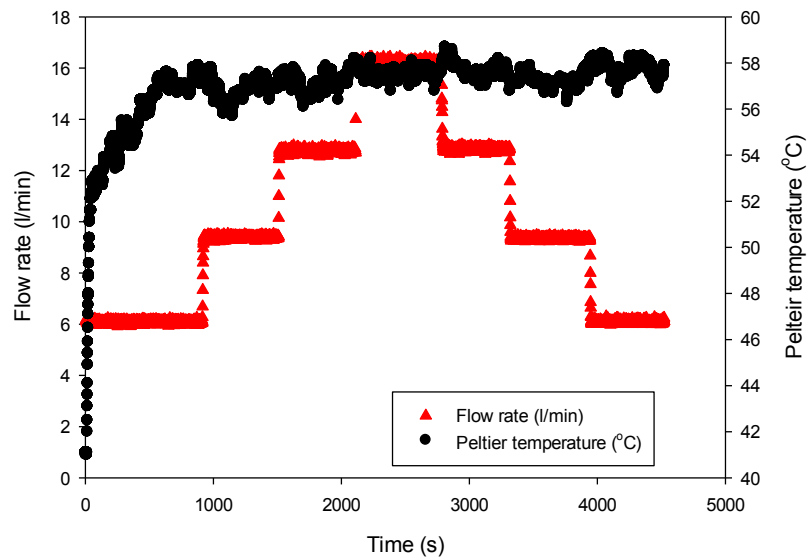


Figure 6.15: Peltier device temperature readings with changes in flow rate

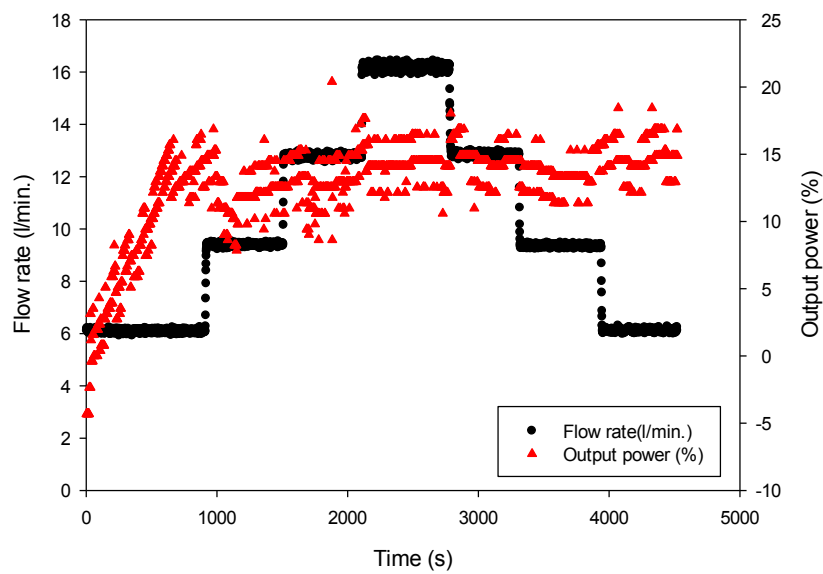


Figure 6.16: Peltier output power (%) readings with changes in flow rate.

6.3.2.2 Evaluation of Peltier response

It is essential to gain an understanding of how Peltier works in order to use it effectively to monitor cleaning deposits. Therefore, an insulation layer was put above the fouled plate to observe the effect of that layer on Peltier response. Both the heat sink and cleaning water temperature were set at 50°C.

Figure 6.17 and Figure 6.18 show that once the cleaning water contact the insulation layer, the Peltier temperature increased gradually in the first 600 seconds, and then plateau can be observed afterwards in the Peltier temperature at 38.8°C. In contrast, a sharp increase in Peltier temperature was seen in case of not using insulation, and reached the thermal stability in the first 200 seconds at Peltier temperature of 54°C. It can be seen that the resultant Peltier temperature increased by 39% and the output power (%) by 29% in case of not using insulation. This result implies that the Peltier device can be used for monitoring the cleaning deposit.

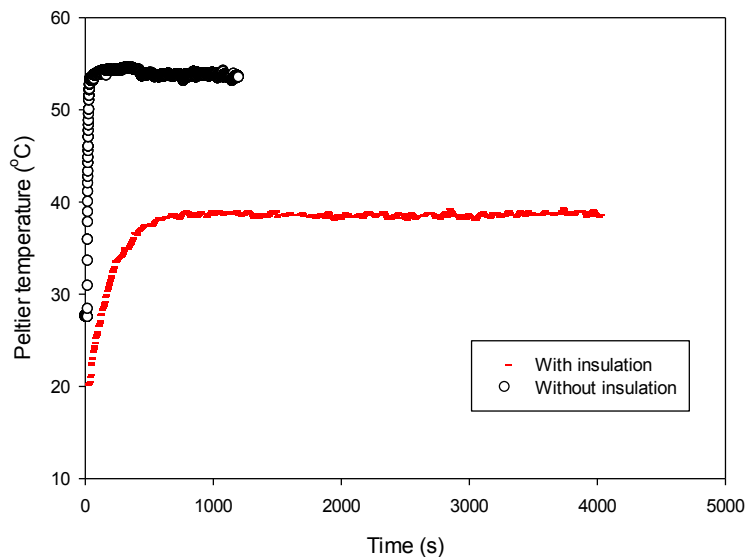


Figure 6.17: The effect of insulation layer on Peltier response in terms of Peltier temperature, heat sink 50°C and cleaning water 50°C.

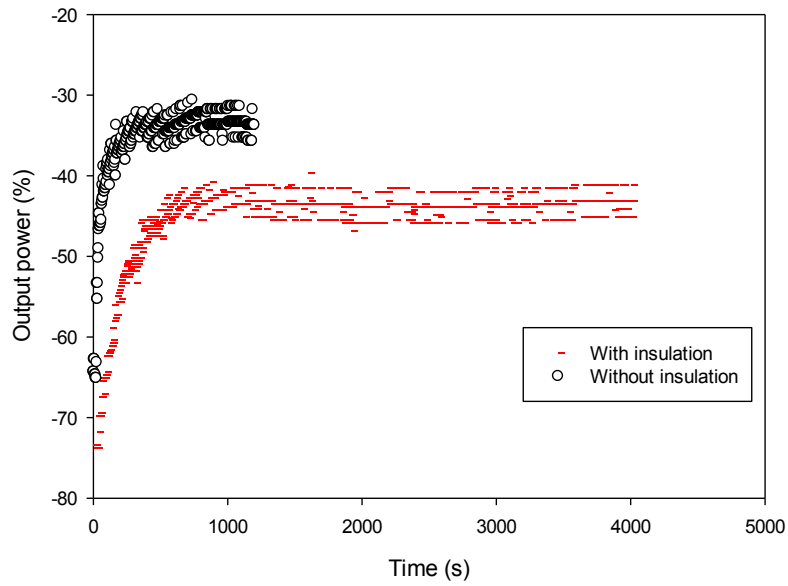


Figure 6.18: The effect of insulation layer on Peltier response in terms of output power (%), heat sink 50°C and cleaning water 50°C.

6.3.2.3 The effect of fan

The heat sink often needs a fan to have sufficiently low thermal resistance and to minimise the size of the sink required. Figure 6.19 and Figure 6.20 show the effective role of using a fan on the Peltier temperature and output power (%). The experiment started with passing water at 70°C through the test section at a constant heat sink temperature of 60°C. The Peltier power and temperature increased in contact with the hot water at 70°C. In order to keep the set point for the heat sink constant, the resultant Peltier power and temperature changed, depending on whether the fan is used or not. It could be observed that when the Peltier device reached the thermal stability, the Peltier temperature and output power (%) increased by ca. 6°C and 40% respectively, without using the fan.

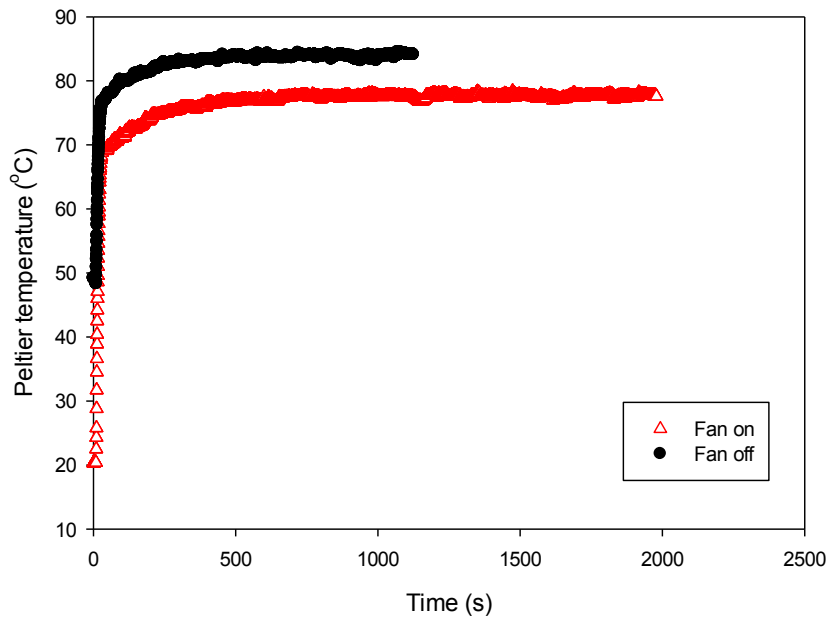


Figure 6.19: The effect of using a fan on the Peltier temperature at heat sink temperature 60°C.

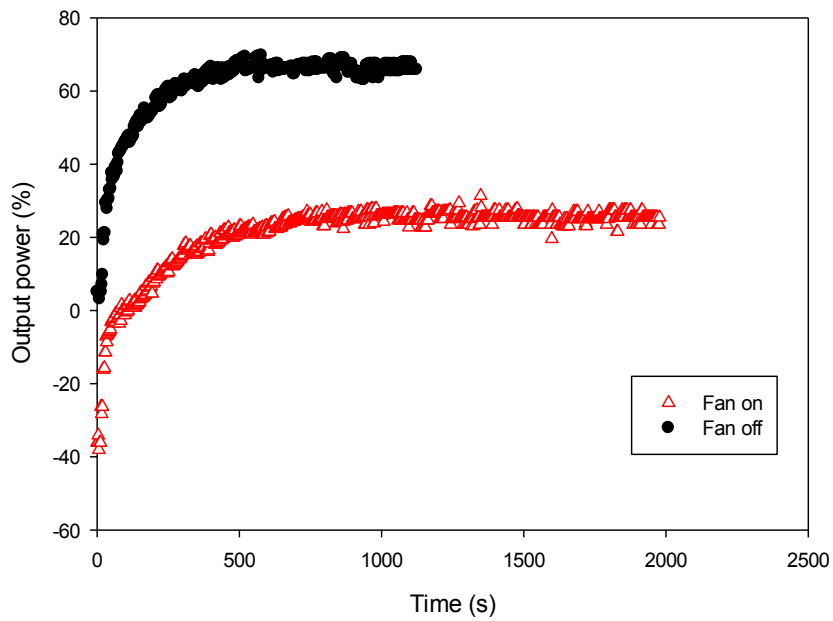


Figure 6.20: The effect of using a fan on the Peltier output power (%) at heat sink temperature 60°C.

6.3.2.4 Effect of controlling one of the two surface temperatures on Peltier response

Peltier has two surfaces: cold and hot. The temperature controller is used to control the temperature of one of the surfaces of the Peltier device. Therefore, the other surface temperature changes during the removal of deposits. To determine the best surface temperature to set in order to get more response during deposit removal, the sensitivity of the Peltier device was initially tested by controlling one of the Peltier surface temperatures. Experiments were carried out by flowing water at two temperatures (50 and 70°C) through the test section of the bench scale rig at different heat sink and Peltier temperatures, as shown in Figure 6.21.

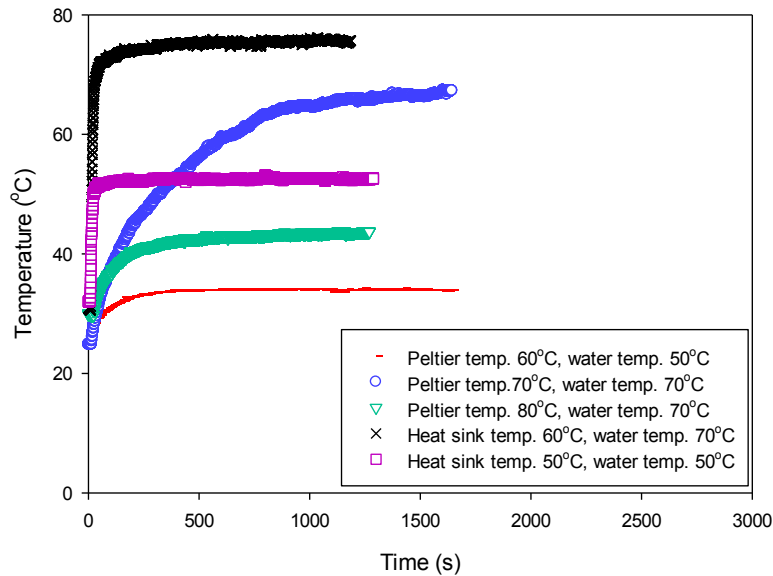


Figure 6.21: Comparison of the response of the Peltier device on controlling one of the two surfaces temperatures.

When the heat sink temperature was controlled, the Peltier temperature increased sharply and reached closer to its maximum range at the initial period (200 sec), i.e. the Peltier

device reached thermal stability in the first 200 seconds. On the other hand, controlling the Peltier surface temperature resulted in the gradual increase in heat sink temperature during flowing water. Heat sink temperature kept rising over time when the Peltier temperature was set to 70°C and at water temperature 70°C. However, as shown in Figure 6.21 that the heat sink temperature showed slower response compared to Peltier temperatures and reached the thermal equilibrium at a later time of 400 seconds when the Peltier temperature was set at the temperature of 80°C. In general, at a low temperature, the Peltier device reached thermal stability at an earlier time, as less power is needed to achieve the thermal stability. Therefore, the figure clearly illustrates that the heat sink temperature should be controlled and thus Peltier temperature reading should be used to monitor the cleaning process.

6.3.2.5 Controlling the heat sink temperature

Understanding the influence of controlling different heat sink temperatures on the Peltier temperature and output power (%) is important in comprehending the Peltier device behaviour. Experiments were carried out by flowing water at 50°C through the test section of the bench scale cleaning rig at different heat sink temperatures as shown in Figure 6.22. Three Peltier temperatures (53.7, 57.2 and 68.8°C) were obtained while the heat sink temperature was set at 30, 35 and 40°C respectively. In contact with water, the Peltier temperature for the three controlled temperatures rose sharply during the first 100 seconds, followed by gradual increases for the two temperatures controlled at (30 and 35°C) and a plateau for the one controlled at temperature 40°C. The two temperatures controlled at 30 and 35°C were found to give the lowest time to reach the thermal stability during 800 seconds, while controlling the heat sink at 40°C gave the quickest time to

reach the thermal stability within the first 200 seconds. This may suggest that the smaller the temperature difference between the heat sink and bulk temperature, the quicker the achievement of thermal stability, which may imply the quicker response of the Peltier device during cleaning.

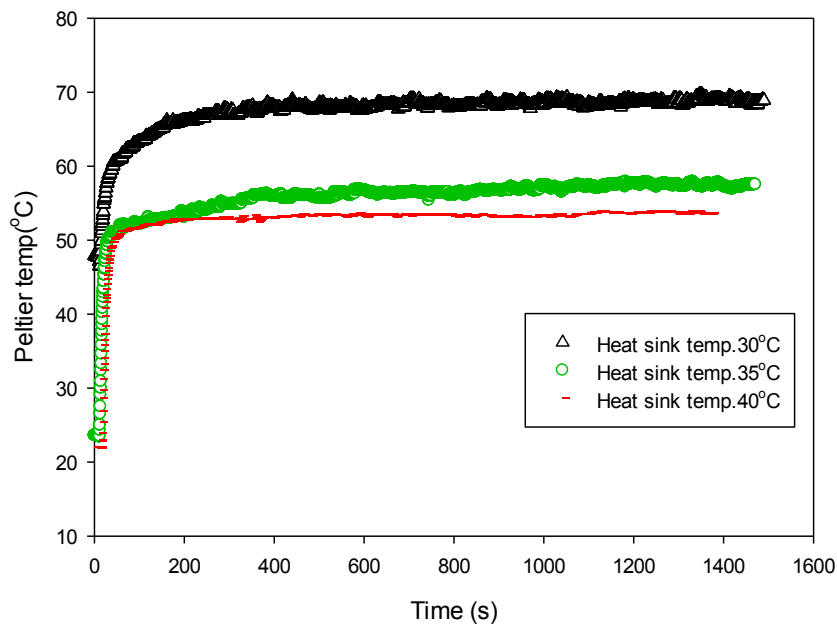


Figure 6.22: The resultant Peltier temperature when controlling the heat sink at 30, 35 and 40°C.

6.3.2.6 Sensitivity of the Peltier throughout the cleaning experiment

Understanding the response of the Peltier during deposit removal is essential to validate the use of this monitoring for such cleaning processes. As mentioned earlier, two deposits were selected; namely, tooth paste and golden syrup and they were investigated separately.

From Figure 6.23 and Figure 6.24, during the cleaning of toothpaste deposit, an initial increase in the Peltier temperature and output power (%) can be observed during the first 200 seconds approximately. During this time, the water entered the test section with a thermal equilibrium being established. Although the plate was fully fouled with tooth paste deposit by this time, the Peltier temperature increased only gradually, probably because of the reason that the tooth paste absorbed water. Distinct changes were observed in the Peltier temperatures between the water and tooth paste deposit curves throughout the removal process. Images showed no significant deposit removal during the first 1080 seconds, as shown in Figure 6.25.

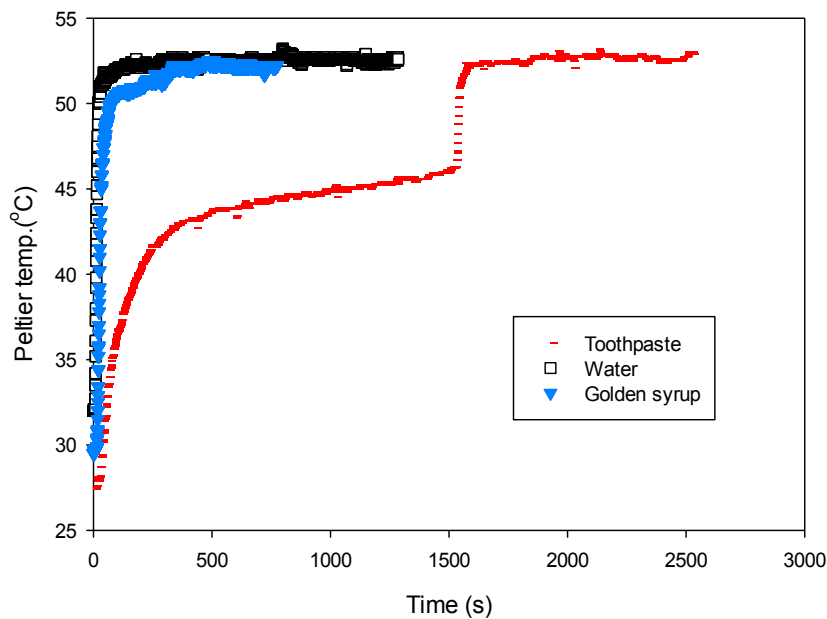


Figure 6.23: Change in the Peltier temperature during cleaning of the tooth paste and golden syrup deposits by controlling heat sink temperature at 50°C.

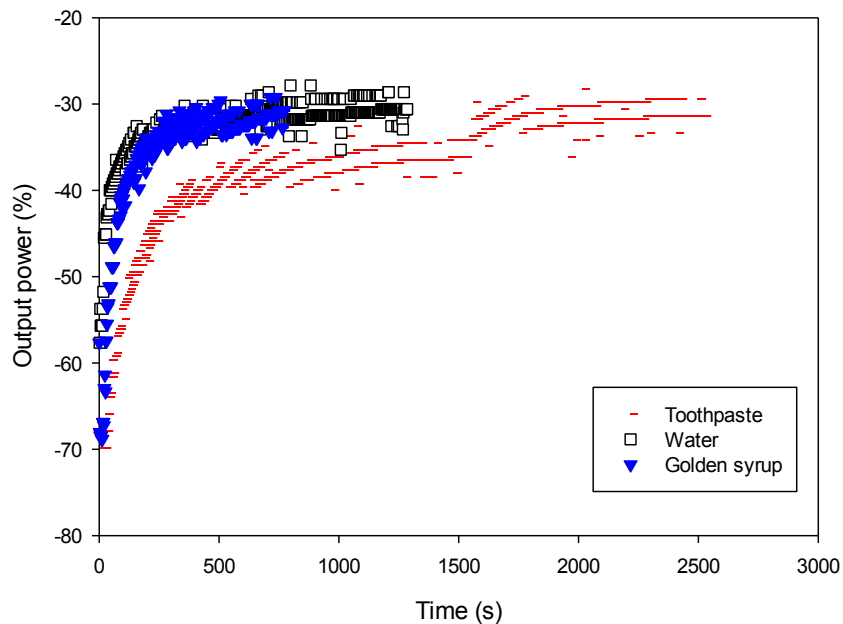


Figure 6.24: Change in output power (%) during cleaning of the tooth paste and golden syrup deposits by controlling heat sink temperature at 50°C.

A plateau in the Peltier temperature can be seen between 1080 seconds and 1440 seconds. During this period, a small island situated outside the area covered by the Peltier was removed corresponding to the small increase in Peltier temperature from 45 to 45.8°C. At 1450 seconds, the Peltier temperature changed rapidly by 6.5°C to 52.3°C, corresponding to a sharp decrease in the amount of the deposits as the deposits fell off as one big chunk. Images show that almost the whole plate was cleaned by this time and that approximately three quarters of the deposit were removed between 1440 and 1620 seconds. A plateau can be seen between 1620 and 2160 seconds, possibly due to the presence of small pieces of deposits attached to the surface, and was detected both by the Peltier corresponding a small temperature rise of 0.5°C between 52.3 and 52.8°C as well as by photographic evidence. This could suggest that the remaining deposit may partially be attached to the surface or that the temperature of deposit may reach the bulk temperature. At 2160 seconds, one island of the deposit remaining at the edge of the fouled plate was not

detected as it laid outside the area covered by the Peltier range (as discussed in section 3.9). Christian (2004) and Aziz (2008) observed similar effects by using MHFS and noted that it did not detect the remaining small islands. They concluded that the resistance from these small islands sometimes cannot be measured by the MHFS.

During the cleaning of the golden syrup deposit, the Peltier temperature increased rapidly which indicates fast removal of the deposit and the cleaning was terminated visually in only 200 seconds, as seen in Figure 6.24.

These results may suggest that the Peltier device could detect the different cleaning behaviour of deposit that has different rheological properties.

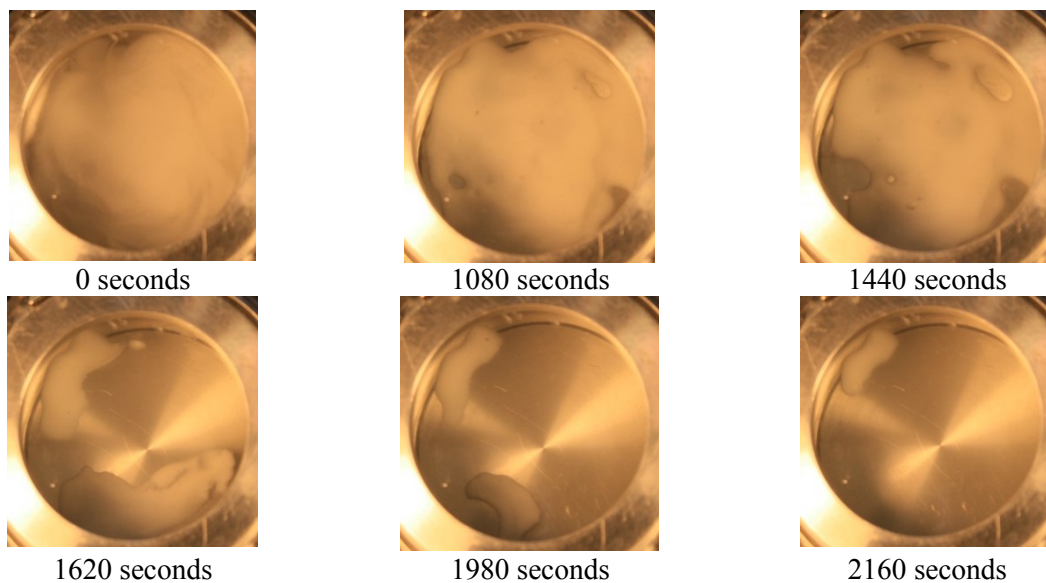


Figure 6.25: Images recorded during cleaning of toothpaste deposit by controlling heat sink temperature.

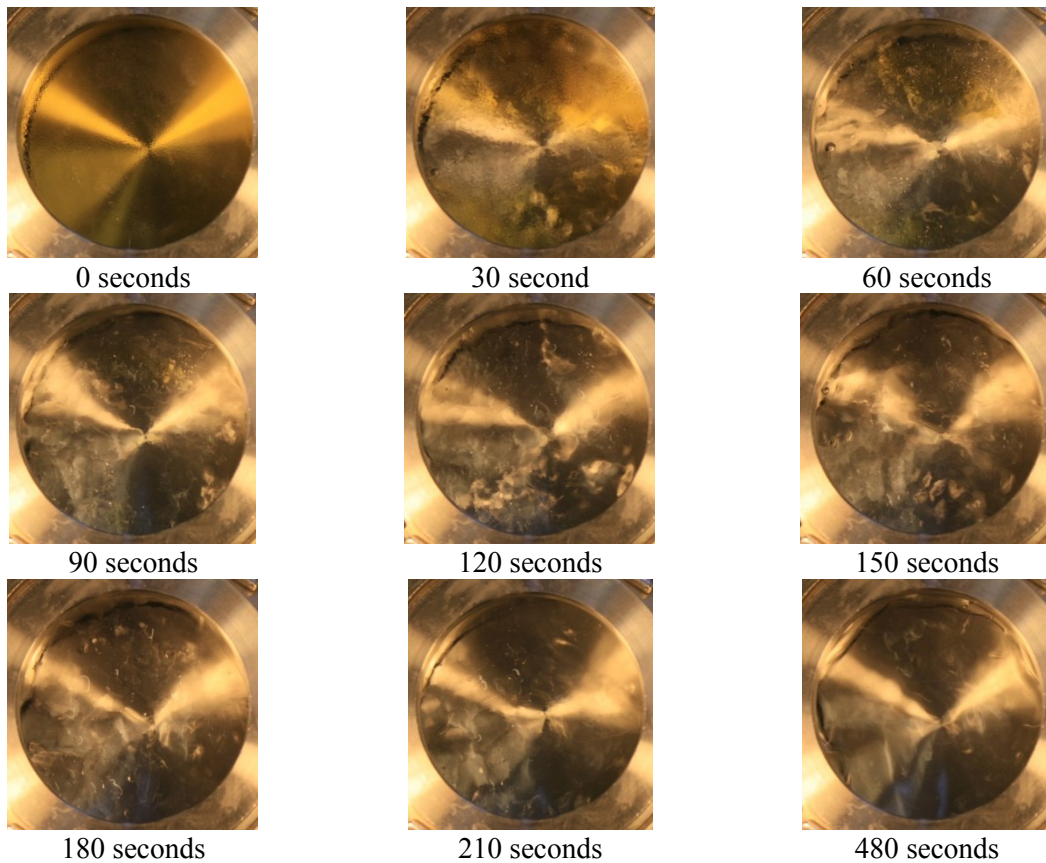


Figure 6.26: Images recorded during cleaning of the golden syrup deposit by controlling heat sink temperature.

6.3.2.7 Effect of controlling the Peltier temperature on cleaning deposit behaviour

During flow diagnostic, controlling the Peltier temperature shows less response to water flow compared to controlled heat sink temperature. This event gave an idea to investigate the behaviour of the Peltier device during deposit removal under controlling the Peltier temperature.

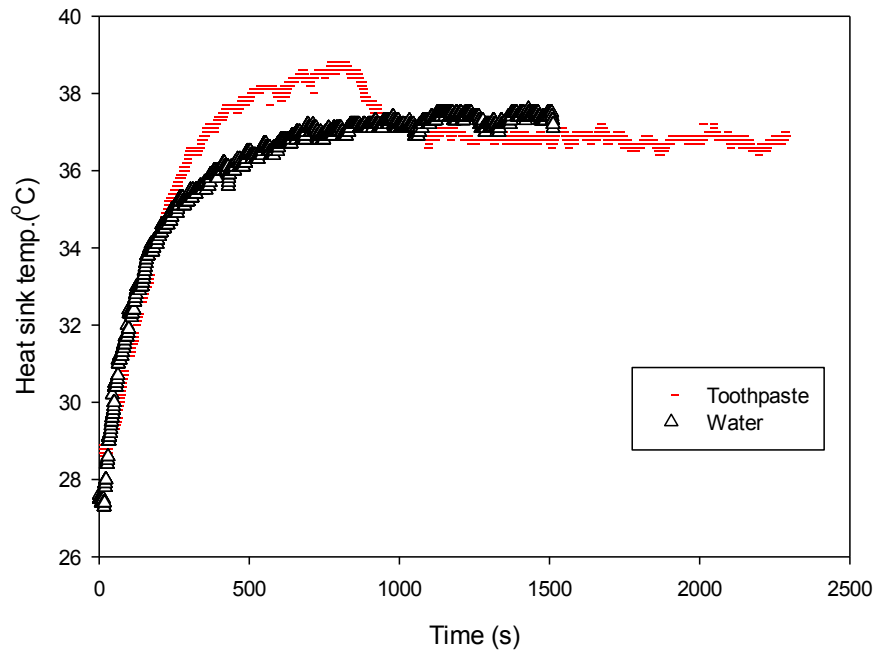


Figure 6.27: Changes in the heat sink temperature during cleaning of tooth paste by controlling the Peltier temperature.

Since setting the Peltier temperature to 70°C gave unstable readings during flow water at 70°C, as seen earlier in Figure 6.21, the Peltier temperature was set to 80°C while the cleaning temperature was 70°C. Once the water flow contacted the tooth paste deposit, the heat sink temperature increased gradually over the 700 seconds and achieved a peak temperature of ca. 39°C, as shown in Figure 6.27. As the exposition of deposit to the flow stream increased over time, the heat sink temperature decreased until the clean state was reached at 36.2°C. Also an image from the digital camera during the cleaning deposit does not reasonably correspond to the change in heat sink temperature. As the cleaning started, an initial increase in heat sink temperature during cleaning of the tooth paste deposit was observed similar to that of the clean state. Significant change occurred between 720 and 900 seconds when the deposit was removed in one piece (see Figure 6.28) which

consequently made the heat sink temperature decrease by only 0.8°C. These figures suggested that the response of this monitoring device at a constant Peltier temperature was not reliable during the deposit removal process.



Figure 6.28: Images recorded during cleaning of the tooth paste deposit by controlling the Peltier temperature.

6.3.2.8 The decrease of thermal recovery during cleaning experiment

Experiments were also conducted in which thermal recovery decreased during the cleaning experiments at a constant heat sink temperature of 40°C. Water at 70°C was passed through the test section of the bench scale rig, which contained the fouled disk. Once the water flow contacted the tooth paste deposit, the Peltier temperature and the output power (%) increased gradually over the 1100 seconds and achieved a peak temperature of 112°C, as shown in Figure 6.29 and Figure 6.30.

During that time, the deposits still covering the fouled plate were formed as an insulating layer between the flow and the Peltier. As the exposition of deposit to the flow stream increased over time, the Peltier temperature and output power (%) decreased until the clean state was reached at 85.3°C and 57% respectively. This experiment may illustrate the potentiality of using this monitoring device in detecting the deposit removal in different direction.

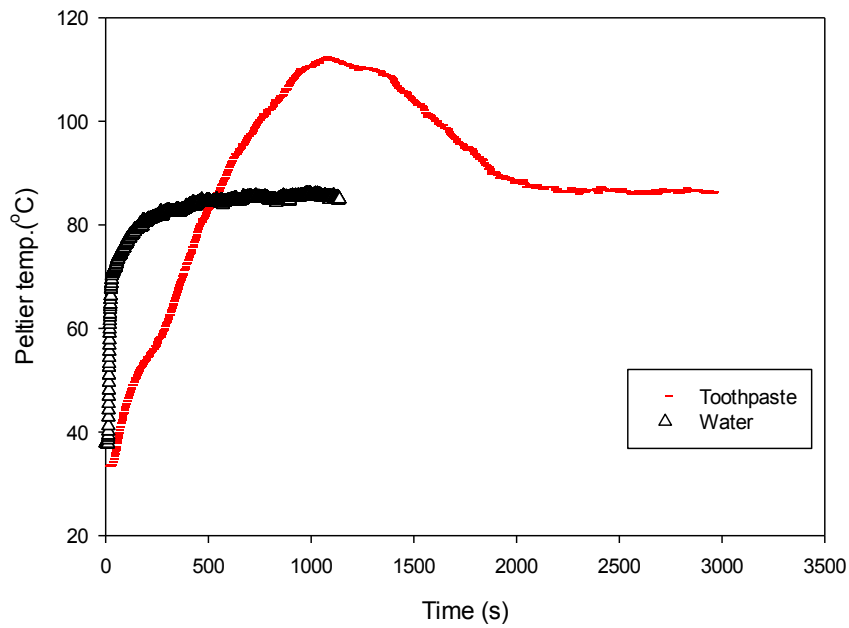


Figure 6.29: Change in the Peltier temperature during cleaning of tooth paste deposit at constant heat sink temperature of 40°C.

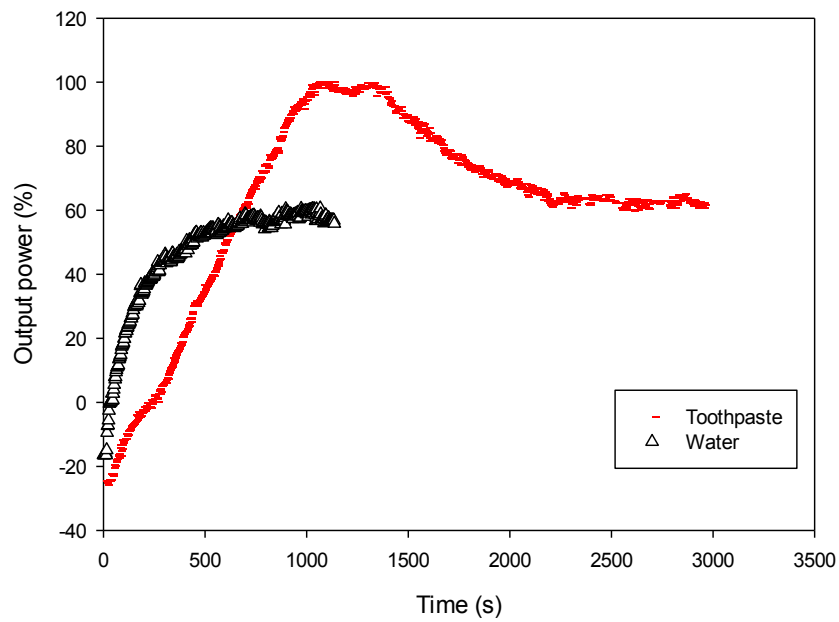


Figure 6.30: Change in output power (%) during cleaning of the tooth paste deposit at constant heat sink temperature of 40°C.

6.4 Conclusion

The first step in optimising CIP is ensuring that the monitoring techniques used are giving reliable data. Data that are measured at the beginning of CIP (where the confidence limit of variation is high) are used to predict the end point of cleaning (where the confidence limit of variation is low). Online application of such a tool would be valuable in optimising CIP.

Three types of deposit formation, followed by the cleaning regime application, were experimented and monitored. The cleaning behaviour of WPC and WPC_m deposit showed considerable differences. Under the conditions investigated, the swelling period appeared mainly to be controlled by temperature; large swelling periods were seen at the lowest temperature suggesting that the deposit is insufficiently degraded to allow rapid removal. Significantly different cleaning times arose for the different conditions investigated. Cleaning temperature and cleaning concentration were all found to influence the cleaning time, with temperature having the greatest effect.

All the four monitoring methods for measuring fouling removal obtained give comparable results. The application of the particles count technique is considered the most sensitive measurement among the four monitoring methods used in this work. However, the disadvantage of this technique is constrained by the strength of the cleaning process to remove all the deposit from the PHE surfaces. This work emphasises the importance of utilising at least two types of monitoring method: the bulk and the surface monitoring.

The sensitivity of the Peltier has been characterised under different conditions using water and two types of deposit, namely, tooth paste and golden syrup. The Peltier was located in contact with the fouled plate, within the bench-scale cleaning rig. The Peltier temperature

and output power (%) results and an imaging technique were used to assess the extent of deposit removal response. These experiments show that the Peltier device can detect the removal of an insulating layer from a surface. The nature of the contact between Peltier and the fouled plate means that it is difficult to obtain identical temperature and output power (%) values under the same conditions. The image technique was able to identify the events during cleaning, i.e. deposit removal.

Cleaning profile experiments show less response to the change of flow rate during flow diagnosis experiments. However, the Peltier temperature and output power (%) rise slightly as a result of increasing the water flow rate. The Peltier temperature and output power (%) increases to the clean value when the image from the camera shows that deposit removal has not yet ceased. The removal of deposit could be detected till at least 15% of the initial deposit. The image from the digital camera allowed the reduction of the deposits over time to be compared and measured to the change in the Peltier temperature and output power (%). In general, a good relationship was found between the Peltier results and the camera images. The availability of images taken during the cleaning process has proven useful in understanding the deposit removal behaviour. Controlling the heat sink temperature clearly showed a fast response to any change over the fouled plate. On the other hand, controlling the Peltier temperature could not show a clear distinction in heat sink temperature and output power (%) between the clean state and cleaning deposit removal curves. It has been observed that the Peltier can be utilised in both directions, with good response to deposit removal when thermally stabilised below and above the Peltier temperature.

It is noteworthy that Peltier needs more work, since every effort is given to optimise the initial operation of the device in cleaning studies. However, the device has a number of disadvantages; having a complex response; it is affected by different factors such as cleaning temperature, deposit type, the heat of the environment, effectiveness of the heat sink, the order of the input electrical power, etc.

CHAPTER 7: CONCLUSION AND FUTURE WORK

Dairy fouling deposits in the heat transfer surface are formed as a result of the thermal instability of certain components in the products. As a result, frequent shut-down of the equipment is required for cleaning. A better understanding of the fouling mechanism may lead to prolonged running times and improve cleaning processes. Differences in the chemistry and thermodynamics of the processes taking place result in the different temperatures at which deposition occurs and composition of the deposit. A review of previous work showed that there is no sufficient research on both the knowledge of the role of surface and bulk temperature in deposit formation as well as a suitable method to monitor fouling and cleaning in closed systems where a variety of conditions have to be considered. Therefore, the purpose of this study was to investigate and to monitor the fouling and cleaning behaviour of dairy deposits formed at pasteurisation temperature in PHE and a lab scale fouling rig.

7.1 Effect of process variable in fouling and cleaning

Fouling experiments conducted on WPC deposits over a range of β -Lg (wt.%) concentrations, minerals added and flow rates, using the PHE, are discussed in Chapter 4. It is necessary to understand how variations in process variables affect fouling, so that the variables may be chosen in order to minimise the effect of fouling. The main conclusions obtained from this study are:

- Fouling increased with increasing protein concentration up to a limit around β -Lg 0.3wt. %. The plateau at that value was explained in terms of fouling becoming controlled by the amount of protein in the laminar sub-layer.
- It was found that whey protein solution with increasing fluid bulk whey protein concentration leads to faster build-up of fouling. Therefore, giving the greatest amount of fouling in section 3 of the PHE at a temperature range of 90 to 95°C. Insignificant fouling was observed in sections 1 and 2 of PHE due to a low bulk temperature; observations made on opening the plate pack confirmed there was little or no deposit present.
- Changing the flow rate will change the surface shear stresses at the heat transfer surface as a result of fluid flow over the surface, the temperature profile across the section of the PHE, and the residence time of fouling fluid in the system and at the wall.
- It was observed that a decrease in deposition thickness takes place with an increasing flow rate. Higher flow velocities also promote deposit re-entrainment through increased fluid shear stresses and the deposit became more compact and smoother. Increasing flow rate from 100 to 150 l/h decreased the Δ (ΔP) fouling rate for β -Lg concentrations 0.1, 0.3 and 0.5wt.% by 34, 70 and 72.7%, respectively.

Owing to WPC being low in minerals, adding calcium and phosphorus to the WPC may alter fouling and cleaning behaviour and, therefore, need investigation. Calcium and phosphorus participate in the denaturation mechanism by lowering the temperature at which β -Lg begins to denature. Three types of fluid were tested in this work, namely WPC_m, WPC_{m/2} and WPC_{mx2}. These fluids refer to WPC solutions with calcium and

phosphorus contents the same as milk, half that of milk and twice that of milk, respectively. The main conclusions obtained from this study are:

- The processing of the three modified model fluids resulted in fouling which showed two major changes in behaviour: (i) fouling rate declined relative to WPC, (ii) deposit distribution in the PHE altered to resemble milk behaviour.
- The three modified model fluids appear to foul mainly in section 2 of PHE, with very little fouling observed in section 1, but fouling in section 3 became negligible when minerals were added, as the added minerals reduced the heat stability of whey protein.
- During preparation of WPC with added minerals, the pH of the solution changed from 6.5 to 5. This reduction in pH might contribute to causing the difference in fouling behaviour observed.

The differences in fouling behaviour of WPC and the three modified fluids had an effect on cleaning behaviour. The cleaning process is affected by differences in deposit chemistry. Initial increases in pressure drop and decreases in heat transfer coefficient could be observed, as a result of contacting protein with alkaline cleaning chemical. Pressure drop changes and increasing in heat transfer correspond to removal of the deposit from the heat surface. The following conclusion can be drawn:

- In all cases, increasing the chemical concentration from 0.1 to 0.5wt.% NaOH decreases the cleaning time; after this concentration, the cleaning time do not decrease significantly. Accordingly, a chemical concentration optimum (at 0.5 wt.%) is found.

- The WPC deposit formed at 150 l/h took considerably longer to be removed from the surface at 0.1 wt. % NaOH, suggesting that the deposit was compact. However, WPC deposits were removed very quickly at 0.5 wt. % NaOH and higher.
- Cleaning the three modified fluids showed a considerable change in cleaning behaviour. At low mineral added WPC_{m/2}, the cleaning behaviour is similar to that of WPC, with no noticeable change in pressure sensor and heat transfer coefficient while the acid cleaning was introduced.
- Increasing the mineral content in WPC solution leads to increases in mineral deposition. Therefore, the swelling peak on contacting the alkaline solution begins to disappear with increasing minerals to double as milk (WPC_{mx2}) since the protein is trapped in the mineral matrix (see Table 5.1). No Pressure peak was observed when cleaning with acid was introduced.

7.2 Bench scale fouling rig

The experiment was carried out to investigate the scalability of PHE fouling findings. The hope is that simple models for fouling can be developed which can be validated against experiments. Experiments have been conducted in a bench scale fouling rig and PHE to compare the deposit generated and also to investigate the effect of bulk temperatures of 70, 80 and 90°C and surface temperatures of 80, 89 and 98°C on fouling behaviour of the two model solutions: (WPC and WPC_m) in terms of deposit thickness, weight and morphology. The following conclusions are drawn from this study:

- It was found that increasing fluid bulk whey protein concentration leads to faster build-up of fouling. Therefore, the increase of the fouling rate was more than double at 70 and 80°C. However, at bulk temperature 90°C, increasing the β -Lg

concentration had no effect on deposit thickness or deposit weight. This could be due to the voluminous nature formed at the higher temperature where re-entrainment of all extra material deposited took place with the fluid and prevented deposition.

- For WPC_m solution and at low bulk temperatures such as 70 and 80°C, the amount of deposit formed was significantly higher than that formed from WPC solution, as the addition of minerals enhances deposition by reducing the heat stability of protein. However, the amount of deposit decreased when bulk temperature rose to 90°C, which may be attributed to the small contribution from a bulk deposition mechanism at 90°C.
- The same trend was observed in PHE, where the amount of deposits decreases drastically by 95% when bulk temperature increases from ca.85°C to 91°C. This suggests that the bench scale fouling rig is able to follow the progress of fouling in PHE quite closely.
- Surface temperature was also the most important influence in initiating fouling. For WPC solution, increasing the surface temperature from 80 to 89°C, at bulk temperature 80°C, leads to increasing the deposit thickness by six fold; however increasing the surface temperature to 90°C increases the deposit thickness by 1.5 times.
- The effect of surface temperature declined when fouling proceeds and the bulk temperature will control the process afterwards. In contrast, for WPC_m solution, the greatest effect on fouling deposition occurred when the surface temperature increased from 89 to 98°C. This may be due to the increases in mineral deposition which, in turn, enhance the deposition by the interactions between Ca and β -Lg.

- Compositional analysis of the WPC_m deposits showed that the mineral content was more predominant than the protein content in the first 20 minutes and bulk temperature was 80°C, and then protein deposition became predominant with time.
- WPC deposits produced at bulk temperature 90°C were cream in colour and fluffy in nature and the attachment to the stainless steel is not as strong as between WPC deposits and the stainless steel, formed at bulk temperature 70 and 80°C.
- WPC_m deposits produced at bulk temperatures 70, 80 and 90°C were white in colour and fouled evenly on the surface.
- The morphology studies showed small clumps, observed at 70°C, and the size of clumps increased with increasing concentration and temperature. In general, for WPC deposit, a more fluffy or cauliflower-like deposit on top at β -Lg 0.6 wt. % followed by a more compact deposit at β -Lg 1wt.%. In contrast, a very fine structure with much smaller particulates was observed for WPC_m deposit than in the WPC deposit. Therefore, the roughness data for WPC_m deposit was lower than the WPC deposit.

7.3 Monitoring device

One of the main challenges for researchers and engineers is to look for cheap, sensitive, small and reliable monitoring devices to monitor the build-up and removal of deposits in order to optimise both the production and cleaning process. Therefore, two novel tools have been developed to evaluate the cleaning process: particles count technique and Peltier device. The particles count technique was used to evaluate the removal of various whey protein deposits from the PHE, while the Peltier device was used to measure the responsiveness of the device during cleaning of two deposits: toothpaste and golden

syrup. Three conventional monitoring devices: pressure sensor, heat transfer coefficient and turbidity were used to assess the particle count technique under cleaning three types of deposit; WPC deposit formed at 95°C, WPC deposit formed at 140°C and WPC_m deposit with additional minerals formed at 140°C. Cleaning experiments have been conducted over two temperatures, cleaning solution concentrations, and two-stages of cleaning solution; alkaline and acid. The main conclusions obtained from this study are as follows:

- At higher temperature of 70°C, the reaction between the cleaning solution and deposit rapidly forms a deposit that is rapidly removed, whereby giving a smaller swelling period. Large swelling periods were occurred at 50°C, suggesting that the deposit is insufficiently degraded to allow rapid removal.
- When both the pressure sensor and heat transfer coefficient reached the cleaning status, the PHE showed fouling, this indicated that both monitoring devices can not detect the remaining small layer of fouling during the cleaning process. The end-point of cleaning was difficult to establish from these measurements.
- Both turbidity and the particles count technique were able to relate their reading with the deposit removal from the surface. The disadvantages of the two latter techniques are being controlled by the strength of the cleaning chemical to remove all the deposit from the PHE surfaces. The particles count technique has an advantage over turbidity, as the former can detect invisible particles to the naked eye.

The Peltier device technique is a fully integrated on-line monitoring system, *in situ* and in real time, providing information about the change of Peltier temperature and output power (%) during the cleaning of deposits. The cleaning deposits were achieved by action of

water alone. The characteristics of the Peltier show (i) the optimal set-up for Peltier in order to catch the best sensitivity of the instrument for monitoring the cleaning process, and (ii) the possibility to detect the cleaning end point. The following conclusions are drawn from this study:

- Cleaning profiles were less responsive to the change of water flow rate; however, different water flow rates resulted in different Peltier temperature outputs.
- Controlling the heat sink temperature shows higher response than that of controlling Peltier surface temperature during the water flow experiment. Monitoring of cleaning deposits showed that the removal of the deposit layer from surface can be detected.
- The end-points determined by the Peltier device were confirmed by images from a digital camera. The availability of images taken during the cleaning process has proven useful information about the sensitivity of the Peltier device.
- Comparison of the Peltier device results with an image from digital camera has shown that the Peltier will not detect removal of deposit from surface not contacted by the Peltier device.

7.4 Contributions

The contributions of this study to its field of research include;

- Chapter 4 introduced an integrated study for the first time that covered the influence of the process parameters (flow rate, cleaning chemicals) and chemical composition (protein and minerals concentration) upon fouling and cleaning behaviours at pasteurisation temperature. The results revealed that the minimum required cleaning chemical concentration can be affected by altering the process variables, i.e. in case

of cleaning deposit formed at flow rate 150 l/hr, there was a significant difference between cleaning deposit at 0.1 wt.% NaOH and other chemical concentrations. The removal time was considerably slower than at any other chemical concentrations. However, chemical concentration at 0.1 wt.% NaOH was sufficient to clean the deposit for the other cases.

They also showed that the increase of the minerals content in the deposits had a significant effect on cleaning behaviour, where the dependency on cleaning chemical concentration (NaOH %) to clean the majority of deposit became less significant.

- It was not practical to dismantle the PHE to measure the fouling in each plate. Therefore, lab scale fouling rig was designed to generate deposit which was similar to that in heat exchanger, to facilitate controlling surface temperature and to quantify fouling locally, together with an easy assembling and dismantling during experimental work. The results revealed that the progress of fouling agreed well with that at PHE. They also showed that the surface temperature was the most significant factor in initiating fouling. The minerals content in the deposit at the beginning of 20 minutes was higher than the protein content. However, the amount of protein in deposit became predominant afterwards. All these findings are necessary to design equipment that minimises the effects of fouling.
- Two novel monitoring cleaning techniques were applied for the first time to improve the cleaning measurements in heat exchangers: particles count technique for the global monitoring and Peltier device for the local monitoring of the cleaning progress. The results illustrated that particles count technique can detect the cleaning end point. The Peltier device results showed that the removal of deposit can be detected till at least 15 wt. % of the initial deposit remains.

7.5 Future work

The fouling and cleaning behaviour of WPC and WPC with additional minerals has been investigated at a two-length scale: PHE and bench scale fouling rig. Chapter 4 results have provided useful information on the mechanisms involved in fouling and cleaning. A range of flow rates and chemical concentrations has been studied. Based on the fact that only one cleaning temperature was used throughout this study, more work could be done to test the removal behaviour at different ranges of temperature using a single stage-cleaning, since the previous research have shown that temperature is the main controlling parameter in removing proteinaceous deposit, due to its influence on the strength of chemical and flow effect.

Results on Chapter 5 have shown that the bench scale fouling rig is able to follow the development of fouling in PHE quite closely at pasteurisation temperature. Only one flow rate was used throughout this work; other ranges of flow rate could be verified to investigate the contribution of fluid velocity to fouling process. If the fouling deposition process is controlled solely by a chemical reaction, which is not influenced by mass transfer, the fouling rate should be independent of fluid velocity.

As the temperature increases above 90°C, fouling from WPC_m decreases. This behaviour is not well understood, due to the highly complex interaction between β -Lg and mineral. Much more work is needed in this area to relate understanding the chemistry of the product to the operating conditions.

Since the bench scale fouling rig is totally suitable to generate fouling deposit at pasteurisation temperature, it is recommended to redesign the fouling rig to be able to heat the product up to 140°C in order to develop a model dairy deposit at UHT for the subsequent investigation of its cleaning behaviour using a bench scale cleaning rig. The

development of a fouling rig will lead to further understanding of high temperature processes.

In removing a deposit during cleaning, both cohesive and adhesive forces must be overcome. An understanding of the interaction between deposits and surfaces is clearly critical in cleaning. Therefore, it would be useful to measure the adhesive/cohesive force between whey protein fouling deposits formed at the UHT process, and the stainless-steel substrate by using the micromanipulation technique. This can be an area which needs a further investigation.

A plate heat exchanger consists of a series of thin, corrugated plates, which in turn increase both fluid turbulence and heat transfer through the plates. In this work, the coupon surface used was flat. Therefore, it would be better to have corrugated coupon surface to simulate the flow pattern and the progress of fouling in PHE.

Surface modification has often been proposed as a solution to the surface interfacial fouling problem. A deeper knowledge on the relation between fouling material and the properties of the fouled surfaces is essential in order to delay or reduce fouling as well as to determine optimal cleaning conditions for a given process. Consequently, it would be useful to modify the coupon surface in order to minimise the effects of protein fouling and decrease the deposit adhesion strength to facilitate a simpler cleaning procedure.

Chapter 6 has shown that the two novel monitoring techniques: particles count and Peltier effect were suitable to be used for monitoring cleaning. The particles count technique used in this work was an off-line retrospective technique. It may be more appropriate to use online particle count techniques to detect the clean end-point correctly. The sensitivity of the Peltier device was only assessed during removal of two deposits, due to the inapplicability of its assessment during fouling because of the following:

- The inlet and the outlet of the circular flow channel containing the Peltier device were not flush with fouled plate that held the Peltier device.
- The circular flow channel was not suitable to simulate the flow pattern in PHE, so it would be better to use rectangular flow channel.

Thus, it would be interesting to study the sensitivity of Peltier during a fouling run.

APPENDIX : COMMISSIONING OF THE PHE

A.1 Operating procedure to achieve standard state of cleanliness at the PHE

The characterisation of PHE was investigated for different flow rates ranging from 50 to 150 l/h. Starting with the lowest flow rate and moving up in small increments to the highest flow rate, afterwards the flow rate was decreased in small increments to 50 l/h as seen in Table A.1. The oil heater temperature was controlled at three different temperatures: 100, 110 and 120°C. The experiments were carried out at different PHE pressures of 10, 200, 400 and 600 kPa by adjusting the back pressure regulator. The PHE was first thermally stabilised using soft water, following the protocol described in section 3.4. Prior to initiating the experiments, all the plant temperatures were allowed to stabilise within $\pm 0.2^\circ\text{C}$ for at least 10 minutes. This gave enough thermally stable data to obtain accurate average performance calculations.

A.2 Characterisation of behavior under clean conditions

Table A.1 and Table A.2 represent the inlet and outlet temperature in each section of PHE; at lower flow rates the PHE reached a higher temperature in the earlier sections at 90.3°C, whilst at 150 l/h this temperature was not reached until the outlet of section 3.

Table A.3 to Table A.8 show the effect of changing the flow rate, oil heater temperature and cooling water flow rate on overall heat transfer in terms of area (UA), whilst operate the PHE. In general, as the flow rate increased, UA increased in each section of the PHE. At the lowest flow rate of 50 l/h, maximum UA was recorded in section 1 followed by

sections 2 and 3. As the flow rate increased from 50 to 150 l/h and the system became fully turbulent, the UA increased by roughly 1.7, 3.4 and 7.2 times for sections 1, 2 and 3, respectively. The UA values were increased by ca. 5% when PHE temperature increased by 10°C.

The change in the cooling water flow rate affected the temperature distribution across the PHE and, in turn the UA. The increasing effect of the cooling water flow rate from 1 to 2 l/min at the PHE flow rate of 50 l/min was observed at section 3 as an approximate 20% change in UA. However, the change of UA at section 3 became less than 3% with an increasing flow rate of 150 l/h. In general, the effect of changing the cooling water flow rate in UA was less noticeable at a PHE flow rate of over 100 l/h, where it was less than 9% of UA in all PHE sections.

As the process fluid flow rate was increased, the rate of removal of heat from the oil (heating fluid) was also increased, reflecting the increase in heat transfer coefficient. Another test of thermal efficiency, and of the accuracy of the equipment, is the heat balance recorded in (see Table A.9 to Table A.14). These compare the heat removed from the oil to that taken up by the process fluid, and are defined in Equation 3.18. The smaller a temperature change across a section, the less accurate the heat balance will be, because of inaccuracies in the temperature readings and the higher thermal losses as a proportion of the heat transferred. Heat transfer efficiency was very high in section 1 at all flow rates; the temperature change across this section was always large. However, in sections 2 and 3 of PHE, below 100 l/h heat transfer efficiencies were very low. Here, for example, very small temperature increases occur in section 3. Above 100 l/h, thermal balances become better, reaching the best values at 150 l/h when all of the three sections displayed efficiencies >90% and within $\pm 5\%$ of their mean. This latter value is very close to that

found by Changani (2000) who found for the PHE under the same condition, that the heat balance was accurate to $\pm 7\%$ for the three PHE sections. As a result of these measurements, a flow rate of 100 and over was used for the fouling experiments.

Figure A.1 and Figure A.2 display the clean thermal behaviour both for the whole PHE and for individual sections. Figure A.1 shows that the relationship between $1/UA$ and $1/\text{flow rate}$ was linear; the correlation coefficient was 0.976 for the whole PHE. Heat transfer efficiencies already discussed above (Table A.3 to Table A.8), showed that good efficiencies were not recorded until flow rates exceeded 100 l/h. Poor thermal efficiency below 100 l/h is one reason for deviation of the $1/UA$ versus $1/\text{flow rate}$ relationship from linearity. Below this flow velocity, the flow patterns in the exchanger may also become laminar.

As found by Schreier (1995) and Changani (2000), a value of $n = 1$ for Equation 3.12 yielded the best straight line fit. This showed that the PHE exhibited the expected thermal behaviour and that behaviour previously recorded for the same PHE was replicated (Schreier, 1995). The highest regression coefficient found was for section 1, $R^2 = 0.98$; but both sections 2 and 3 exhibited lowest regression coefficients, $R^2 = 0.95$ and 0.94 respectively. The fit to data is reasonable, showing that this form of analysis is a good starting point for characterisation.

Table A.15 to Table A.18 show the values of ΔP calculated for the different flow rates tested. This clean hydraulic behaviour has been plotted as ΔP versus flow rate for the individual sections and the whole PHE in Figure A.3 to Figure A.7. Curves have been fitted to the data for each of the section (in each case $\Delta P \propto Q^2$ (see Equation 3.20)). As the PHE pressure was increased, the pressure drop was also increased. However, the pressure drop at section 2 decreased with increasing PHE

pressure. The reading of pressure drop for section 2 at PHE pressure equal to 10 kPa and is close to section 1 while at PHE pressure equal to 600 kPa, the reading of pressure drop for section 2 is closer to section 3, as seen in Figure A.6. All curves that were fitted gave a very high correlation coefficient; the lowest was 0.99 (for section 1). It should be noted that some of the pressure sensor values were negative. This was probably due to a calibration problem with one of the intermediate pressure transducers. All pressure transducers were checked and adjusted where necessary and subsequent experiments no longer gave negative readings. This difference did not affect the results discussed here because the calculation of pressure drop essentially removes this error.

| Flow rate (l/h) | Temperature (°C) Pre-heat | Temperature (°C) Section 1 | Temperature (°C) Section 2 | Temperature (°C) Section 3 | Fluid type |
|-----------------|---------------------------|----------------------------|----------------------------|----------------------------|------------|
| 50 | 38.6 | 90.3 | 93.7 | 95.4 | Water |
| | 76.3 | 93.4 | 95.6 | 97.6 | Oil |
| 80 | 45.9 | 85.5 | 92.4 | 95.8 | Water |
| | 69.9 | 90.4 | 94.9 | 97.9 | Oil |
| 100 | 50.2 | 80.3 | 89.6 | 95.3 | Water |
| | 66.6 | 86.4 | 93.3 | 98.0 | Oil |
| 120 | 52.8 | 75.0 | 85.7 | 94.0 | Water |
| | 63.8 | 81.6 | 90.6 | 98.0 | Oil |
| 150 | 54.7 | 67.5 | 78.1 | 90.0 | Water |
| | 60.4 | 73.8 | 85.0 | 98.0 | Oil |

Table A.1: Typical outlet temperature in each section during clean operation of the PHE, at oil heater temperature 100°C and various flow rates (cooling flow rate 1 l/min).

| Flow rate (l/h) | Temperature (°C) Pre-heat | Temperature (°C) Section 1 | Temperature (°C) Section 2 | Temperature (°C) Section 3 | Fluid type |
|-----------------|---------------------------|----------------------------|----------------------------|----------------------------|------------|
| 50 | 28.7 | 90.1 | 94.0 | 95.4 | Water |
| | 73.3 | 93.6 | 95.9 | 98.0 | Oil |
| 80 | 32.8 | 84.3 | 93.1 | 96.5 | Water |
| | 63.8 | 90.4 | 95.5 | 98.5 | Oil |
| 100 | 38.1 | 76.7 | 88.8 | 95.3 | Water |
| | 59.1 | 84.6 | 93.1 | 98.6 | Oil |
| 120 | 40.5 | 68.0 | 82.4 | 93.4 | Water |
| | 54.2 | 76.9 | 89.0 | 98.8 | Oil |
| 150 | 43.2 | 58.1 | 71.8 | 88.2 | Water |
| | 50.1 | 66.3 | 81.0 | 98.7 | Oil |

Table A.2: Typical outlet temperature in each section during clean operation of the PHE, at oil heater temperature 100°C and various flow rates (cooling flow rate 2 l/min).

| Flow rate (l/h) | UA (kW/K) (Section 1) | UA(kW/K) (Section 2) | UA(kW/K) (Section 3) |
|-----------------|-----------------------|----------------------|----------------------|
| 50 | 0.217 | 0.082 | 0.046 |
| 80 | 0.303 | 0.178 | 0.137 |
| 100 | 0.338 | 0.229 | 0.209 |
| 120 | 0.359 | 0.260 | 0.261 |
| 150 | 0.376 | 0.284 | 0.304 |
| 100 | 0.348 | 0.238 | 0.211 |
| 50 | 0.226 | 0.087 | 0.044 |

Table A.3: Typical clean overall heat transfer coefficient in terms of area for each section at various flow rates (oil set to 100°C, cooling water flow rate 1 l/min).

| Flow rate (l/h) | UA (kW/K) (Section 1) | UA (kW/K) (Section 2) | UA (kW/K) (Section 3) |
|-----------------|-----------------------|-----------------------|-----------------------|
| 50 | 0.224 | 0.088 | 0.037 |
| 100 | 0.334 | 0.237 | 0.200 |
| 150 | 0.350 | 0.277 | 0.292 |
| 120 | 0.348 | 0.264 | 0.256 |
| 80 | 0.311 | 0.197 | 0.127 |

Table A.4: Typical clean overall heat transfer coefficient terms of area for each section at various flow rates (oil set to 100°C, cooling water flow rate 2 l/min).

| Flow rate (l/h) | UA (kW/K) (Section 1) | UA(kW/K) (Section 2) | UA(kW/K) (Section 3) |
|-----------------|-----------------------|----------------------|----------------------|
| 50 | 0.221 | 0.079 | 0.045 |
| 80 | 0.313 | 0.178 | 0.138 |
| 100 | 0.351 | 0.232 | 0.211 |
| 120 | 0.376 | 0.268 | 0.268 |
| 150 | 0.397 | 0.298 | 0.318 |
| 100 | 0.364 | 0.245 | 0.218 |
| 50 | 0.226 | 0.081 | 0.042 |

Table A.5: Typical clean overall heat transfer coefficient in terms of area for each section at various flow rates (oil set to 110°C, cooling water flow rate 1 l/min).

| Flow rate (l/h) | UA (kW/K) (Section 1) | UA (kW/K) (Section 2) | UA (kW/K) (Section 3) |
|--------------------|-----------------------------|-----------------------------|-----------------------------|
| 50 | 0.227 | 0.084 | 0.037 |
| 100 | 0.348 | 0.241 | 0.201 |
| 150 | 0.372 | 0.290 | 0.307 |
| 120 | 0.365 | 0.273 | 0.260 |
| 80 | 0.323 | 0.198 | 0.126 |

Table A.6: Typical clean overall heat transfer coefficient in terms of area for each section at various flow rates (oil set to 110°C, cooling water flow rate 2 l/min).

| Flow rate (l/h) | UA (kW/K) (Section 1) | UA (kW/K) (Section 2) | UA (kW/K) (Section 3) |
|--------------------|-----------------------------|-----------------------------|-----------------------------|
| 50 | 0.223 | 0.078 | 0.046 |
| 80 | 0.322 | 0.180 | 0.140 |
| 100 | 0.364 | 0.237 | 0.215 |
| 120 | 0.391 | 0.275 | 0.270 |
| 150 | 0.429 | 0.318 | 0.333 |
| 100 | 0.374 | 0.245 | 0.217 |
| 50 | 0.233 | 0.081 | 0.045 |

Table A.7: Typical clean overall heat transfer coefficient in terms of area for each section at various flow rates (oil set to 120°C, cooling water flow rate 1 l/min).

| Flow rate (l/h) | UA (kW/K) (Section 1) | UA (kW/K) (Section 2) | UA (kW/K) (Section 3) |
|--------------------|-----------------------------|-----------------------------|-----------------------------|
| 50 | 0.229 | 0.082 | 0.039 |
| 80 | 0.323 | 0.187 | 0.124 |
| 100 | 0.360 | 0.245 | 0.201 |
| 120 | 0.382 | 0.282 | 0.275 |
| 150 | 0.394 | 0.306 | 0.325 |
| 100 | 0.368 | 0.252 | 0.205 |
| 50 | 0.231 | 0.080 | 0.034 |

Table A.8: Typical clean overall heat transfer coefficient in terms of area for each section at various flow rates (oil set to 120°C, cooling water flow rate 2 l/min).

| Flow rate (l/h) | Heat Balance (%) (Section 1) | Heat Balance (%) (Section 2) | Heat Balance (%) (Section 3) | Heat Balance (%) Whole |
|-----------------|------------------------------|------------------------------|------------------------------|------------------------|
| 50 | 114 | 58 | 30 | 96 |
| 80 | 112 | 89 | 66 | 101 |
| 100 | 112 | 99 | 86 | 103 |
| 120 | 110 | 103 | 98 | 103 |
| 150 | 107 | 105 | 105 | 103 |
| 100 | 113 | 100 | 87 | 104 |
| 50 | 112 | 59 | 29 | 98 |

Table A.9: Typical clean heat balance for each section and the whole at various flow rates (oil set to 100°C, cooling water flow rate 1 l/min).

| Flow rate (l/h) | Heat Balance (%) (Section 1) | Heat Balance (%) (Section 2) | Heat Balance (%) (Section 3) | Heat Balance (%) Whole |
|-----------------|------------------------------|------------------------------|------------------------------|------------------------|
| 50 | 112 | 63 | 25 | 98 |
| 100 | 111 | 102 | 85 | 103 |
| 150 | 104 | 103 | 101 | 100 |
| 120 | 109 | 104 | 97 | 103 |
| 80 | 113 | 96 | 62 | 102 |

Table A.10: Typical clean heat balance for each section and the whole at various flow rates (oil set to 100°C, cooling water flow rate 2 l/min).

| Flow rate (l/h) | Heat Balance (%) (Section 1) | Heat Balance (%) (Section 2) | Heat Balance (%) (Section 3) | Heat Balance (%) Whole |
|-----------------|------------------------------|------------------------------|------------------------------|------------------------|
| 50 | 112 | 55 | 29 | 97 |
| 80 | 114 | 88 | 64 | 102 |
| 100 | 113 | 98 | 85 | 103 |
| 120 | 112 | 103 | 98 | 104 |
| 150 | 110 | 106 | 106 | 105 |
| 100 | 114 | 100 | 87 | 105 |
| 50 | 113 | 55 | 27 | 98 |

Table A.11: Typical clean heat balance for each section and the whole at various flow rates (oil set to 110°C, cooling water flow rate 1 l/min).

| Flow rate (l/h) | Heat Balance (%) (Section 1) | Heat Balance (%) (Section 2) | Heat Balance (%) (Section 3) | Heat Balance (%) Whole |
|-----------------|------------------------------|------------------------------|------------------------------|------------------------|
| 50 | 113 | 59 | 24 | 98 |
| 100 | 112 | 101 | 83 | 104 |
| 150 | 106 | 104 | 103 | 102 |
| 120 | 110 | 105 | 96 | 104 |
| 80 | 114 | 95 | 62 | 104 |

Table A.12: Typical clean heat balance for each section and the whole at various flow rates (oil set to 110°C, cooling water flow rate 2 l/min).

| Flow rate (l/h) | Heat Balance (%) (Section 1) | Heat Balance (%) (Section 2) | Heat Balance (%) (Section 3) | Heat Balance (%) Whole |
|-----------------|------------------------------|------------------------------|------------------------------|------------------------|
| 50 | 112 | 52 | 29 | 96 |
| 80 | 114 | 86 | 63 | 102 |
| 100 | 114 | 98 | 84 | 104 |
| 120 | 113 | 104 | 97 | 106 |
| 150 | 113 | 107 | 108 | 107 |
| 100 | 115 | 98 | 85 | 105 |
| 50 | 113 | 55 | 29 | 98 |

Table A.13: Typical clean heat balance for each section and the whole at various flow rates (oil set to 120°C, cooling water flow rate 1 l/min).

| Flow rate (l/h) | Heat Balance (%) (Section 1) | Heat Balance (%) (Section 2) | Heat Balance (%) (Section 3) | Heat Balance (%) Whole |
|-----------------|------------------------------|------------------------------|------------------------------|------------------------|
| 50 | 113 | 56 | 24 | 98 |
| 80 | 114 | 90 | 59 | 103 |
| 100 | 113 | 101 | 82 | 105 |
| 120 | 112 | 106 | 99 | 105 |
| 150 | 109 | 107 | 106 | 105 |
| 100 | 114 | 102 | 83 | 106 |
| 50 | 113 | 56 | 22 | 99 |

Table A.14: Typical clean heat balance for each section and the whole at various flow rates (oil set to 120°C, cooling water flow rate 2 l/min).

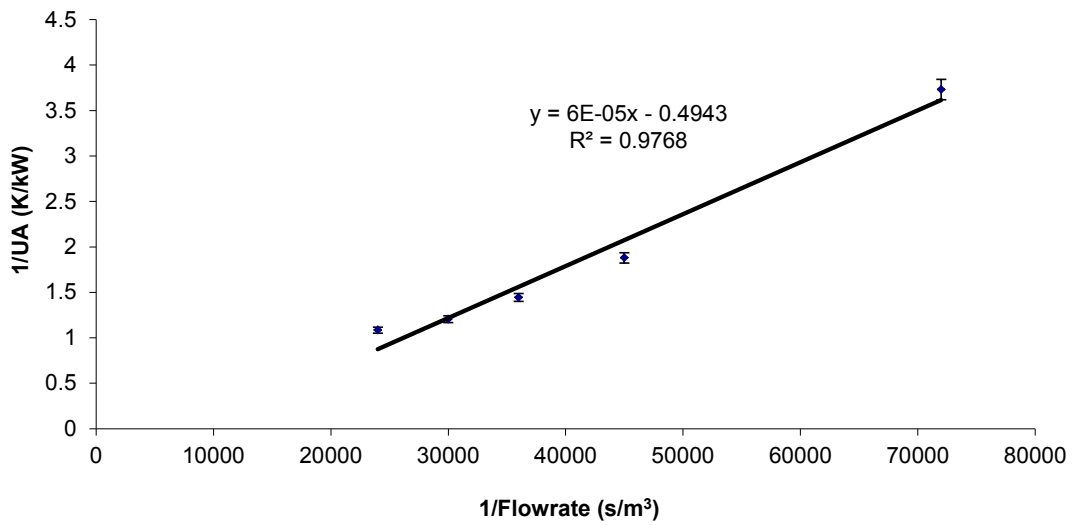


Figure A.1: Clean thermal conditions for the whole PHE. 1/UA vs 1/flow rate, at section 3 outlet temperature 95°C and flow rate range 50-150 l/h.

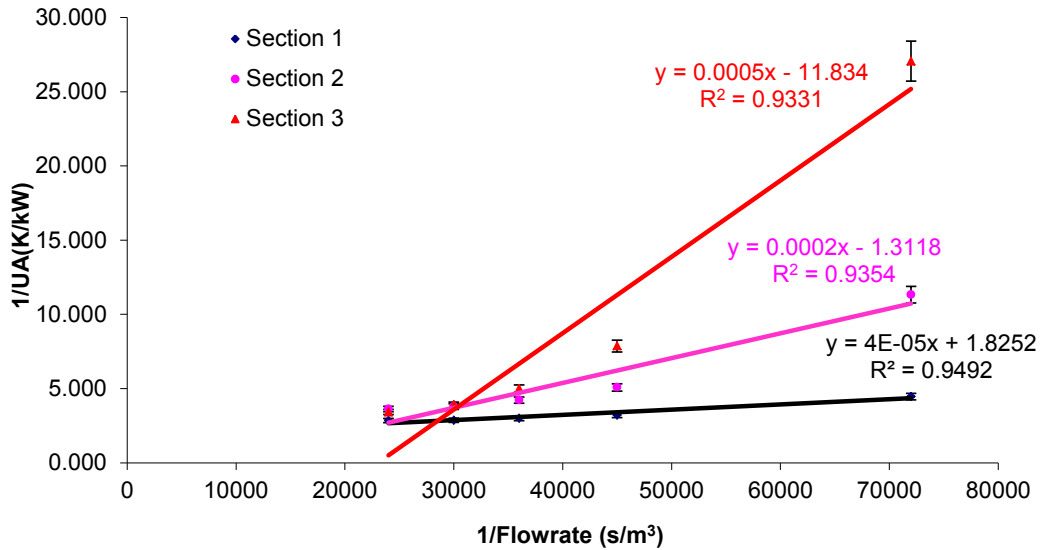


Figure A.2: Clean thermal conditions for sections 1, 2 and 3 of the PHE. 1/UA vs 1/flow rate, at section 3 outlet temperature 95°C and flow rate range 50-150 l/h.

| Flow rate (l/h) | ΔP (kPa) (preheat) | ΔP (kPa) (Section 1) | ΔP (kPa) (Section 2) | ΔP (kPa) (Section 3) | ΔP (kPa) Whole |
|--------------------|------------------------------------|------------------------------------|------------------------------------|------------------------------------|------------------------------|
| 51.0 | 9.4 | 3.7 | 8.2 | -3.7 | 8.2 |
| 79.3 | 11.3 | 8.0 | 11.0 | -0.5 | 18.5 |
| 100.2 | 15.9 | 12.2 | 13.7 | 2.5 | 28.4 |
| 119.4 | 19.6 | 16.4 | 16.9 | 5.7 | 39.0 |
| 149.0 | 27.9 | 24.4 | 22.2 | 11.5 | 58.1 |

Table A.15: Clean pressure drop for each section of PHE, and whole PHE for flow rates ranging from 50-150 l/h, at section 3 outlet pressure 10 kPa.

| Flow rate (l/h) | ΔP (kPa) (preheat) | ΔP (kPa) (Section 1) | ΔP (kPa) (Section 2) | ΔP (kPa) (Section 3) | ΔP (kPa) Whole |
|--------------------|------------------------------------|------------------------------------|------------------------------------|------------------------------------|------------------------------|
| 52.2 | 1.8 | 6.3 | 6.7 | -1.8 | 11.2 |
| 80.5 | 6.5 | 10.8 | 9.6 | 1.3 | 21.7 |
| 99.0 | 10.6 | 14.3 | 12.1 | 4.0 | 30.4 |
| 119.2 | 15.9 | 18.8 | 15.3 | 7.2 | 41.3 |
| 149.6 | 24.8 | 27.1 | 20.7 | 13.1 | 60.9 |

Table A.16: Clean pressure drop for each section of PHE, and whole PHE for flow rates ranging from 50-150 l/h, at section 3 outlet pressure 200 kPa.

| Flow rate (l/h) | ΔP (kPa) (preheat) | ΔP (kPa) (Section 1) | ΔP (kPa) (Section 2) | ΔP (kPa) (Section 3) | ΔP (kPa) Whole |
|--------------------|------------------------------------|------------------------------------|------------------------------------|------------------------------------|------------------------------|
| 51.4 | -0.5 | 7.6 | 5.0 | -1.0 | 11.7 |
| 80.3 | 3.4 | 12.7 | 7.9 | 2.6 | 23.2 |
| 99.7 | 7.4 | 16.9 | 10.3 | 5.6 | 32.7 |
| 120.2 | 12.5 | 21.5 | 13.6 | 9.0 | 44.1 |
| 148.4 | 20.9 | 29.2 | 18.4 | 14.7 | 62.3 |

Table A.17: Clean pressure drop for each section of PHE, and whole PHE for flow rates ranging from 50-150 l/h, at section 3 outlet pressure 400 kPa.

| Flow rate (l/h) | ΔP (kPa) (preheat) | ΔP (kPa) (Section 1) | ΔP (kPa) (Section 2) | ΔP (kPa) (Section 3) | ΔP (kPa) Whole |
|-----------------|------------------------------|------------------------------|------------------------------|------------------------------|------------------------|
| 51.0 | -3.0 | 8.8 | 3.9 | -0.3 | 12.5 |
| 78.9 | 1.0 | 13.0 | 6.2 | 2.9 | 22.1 |
| 98.9 | 4.6 | 16.7 | 8.4 | 6.0 | 31.1 |
| 121.1 | 9.3 | 22.1 | 11.3 | 9.9 | 43.3 |
| 149.5 | 17.2 | 30.9 | 16.7 | 16.0 | 63.6 |

Table A.18: Clean pressure drop for each section of PHE, and whole PHE for flow rates ranging from 50-150 l/h, at section 3 outlet pressure 600 kPa.

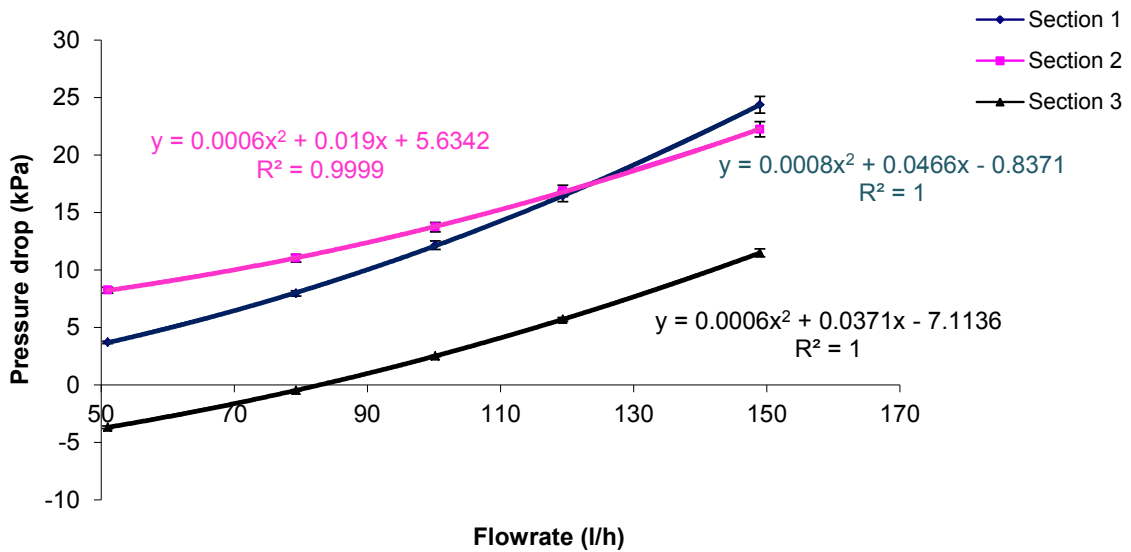


Figure A.3: Clean hydraulic condition for each section of PHE for ranging flow rates from 50-150 l/h, at section 3 outlet pressure 10 kPa.

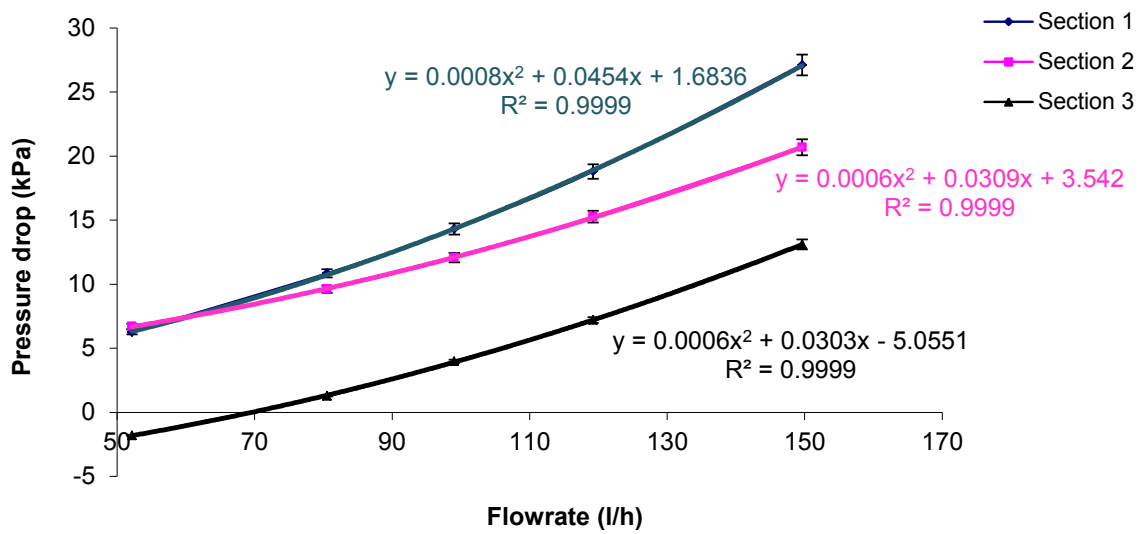


Figure A.4: Clean hydraulic condition for each section of PHE for ranging flow rates from 50-150 l/h, at section 3 outlet pressure 200 kPa.

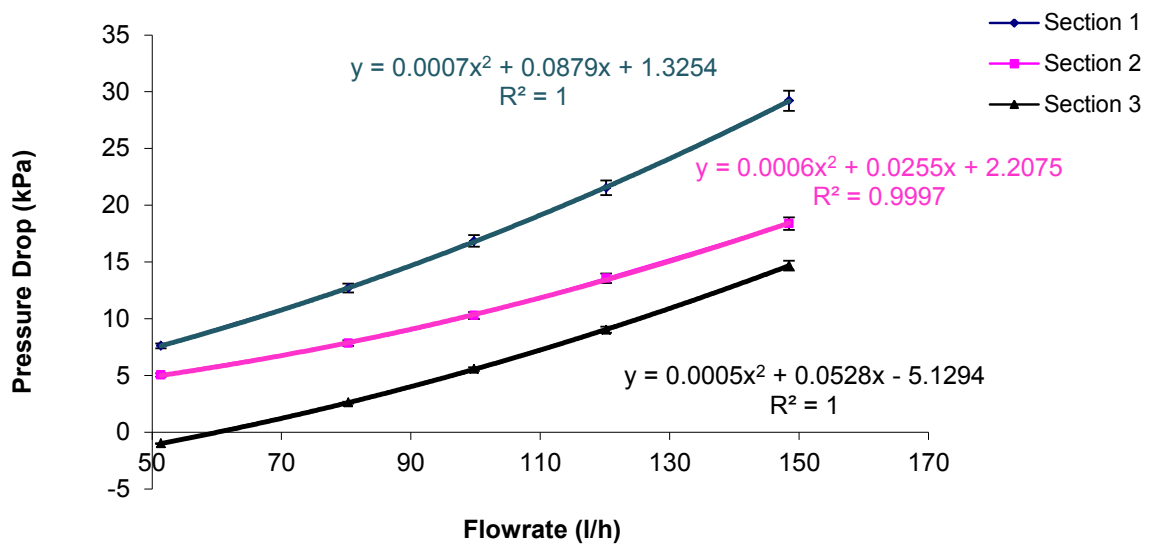


Figure A.5: Clean hydraulic condition for each section of PHE for ranging flow rates from 50-150 l/h, at section 3 outlet pressure 400 kPa.

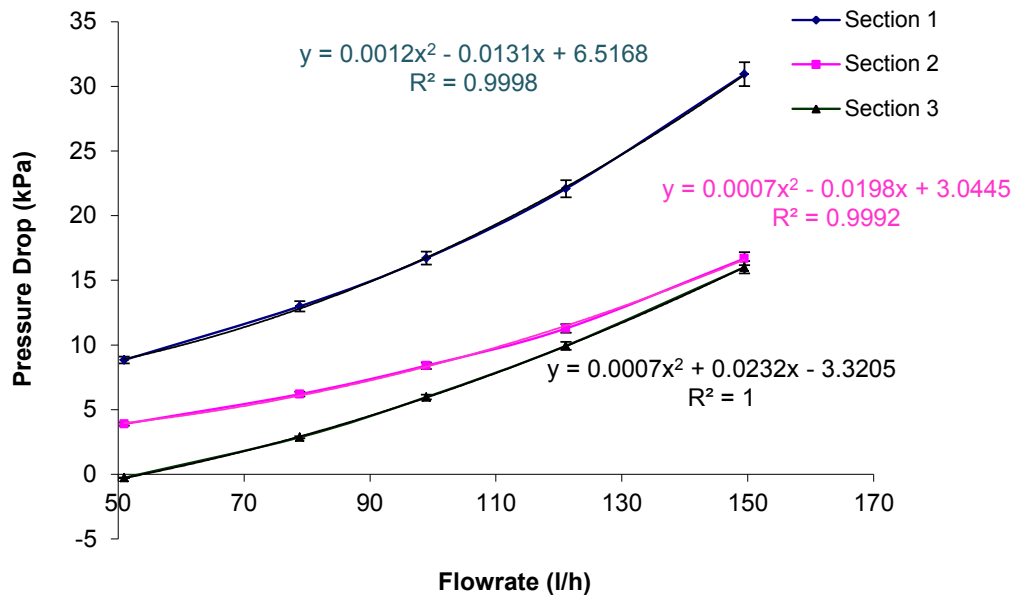


Figure A.6: Clean hydraulic condition for each section of PHE for ranging flow rate from 50-150 l/h, at section 3 outlet pressure 600 kPa.

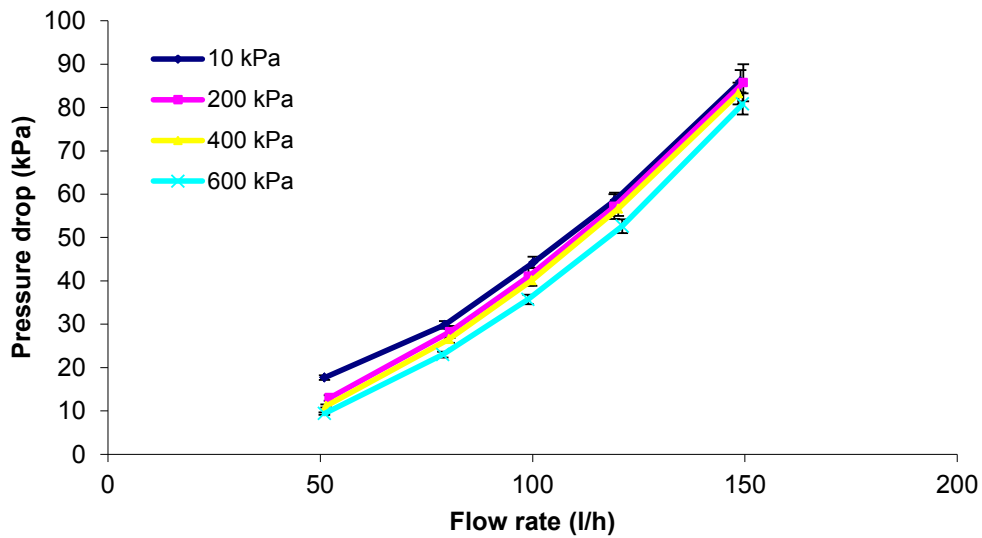


Figure A.7: Clean hydraulic condition of the whole PHE; ranging flow rate from 50-150 l/h, and various pressure drops.

REFERENCES

- ANDRITSOS, N., YIANTSIOS, S. G. & KARABELAS, A. J. 2002. Calcium Phosphate Scale Formation from Simulated Milk Ultrafiltrate Solutions. *Food and Bioproducts Processing*, 80, 223-230.
- ANEMA, S. G. & LI, Y. 2003. Association of denatured whey proteins with casein micelles in heated reconstituted skim milk and its effect on casein micelle size. *Journal of Dairy Research*, 70, 73-83.
- ARNEBRANT, T., BARTON, K. & NYLANDER, T. 1987. Adsorption of α -lactalbumin and β -lactoglobulin on metal surfaces versus temperature. *Journal of Colloid and Interface Science*, 119, 383-390.
- AZIZ, N. S. 2008. *Factors that affect cleaning process efficiency*. PhD Thesis, University of Birmingham.
- BANSAL, B. & CHEN, X. D. 2006. A Critical Review of Milk Fouling in Heat Exchangers. *Comprehensive Reviews in Food Science and Food Safety*, 5, 27-33.
- BELL, R. & SANDERS, C. 1944. Prevention of Milestone Formation in a High-Temperature-Short-Time Heater by Preheating Milk, Skim Milk and Whey. *Journal of Dairy Science*, 27, 499-504.
- BELMAR-BEINY, M. T., GOTHAM, S. M., PATERSON, W. R., FRYER, P. J. & PRITCHARD, A. M. 1993. The effect of Reynolds number and fluid temperature in whey protein fouling. *Journal of Food Engineering*, 19, 119-139.
- BIRD, M. & FRYER, P. 1991. Experimental study of the cleaning of surfaces fouled by whey proteins. *Food and Bioproducts Processing*, 69, 13-21.
- BIRD, M. R. 1992. *Cleaning of food process plant*. University of Cambridge.
- BODE, K., HOOPER, R. J., PATERSON, W. R., IAN WILSON, D., AUGUSTIN, W. & SCHOLL, S. 2007. Pulsed flow cleaning of whey protein fouling layers. *Heat transfer engineering*, 28, 202-209.
- BOTT, T. R. 1995. *Fouling of heat exchangers*, Access Online via Elsevier.
- BURTON, H. 1966. A comparison between a hot-wire laboratory apparatus and a plate heat exchanger for determining the sensitivity of milk to deposit formation. *Journal of Dairy Research*, 33, 317-324.
- BURTON, H. 1968. Section G. Deposits from whole milk in heat treatment plant—a review and discussion. *Journal of Dairy Research*, 35, 317-330.
- BURTON, H. 1994. *Ultra-high-temperature processing of milk and milk products*, Blackie Academic & Professional.
- BYLUND, G. 1995. *Dairy processing handbook, Tetra Pak Processing Systems AB*.
- CHANGANI, S. 2000. *An investigation into the fouling and cleaning behaviour of dairy deposit*. PhD, University of Birmingham.
- CHANGANI, S. D., BELMAR-BEINY, M. T. & FRYER, P. J. 1997. Engineering and chemical factors associated with fouling and cleaning in milk processing. *Experimental Thermal and Fluid Science*, 14, 392-406.

- CHAPLIN, L. G. & LYSTER, R. L. J. 1988. Effect of temperature on the pH of skim milk. *Journal of Dairy Research*, 55, 277-280.
- CHEN, X. & BALA, P. 1998. Investigation of the influences of surface and bulk temperatures upon fouling of milk components onto a stainless steel probe. *Proceedings of Fouling and Cleaning in Food Processing, Jesus College, Cambridge, England*, 25-32.
- CHEN, X. D., LI, D. X., LIN, S. X. & ÖZKAN, N. 2004. On-line fouling/cleaning detection by measuring electric resistance—equipment development and application to milk fouling detection and chemical cleaning monitoring. *Journal of food engineering*, 61, 181-189.
- CHENOWETH, J. 1987. Fouling problems in heat exchangers. *Heat Transfer in High Technology and Power Engineering*, 406-419.
- CHRISTIAN, G. 2004. *Cleaning of carbohydrate and dairy protein deposits*. PhD, University of Birmingham.
- CHRISTIAN, G., CHANGANI, S. & FRYER, P. 2002. The effect of adding minerals on fouling from whey protein concentrate: development of a model fouling fluid for a plate heat exchanger. *Food and bioproducts processing*, 80, 231-239.
- CHRISTIAN, G. & FRYER, P. 2002. Pulsed cleaning: physical and chemical effects on cleaning of a dairy fouled pilot scale plate heat exchanger (PHE). *Fouling, Cleaning and Disinfection in Food Processing*, 135-142.
- CHRISTIAN, G. & FRYER, P. 2006. The effect of pulsing cleaning chemicals on the cleaning of whey protein deposits. *Food and bioproducts processing*, 84, 320-328.
- COLE, P. A., ASTERIADOU, K., ROBBINS, P. T., OWEN, E. G., MONTAGUE, G. A. & FRYER, P. J. 2010. Comparison of cleaning of toothpaste from surfaces and pilot scale pipework. *Food and Bioproducts Processing*, 88, 392-400.
- CORREDIG, M. & DALGLEISH, D. G. 1996. Effect of temperature and pH on the interactions of whey proteins with casein micelles in skim milk. *Food Research International*, 29, 49-55.
- CREAMER, L. K. & MATHESON, A. 1980. Effect of heat treatment on the proteins of pasteurized skim milk. *New Zealand Journal of Dairy Science and Technology*, 15, 37-49.
- DAUFIN, G., LABBE, J. P., QUERMERAI, A., BRULE, G., MICHEL, F. & ROIGNANT, M. 1987. Fouling of a heat exchanger surface by whey, milk and model fluids. An analytical study. *Le Lait*, 67, 339-64.
- DAVIES, T., HENSTRIDGE, S., GILLHAM, C. & WILSON, D. 1997. Investigation of whey protein deposit properties using heat flux sensors. *Food and Bioproducts processing*, 75, 106-110.
- DE GOEDEREN, G., PRITCHARD, N. & HASTING, A. Improved cleaning processes for the food industry. *Fouling and Cleaning in Food Processing*, 1989. 115-130.
- DE JONG, P. 1997. Impact and control of fouling in milk processing. *Trends in Food Science & Technology*, 8, 401-405.
- DE JONG, P., BOUMAN, S. & VAN DER LINDEN, H. 1992. Fouling of heat treatment equipment in relation to the denaturation of β -lactoglobulin. *Journal of the Society of Dairy Technology*, 45, 3-8.
- DE JONG, P., VAN DER HORST, H. & WAALEWIJN, R. Reduction of protein and mineral fouling. *Fouling and Cleaning in Food Processing*, 1998. 39-46.
- DELAPLACE, F., LEULIET, J. & TISSIER, J. 1994. Fouling experiments of a plate heat exchanger by whey protein solutions. *Trans. IChemE*, 72, 163-169.

- DELPLACE, F., LEULIET, J. C. & LEVIEUX, D. 1997. A reaction engineering approach to the analysis of fouling by whey proteins of a six-channels-per-pass plate heat exchanger. *Journal of Food Engineering*, 34, 91-108.
- DELSING, B. & HIDDINK, J. 1983. Fouling of heat transfer surfaces by dairy liquids. *Netherlands Milk and Dairy Journal*, 37.
- DU, S., KENDALL, K., MORRIS, S. & SWEET, C. 2010. Measuring number-concentrations of nanoparticles and viruses in liquids on-line. *Journal of Chemical Technology & Biotechnology*, 85, 1223-1228.
- ELOFSSON, U. M., PAULSSON, M. A., SELLERS, P. & ARNEBRANT, T. 1996. Adsorption during Heat Treatment Related to the Thermal Unfolding/Aggregation of β -Lactoglobulins A and B. *Journal of Colloid and Interface Science*, 183, 408-415.
- FICKAK, A., AL-RAISI, A. & CHEN, X. D. 2011. Effect of whey protein concentration on the fouling and cleaning of a heat transfer surface. *Journal of Food Engineering*, 104, 323-331.
- FOSTER, C. L., BRITTEN, M. & GREEN, M. L. 1989. A model heat-exchange apparatus for the investigation of fouling of stainless steel surfaces by milk I. Deposit formation at 100 °C. *Journal of Dairy Research*, 56, 201-209.
- FOSTER, C. L. & GREEN, M. L. 1990. A model heat exchange apparatus for the investigation of fouling of stainless steel surfaces by milk II. Deposition of fouling material at 140 °C, its adhesion and depth profiling. *Journal of Dairy Research*, 57, 339-348.
- FOX, P. 1989. The milk protein system. *Developments in dairy chemistry. 4. Functional milk proteins.*, 1-53.
- FRYER, P. & ASTERIADOU, K. 2009. A prototype cleaning map: a classification of industrial cleaning processes. *Trends in Food Science & Technology*, 20, 255-262.
- FRYER, P. & BIRD, M. 1994. Factors which affect the kinetics of cleaning dairy soils. *Food Science and Technology Today*, 8.
- FRYER, P., CHRISTIAN, G. & LIU, W. 2006. How hygiene happens: physics and chemistry of cleaning. *International journal of dairy technology*, 59, 76-84.
- FRYER, P., PYLE, D. & RIELLY, C. 1997. *Chemical engineering for the food industry*, Blackie Academic & Professional.
- FRYER, P. J. 1986. *Modelling Heat Exchanger Fouling*. PhD Thesis, University of Cambridge.
- FRYER, P. J. 1989. The uses of fouling models in the design of food process plant*. *International Journal of Dairy Technology*, 42, 23-29.
- FRYER, P. J. & BELMAR-BEINY, M. T. 1991. Fouling of heat exchangers in the food industry: a chemical engineering perspective. *Trends in Food Science & Technology*, 2, 33-37.
- FRYER, P. J., BELMAR, M. T. & SCHREIER, P. J. R. 1995. Thermal processing of milk-processes and equipment. In: FOX, P. F. (ed.) *Heat-induced changes in milk*. 2 ed.
- FRYER, P. J. & ROBBINS, P. T. 2005. Heat transfer in food processing: ensuring product quality and safety. *Applied Thermal Engineering*, 25, 2499-2510.
- FRYER, P. J., ROBBINS, P. T., GREEN, C., SCHREIER, P. J. R., PRITCHARD, A. M., HASTING, A. P. M., ROYSTON, D. G. & RICHARDSON, J. F. 1996. A Statistical Model for Fouling of a Plate Heat Exchanger by Whey Protein Solution at UHT Conditions. *Food and Bioproducts Processing*, 74, 189-199.

- FRYER, P. J. & SLATER, N. K. H. 1985. A direct simulation procedure for chemical reaction fouling in heat exchangers. *The Chemical Engineering Journal*, 31, 97-107.
- GALLOT-LAVALLEE, T., LALANDE, M. & CORRIEU, G. 1984. CLEANING KINETICS MODELING OF HOLDING TUBES FOULED DURING MILK PASTEURIZATION. *Journal of Food Process Engineering*, 7, 123-142.
- GILLHAM, C., FRYER, P., HASTING, A. & WILSON, D. 2000. Enhanced cleaning of whey protein soils using pulsed flows. *Journal of Food Engineering*, 46, 199-209.
- GILLHAM, C. R. 1997. *Enhanced cleaning of surfaces fouled by whey proteins*. PhD, University of Cambridge.
- GILLHAM, C. R., FRYER, P. J., HASTING, A. P. M. & WILSON, D. I. 1999. Cleaning-in-Place of Whey Protein Fouling Deposits: Mechanisms Controlling Cleaning. *Food and Bioproducts Processing*, 77, 127-136.
- GOODE, K., ASTERIADOU, K., FRYER, P., PICKSLEY, M. & ROBBINS, P. 2010. Characterising the cleaning mechanisms of yeast and the implications for Cleaning In Place (CIP). *Food and Bioproducts Processing*, 88, 365-374.
- GOODE, K. R. 2012. *Characterising the cleaning behaviour of brewery foulants*. PhD, University of Birmingham.
- GOTHAM, S. M. 1990. *Mechanisms of protein fouling in heat exchanger*. PhD, University of Cambridge.
- GOTHAM, S. M., FRYER, P. J. & PRITCHARD, A. M. 1992. β -lactoglobulin denaturation and aggregation reactions and fouling deposit formation: a DSC study. *International Journal of Food Science & Technology*, 27, 313-327.
- GRABHOFF, A. 1997. Cleaning of heat treatment equipment. *Fouling and Cleaning in heat treatment equipment, IDF Monograph*, 32-44.
- GRASSHOFF, A. 1989. Environmental aspects of the use of alkaline cleaning solutions. *Fouling and cleaning in food processing. Munich, Germany: Munich University*.
- GRASSHOFF, A. 1996. Efficiency assessment of a multiple stage CIP-procedure for cleaning a dairy plate heat exchanger. *EUR*, 117-124.
- HALLSTROEM, B., LUND, D. & TRAEGAARDH, C. 1981. *Fundamentals and Applications of Surface Phenomena Associated with Fouling and Cleaning in Food Processing*, Lund University.
- HANKINSON, D. J. & CARVER, C. E. 1968. Fluid Dynamic Relationships Involved in Circulation Cleaning. *Journal of Dairy Science*, 51, 1761-1767.
- HEGE, W. & KESSLER, H. 1986. Deposit formation of protein containing dairy liquids. *Milchwissenschaft*, 41, 356-360.
- HOFFMANN, M. A. & VAN MIL, P. J. 1997. Heat-induced aggregation of β -lactoglobulin: role of the free thiol group and disulfide bonds. *Journal of Agricultural and Food Chemistry*, 45, 2942-2948.
- JENNINGS, W. 1959. Circulation cleaning. III. The kinetics of a simple detergent system. *Journal of Dairy Science*, 42, 1763-1771.
- JENNINGS, W., MCKILLOP, A. & LUICK, J. 1957. Circulation cleaning. *Journal of Dairy Science*, 40, 1471-1479.
- JEURNINK, T. & DE KRUIF, K. 1995. Calcium concentration in milk in relation to heat stability and fouling. *Nederlands melk en Zuiveltijdschrift*, 49, 151-165.
- JEURNINK, T. J. 1992. Changes in milk on mild heating: turbidity measurements. *Netherlands Milk and Dairy Journal*, 46.

- JEURNINK, T. J. & DE KRUIF, K. G. 1993. Changes in milk on heating: viscosity measurements. *Journal of Dairy Research*, 60, 139-139.
- JEURNINK, T. J., WALSTRA, P. & DE KRUIF, C. 1996. Mechanisms of fouling in dairy processing. *Nederlands melk en Zuiveltijdschrift*, 50, 407-426.
- JEURNINK, T. J. M. & BRINKMAN, D. W. 1994. The cleaning of heat exchangers and evaporators after processing milk or whey. *International Dairy Journal*, 4, 347-368.
- JEYARAJAH, S. & ALLEN, J. C. 1994. Calcium binding and salt-induced structural changes of native and preheated β -lactoglobulin. *Journal of Agricultural and Food Chemistry*, 42, 80-85.
- JUN, S. & IRUDAYARAJ, J. M. 2009. *Food Processing Operations Modeling: Design and Analysis*, CRC Press.
- KANE, D. R. & MIDDLEMISS, N. E. Cleaning chemicals-state of the knowledge in 1985. Fouling and Cleaning in Food Processing, 1985. 312-355.
- KANEGSBURG, B. & KANEGSBURG, E. 2011. *Handbook for Critical Cleaning: Cleaning Agents and Systems*, CRC press.
- KARLSSON, C. A. C., WAHLGREN, M. C. & CHRISTIAN TRÄGÅRDH, A. 1998. Some Surface-related Aspects of the Cleaning of New and Reused Stainless-steel Surfaces Fouled by Protein. *International Dairy Journal*, 8, 925-933.
- KESSLER, H.-G. & BEYER, H.-J. 1991. Thermal denaturation of whey proteins and its effect in dairy technology. *International Journal of biological macromolecules*, 13, 165-173.
- LALANDE, M. & RENE, F. 1988. Fouling by Milk and Dairy Product and Cleaning of Heat Exchange Surfaces. In: MELO, L. F., BOTT, T. R. & BERNARDO, C. A. (eds.) *Fouling Science and Technology*. Springer Netherlands.
- LALANDE, M. & TISSIER, J.-P. 1985. Fouling of Heat Transfer Surfaces Related to β -Lactoglobulin Denaturation During Heat Processing of Milk. *Biotechnology Progress*, 1, 131-139.
- LEWIS, M. & HEPPELL, N. 2000. Fouling, cleaning, and disinfecting. *Continuous thermal processing of foods*. Gaithersburg, Md.: Aspen Publishers.
- LIU, W., CHRISTIAN, G., ZHANG, Z. & FRYER, P. 2002. Development and use of a micromanipulation technique for measuring the force required to disrupt and remove fouling deposits. *Food and bioproducts processing*, 80, 286-291.
- LYSTER, R. L. J. 1965. The composition of milk deposits in an ultra-high-temperature plant. *Journal of Dairy Research*, 32, 203-208.
- LYSTER, R. L. J. 1970. The denaturation of α -lactalbumin and β -lactoglobulin in heated milk. *Journal of Dairy Research*, 37, 233-243.
- MARTIN, E., MONTAGUE, G. & ROBBINS, P. 2013. A quality by design approach to process plant cleaning. *Chemical Engineering Research and Design*, 91, 1095-1105.
- MASS, A., LALANDE, M., HIDDINK, J., LUND, D., PLETT, E. & SANDU, C. 1985. Fouling of a plate heat exchanger by whipping cream. *Fouling and Cleaning in Food Processing*, LUND, PLETT, SANDU editors, University of Madison, Wisconsin, USA, 217-225.
- MERCADÉ-PRIETO, R. & CHEN, X. D. 2005. Caustic-induced gelation of whey deposits in the alkali cleaning of membranes. *Journal of membrane science*, 254, 157-167.

- MERCADÉ-PRIETO, R., PATERSON, W. R., DONG CHEN, X. & IAN WILSON, D. 2008. Diffusion of NaOH into a protein gel. *Chemical Engineering Science*, 63, 2763-2772.
- MERHEB, B., NASSAR, G., NONGAILLARD, B., DELAPLACE, G. & LEULIET, J. 2007. Design and performance of a low-frequency non-intrusive acoustic technique for monitoring fouling in plate heat exchangers. *Journal of food engineering*, 82, 518-527.
- MLEKO, S. 1999. Effect of protein concentration on whey protein gels obtained by a two-stage heating process. *European Food Research and Technology*, 209, 389-392.
- MORISON, K. R. & LARSEN, S. 2005. SPINNING DISC MEASUREMENT OF TWO-STAGE CLEANING OF HEAT TRANSFER FOULING DEPOSITS OF MILK. *Journal of Food process engineering*, 28, 539-551.
- MOTTAR, J. & MOERMANS, R. 1988. Optimization of the forewarming process with respect to deposit formation in indirect ultra high temperature plants and the quality of milk. *Journal of Dairy Research*, 55, 563-568.
- NEWSTEAD, D., GROUBE, G., SMITH, A. & EIGER, R. Fouling of UHT plants by recombined and fresh milk: some effects of preheat treatment. *Fouling and Cleaning in Food Processing*, 1998. 17-24.
- O'KENNEDY, B. T. & MOUNSEY, J. S. 2009. The dominating effect of ionic strength on the heat-induced denaturation and aggregation of β -lactoglobulin in simulated milk ultrafiltrate. *International Dairy Journal*, 19, 123-128.
- OBENG, E. & HOARE, M. 1988. Heat Transfer to Protein Concentrates. *1ChemE. Syrup. Ser.*, 88, 1213-1222.
- OLDFIELD, D. J., SINGH, H., TAYLOR, M. W. & PEARCE, K. N. 1998. Kinetics of Denaturation and Aggregation of Whey Proteins in Skim Milk Heated in an Ultra-high Temperature (UHT) Pilot Plant. *International Dairy Journal*, 8, 311-318.
- PATERSON, W. & FRYER, P. 1988. A reaction engineering approach to the analysis of fouling. *Chemical engineering science*, 43, 1714-1717.
- PATIL, G. & REUTER, H. 1986. Deposit formation in UHT plants. I. Effect of forewarming in indirectly heated plants. *Milchwissenschaft*, 41, 337-339.
- PEREIRA, A., MENDES, J. & MELO, L. 2009. Monitoring cleaning-in-place of shampoo films using nanovibration technology. *Sensors and Actuators B: Chemical*, 136, 376-382.
- PEREIRA, A., MENDES, J. & MELO, L. F. 2008. Using nanovibrations to monitor biofouling. *Biotechnology and bioengineering*, 99, 1407-1415.
- PEREIRA, A., ROSMANINHO, R., MENDES, J. & MELO, L. F. 2006. Monitoring Deposit Build-up using a Novel Mechatronic Surface Sensor (MSS). *Food and Bioproducts Processing*, 84, 366-370.
- PERRY, R. H., GREEN, D. 1984. *Green D. Perry's chemical engineers' handbook*, McGraw-Hill, New York
- PRITCHARD, N., DE GOEDEREN, G. & HASTING, A. 1988. The removal of milk deposits from heated surfaces by improved cleaning processes. *Fouling in Process Plant*, 465-475.
- RAKES, P. A., SWARTZEL, K. R. & JONES, V. A. 1986. Deposition of Dairy Protein-Containing Fluids on Heat Exchange Surfaces. *Biotechnology Progress*, 2, 210-217.
- RAUSCH, K. D. & POWELL, G. M. 1997. Dairy processing methods to reduce water use and liquid waste load. Department of Agricultural and Biological Engineering.

Report # MF- 2071: Cooperative Extension Service, Kansas State University, Manhattan, Kansas.

- REBELLO, W. J., RICHLIN, S. L. & CHILDS, F. 1988. The cost of heat exchanger fouling in the US industries. Department of Energy, Washington DC. Report no. EGG-M-39187.
- ROBBINS, P., ELLIOTT, B., FRYER, P., BELMAR, M. & HASTING, A. 1999. A comparison of milk and whey fouling in a pilot scale plate heat exchanger: implications for modelling and mechanistic studies. *Food and bioproducts processing*, 77, 97-106.
- ROEFS, S. P. & KRUIF, K. G. 1994. A Model for the Denaturation and Aggregation of β -Lactoglobulin. *European Journal of Biochemistry*, 226, 883-889.
- ROMNEY, A. 1990. *CIP: cleaning in place*, Society of Dairy Technology.
- SANTOS, O., NYLANDER, T., RIZZO, G., MÜLLER-STEINHAGEN, H., TRÄGÅRDH, C. & PAULSSON, M. 2003. Study of whey protein adsorption under turbulent flow rate. *Proceedings of Heat Exchanger Fouling and Cleaning-Fundamentals and Applications, Santa Fe, USA*.
- SAWYER, W. H. 1968. Heat Denaturation of Bovine β -Lactoglobulins and Relevance of Disulfide Aggregation. *Journal of dairy science*, 51, 323-329.
- SCHREIER, P., GREEN, C., HASTINGS, A. & FRYER, P. 1996. Heat exchanger fouling by whey protein solutions. *EUR*, 9-17.
- SCHREIER, P. J. R. 1995. *Monitoring and modelling of heat exchanger fouling*. PhD, University of Cambridge.
- SCHREIER, P. J. R. & FRYER, P. J. 1995. Heat exchanger fouling: A model study of the scaleup of laboratory data. *Chemical Engineering Science*, 50, 1311-1321.
- SIMMONS, M. J. H., JAYARAMAN, P. & FRYER, P. J. 2007. The effect of temperature and shear rate upon the aggregation of whey protein and its implications for milk fouling. *Journal of Food Engineering*, 79, 517-528.
- SINGH, H. & CREAMER, L. K. 1991. Changes in Size and Composition of Protein Aggregates on Heating Reconstituted Concentrated Skim Milk at 120°C. *Journal of Food Science*, 56, 671-677.
- SKUDDER, P. J., BROOKER, B. E., BONSEY, A. D. & ALVAREZ-GUERRERO, N. R. 1986. Effect of pH on the formation of deposit from milk on heated surfaces during ultra high temperature processing. *Journal of Dairy Research*, 53, 75-87.
- SMITS, P. & BROUWERSHAVEN, J. H. V. 1980. Heat-induced association of β -lactoglobulin and casein micelles. *Journal of Dairy Research*, 47, 313-325.
- SPX 2012. *CIP and Sanitation of Process Plant*.
- SRICHANTRA, A., NEWSTEAD, D., MCCARTHY, O. & PATERSON, A. 2006. Effect of preheating on fouling of a pilot scale UHT sterilizing plant by recombined, reconstituted and fresh whole milks. *Food and bioproducts processing*, 84, 279-285.
- STEWART, J., SEIBERLING, D. & CHOWDHURY, J. 1996. The secret's out clean in place. *Chemical engineering*, 103, 72-79.
- TAMIME, A. Y. 2009. *Cleaning-in-place: dairy, food and beverage operations*, John Wiley & Sons.
- THERMOELECTRIC, C. 2013. *Peltier Analysis* [Online]. Available: http://www.customthermoelectric.com/Peltier_analysis.html [Accessed 19 July 2013].

- TIMPERLEY, D. A. & SMEULDERS, C. N. M. 1987. Cleaning of dairy HTST plate heat exchangers: comparison of single- and two-stage procedures. *International Journal of Dairy Technology*, 40, 4-7.
- TISSIER, J. & LALANDE, M. 1986. Experimental device and methods for studying milk deposit formation on heat exchange surfaces. *Biotechnology progress*, 2, 218-229.
- TISSIER, J., LALANDE, M. & CORRIEU, G. 1984. A study of milk deposit on a heat exchange surface during ultra-high-temperature treatment, Engineering and Food, 1: Engineering Sciences in the Food Industry, ed. McKenna, BM. Applied Science Publishers.
- TOYODA, I., SCHREIER, P. & FRYER, P. 1994. A computational model for reaction fouling from whey protein solutions. *Proceedings of Fouling Cleaning in Food Processing, Cambridge, England*, 222-229.
- TRUONG, T., ANEMA, S., KIRKPATRICK, K. & CHEN, H. 2002. The use of a heat flux sensor for in-line monitoring of fouling of non-heated surfaces. *Food and bioproducts processing*, 80, 260-269.
- TULADHAR, T., PATERSON, W., MACLEOD, N. & WILSON, D. 2000. Development of a novel non-contact proximity gauge for thickness measurement of soft deposits and its application in fouling studies. *The Canadian Journal of Chemical Engineering*, 78, 935-947.
- TULADHAR, T., PATERSON, W. & WILSON, D. 2002. Investigation of alkaline cleaning-in-place of whey protein deposits using dynamic gauging. *Food and bioproducts processing*, 80, 199-214.
- VAN ASSELT, A., VAN HOUWELINGEN, G. & TE GIFFEL, M. 2002. Monitoring system for improving cleaning efficiency of cleaning-in-place processes in dairy environments. *Food and bioproducts processing*, 80, 276-280.
- VISSER, H., JEURNINK, T. J., SCHRAML, J., FRYER, P. & DELPLACE, F. 1997. Fouling of heat treatment equipment. *Bulletin of the IDF*, 328, 7-31.
- VISSER, J. & JEURNINK, T. J. M. 1997. Fouling of heat exchangers in the dairy industry. *Experimental Thermal and Fluid Science*, 14, 407-424.
- WALLHÄUBER, E., HUSSEIN, M. A. & BECKER, T. 2012. Detection methods of fouling in heat exchangers in the food industry. *Food Control*, 27, 1-10.
- WINQUIST, F., BJORKLUND, R., KRANTZ-RÜLCKER, C., LUNDSTRÖM, I., ÖSTERGREN, K. & SKOGLUND, T. 2005. An electronic tongue in the dairy industry. *Sensors and Actuators B: Chemical*, 111, 299-304.
- WITHERS, P. M. 1996. Ultrasonic, acoustic and optical techniques for the non-invasive detection of fouling in food processing equipment. *Trends in food science & technology*, 7, 293-298.
- XIONG, Y. L. 1992. Influence of pH and ionic environment on thermal aggregation of whey proteins. *Journal of Agricultural and Food Chemistry*, 40, 380-384.
- YANG, A., MARTIN, E., MONTAGUE, G. & FRYER, P. 2008. Towards improved cleaning of FMCG plants: a model-based approach. *Computer Aided Chemical Engineering*, 25, 1161-1166.
- ZELVER, N., ROE, F. & CHARACKLIS, W. 1985. Potential for monitoring fouling in the food industry. *Fouling and Cleaning in Food Processing, Madison, WI: Univ. of Wisconsin, Department of Food Science*, 255-262.

